

Synthesis of 2'-bromo-2'-fluoro-2'-deoxycytidine derivatives towards [^{18}F]gemcitabine

Roderick Thomas Stark

This thesis is submitted for the degree of Doctor of Philosophy
(PhD) at Cardiff University

March 2020



Contents

Abstract	v
Acknowledgements	vi
Abbreviations	viii
1 – Introduction	1
1.1 – Gemcitabine	1
1.1.1 – Synthesis of gemcitabine	5
1.1.1.1 – Original synthesis	5
1.1.1.2 – Protecting groups	10
1.1.1.3 – Leaving group	14
1.1.1.4 – Pyrimidine ring formation	21
1.1.2 – Ribonolactone halogenation	23
1.1.2.1 – Mixed halogen ribofuranoses	28
1.1.3 – Gemcitabine prodrug and ProTide strategies	36
1.1.3.1 – LY2334737	36
1.1.3.2 – NUC-1031 and ProTide strategies	38
1.1.3.3 – Clavis	44
1.2 – Positron emission tomography	46
1.2.1 – Principles of PET	46
1.2.2 – ^{18}F production	49
1.2.3 – Application and principles of radiotracers	51
1.2.4 – ^{18}F radiochemistry	54
1.2.4.1 – Electrophilic fluorination	54
1.2.4.2 – Nucleophilic fluorination	59

1.2.5 – Radiofluorination of nucleosides	61
1.2.5.1 – Early-stage fluorination	61
1.2.5.2 – Late-stage fluorination	63
2 – Research aims and objectives	70
3 – Results and discussion	71
3.1 – Synthetic route 1	71
3.1.1 – Disconnection strategy	71
3.1.2 – Synthesis	71
3.2 – Synthetic route 2	76
3.2.1 – Disconnection strategy	76
3.2.2 – Synthesis	76
3.2.2.1 – Ring construction and protection	76
3.2.2.2 – α -halogenation	78
3.2.2.3 – Lactone deprotection	84
3.2.2.4 – Mesyl-O-lactol formation	86
3.2.2.5 – Glycosylation	89
3.2.2.6 – Radiolabelling precursor synthesis	96
3.2.3 – α -hydroxy lactone formation	98
3.3 – Scale up of synthetic route 2	102
3.4 – Fluorination	107
3.4.1 – Cold ^{19}F fluorination	107
3.4.2 – Radiofluorination	112
3.4.3 – Conclusions and outlook	114
3.5 – Tissue culture work	116

3.5.1 – Conclusions and outlook	121
4 – Conclusion	123
5 – Experimental	125
5.1 – General information	125
5.2 – Synthetic route 1	127
5.3 – Synthetic route 2	130
5.4 – Synthesis of reference compounds	156
5.5 – Fluorination	160
5.6 – Cell culture details	161
6 – Appendix	162
6.1 – HPLC traces of selected compounds	162
6.2 – Selected NMR spectra	164
6.3 – HRMS report	171
References	172

Abstract

Gemcitabine is a frequently used chemotherapeutic agent against a range of cancers – pancreatic cancer in particular. One of its disadvantages is its poor specificity, needing to overcome many deactivation pathways in order to impart its anticancer properties. As such, a fluorine-18 labelled gemcitabine would provide *in vivo* pharmacokinetic information specific for each patient in a step towards personalised treatment.

Herein described is a synthetic route towards compounds that may be screened as a fluorine-18 radiolabelling precursors for the synthesis of [¹⁸F]gemcitabine. The developed strategy centres on the synthesis of key 2-bromo-2-fluororibonolactone, which was produced in a diastereoselective fashion. The synthesised lactone was then reacted with cytosine derivatives to deliver the radiofluorination substrates.

Fluorination with fluorine-19 demonstrated the suitability of the substrates towards substitution, with initial [¹⁸F]fluorination studies also conducted. Tissue culture studies were also carried out, in order to evaluate the bioactivity of the synthesised compounds, relative to gemcitabine.

Acknowledgements

I would like to take this opportunity to thank the many people involved with the work presented in this thesis, as many people have contributed in supporting me along the way.

Let's start at the very beginning – my supervisor Dr. Ian Fallis, for his vast knowledge and guidance throughout this project. I know this has been a project Ian has worked on for a number of years and count myself incredibly lucky to work on such an interesting and meaningful project. Thanks for guiding me along the way, while encouraging me to push myself further than I thought possible. I would also like to Dr. Duncan Browne, who has co-supervised me and overseen the majority of my work. Over the time spent in Duncan's research group, he has challenged me and driven me to new levels for which I cannot thank him enough, while offering new and exciting opportunities I would never have thought of doing.

The nature of this project has meant significant collaborations, which must be recognised. I would like to thank Prof. Chris Marshall, Dr. Peter Llywelyn and the rest of the Production Team and staff at PETIC in UHW for providing the opportunity to work with you all. The chance to work with ^{18}F is rare, and the training you provided for FDG synthesis was incredible. Latterly, thank you to Dr. Steve Paisey and Dr. Matt Tredwell for their help with the radiochemistry. Thanks to Dr. Catherine Hogan for the opportunity to conduct tissue culture experiments and training me, along with Anna Richards for helping me with any other issues I had.

I must also thank my funders, who made this project possible. To Tenovus Cancer Care and Tim Banks, your support was much appreciated, and I hope this work reflects the good work you and the charity continue to do. Thanks to the KESS II scheme and team involved, notably Esther Meadows, for providing the platform for research such as this to be conducted.

A huge amount of credit must go to Dr. JieXiang Yin, who came in to help the project and really helped provide synthetic experience and a calming influence – which cannot be understated. Not only a wizard at organic chemistry (and whistling), he helped teach me so many valuable lessons ("*more silica gel!*") and I wish him and his young family all the very best. Some of his work is presented in this thesis (Schemes 3.03 and 3.04)

Onto my fellow DLB group members. Firstly, to Christiane and Joey. The amount of help you gave and time you both invested in me, especially at the start of my PhD, was something I didn't really appreciate. You helped me when I needed it most, thank you so much. During my time in the group, many people have come and gone but those that have stuck around long enough to endure my singing must be recognised. So thanks to Qun, Tom, Will, Yerbol and Andy; you have all helped me at many points over the course of my PhD. Be it in the lab, the pub or at home with a cup of tea – you've helped keep me on the straight and narrow, while condoning my awful jokes (but really, you know they're very good).

I would like to thank members of other groups in the department that have helped me along the way. Firstly, James, Kurt, Ben R-B, Alex and latterly Ben A., from the LCM group who offered advice in the lab, group meetings and life. Thanks to Andy, Siôn and others from Ian's group for support when I needed it. And to all my hall-way friends, for the half-hearted smiles we share.

Outside of university life, I have an amazing friendship group who always have a plan in the mix that help keep me motivated and remind me of life outside of the PhD bubble. Shout out to Mark "M.J." Sullivan, who has had the pleasure/misery of living with me for the duration of our PhDs.

I'd like to give a special mention to my girlfriend Meg – thanks for supporting me during the good and the bad, for when I need a reminder to switch off and everything else in between. You've been my constant, thank you so much.

Thanks to my family for their continued support over the years. This is something we can all be proud of, and I'm so grateful for everything you've done for me. This one is for you.

Finally, I'd like to thank my legs for always supporting me, my arms for being by side and my fingers, because I can always count on them.

Abbreviations

Ac	Acetyl
AIBN	Azobisisobutyronitrile
app.	Apparent
Boc	<i>tert</i> -Butyloxycarbonyl
BOPCl	Bis(2-oxo-3-oxazolidinyl)phosphinic chloride
BSA	<i>N,O</i> -Bis(trimethylsilyl)acetamide
Bz	Benzoyl
calc.	Calculated
CDI	Carbonyl diimidazole
COSY	Correlation spectroscopy
Cp	Cyclopentadienyl
DABCO	1,4-Diazobicyclo[2.2.2]octane
DBU	1,8-Diazabicyclo(5.4.0)undec-7-ene
DCC	Dicyclohexylcarbodiimide
DCE	1,2-dichloroethane
DCM	Dichloromethane
DHP	3,4-Dihydropyran
DIBAL-H	Diisobutylaluminium hydride
DIPEA	<i>N,N</i> -Diisopropylethylamine
DMAP	4-Dimethylaminopyridine
DMF	<i>N,N</i> -Dimethylformamide
DMP	Dess-Martin Periodinane
DMPU	<i>N,N'</i> -Dimethylpropyleneurea
DMSO	Dimethylsulfoxide
DMTr	4,4'-Dimethoxytrityl

DOTA	1,4,7,10-Tetraazacyclododecane-1,4,7,10-tetraacetic acid
d.r.	Diastereomeric ratio
EDC.HCl	1-Ethyl-3-(3-dimethylaminopropyl)carbodiimide hydrochloride
Et ₂ O	Diethyl ether
FAC	1-(2'-Deoxy-2-fluoro-β-D-arabinofuranosyl)cytosine
FBS	Fetal bovine serum
GC-MS	Gas chromatography-mass spectrometry
HMDS	Hexamethyldisilazane
HOBt	Hydroxybenzotriazole
HPLC	High performance liquid chromatography
HRMS	High resolution mass spectrometry
ⁱ Pr	Isopropyl
IR	Infrared
K ₂₂₂	4,7,13,16,21,24-Hexaoxa-1,10-diazabicyclo[8.8.8]hexacosane, Kryptofix® 222
KHMDS	Potassium hexamethyldisilazide
LDA	Lithium diisopropylamine
LiHMDS	Lithium hexamethyldisilazide
LTBA	Lithium tri(<i>tert</i> -butoxy)aluminium hydride
<i>m</i>	Atomic mass of (radio)nuclide
mCPBA	<i>meta</i> -chloroperbenzoic acid
MeCN	Acetonitrile
min	Minute(s)
Ms	Mesyl/methanesulfonyl
MTBE	Methyl <i>tert</i> -butyl ether
<i>N</i> _A	Avagadro's number

NBS	<i>N</i> -Bromosuccinimide
n.d.	Not disclosed
NDCY	Non-decay corrected yield
NFSI	<i>N</i> -Fluorobenzenesulfonamide
NMI	<i>N</i> -Methylimidazole
NMM	<i>N</i> -Methylmorpholine
NMR	Nuclear Magnetic Resonance
NOESY	Nuclear Overhauser effect spectroscopy
Nuc.	Nucleophile
ONs	<i>para</i> -Nitrobenzenesulfonate (nosylate)
OTf	Triflate
PBS	Phosphate buffered saline
PLE	Pig liver esterase
PMBz	<i>para</i> -Methoxy benzoyl
PPY	4-Pyrrolidinopyridine
<i>p</i> TSA	<i>para</i> -Toluenesulfonic acid
Py	Pyridine
quant.	Quantitative
RCC	Radiochemical conversion
RCY	Radiochemical yield
R_f	Retention factor
RedAl	Sodium bis(2-methoxyethoxy)aluminium hydride
RPMI	Roswell Park Memorial Institute (medium)
TBAF	Tetrabutylammonium fluoride
TBDMS	<i>tert</i> -butyldimethylsilyl
TBDPS	<i>tert</i> -butyldiphenylsilyl

^t Bu	<i>tert</i> -butyl
TES	Triethylsilyl
TFA	Trifluoroacetic acid
THF	Tetrahydrofuran
THP	Tetrahydropyran
TIPSDCl ₂	1,3-dichloro-1,1,3,3-tetraisopropylidisiloxane
TLC	Thin layer chromatography
TMAF	Tetramethylammonium fluoride
TMS	Trimethylsilyl
TIPS	Triisopropylsilyl
Tr	Trityl

1 – Introduction

1.1 – Gemcitabine

2',2'-Difluoro-2'-deoxycytidine (dFdC; **1**, Figure 1.01) marketed commercially in 1988 as Gemzar® as the hydrochloride salt, is a nucleoside analogue of 2-deoxycytidine (**2**), with geminal fluorine atoms at the 2' position, hence the common name gemcitabine. It is a frequently used chemotherapeutic agent as a combatant against a range of cancers, such as ovarian, breast and pancreatic cancer.

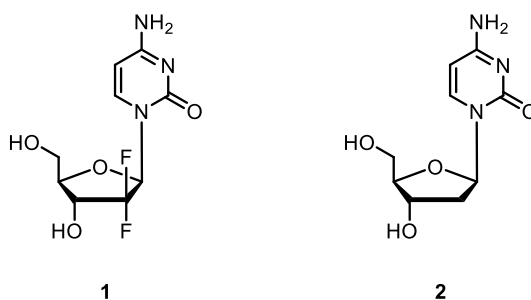


Figure 1.01: Structures of gemcitabine (**1**) and 2-deoxycytidine (**2**).

Additionally, it is commonly used as a combination therapy, with platinum based compounds such as *cis*-platin (**3**) and carboplatin (**4**) for bladder and ovarian cancer, respectively. For pancreatic cancer, gemcitabine is typically administered as the sole chemotherapeutic agent as a first-line treatment, but has limitations in its effectiveness.

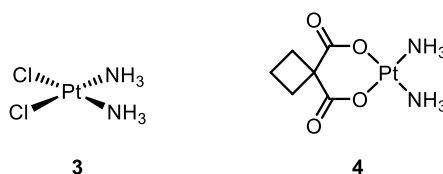
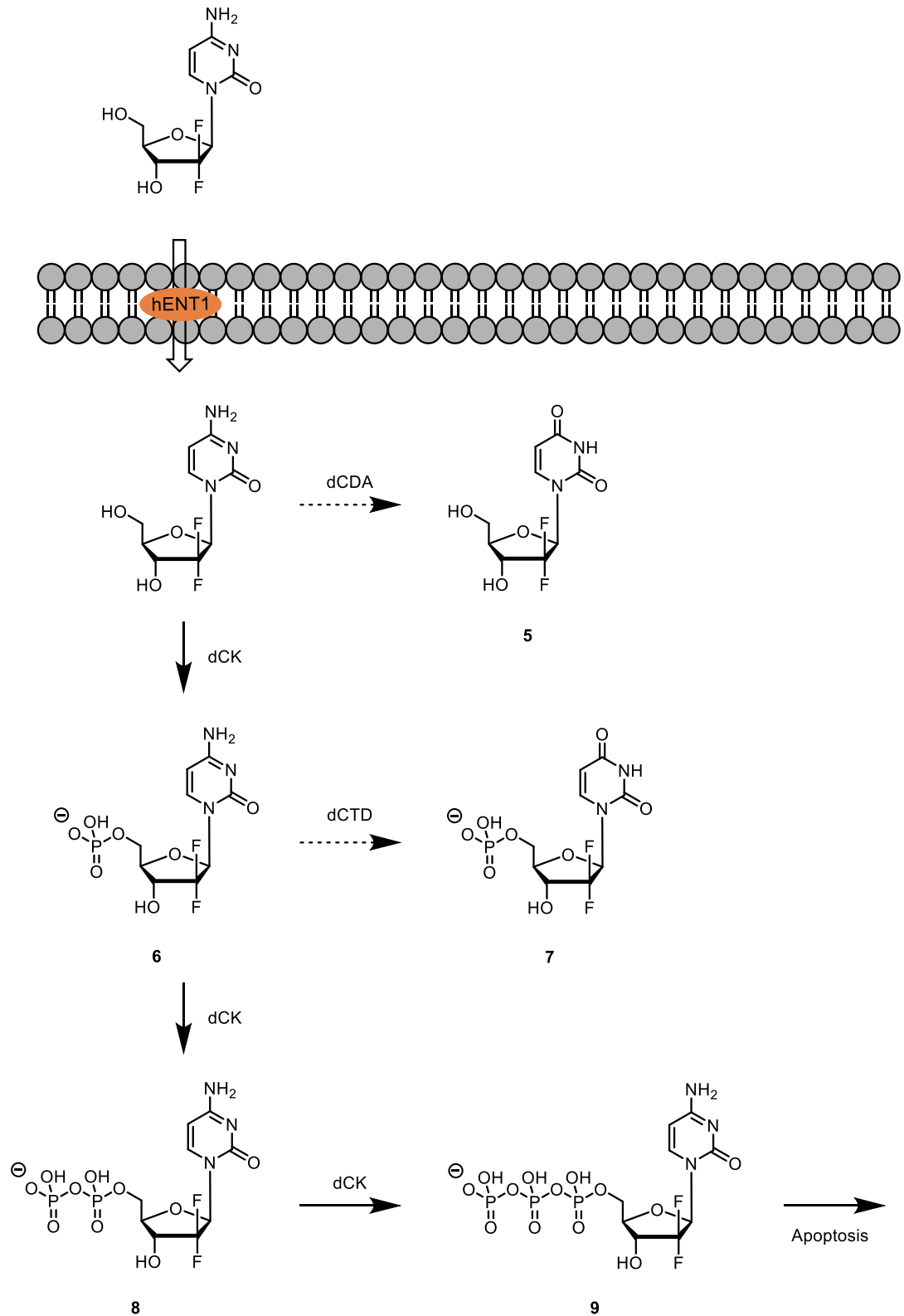


Figure 1.02: Structures of *cis*-platin (**3**) and carboplatin (**4**).

Gemcitabine is delivered as the prodrug into the patient, and metabolised into the active chemotherapeutic agent. Due to its highly hydrophilic nature, the drug is not actively taken up into cancer cells across the plasma lipid bilayer found in the pancreas, demonstrating poor bioavailability. Kinetic studies have illustrated that gemcitabine uptake across a cell membrane is mediated by range of transporter proteins, such as human equilibrative nucleoside transporters (hENT), specifically hENT1. It has also been

found to be transported via human concentrative nucleosides (hCNT) although to a lower extent, in particular hCNT1 which is known to favour transporting pyrimidine nucleosides.^[1] With a human terminal plasma half-life of 17 minutes,^[2] intracellular gemcitabine is rapidly consumed with approximately 90% of uptaken **1** being deactivated by deoxycytidine deaminase (dCDA), to the inactive 2',2'-difluoro-2'-deoxyuridine equivalent.^[3]

Gemcitabine that remains intact in cells is first phosphorylated at the 5' position by deoxycytidine kinase (dCK) in the rate limiting step, to form 2',2'-difluoro-2'-deoxycytidine-5'-O-phosphate, shown in Scheme 1.01. This intermediate may also be deactivated, noted by dashed arrows, in a process facilitated by deoxycytidylate deaminase which converts it to mono-phosphorylated uridine **7**. dFdCMP may be sequentially further phosphorylated to produce the corresponding diphosphate (**8**, dFdCDP) and triphosphate (**9**, dFdCTP) – both considered to be active cytotoxic metabolites *in vivo*. dFdCTP acts as a masked chain terminant, addition of a subsequent natural nucleotide renders the compound less susceptible to DNA repair by base pair excision,^[4] inhibiting DNA strand growth and inducing apoptosis within the cell. In addition, gemcitabine also possesses a self-potentiating mechanism; dFdCDP inhibits ribonucleotide reductase (RNR), which catalyses the production of other deoxyribonucleotides needed for continued synthesis and repair of DNA. As a result of this inhibition, the concentration of DNA nucleobases and their corresponding phosphates is reduced. Ramos and co-workers go on to say that the effect of inhibiting RNR is profound, as the intracellular equilibrium is shifted leading to an overall increase in active uptake of deoxyribonucleotides, including gemcitabine, increased rates of phosphorylation, and decreased deactivation by dCDA.^[5]



Scheme 1.01: Intracellular mode of action of gemcitabine, where **9** acts as a masked chain terminator.

hENT1 = human equilibrative nucleoside transporter. dCDA = deoxycytidine deaminase. dCK = deoxycytidine kinase. dCTD = deoxycytidylate deaminase.

In summary, the *in vivo* release of gemcitabine is dependent on three factors:^[6]

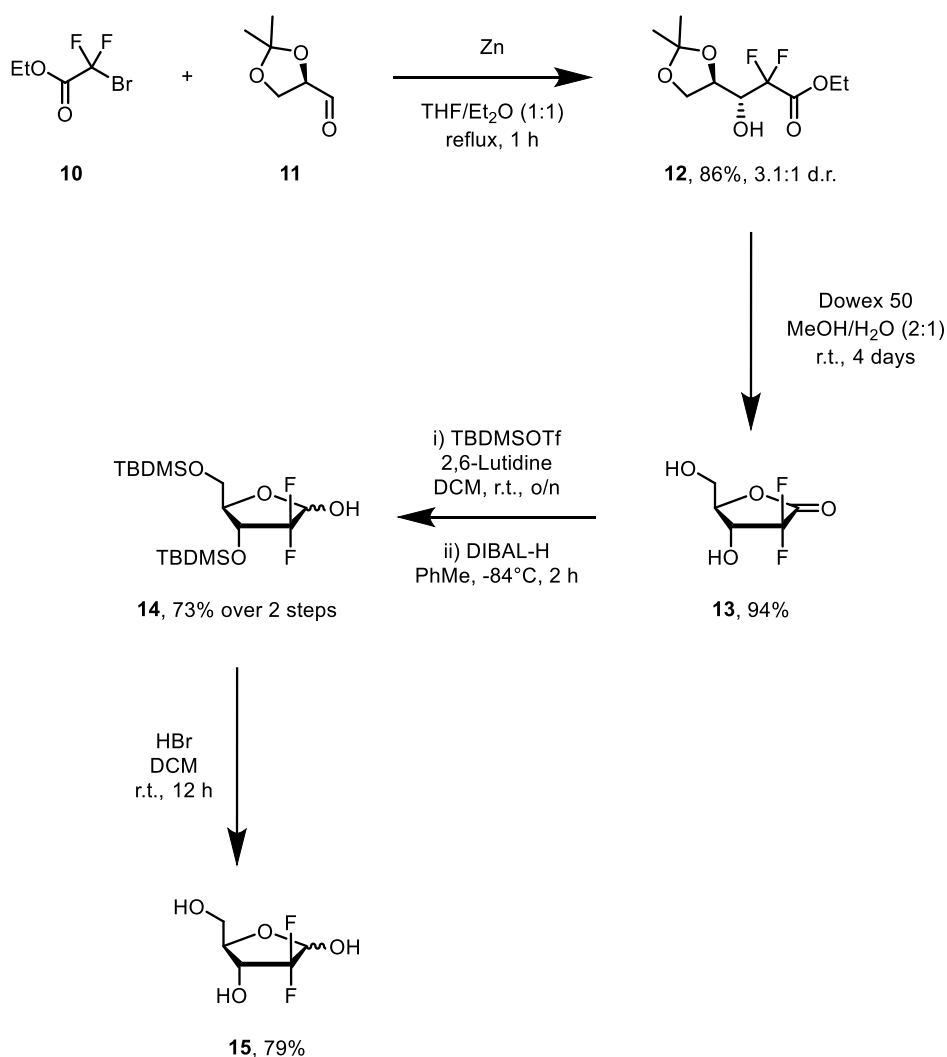
- i. Regulation of dCK, which is necessary for the initial phosphorylation.
- ii. Regulation of enzymes, such as CDA, contributing to undesirable degradation pathways of gemcitabine.
- iii. Expression of nucleoside transporters, such as hENT1, for uptake into cells.

Alternative strategies have been developed in order to overcome the observed deactivation pathways of gemcitabine. McGuigan and co-workers successfully established the field of ProTide drug delivery, in which the nucleotide is introduced with a pseudo phosphate group already installed at the 5' position as to avoid deactivation by dCDA.^[7] Additionally, this strategy circumvents the rate limiting phosphorylation of gemcitabine *in vivo*, and dependence on nucleoside transporters such as hENT1. One drawback of this improved activity and availability is a simultaneous loss of specific targeting.

1.1.1 – Synthesis of gemcitabine

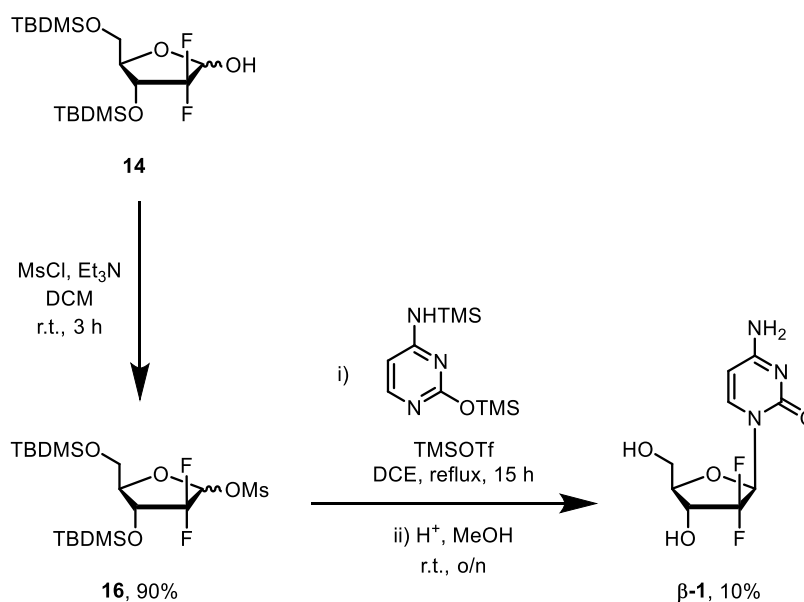
1.1.1.1 – Original synthesis

Gemcitabine was first successfully synthesised by Hertel *et al* in 1998,^[8] with the aim of synthesising fluorinated nucleosides as potential anticancer/antiviral agents. The synthesis (Scheme 1.02) was realised by combining (*R*)-2,3-*O*-isopropylidene-D-glyceraldehyde, accessed from D-mannitol in two steps,^[9] with ethyl bromodifluoroacetate (**10**) and zinc in a Reformatsky reaction, furnishing the desired β -hydroxy ester in 65% yield. Subsequent acidic deprotection of the acetal moiety and lactonisation afforded the integral 2-deoxy-2,2-difluoro-D-ribonolactone (**13**) (Scheme 1.02). Protection of **13** as the *tert*-butyl dimethyl silyl ether and reduction by DIBAL-H to yield the corresponding protected or deprotected ribofuranose (**14** and **15** respectively).



Scheme 1.02: The synthesis of protected and unprotected difluorolactols (**14**) and (**15**) by zinc-based Reformatsky and lactonisation.

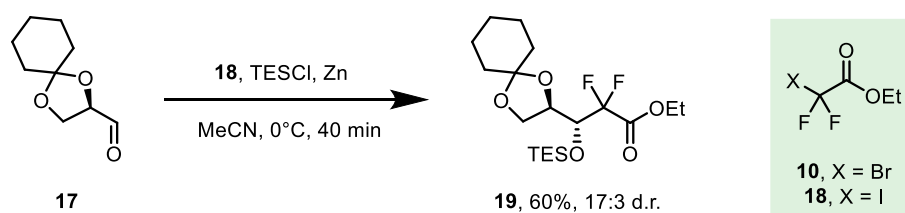
Ribofuranose **14** was subsequently treated with methanesulfonyl chloride to afford **16**, which upon reacting with *bis*-TMS protected cytosine and acid hydrolysis, affords gemcitabine (Scheme 1.03, **β -1**). The lack of anomer selectivity observed was attributed to the *gem*-fluoro moiety deactivating the mesylate leaving group, leading to increased S_N2 character during the ring appending reaction. Consequently, the α -anomer was formed in 40% yield (Scheme 1.03).



Scheme 1.03: The synthesis of gemcitabine (**1**) by mesylation and glycosylation.

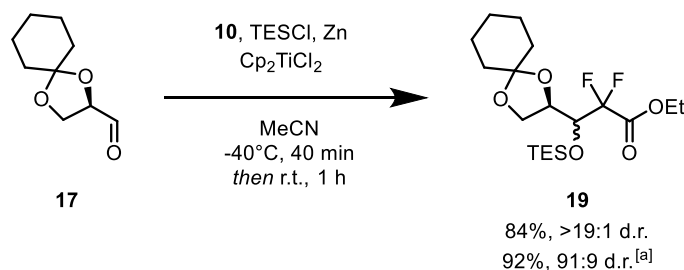
The seminal work by Hertel^[8] demonstrated the value of the difluoromethylene moiety in this class of chemotherapeutic agents and paved the way for alternative synthetic routes to be explored.

Building on the original zinc-based synthesis, Yasuda and co-workers investigated the use of various Lewis acids to promote the addition to unactivated protected glyceraldehydes.^[10] In the absence of activator, combining ethyl difluoroiodoacetate with (*R*)-cyclohexylideneglyceraldehyde in the presence of zinc powder and triethylsilylchloride, the silyl protected product **19** was isolated in a moderate 60% yield with good selectivity for the desired *anti* diastereomer, in a 17:3 ratio over the *syn* isomer (Scheme 1.04).



Scheme 1.04: The synthesis of **19** by zinc-mediated addition reaction using (*R*)-cyclohexylidene-glyceraldehyde (**17**).

Changing the latent nucleophile to ethyl bromodifluoroacetate, and screening a number of Lewis acids, they found that stoichiometric bis(cyclopentadienyl)titanium (IV) dichloride not only afforded higher yields (84%), but also further promoted the formation of the *anti*-diastereoisomer, in a ratio greater than 19:1. Furthermore, the observed enhanced selectivity and reactivity illustrated in Scheme 1.05 was also possible with catalytic Cp_2TiCl_2 which delivered **19** in 92% yield, albeit with slightly lower *anti:syn* ratio of 91:9.



^[a] 10 mol% of Cp_2TiCl_2 used.

Scheme 1.05: The modification of the reaction shown in Scheme 1.04, utilising Cp_2TiCl_2 as Lewis acid.

The authors attribute the diastereoselectivity of the reaction to the coordination of the Lewis acid to the aldehyde oxygen, with the *in situ* produced nucleophile attacking from the less sterically hindered *si* face,^[10] illustrated by the Felkin-Anh model in Figure 1.03.

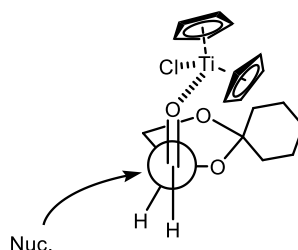
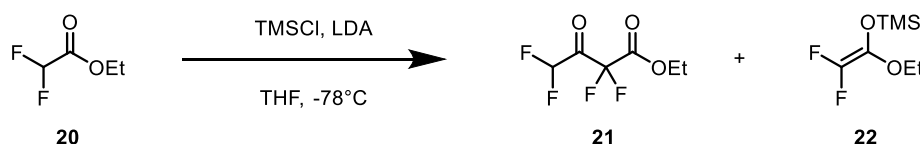


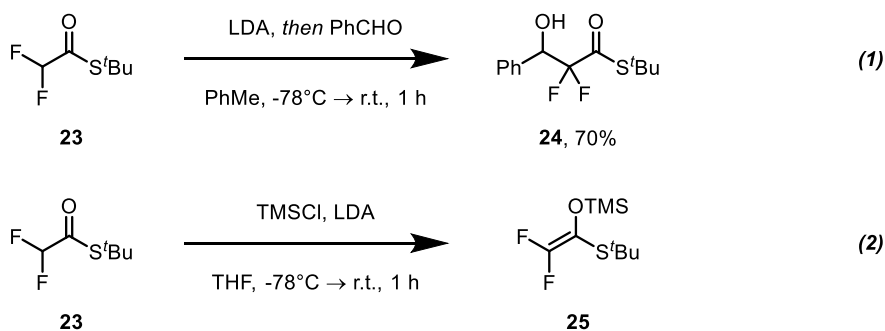
Figure 1.03: The Felkin-Ahn model to rationalise the observed selectivity of the reaction shown in Scheme 1.05, utilising Cp_2TiCl_2 .

Alternative strategies to installing the CF_2 group have had limited success outside of the Reformatsky reaction centred approach. Use of ethyl difluoroacetate with LDA and TMSCl was found to predominantly yield the self-Claisen condensation product **21**, not the desired silyl enol ether **22**, as shown in Scheme 1.06.



Scheme 1.06: The LDA mediated reaction of ethyl difluoroacetate and the mixture of products obtained.¹¹

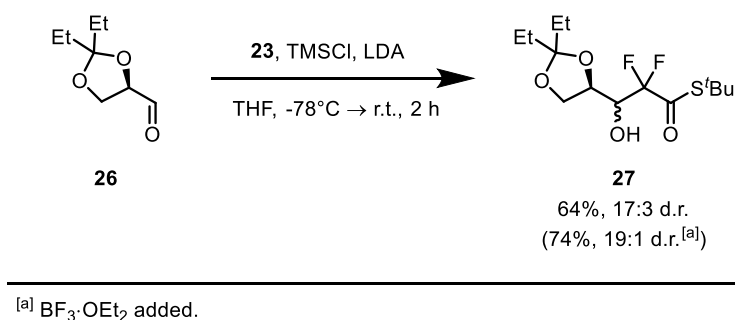
Weigel overcame this issue,^[11] using *tert*-butyl thioester **23** as the latent nucleophile in conjunction with LDA as base and benzaldehyde as electrophile, affording β -hydroxy thioester **24** in 70% isolated yield (Scheme 1.07(1)). The improved selectivity was due to a less nucleophilic lithium enolate generated *in situ*, although the self-condensation product was detected at 10% ^{19}F NMR yield.



Scheme 1.07: The LDA mediated reactions of *S*-(*tert*-butyl) 2,2-difluoroethanethioate (**23**), with benzaldehyde as electrophile (*top*, (1)) and TMSCl (*bottom*, (2)).

Conditions were also altered to include TMSCl, resulting in formation of silyl enol ether **25** as the sole product by ^{19}F NMR. The yield of **25** was not given but was used *in situ* for further reactions, and not isolated due to its hydrolytic instability (Scheme 1.07 (**2**)),

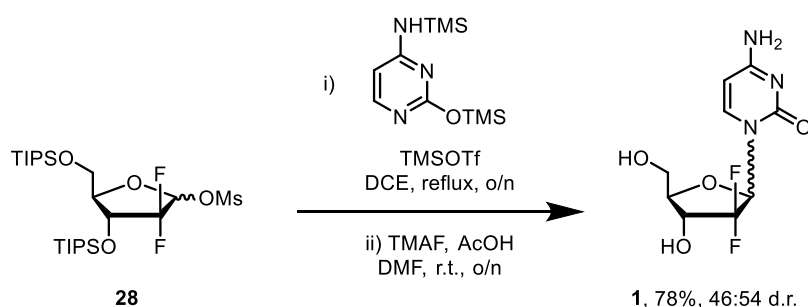
With appropriate conditions for the formation of **25**, **23** was combined with protected glyceraldehyde **26** furnishing 64% yield of β -hydroxy thioester **27**, shown in Scheme 1.08. Inclusion of Lewis acid $\text{BF}_3 \cdot \text{Et}_2\text{O}$ to activate aldehyde **26** increased the yield and diastereoselectivity of the reaction, preferentially forming the *anti*-isomer, an observation attributed to the steric bulk of the *tert*-butyl thioester in both instances.



Scheme 1.08: The LDA mediated reaction of **23** and production of β -hydroxythioester **27**.

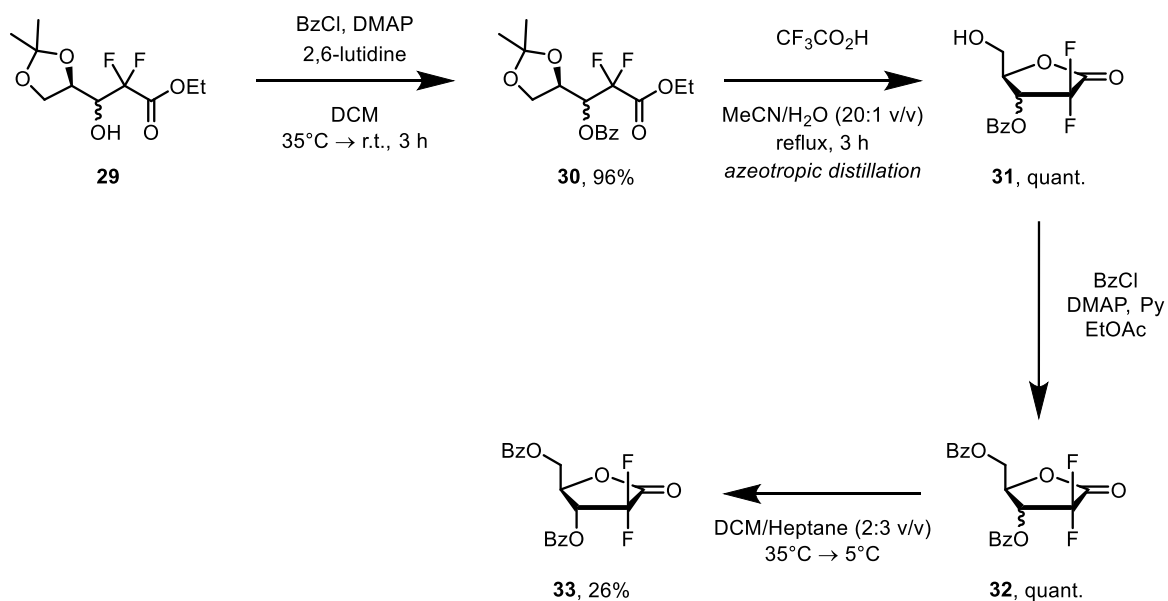
1.1.1.2 – Protecting groups

Cen and Sauve found that utilising the difluororibofuranose protected as the bis(triisopropyl)silyl ether increased the anomeric selectivity of the silyl-Hilbert-Johnson reaction (Scheme 1.09), improving Hertel's original methodology.^[12] By changing from TBDMS to TIPS, the increased sterics of the 3-O-silyl group resulted in improved β -anomer formation. In the presence of Lewis acid TMSOTf in refluxing DCE and subsequent deprotection by TMAF and acetic acid, anomerically pure gemcitabine was produced in 36% yield after HPLC purification. The undesired α -anomer was produced in a slight excess, at 42% isolated yield (overall 78% yield).



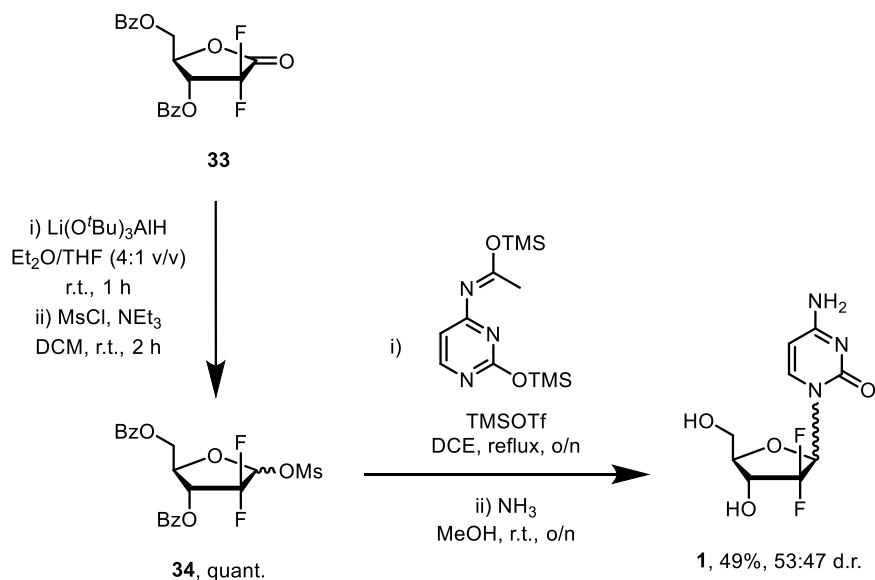
Scheme 1.09: The Vorbruggen glycosylation reaction of **28** and TMAF mediated deprotection to yield an anomeric mixture of **1**.

Esters have also been employed as protecting groups for the 3- and 5-hydroxyl groups once 2-deoxy-2,2-difluororibofuranose has been synthesised. Chou *et al* further developed the synthesis of gemcitabine, following Hertel's synthesis of the requisite β -hydroxy ester, by converting intermediate **29** into its benzoyl ester; through benzoyl chloride, catalytic DMAP, and 2,6-lutidine as base in DCM.^[13] Depicted in Scheme 1.10, concomitant deprotection and cyclisation affords lactone **31**, which is in turn benzoylated to afford 3,5-di-O-benzoyl-2-deoxy-2,2-difluoro-D-ribonic acid-1,4-lactone **32**, from which the desired *ribo*-stereomer may be selectively crystallised, albeit in a low yield of 26%.



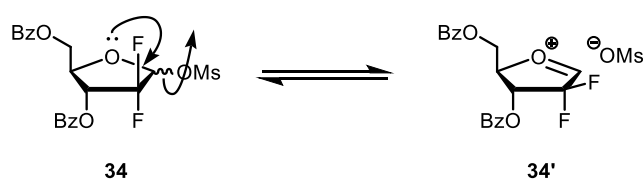
Scheme 1.10: The synthesis of key protected difluorolactone **33**.

From **33**, reduction by LTBA in THF/Et₂O quantitatively delivered intermediate ribofuranose as a mixture of anomers, which was then mesylated to afford **34** in quantitative yield. Subsequently, subjecting **34** to the Vorbruggen reaction and debenzoylation by ammonia in methanol furnished **1** as a near 1:1 anomeric mixture, with the α -anomer being formed in a slight excess (Scheme 1.11).



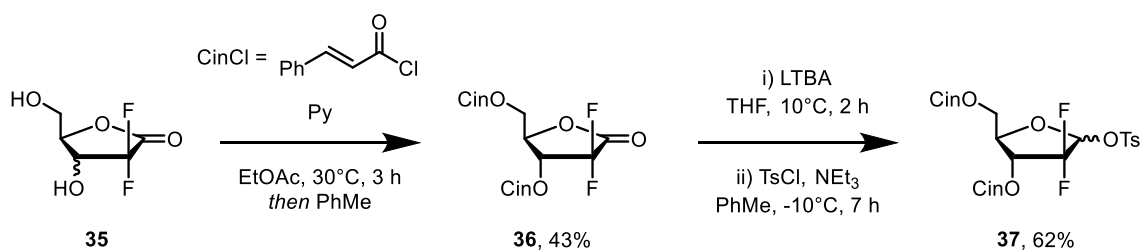
Scheme 1.11: The synthesis of **1** as an anomeric mixture by sequential reduction, glycosylation and deprotection.

The desired β -anomer was selectively crystallised out as the hydrochloride salt firstly by recrystallisation from hot i PrOH, and then triturated with water/acetone (1:12 v/v) mixture. Chou's method demonstrated considerable improvement in the anomeric selectivity of the silyl-Hilbert-Johnson reaction, increasing the ratio of β : α -anomer ratio from 1:4 to near 1:1. The authors noted that regardless of the diastereomeric ratio of mesylate **34** input into the reaction, the near 1:1 β : α -anomer ratio was consistently achieved. This observation was attributed to the reaction profile following a S_N1 mechanism, with an oxocarbenium intermediate, shown in Scheme 1.12. Subjecting α -**1** to the Vorbruggen reaction conditions resulted in no anomerisation and formation of β -**1**, inferring that alteration of the anomeric ratio does not occur post-nucleobase attack.



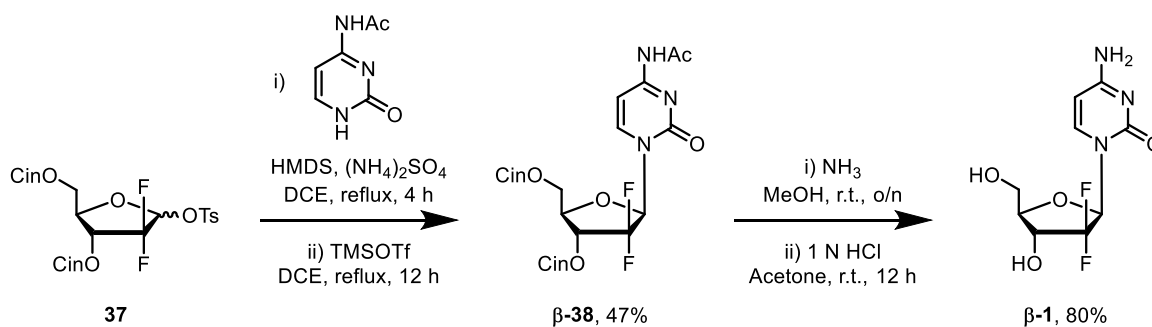
Scheme 1.12: The proposed formation of oxocarbenium **34'** as reactive intermediate.

The approach of using esters for stereospecific crystallisation was capitalised on by Shen and co-workers, who developed a synthetic route which utilised the *trans*-cinnamoyl esters to improve selectivity of the Vorburggen reaction.^[14] Starting from **35** as a mix of *ribo*- and *xylo*- diastereomers following lactonisation,^[8] both 3- and 5-alcohol groups were acylated with *trans*-cinnamoyl chloride with pyridine in ethyl acetate, followed by selective crystallisation of the desired *ribo*- stereomer, delivering **36** in 43% (Scheme 1.13). The diastereomeric ratio of **36** was not disclosed, but Hertel's previous work notes a 3:1 mixture of the desired configuration prior to lactonisation.^[8] Reduction by freshly prepared LTBA in THF and base mediated tosylation of the intermediate lactol produced **37** as a crystalline solid in 62% over two steps. Interestingly, the authors comment that the nature of the base used for the tosylation step directly affects the diastereomeric nature, although no quantification data is given.



Scheme 1.13: The synthesis of crystalline intermediate **37**.

Shen and co-workers found that they obtained a one-to-one mixture of anomers when subjecting **37** to Vorbruggen's reaction conditions, regardless of the diastereomeric ratio of the starting material. Their observation agrees with Chou's previous investigation and conclusion that the reaction likely proceeds via a $\text{S}_{\text{N}}1$ mechanism, delivering β -**38** in 47% yield (Scheme 1.14). Subsequent deprotection of the cinnamoyl esters and acetamide motif furnished pure gemcitabine in 80% yield.



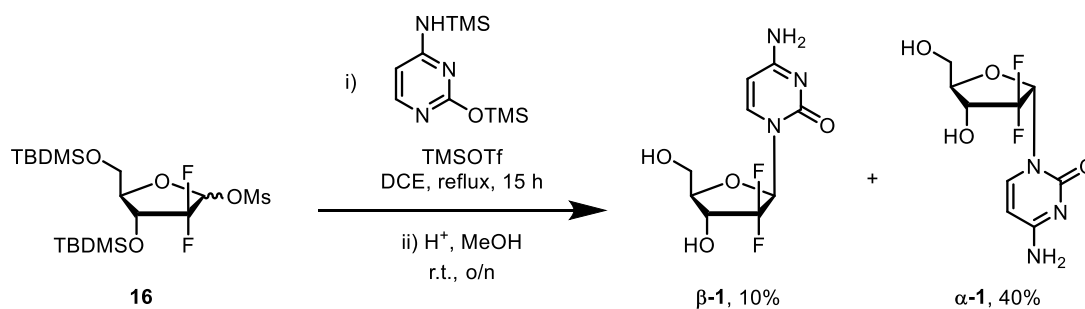
Scheme 1.14: The synthesis of anomerically pure gemcitabine from **37**.

Shen's research demonstrates that employing groups that impart greater crystallinity during the synthesis of the intermediates may allow for enhanced processing by crystallisations, leading to an overall anomerically enriched synthesis.

1.1.1.3 – Leaving group

The Vorbrüggen reaction (also known as the silyl-Hilbert-Johnson reaction) employs nucleobases that are typically protected as their silylated equivalents and used directly for the subsequent reaction with a primed ribofuranose. Of particular note is the lack of selectivity of the desired β -anomer from the silyl-Hilbert-Johnson reaction of ribofuranose **16** and the masked nucleobase. This reaction is more challenging due to the electron withdrawing nature of the geminal difluoro motif adjacent to the anomeric position.

One such factor that may affect the anomeric selectivity is the nature of the leaving group at the anomeric position. Hertel's original synthesis utilised the mesylate leaving group, affording the desired β -anomer in an undesired 1:4 β : α ratio at 50% overall yield, delivering an effective 10% yield of **β -1**, shown in Scheme 1.15.

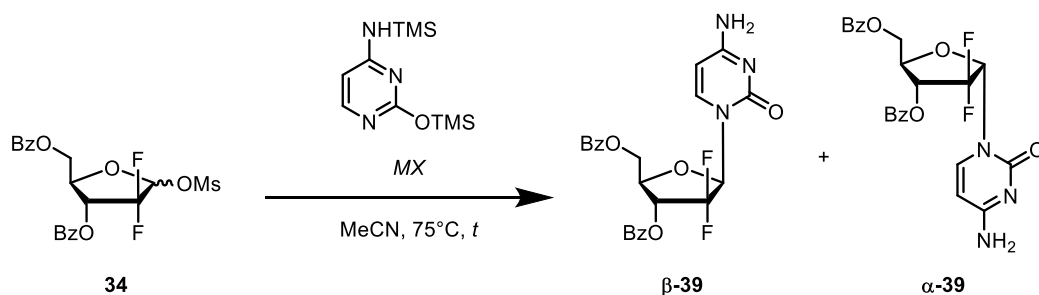


Scheme 1.15: The synthesis of gemcitabine as an anomeric mixture by glycosylation with bis-(TMS)-cytosine.

The role of different Lewis acids was reported in a patent by Kjell, in an attempt to improve β -selectivity, listed in Table 1.01.^[15] Using 2-deoxy-2,2-difluoro-D-ribofuranosyl-3,5-dibenzoyl-1- α -methane-sulfonate as model substrate in combination with bis(TMS)-cytosine, it was shown that the selectivity may be improved simply by using anisole as solvent, delivering 77% yield of an anomeric mixture, favouring the β -anomer in a 3.4 to 1 ratio.

A range of inorganic Lewis acids were subsequently screened and were found to enhance the formation of the desired β -anomer – apart from potassium nonaflate (Table 1.01, Entry 2). One drawback of this methodology was that bis(TMS)-cytosine was frequently used in greater than 10 fold excess, which is not atom economical in a drug development context, but is irrelevant for positron emission tomography (PET) studies. The varying lengths of reaction were not discussed but would presumably be based on consumption of one of the starting materials. In general, there appears to be a trend of

lower yielding reactions delivering improved selectivity (Entries 3-8). Larger cations caesium and barium demonstrated marked β -selectivity with the sulfate salts improving the anomeric selectivity to greater than 90% (Entries 6 and 7), although barium sulfate delivers β -**39** in greater yield. Employing barium triflate yielded **39** in a comparable 25% yield with very good selectivity (Entry 8); however, using caesium triflate significantly improved the yield to 65% while maintaining a high degree of β -selectivity at a ratio of 7.2:1, resulting in a greater than doubling of the effective yield of β -**39** to at 57%. By using potassium carbonate, the yield was slightly improved to 70% (Entry 10), while maintaining β -enrichment.

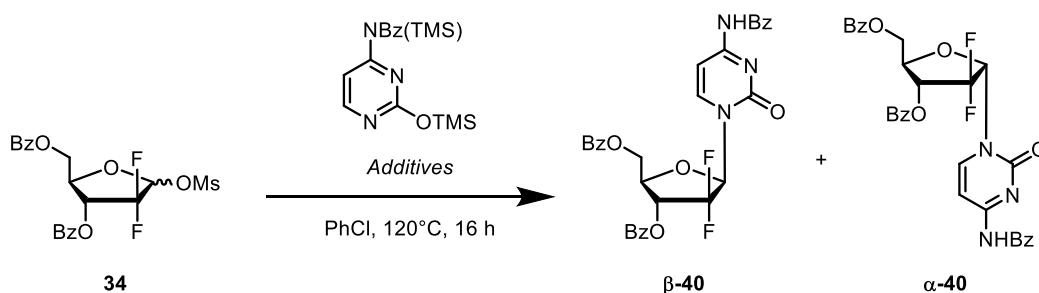


Entry	MX	Time / h	Overall Yield ^[a]	β - 39 : α - 39 Ratio
1 ^[b]	-	20	77%	3.4:1
2 ^[c]	C ₄ F ₉ SO ₃ K	16	33%	3:1
3 ^[c]	K ₂ SO ₄	72	65%	4.7:1
4 ^[d]	KOTf	21	59% ^[e]	6.7:1
5	TBAOTf	4	45%	7.1:1
6	BaSO ₄	20.5	36%	11.2:1
7	Cs ₂ SO ₄	21	24%	14.9:1
8	Ba(OTf) ₂	20.5	25%	14.4:1
9	CsOTf	20.5	65%	7.2:1
10	K ₂ CO ₃	45	70%	7.2:1

^[a] HPLC yield. ^[b] 110°C in anisole. ^[c] 80°C. ^[d] 90°C in propionitrile. ^[e] Isolated yield.

Table 1.01: The influence of various inorganic Lewis acids on the anomeric ratio of **39** from bis-(TMS)-cytosine.

A complementary study was conducted by Liu *et al.*,^[16] in which they screened a range of conditions for the reaction of **34** with bis(trimethylsilyl)-*N*⁴-benzoyl cytosine to form **40** stereoselectively. Initially tin (IV) chloride was employed as stoichiometric Lewis acid in refluxing chlorobenzene and delivered **40** in a combined yield of 43% (Table 1.02, Entry 1). Changing Lewis acid to trimethylsilyl trifluoromethane sulfonate (Entry 2) inverted the anomeric selectivity in preference of α -**40** in a 20:11 fashion, in a slightly lower yield of 44%.



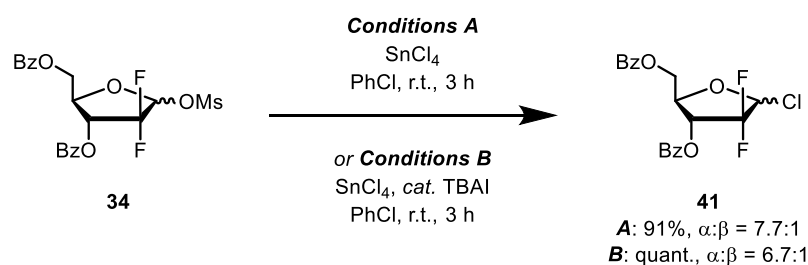
Entry	Additives ^[a]	Yield ^[b]	β - 40 : α - 40 Ratio ^[c]
1	SnCl ₄	43%	4.9:1
2	TMSOTf	44%	11:20
3	SnCl ₄ , <i>cat.</i> TMSOTf	58%	6.3:1
4	SnCl ₄ , <i>cat.</i> TBAOTf	62%	6.7:1
5	SnCl ₄ , <i>cat.</i> TBAC	76%	5.9:1
6	SnCl ₄ , <i>cat.</i> TBAB	68%	6.6:1
7	SnCl ₄ , <i>cat.</i> TBAI	82%	8.0:1
8 ^[d]	SnCl ₄ , <i>cat.</i> TBAI	<5%	-
9 ^[e]	SnCl ₄ , <i>cat.</i> TBAI	43%	1.7:1

2.65 equiv. of silylated nucleobase. **34** α : β = 1.6:1. ^[a] 6 equiv. of SnCl₄/TMSOTf, 8 mol% of *cat.* ^[b] Isolated yield after chromatographic purification. ^[c] Determined by ¹H NMR. ^[d] Bis(TMS)-cytosine used as nucleobase instead. ^[e] 2 equiv. of SnCl₄.

Table 1.02: The influence of various inorganic Lewis acids on the anomeric ratio of **40** from bis-(TMS)-*N*⁴-Bz-cytosine.

Combining the two activators, SnCl₄ and catalytic amounts of TMSOTf, improved both the yield of **40** and the selectivity towards β -**40** (Entry 3). Following from this, a range of alternative tetrabutyl ammonium salts were screened in catalytic quantities (Table 1.02, Entries 4-7).

It was found that their inclusion promoted the selective formation of β -**40** in good yields, with tetrabutylammonium iodide being the most selective and highest yielding (Entry 7). The observed effect could be due to an *in-situ* formation of the 1-iodoribofuranose intermediate, prior to attack of the nucleoside.^[16] Use of non-*N*⁴-functionalised cytosine did not afford the desired product (Entry 8), while decreasing the equivalents of SnCl₄ had a deleterious effect on the reaction.



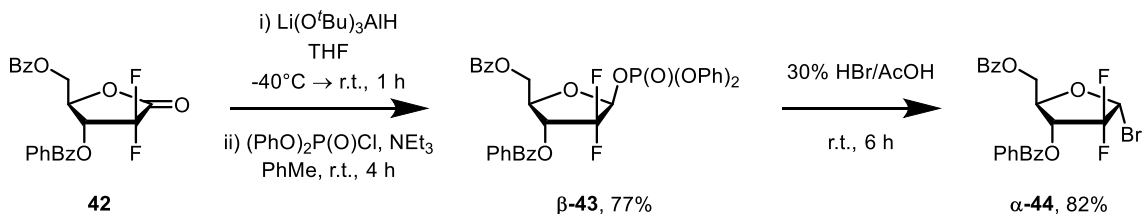
Scheme 1.16: The comparison of conditions for the synthesis of **41**.

Interestingly, they found that treatment of an anomeric mixture of **34** (Scheme 1.16) with tin(IV) chloride generated 1-chlororibofuranose, which may be the active electrophile in the glycosylation reaction. Notably, **41** was formed as the α -anomer predominantly in a ratio of 7.7:1, shown in Scheme 1.16. The inclusion of tetrabutylammonium iodide improved the conversion of the transformation to quantitative, without significantly affecting the anomeric ratio of **41**, again potentially invoking the *in-situ* formation the 1-iodoribofuranose.

The tosyl leaving group has also been employed by Shen and co-workers, as discussed previously,^[14] and while although not shown to improve the anomeric selectivity, did improve the crystallinity of the intermediates synthesised.

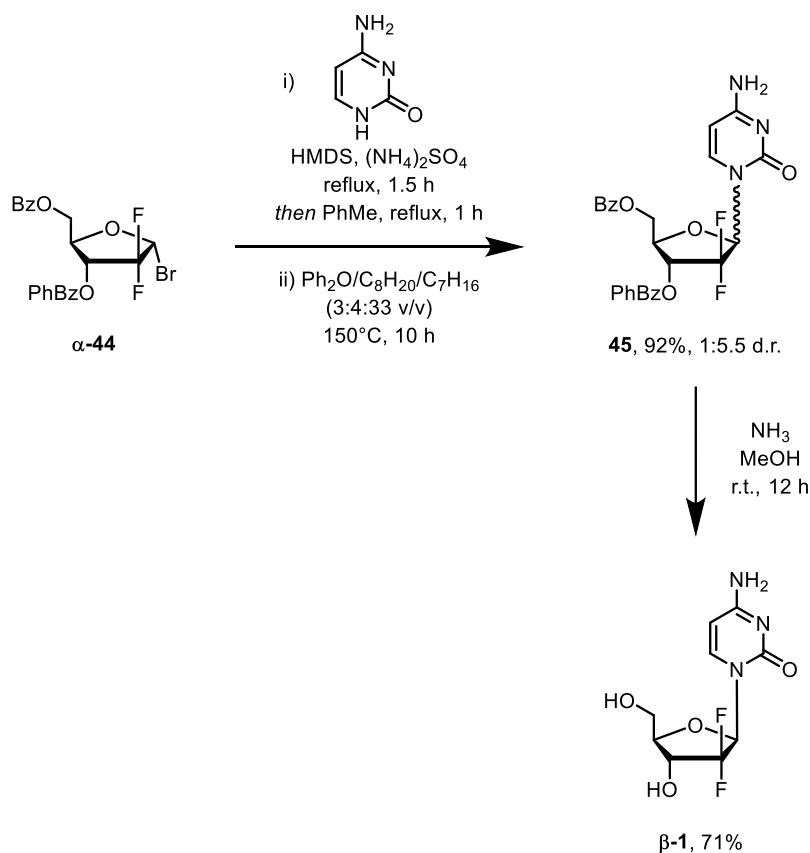
Researchers have also targeted 1-halo-ribofuranose systems directly, and not the apparent *in situ* generation highlighted methodologies previously mentioned. One such example was the work by Chang *et al*, who targeted the 1-bromo-2,2-difluoro-ribofuranose.^[17] Having successfully accessed **42** by adaptation of the Reformatsky style synthesis (not shown), sequential reduction by LTBA and phosphorylation with diphenylphosphoryl chloride in toluene with triethylamine to afforded β -**43** selectively, in

77% yield over two steps and recrystallisation from *i*PrOH/H₂O (3:1 v/v). Treatment of **β-43** with 30% hydrogen bromide in acetic acid delivered an 82% yield of **α-44**, following recrystallisation from isopropanol. The overall transformation is depicted in Scheme 1.17.



Scheme 1.17: The synthesis of **α-44** by sequential reduction, lactol activation and bromination. PhBz = 4-phenylbenzoyl.

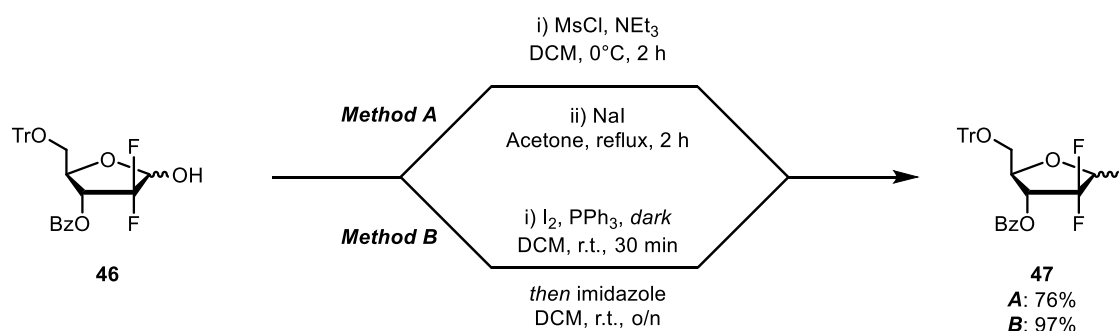
Treatment of **α-44** with bis-TMS-cytosine, using heptane to aid in the distillation of by product TMSBr from the reaction mixture, afforded 92% of **45** as a mixture of anomers, preferentially forming the desired β -nucleoside in a 5.5:1 ratio (Scheme 1.18). Subsequent treatment of **45** with methanolic ammonia cleaved the ester protecting groups, delivering anomerically pure gemcitabine hemihydrate, in 71% yield.



Scheme 1.18: The synthesis of anomerically pure gemcitabine from **α-44**.

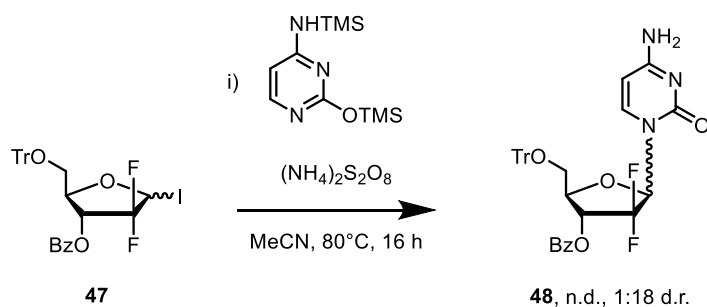
Notably in Chang's work, there seems to be a large degree of S_N2 character to the glycosylation reaction, with a configuration inversion at the anomeric position from pure α -**44** to β -**45** as the major product. This is somewhat contradictory to previous reports which suggest a S_N1 pathway.^[13,14]

One explanation for this observation was described in a patent by Hwang and co-workers, who were targeting the synthesis of gemcitabine via the analogous 1-iodo-2,2-difluoro-ribofuranose,^[18] shown in Scheme 1.19. They achieved the synthesis of **47** by two methods; firstly by sequentially reacting tritylated lactol **46** with mesyl chloride under basic conditions, followed by mesyl displacement by iodide, delivering **47** in 76% yield. Their alternative methodology was an adapted Appel reaction, using iodine and triphenylphosphine in the dark, which yielded 97% of **47**. In both examples, the diastereomeric ratio of the product was omitted.



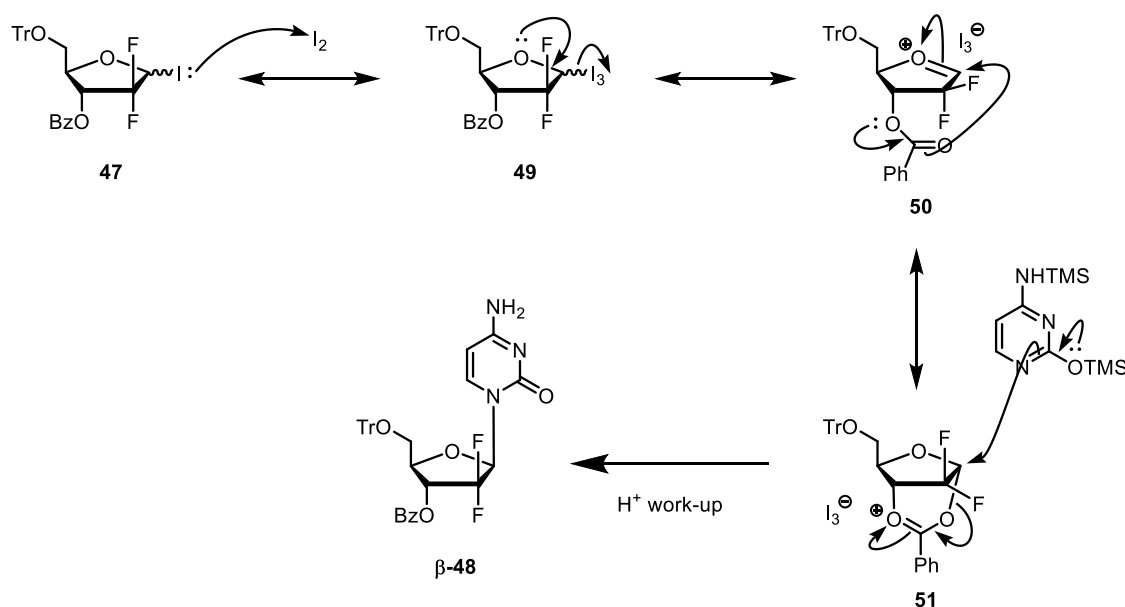
Scheme 1.19: The comparison of synthetic methods for the production of intermediate **47**.

Hwang found that combining iodo precursor **47** with bis-TMS-cytosine (Scheme 1.20) in the presence of ammonium persulfate as oxidant in hot acetonitrile delivered the β -anomer with remarkable selectivity, in an 18:1 fashion over the α -anomer, although no yield was noted.



Scheme 1.20: The formation of **48** by glycosylation reaction of **47**.

The impressive selectivity was attributed to the involvement of the 3-O-benzoyl group, in a process that may be described as neighbouring group participation. Illustrated in Scheme 1.21, 1-iodo-ribofuranose **47** may attack iodine, which is generated *in situ* by the oxidation of iodide by persulfate, following iodide exclusion from **47**. Subsequent formation of oxocarbenium intermediate **49** by triiodide displacement facilitates attack of the carbonyl oxygen of the 3-O-benzoyl motif onto the 1-position, forming an alternative 6-membered oxocarbenium intermediate, which provides an additional stabilising resonance form (**50**). Attack of bis-TMS-cytosine onto intermediate **51** results in breaking the charged heterocycle and reforming the benzoyl group, yielding β -**48**. The anchimeric assistance of the 3-O-ester group helps selectively form the beta anomer of **48**. This mechanistic proposal would also support Chang's observation,^[17] as their glycosylation substrate contains a 3-O-ester group that could be involved in a neighbouring group participation style process.

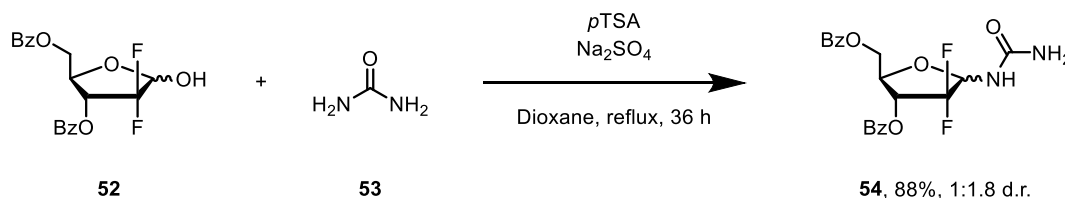


Scheme 1.21: The proposed reaction mechanism explaining the observed anomeric selectivity when using **47**.

1.1.1.4 – Pyrimidine ring formation

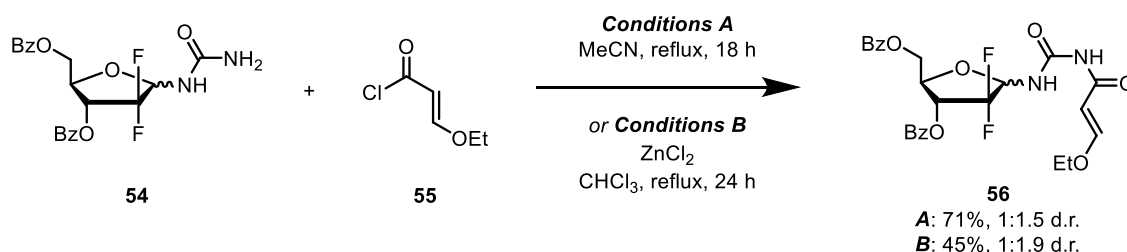
While construction of the ribofuranose ring is critical for the introduction of the geminal difluoro motif, less attention is paid to the construction of the pyrimidine ring. One of the primary reasons for this is that the ring may be easily accessed and installed from a protected cytosine. If a complementary methodology were realised offering improved anomeric selectivity, it would be a useful tool.

Linclau and co-workers investigated the construction of the pyrimidine ring beginning from commercially available lactol **52**.^[19] Treatment of **52** in combination with urea in the presence of *para*-toluenesulfonic acid and dehydrating sodium sulfate delivered **54** in 88% yield after 36 hours of reflux (Scheme 1.22).



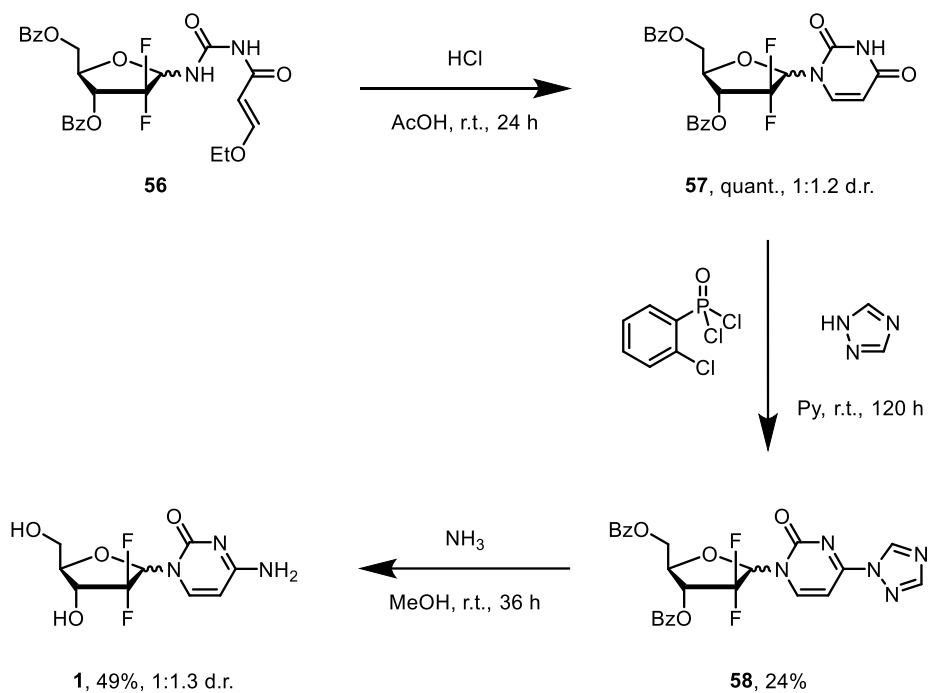
Scheme 1.22: The formation of urea-derivative **54** from **52** and urea.

The ratio of diastereomers of **54** was noted, but the relative assignment wasn't possible. Taking **54** as a mixture forward, reacting it with acyl chloride **55**, furnished urea derivative **56** in 71% yield in a lower anomeric ratio. The anomerisation was attributed to ring opening of the ribofuranose by deprotonation of the urea motif, aided by the electron withdrawing difluoro moiety. Switching solvent to chloroform and use of zinc chloride as Lewis acid aided in maintaining the anomeric ratio from before, albeit, with a diminished yield of 45%, shown below in Scheme 1.23.



Scheme 1.23: The synthesis of *N*-acrylurea derivative **56**.

Acid mediated ring closure yielded uracil congener **57** quantitatively, with diminished anomeric ratio. Subsequent treatment with 2-chlorophenyl phosphorodichloridate as chlorinating agent and 1,2,4-triazole for 5 days at ambient temperature in pyridine furnished 24% of impure **58**, which was then treated with methanolic ammonia for 36 hours to produce gemcitabine in 49% yield as a mixture of anomers (Scheme 1.24).

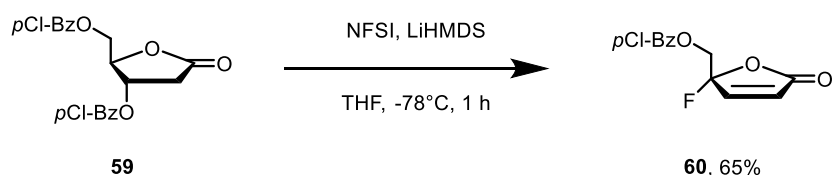


Scheme 1.24: The acid-promoted ring closure of **56**, chlorination and 1,2,4-triazole attack for intermediate **57**, and ammonia-mediated transformation for the synthesis of **1**.

1.1.2 – Ribonolactone halogenation

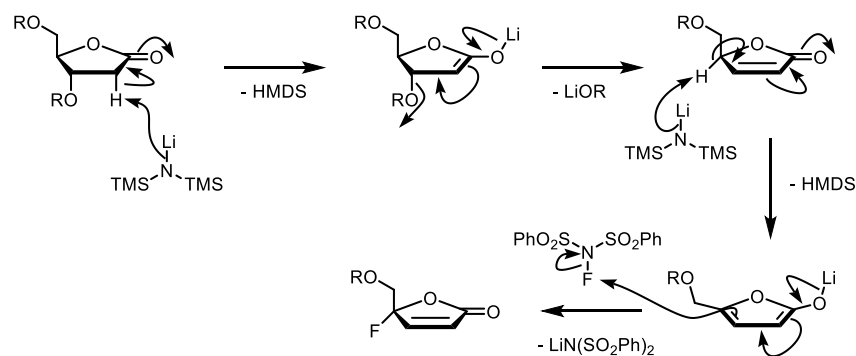
One potential drawback of the aforementioned methodologies is the installation of the geminal difluoro moiety from an early stage by Reformatsky reaction. Modification of this strategy to include alternative halogens is unattractive given the susceptibility of other halogens to partake in zinc-based reactions. The opportunity to functionalise a mono- and di-fluorinated analogue of intermediate ribonolactone **61** was realised by Cen and Sauve, from protected 2-deoxy-D-ribonic acid-1,4-lactone.^[20] They were investigating the diastereoselective fluorination (and difluorination) of γ -lactones, accessed via enolate chemistry and appropriate electrophilic halogenating reagents. This methodology allows for installation of the desired motif via two succinctly different steps, which arguably may not be as efficient but allows for tunability and modification – which is a key attribute when designing the synthetic route of a radiolabelling precursor and associated derivatives for PET studies.

Their preliminary findings, employing *para*-chloro-benzoyl ester protecting groups – which have previously found extended use in the synthesis of similar ribonolactones – had a deleterious effect on the reaction. Initial α -fluorination of **59** was attempted utilising NFSI and LiHMDS, which yielded the α,β -unsaturated γ -lactone, fluorinated at the 4- position (Scheme 1.25).



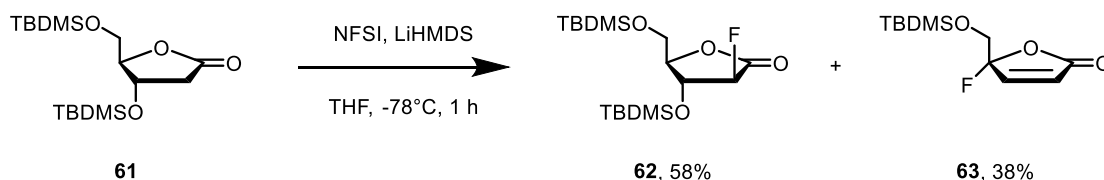
Scheme 1.25: The fluorination/elimination of **59** by NFSI and LiHMDS.

The formation of the α,β -unsaturated- γ -fluoro- γ -lactone can be explained when considering the mechanism of the reaction (Scheme 1.26). Basic LiHMDS deprotonates the most acidic proton, at the alpha position of the lactone, to form the lithium enolate, which then cascades in an E1cB fashion, eliminating an alkoxide from the 3- position of the tetrahydrofuran ring. A second equivalent of LiHMDS can subsequently deprotonate at the γ -position of the α,β -unsaturated lactone, funnelling through to the lithium 1,2-3,4-dienolate, which in turn will cascade back around the ring to pick up the electrophilic fluorine from NFSI at the γ -position. The observation was further rationalised by considering the pK_a of the conjugate acid of the carboxylate (*c.f.* pK_a [H₂O] \approx 4).

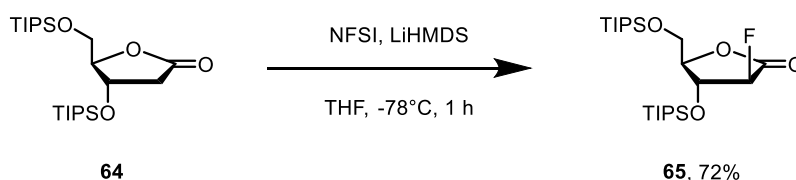


Scheme 1.26: A proposed reaction mechanism for the formation of **60**. R = *p*Cl-Bz.

Consequently, alternative protecting groups were explored – which may be conveniently accessed from commercially available 2-deoxy-D-ribo-1,4-lactone. Therein switching to TBDMS protected alcohols, mono-fluorinated product **62** was successfully synthesised in 58% yield under the same reaction conditions. Unfortunately, 38% of the equivalent α,β -unsaturated- γ -fluoro- γ -lactone was also obtained, shown in Scheme 1.27. While demonstrating an improvement on their previous methodology, unwanted side reactions remained an issue.



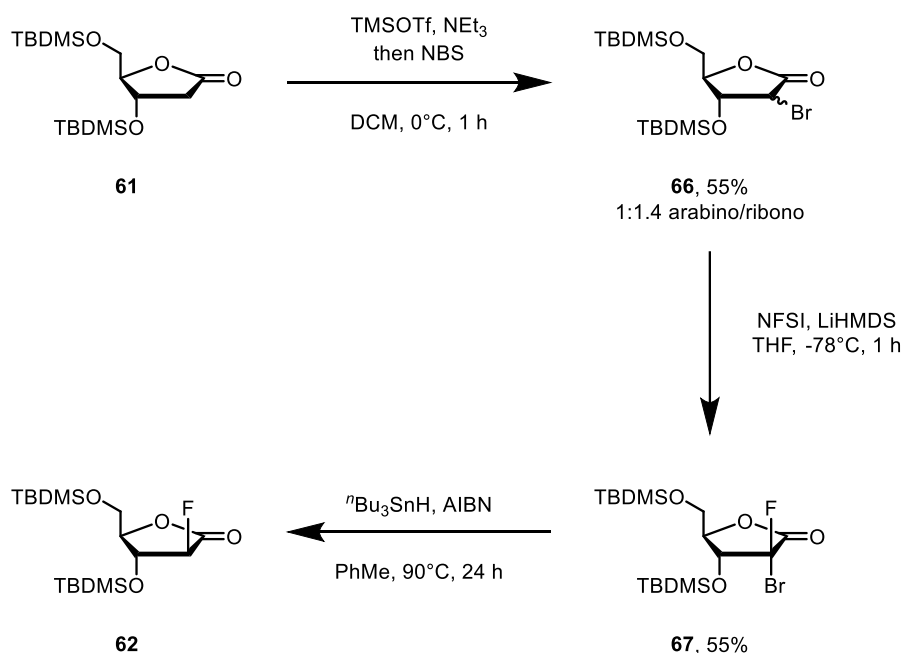
Scheme 1.27: The mixture of products obtained by reacting **61** with NFSI and LiHMDS.



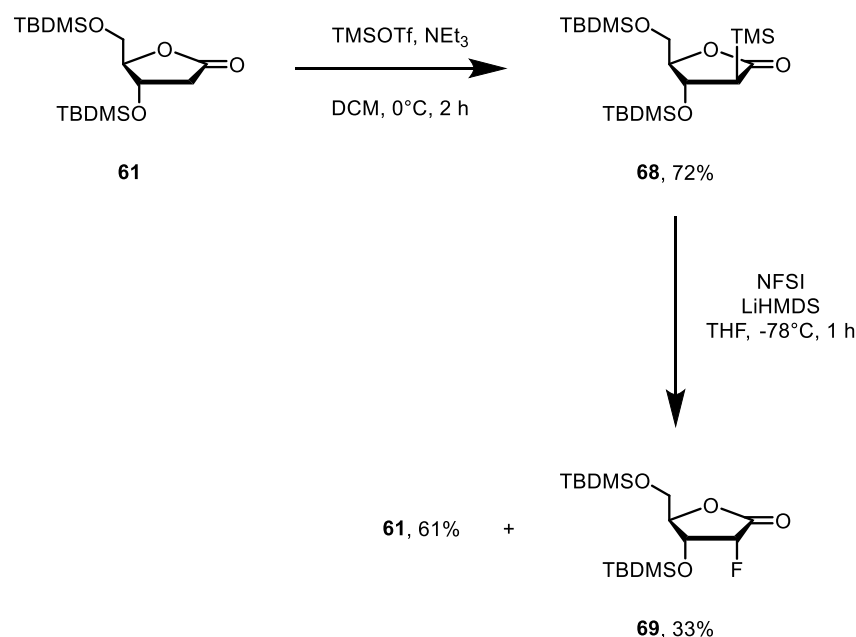
Scheme 1.28: The diastereoselective fluorination of **64** by NFSI and LiHMDS.

The alternative reactivity was circumvented using bulkier triisopropylsilyl protected alcohols, in which no eliminated product was detected, isolating the α -fluorinated lactone **65** in 72% yield in diastereoselective fashion (Scheme 1.28). This was attributed to a less favourable leaving group (pK_a of silanol ≈ 11 ^[21]), and the bulky silyl ether inducing a puckered ring conformation to minimise steric interactions. The puckered conformation also enforced a geometry whereby elimination of the silanoate would be reduced.^[20]

Alternatively, **68** may also be accessed via a circuitous 3-step strategy shown in Scheme 1.29 – although the author's goal was to access the ribono stereoisomer. Initially, lactone **61** was sequentially treated with triethylamine and TMSOTf, then NBS to furnish a diastereomeric mixture of α - brominated lactone **66** in 55% isolated yield. Fluorination of **66** by treatment with NFSI and LiHMDS delivered **67** as a single diastereomer, in 55% yield. Use of catalytic azobisisobutyronitrile as radical initiator and tributyltin hydride for the radical bromide abstraction of **67** yielded only arabino **68**, although no yield for the final product was reported.



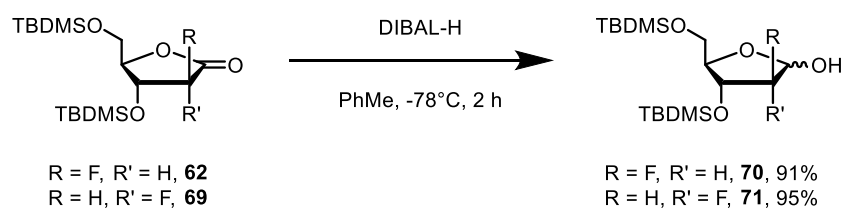
Scheme 1.29: The three-step strategy towards the synthesis of arabino **61**.



Scheme 1.30: The two-step strategy towards the synthesis of ribono **69**.

Synthesis of the ribono stereoisomer **69**, illustrated by Scheme 1.30, was achieved by treating protected lactone **61** with NEt_3 and TMSOTf to yield intermediate **68** in 72% yield. Reacting **68** with NFSI and LiHMDS yielded 33% of **69**, but also 61% of initial starting material **61** was recovered and may be reused.

With both mono-fluorinated diastereomers in hand, DIBAL mediated reduction afforded the corresponding lactol (Scheme 1.31) in excellent yields.

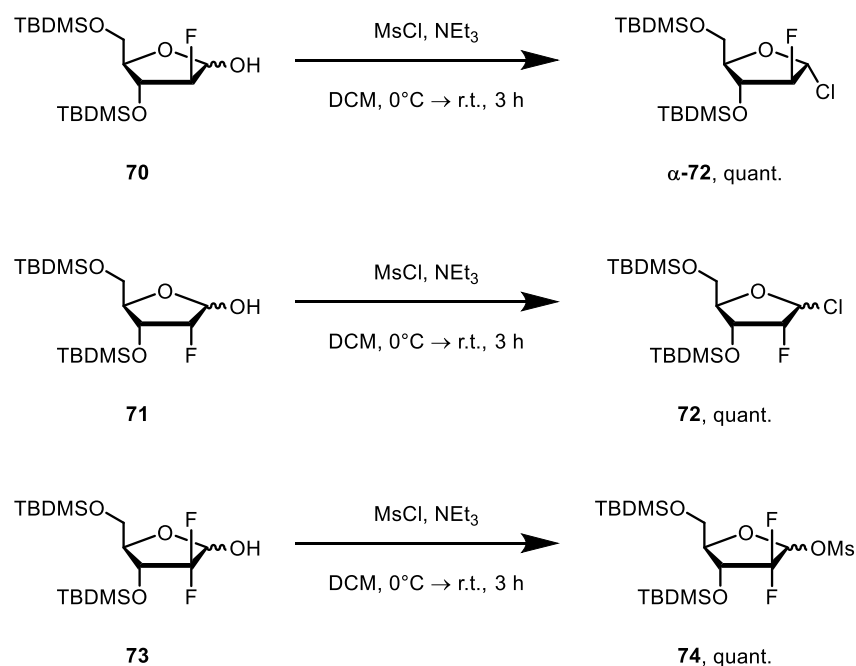


Scheme 1.31: The reduction of diastereomers **62** and **69** by DIBAL-H.

Subsequent treatment of **70** with MsCl and triethylamine quantitatively yielded the chlorinated furanose solely as the α - anomer (**72**, Scheme 1.32). Similarly, reacting **71** with NEt_3 and MsCl yielded chlorinated ribofuranose in quantitative yield, this time as an anomeric mixture. By comparison, reacting difluororibolactol **73** under the same conditions delivered the *O*-mesyl compound. This observation was ascribed to a

deactivation of **73** by the geminal difluoro motif towards chlorination, not observed in the cases of **70** and **71**.

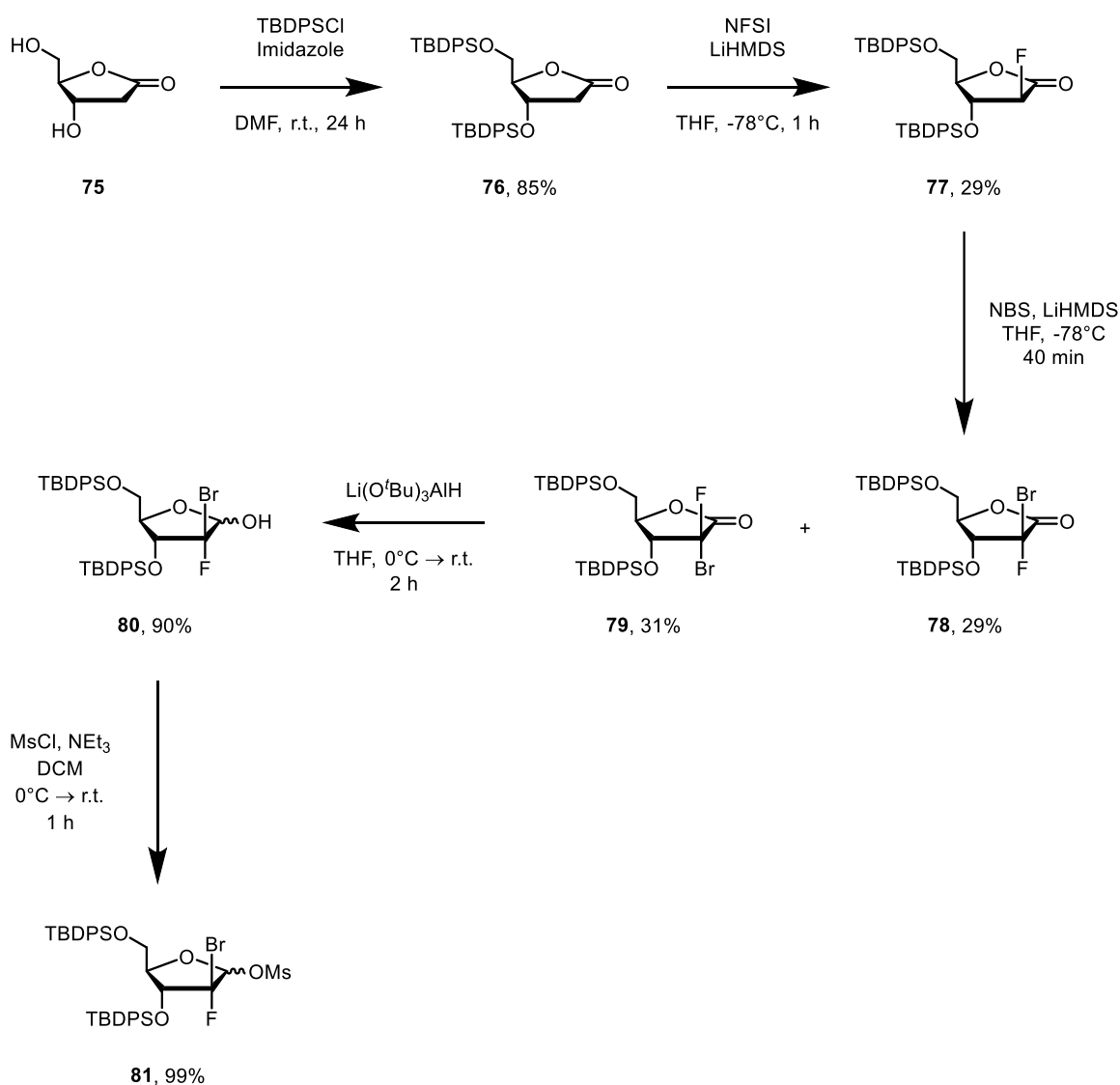
Crucially, Cen and Sauve demonstrated that diastereocontrolled α -fluorination of suitably protected lactones was possible, while also illustrating the potential for alternative halogens to be introduced.



Scheme 1.32: The mesylation of **70**, **71** and **73** under basic conditions delivering different compounds depending on configuration at the 2-position of the lactol.

1.1.2.1 – Mixed halogen ribofuranoses

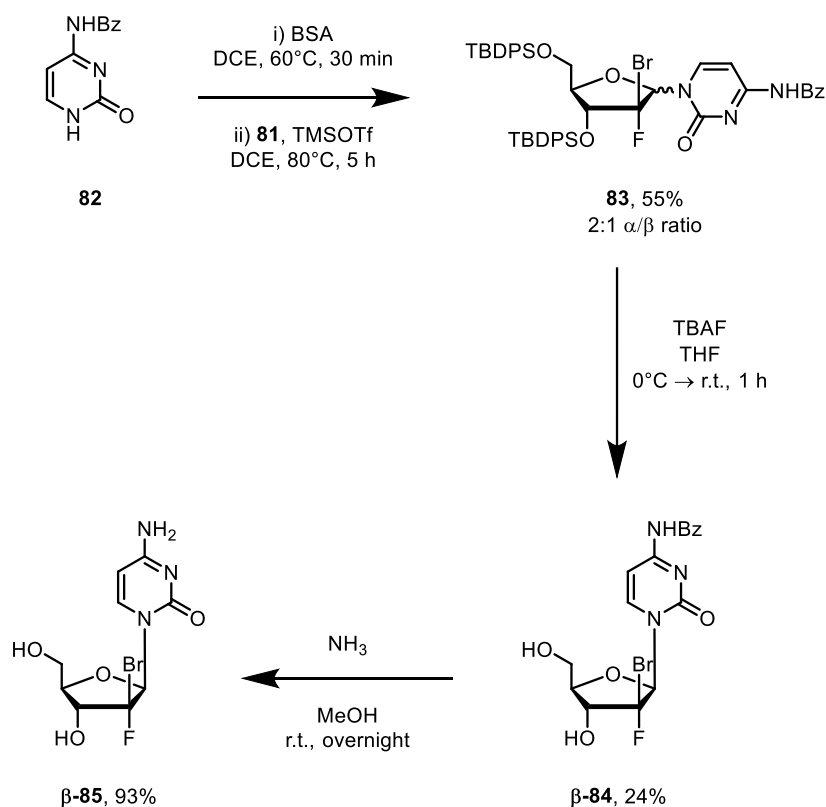
Following Cen and Sauve's seminal work, Schinazi and co-workers reported the synthesis of 2'-bromo-2'-fluoro-nucleosides, in their phosphoramidate Protide form (discussed later), as pharmaceutical agents for the treatment of hepatitis C virus (HCV).^[22] The utilised strategy related to that developed by Cen and Sauve, whereby they initially protected 2-deoxy-D-ribose-1,4-lactone **75** using TBDPSCI and imidazole in DMF to furnish silyl ether **76** in 85% yield (Scheme 1.33). Combining **76** with NFSI and LiHMDS furnished 29% of the protected 2-fluoro arabinolactone **77** in a low yielding reaction.



Scheme 1.33: The synthesis of bromo-fluoro intermediate **79** from 2-deoxy-D-ribose-1,4-lactone (**75**) by fluorination-bromination strategy.

Subsequent treatment with NBS and LiHMDS yielded a near one-to-one diastereomeric mixture of the geminal dihalogenated γ -lactone (**78** and **79**). Taking the desired β -diastereomer forward (**79**), reduction by lithium tri(*tert*-butoxy)aluminium hydride effectively delivered lactol **80**, before quantitative mesylation to produce **81**.

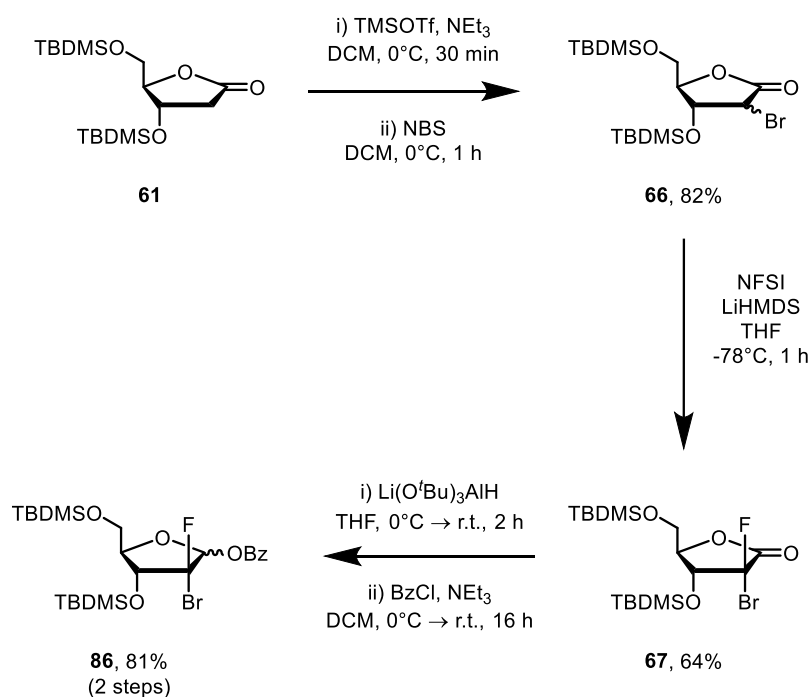
Notably the activated lactol is observed as the *O*-mesyl compound thus agreeing with Cen and Sauve's observation that adjacent geminal dihalogenated ribofuranoses preferentially form compounds akin to **74** (Scheme 1.32), and not the chlorinated congener. A drawback of this strategy is evident in the product yields for the fluorination and bromination steps, with both returning target materials at isolated yields less than 30%, equating to an 8% across two steps.



Scheme 1.34: The synthesis of anomerically pure **85** from **81**.

Treating activated lactol **81** with *in situ* silylated *N*⁴-benzoyl cytosine furnished the Vorbruggen product **83** in a combined yield of 55%. Subjecting the anomeric mixture to deprotection by TBAF delivered 24% of **84** as the pure β -epimer (Scheme 1.34). Subsequent removal of the benzoyl protecting group by methanolic ammonia produced **85** in excellent yield.

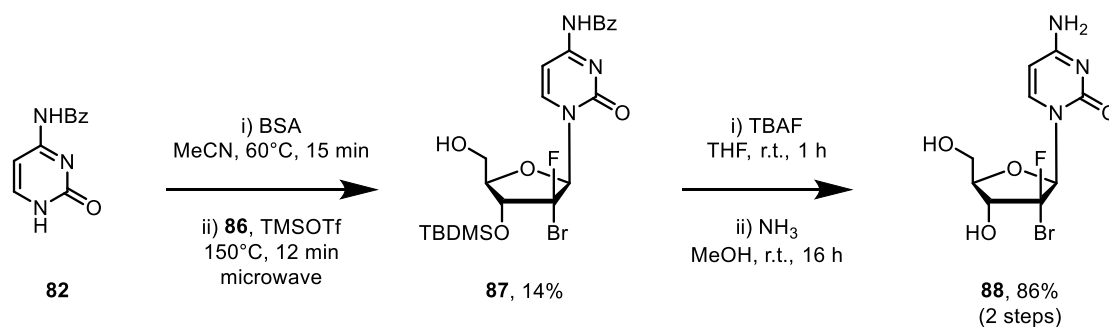
Following this, Schinazi and coworkers changed tact targeting the alternative diastereomer, in order to evaluate its cytotoxicity against HCV.^[23] Similarly, they commenced from a silyl ether protected ribonolactone (**61**, Scheme 1.30) only this time brominated first prior to electrophilic fluorination to yield **67** as the sole diastereomer, in yields of 82% and 64% respectively (Scheme 1.35). Formation of the primed lactol was achieved via sequential reduction of **67** by LTBA and activation by benzoyl chloride delivered **86** in 81% across two steps. This approach illustrated that activated lactol **86** could be achieved in 43% over 4 steps from **61**, with good yields across the board.



Scheme 1.35: The synthesis of α -bromo- β -fluoro intermediate **86** from **61** by bromination-fluorination strategy.

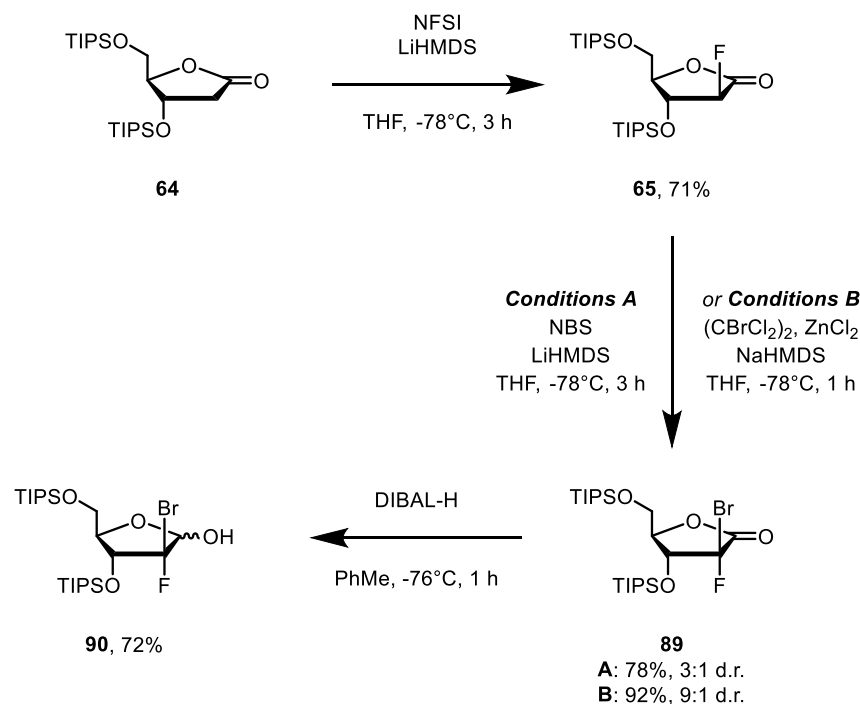
As previously, appending **86** with *N*²-benzoyl cytosine in the presence of TMSOTf under microwave irradiation yielded **87** as the coupled product, isolated as the pure β -anomer, which somewhat surprisingly had been deprotected during the Vorbruggen reaction. This observed reactivity was accredited due to increased reaction times, under microwave conditions. Like their previous report, the undesired α -epimer was formed preferentially in a 2:1 ratio.

Complete removal of the silyl ether protecting group mediated by fluoride, followed by benzoyl removal to produce free nucleoside **88** in 86% yield over two steps (Scheme 1.36).



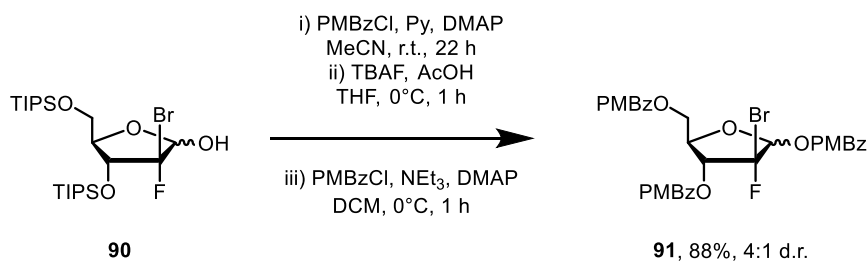
Scheme 1.36: The synthesis of 2'-deoxy-2'- α -bromo-2'- β -fluorocytidine (**88**).

Related to work conducted by Schinazi and co-workers, Voight *et al* were simultaneously investigating 2'-bromouridine derivatives for HCV treatment.^[24] Shown in Scheme 1.37, their synthetic strategy was closely connected, where **64** was treated with NFSI and LiHMDS to deliver 71% of **65** as a single diastereomer, as observed previously – although inconsequential. Initially, electrophilic bromination was successfully achieved through NBS and LiHMDS (conditions A, Scheme 1.37) to generate **89** in 78% as an inseparable diastereomeric mixture, in favour of the desired α -fluoro- β -bromo-configuration intermediate lactone **90**. Changing the source of electrophilic bromine to dibromotetrachloroethane with zinc chloride not only increased the reaction yield to 92% but crucially the diastereoselectivity. The authors state that the inclusion of ZnCl₂ delivers an *in situ* zinc enolate intermediate, manifesting an improved selectivity. Conversion of **65** produced *via* conditions B of Scheme 1.37, to lactol **90** by DIBAL-H proceeded well in 72% yield.



Scheme 1.37: The synthesis of α -fluoro- β -bromo intermediate **90** from **64** by fluorination-bromination strategy.

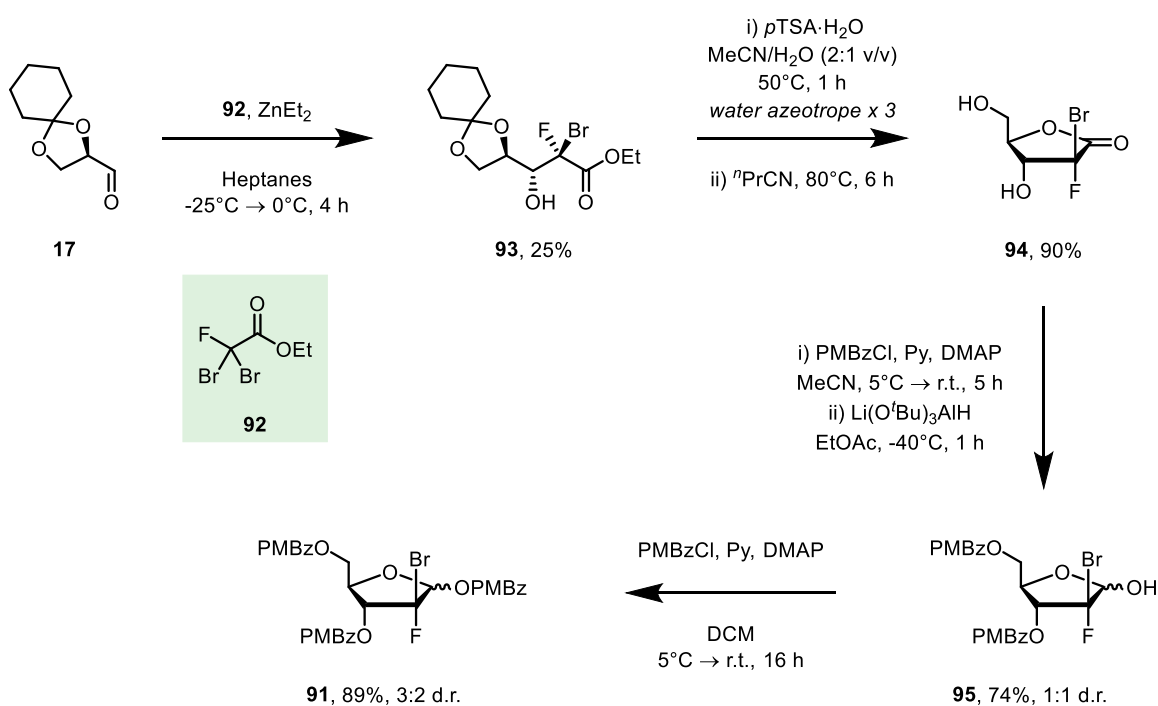
After initially attempting activation and glycosylation through benzoylation and reacting with *in situ* silylated *N*⁴-Bz-cytosine, the desired β -anomer of the intermediate was delivered only in 5% yield, in a 1:9 ratio of the β : α epimers. Alternatively, changing the protecting groups and lactol leaving group was explored, whereby use of the same motif for both the leaving group and protecting groups facilitated a cleaner reaction. As such, reacting lactol **90** with *para*-methoxybenzoyl chloride, followed by deprotection by TBAF and reprotection as the PMBz esters yielded **91** in 88% over 3 steps (Scheme 1.38).



Scheme 1.38: The activation of lactol **90** by *para*-methoxybenzoyl chloride, TBAF deprotection and reprotection with *para*-methoxybenzoyl chloride to form **91**.

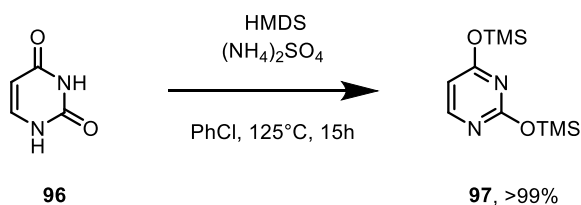
The authors contextualise the synthetic strategy towards forming **85**, shown in Scheme 1.34, as impractical on multi-kilogram scale, given the need for two cryogenic reaction steps for the key halogenation steps and purification by column chromatography. Additionally, the use of TIPS as hydroxyl protecting groups – key for the halogenation reactions – was inefficient as they required replacement prior to glycosylation, in order to afford a cleaner reaction profile.

Much like Hertel's original synthesis, the second strategy (Scheme 1.39) towards construction of **85** began with a protected glycer aldehyde (**17**), in combination with ethyl dibromofluoroacetate and ZnEt_2 as zinc source, delivering **93** as a single diastereomer in a low 25% yield. Although selectivity was poor, the product could be separated effectively by crystallisation – a factor critical in the choice of the cyclohexylidene ketal as protecting group, as other protecting groups investigated were non-crystalline. Deprotection of cyclohexylidene ketal **93** by *p*TSA in acetonitrile/water mixture delivered triol ester as an intermediate. The hydrolysis was driven to completion by azeotropic distillation of the reaction mixture to remove by-product cyclohexanone. Lactonisation in butyronitrile delivered crude **94**, purified by crystallisation from chlorobenzene and DCM as antisolvent, affording hydrolytically unstable lactone **94** in 90% yield.



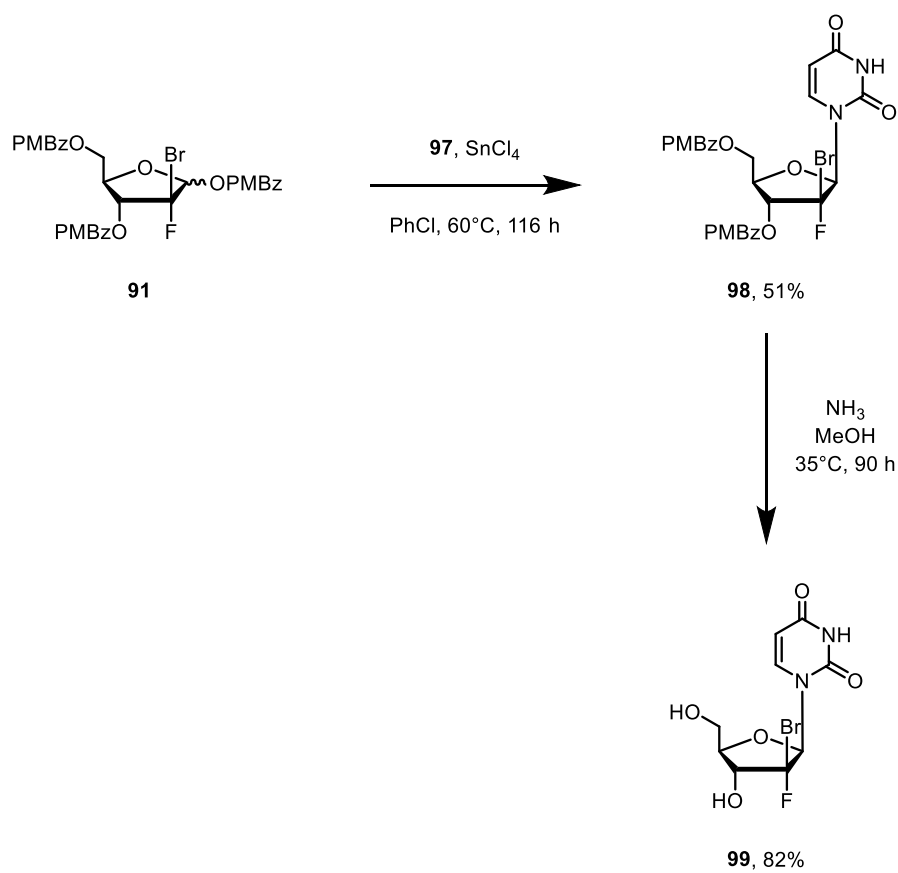
Scheme 1.39: The activation of lactol **95** by *para*-methoxybenzoyl chloride, TBAF deprotection and reprotection with *para*-methoxybenzoyl chloride to form **91**.

Protection of **94** with *para*-methoxy benzoyl chloride, catalytic DMAP and pyridine as base, followed by reduction by LTBA yielded 74% of lactol **95**, in a 1:1 ratio of diastereomers. Reacting **95** with *para*-methoxy benzoyl chloride delivers activated lactol **91** in 89% yield, as 3:2 mix of anomers. An important aspect of the developed methodology illustrated in Scheme 1.39 is the purification of the intermediates by crystallisation (where possible) – **95** crystallised from heptanes/EtOAc, and **91** from *i*PrOH – avoiding purification by column chromatography.



Scheme 1.40: The protection of uracil by HMDS with catalytic ammonium sulfate to form **97**.

Prior to glycosylation, uracil (**96**) was protected using HMDS as TMS source with catalytic ammonium sulfate in chlorobenzene to form **97** quantitatively (Scheme 1.40). The resulting *bis*-TMS uracil derivative was reacted with **91** under Vorbruggen like conditions to yield **98** selectively in 51% yield. The researchers evaluated the parameters and conditions of the glycosylation reaction, revealing that lower temperatures reduced **97** reacting with a second equivalent of **91**. Consequently, reaction time was increased to allow the reaction to proceed to completion. Omitting TMSOTf from the reaction mixture produced the cleanest reaction profile, using tin(IV) chloride as the sole Lewis acid. Subsequent deprotection yielded 2'-deoxy-2'- α -fluoro-2'- β -bromouridine (**99**, Scheme 1.41) in 82% isolated yield.



Scheme 1.41: The glycosylation of **91** with **97** and ammonia deprotection to yield 2'-deoxy-2'- α -fluoro-2'- β -bromouridine (**99**).

1.1.3 – Gemcitabine prodrug and ProTide strategies

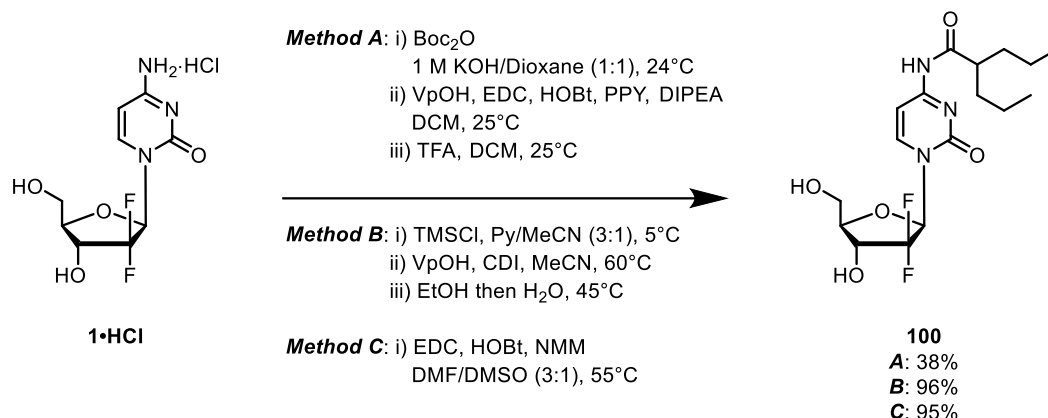
As previously mentioned, one of the issues with the efficacy of gemcitabine is its hydrophilicity and hence poor uptake into fatty pancreatic cells. As such, substantial efforts have been made in order to improve the compound's lipophilicity hence it's bioavailability. Additionally, high dose treatments of orally delivered gemcitabine has been found to increase the risk of hepatotoxicity and gastrointestinal toxicity likely due to lack of selectivity in targeting specific areas of the body.

From a PET perspective, the application of this approach would also be attractive as improved bioavailability would allow for the radiolabelled agent to target the problem area with improved effectiveness and at shorter times. Moreover, utilisation of ^{18}F PET would also offer an excellent diagnostic tool in drug development in candidate therapeutic agents and screening patients.

1.1.3.1 – LY2334737

One such example is that investigated by Eli Lilly, who focussed on modifying gemcitabine at the N^4 position on the cytidine ring.^[25] They targeted an amide linker in order to circumvent the deleterious effect of dCDA, while the functionality would also remain stable under enzymatic and chemical hydrolysis conditions. The compound investigated by Bender *et al* contained a valproamide moiety, and was coined LY2334737 (**100**, Scheme 1.42). The prodrug is hydrolysed by enzyme carboxylesterase 2 (CES2) to liberate the active agent (pre-phosphorylation) and valproic acid.

The synthetic methodologies discussed always commenced from gemcitabine (hydrochloride) and explored 3 different routes by which to synthesise **100** (Scheme 1.42). The first route appended valproic acid to a *bis*-Boc protected gemcitabine^[26] using EDC coupling conditions, prior to TFA mediated deprotection to afford LY2334737 in 42% yield over 2 steps (38% over 3 steps). Alternatively, utilising CDI and valproic acid with a *bis*-TMS protected intermediate yielded 96% of **100** after work up. Interestingly, a synthetic route was developed that avoided using protecting groups, by switching solvent system and employing peptide coupling conditions (EDC, HOBt, NMM), producing **100** in excellent yield (95%). Their preliminary results demonstrate that LY2334737 is highly stable to both chemical hydrolysis, by investigating stability under a range of pHs, and enzymatic hydrolysis against small intestine homogenates.



Scheme 1.42: The different synthetic routes towards LY2334737 (**100**) from gemcitabine hydrochloride developed by Eli Lilly.

Having successfully synthesised **100**, it was screened against human colon HCT-116 cells in mice and was found to overcome deamination by dCDA and display comparable tumour reduction (% vehicle) to gemcitabine.

Further Phase I studies then commenced using LY2334737, in order to ascertain maximum tolerated dose (MTD) and dose limiting toxicities (DLTs) of the orally taken compound. The MTD of **100** was found to be 40 mg, as a standalone treatment or a combination therapy with erlotinib.^[27] Schellens and co-workers noted that only 2 out of 65 European patients suffered hematologic toxicity – a principal DLT observed when patients are treated with gemcitabine. This observation was attributed to a lower effective gemcitabine concentration over the course of LY2334737 administration vs intravenous gemcitabine regimes. It was also mentioned that dFdU was observed over the course of **100** regime, but 0.75 fold lower than gemcitabine over a two week treatment course demonstrating a marked improvement.^[27]

A second European study focussed on the potential to increase the MTD limit as the recommended dosage ahead of Phase II trials of patients with advanced/metastatic solid tumours.^[28] 3 Patients exhibited DLTs when the dose level was increased to 100 mg; therefore 90 mg for a 21 day dose regime (followed by 7 days rest) was considered the new MTD. The new dosage was found to display linear pharmacokinetics and safety profiles of a sufficient standard. Raymond and co-workers also reported that administration schedules played a role in DLTs exhibited, in agreement with other literature findings,^[27–29] where administering the drug every other day (QD treatment) led to less DLTs.

Further studies investigated the MTD and found ethnicity to be a factor. Tamura and co-workers found that the MTD was lower for their work, carried out on 13 Japanese patients with advanced or metastatic solid tumours.^[29] Alarming, 3 out of 4 patients on the 40 mg course suffered DLTs such as hepatic toxicities and disseminated intravascular coagulation when on a QD treatment course. It was found that 30 mg was the MTD cut off point, attributed to lower body surface area that Japanese patients possess leading to increased area under the curve (AUC). In Tamura's studies, the mean AUC of LY2334737 was 328 ng.h mL⁻¹, compared to 244 ng.h mL⁻¹ in Schellens' work – although it is noted that clinical relevance of these findings is unclear.

A concurrent Phase 1b study by Adjei and co-workers into a combinative QD therapy of LY2334737 and capecitabine was halted due to Tamura's findings,^[30] resulting in the MTD not being established for the investigated combination regime. They noted that QD administration of LY2334737 for 21 days, followed by 7 days rest, is not optimal for risk/benefit ratio.

Further Phase 1 investigation by Llombart and co-workers looked into using docetaxel in conjunction with **100**, revealing a 30 mg QD regime of **100** and 70 mg of docetaxel gave rise to a detrimental toxicity profile, leading to an eventual MTD of 10 mg day⁻¹. Their finding infers a negative effect of docetaxel, despite its successful combination with gemcitabine,^[31] although no reason is offered for the observed impact. Llombart's work was also suspended following Tamura's findings, which ultimately led to further trials into LY2334737 being discontinued.

1.1.3.2 – NUC-1031 and ProTide strategies

Alternatively, improved cell membrane permeation of gemcitabine has been targeted via pre-installation of a phosphate group at the 5' hydroxyl group of the compound. Converting the nucleoside to a monophosphate nucleotide overcomes the rate limiting step of initial phosphorylation by dCK, which in turn reduces deleterious conversion to dFdU. This strategy was termed ProTide and pioneered by McGuigan and coworkers.^[7,32] However, introduction of the 5'-O-monophosphate derivatives would be ineffective, showing poor efficacy due to their negative charge under physiological conditions and may be prone to dephosphorylation. As such, the ProTide strategy underwent a period of refinement and found that aryloxy phosphoramidates demonstrate the greatest selectivity for uptake into cells. These derivatives were chosen due to their tunability, illustrated in Figure 1.04 with 3'-azido-3'-deoxythymidine as the nucleoside core. The modular components can be broken down into three distinct areas:

- i. Carboxyl ester – modified to increase cellular uptake, by using lipophilic groups such as benzyl or 2-naphthyl. It was noted; however, that it is critical to balance the improved uptake with efficient ester hydrolysis *in vivo*; use of *tert*-butyl esters increased incorporation into cells but was resistant to hydrolysis by PLE.^[33] Other esterases (such as cathepsin A) have been found to play a predominant role in hydrolysing the ester to the acid congener.^[34]

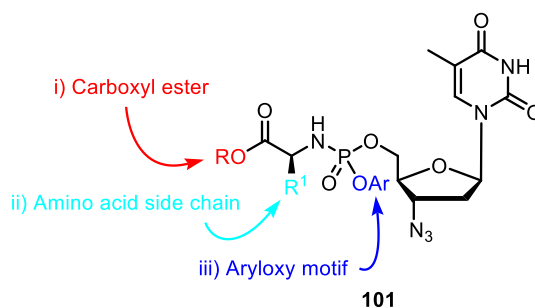
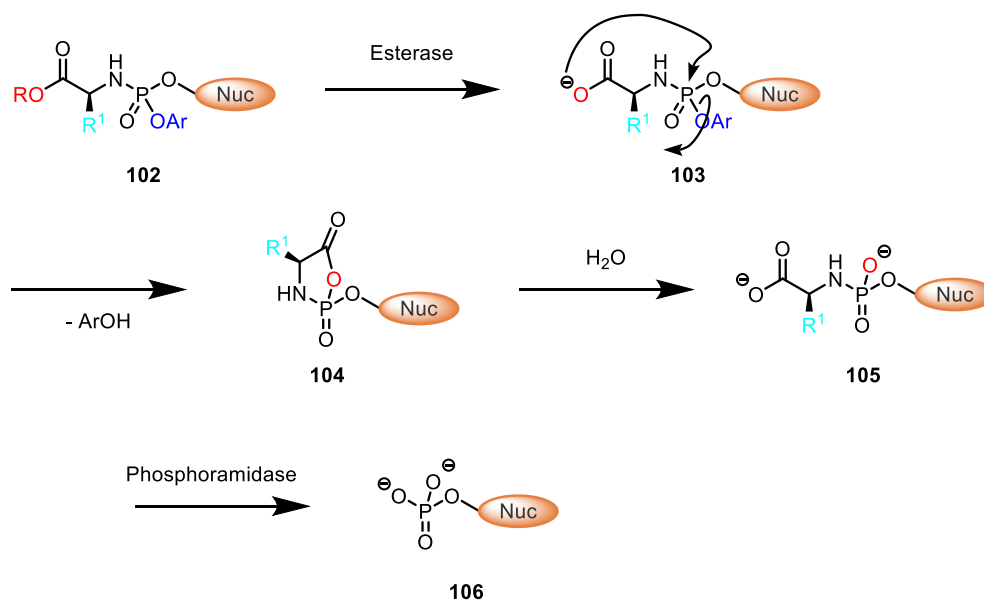


Figure 1.04: The general structure of a ProTide prodrug, with 3'-azido-3'-deoxythymidine (**101**) as model nucleobase.

- ii. Amino acid side chain – demonstrates indirect effect on ester hydrolysis. Steric bulk was found to restrict hydrolysis when using cathepsin A as the esterase for isoleucine,^[34] but cathepsin G efficiently cleaved phenylalanine containing prodrugs.^[35] Interestingly, use of glycine as the amino acid yielded a less cytotoxic prodrug than cysteine – however, alanine containing prodrugs were the most active when tested against 2',3'-didehydro-2',3'-dideoxythymidine.^[36] Wagner and co-workers also observed that altering the amino acid stereochemistry, from L- to D-phenylalanine, could produce up to a 200-fold increase in activity.^[37]
- iii. Aryloxy motif – its primary function is as a leaving group to form the active monophosphate. Aryloxy moieties were found to demonstrate significantly greater antiviral activity over alkoxy motifs, which shows little to no meaningful antiviral activity.^[38] Substituted phenoxy groups were investigated by Siddiqui *et al*, and found mildly electron withdrawing substituents, such as 4-chloro, corresponded to increased activity *in vitro*.^[39] Further research typically utilised non-substituted phenyl.^[40] Moreover, the aryloxy group imparts further lipophilicity to the prodrug, with phenyl or naphthyl motifs targeted.



Scheme 1.43: The *in vivo* mechanism of prodrug **102** by sequential esterase and phosphoramidase cleavage process to yield 5'-O-monophosphate **106**.

The mode of action is depicted in Scheme 1.43 and helps rationalise some of the aforementioned points. Once the ProTide has been taken across the cell membrane, the amino acid ester functionality is hydrolysed by esterases, such as cathepsin A,^[34] to form **103** which exists as the carboxylate anion under physiological conditions. The newly formed carboxylate motif then nucleophilically attacks the phosphoramidate, releasing the aryloxy leaving group and forming mixed cyclic anhydride **104**. It is interesting to note that there is little discussion surrounding the effect of the liberated aryloxy species and its potential effect on bioactivity. For example, when Ar = Ph, the cleavage of phenol/phenoxide would likely impart some toxicity given that phenol is a known toxin. Metabolite **104** is then rapidly ring opened by water, which can do so by attacking either the carbonyl or phosphorous centre, generating **105**. Attack at either position yields the same product, although no cleavage of the P-N bond has been observed.^[41] The final step is cleavage of the P-N bond, the rate of which has been found to correlate to bioactivity.^[37] The cleavage liberates the amino acid and nucleoside monophosphate **106**, and is facilitated by a phosphoramidase enzyme.^[42] Thereafter **106** is converted to the diphosphate and triphosphate in turn by phosphate kinases.^[42]

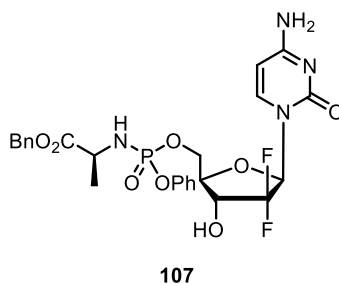
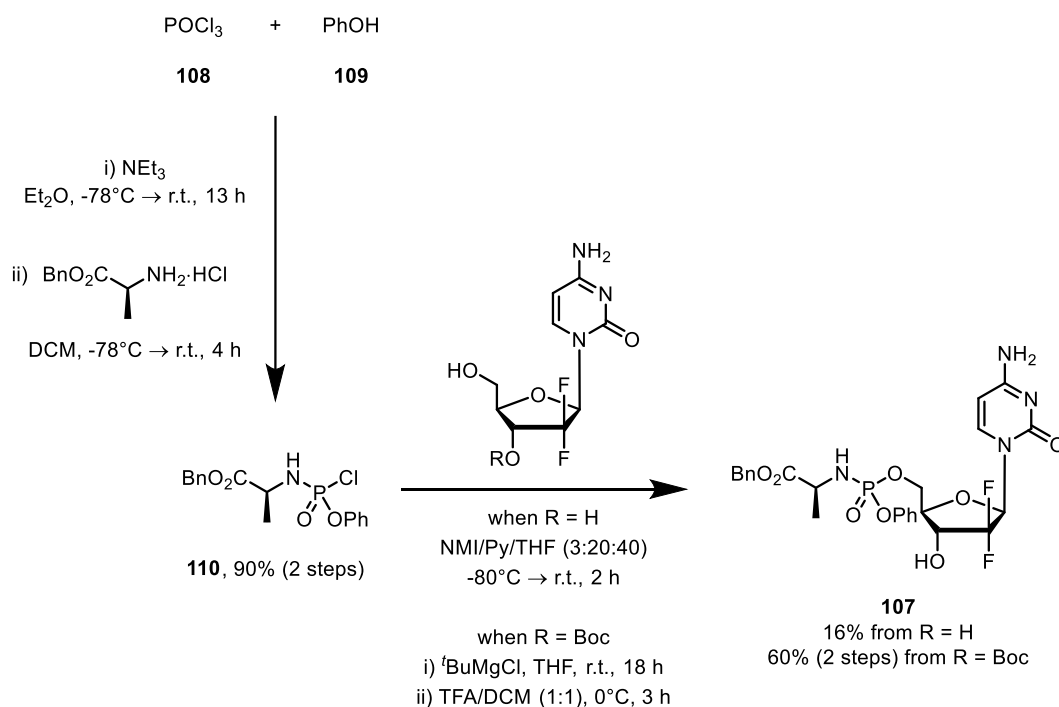


Figure 1.05: The structure of gemcitabine-phosphoramidate NUC-1031, **107**.

Given gemcitabine's poor conversion *in vivo* to the active dFdCDP and dFdCTP metabolites, it was an ideal candidate to be explored under the ProTide strategy. Investigative work by McGuigan and co-workers, in collaboration with NuCanna, synthesised and evaluated a range of gemcitabine protides.^[6] Extensive research culminated in **107** (NUC-1031, Acelarin®) being identified as the most suitable candidate to pursue clinical trials with. The L-Ala-OBn phenyl protide was chosen over other candidates due to its high cytotoxicity and metabolic stability, where a mid-range half-life in human hepatocytes was targeted. **107** overcame the three parameters for gemcitabine deactivation highlighted previously (Page 3), with a key observation being that NUC-1031 is not dependent on hENT1 in order to exert its anticancer effect. The 5-O functionalisation also inhibited deleterious deamination to toxic dFdU or derivatives thereof.^[43]

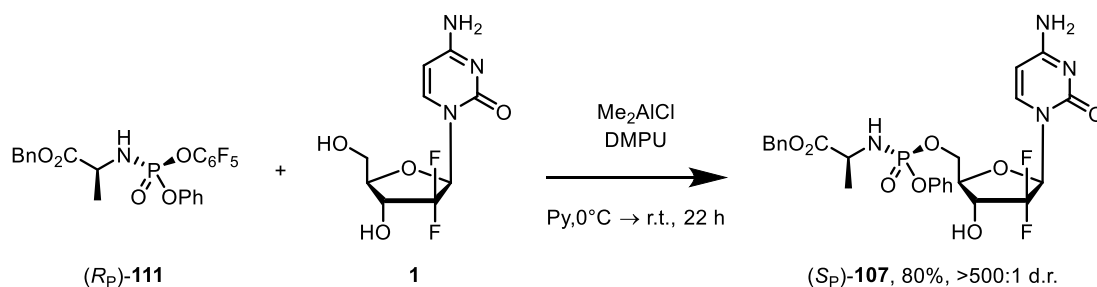
The most common strategy for synthesising the aryloxy phosphoramidate begins by reacting the aryl alcohol with phosphoryl chloride before combining the product of that with the appropriate amino acid. In the context of NUC-1031, phenol is reacted with phosphoryl chloride with triethyl amine as base in anhydrous diethyl ether affording phenyl phosphorodichloridate,^[44] which is subsequently reacted with L-alanine benzyl ester hydrochloride in dry DCM using triethyl amine as base, yielding **110** in 90% over two steps after column chromatography (Scheme 1.44).



Scheme 1.44: The synthetic route developed by McGuigan and co-workers towards the production of **107**.

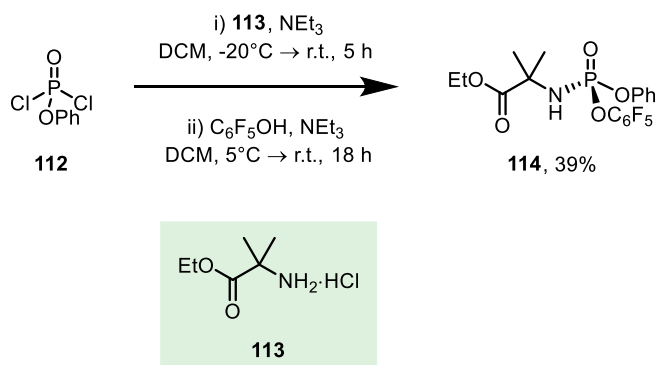
Reacting aryl aminoacyl phosphorochlorodate **110** with gemcitabine affords **107** in 16% yield in a rather unselective fashion,^[45] with side reactions likely occurring. Later findings by Slusarczyk *et al* use 3-*O*-Boc protected gemcitabine, which affords NUC-1031 in 60% yield over 2 steps, in a more controlled approach.^[6] Alternative approaches involved similar construction of the aryloxy phosphoramidate; Silverman and co-workers utilised pentafluorophenol as the leaving group,^[46] in conjunction with catalytic dimethyl aluminium chloride as Lewis acid (Scheme 1.45). Their method avoided employing protecting groups, resulting in an improved, highly selective 5-*O* functionalisation of **1** and delivered an 80% yield of NUC-1031. It is interesting to note that these compounds are chiral at phosphorous and are illustrated as such through ^{31}P NMR analysis, revealing two phosphorous environments equating to the two diastereomers formed.^[46] In Silverman's case, the use of enantiopure phosphoramidate (R_P)-**111** allowed diastereoselective formation of (S_P)-**107** through a phosphorous S_N2 -type mechanism,^[46] with alternative approaches dependent on selective crystallisation or HPLC separation. Although both stereogenic phosphorus centres demonstrate anti-viral activity,^[47,48] the chosen diastereomer can have a pronounced effect resulting in a 10-fold or greater *in vitro* potency,^[49] due to diastereospecific enzyme binding.^[42]

Clinical trials are ongoing using NUC-1031, although recent setbacks have appeared when using **107** in Phase II studies.^[50]



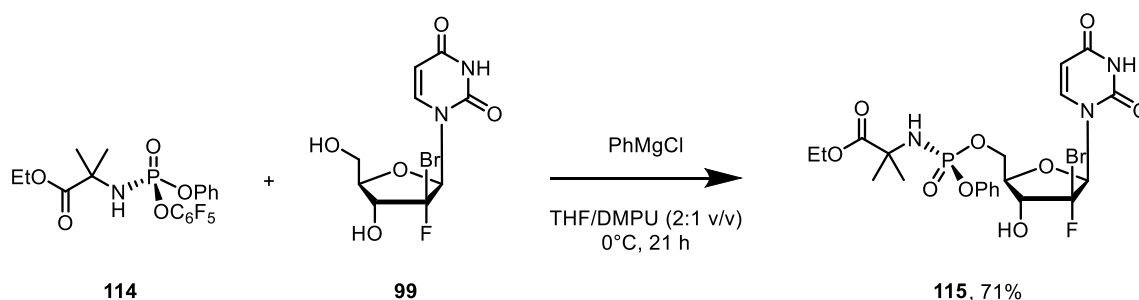
Scheme 1.45: The improved coupling of gemcitabine and **111** for the synthesis of **(S_P)-107**.

Similarly, Voight *et al* utilised the pentafluorophenoxy leaving group in their synthesis of ABBV-168.^[24] Depicted in Scheme 1.46 is the sequential treatment of phenyl dichlorophosphate (**112**) with 2-amino-isobutyric acid ethyl ester hydrochloride (**113**) and pentafluorophenol under basic conditions, which furnished **114** in 39%, following purification by HPLC.



Scheme 1.46: The synthesis of **114** by sequential addition of nucleophiles **113** and pentafluorophenol to phenyl dichlorophosphate.

From **114**, extensive optimisation led to identification of phenyl magnesium chloride as base, in a solvent mixture of THF and DMPU in a 2:1 ratio, which produced **115** in 71% yield. The quoted conditions suppress side reactions, such as epimerisation at the phosphorous centre and diphosphoramidation at the 5' and 3' hydroxyl groups. Although the product **115** doesn't include an amino acid in the phosphoramidate motif, the research depicted in Scheme 1.47 demonstrates the potential for alternative amine moieties in ProTides, in addition to the pentafluorophenoxy leaving group to improve selectivity.



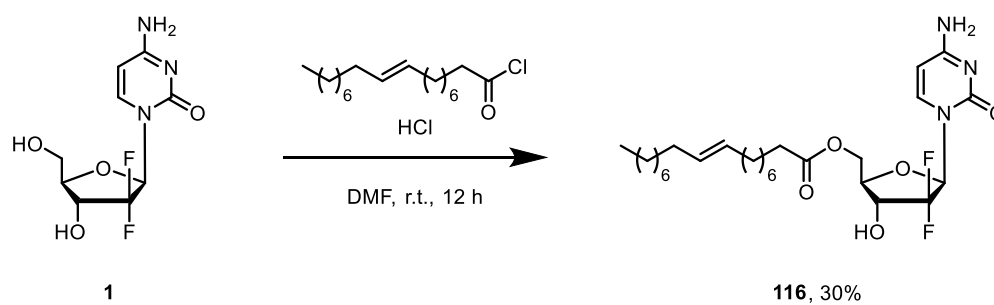
Scheme 1.47: The synthesis of **115** using **114** in combination with 2'-deoxy-2'-α-fluoro-2'-β-bromouridine (**99**).

1.1.3.3 – Clavis

Unprotected 3' hydroxyl groups have been shown to be critical for enzyme mediated deamination to the uridine congener to occur, while altering the 5' substituent did not dramatically alter deamination.^[51] Later research by Amidon and coworkers revealed that 5'-O-amino acid derivatives of gemcitabine were highly resistant to deamination by CDA, compared to gemcitabine itself.^[43] As such, synthesis of 5'-O functionalised gemcitabine was targeted by a number of pharmaceutical companies. One such example was the elaidic acid ester derivative of gemcitabine, developed by Norwegian pharmaceutical company Clavis Pharma. Their rationale for the monounsaturated aliphatic ester was the improved lipophilicity towards the treatment of solid tumours, which could be enzymatically hydrolysed *in situ* to gemcitabine. Such targeted moieties were part of the company's Lipid Vector Technology, which aimed to overcome agent uptake dependence on the expression of nucleoside transporters such as hENT1.

Its synthesis was reported in 1997,^[52] in which gemcitabine was treated with elaidic acid chloride in acidic DMF, yielding the 5'- functionalised prodrug in 30% isolated yield after column chromatography (Scheme 1.48). The approach was unselective, with a small amount of the 3'-O congener also produced.

Initial clinical studies demonstrated lower half maximal inhibitory concentration for elaidic acid derivative **116** than gemcitabine, for the four cell lines tested. The improved cytotoxicity was attributed to an improved *in vivo* half-life over gemcitabine, arising from a poor binding mode of the modified chemotherapeutic agent **116** to CDA. Consequently, less **116** undergoes deactivating deamination. Additionally, inclusion of the monounsaturated motif means an independence on the nucleoside transporters gemcitabine is reliant on.^[53]



Scheme 1.48: The reaction of gemcitabine with elaidic acid chloride to form **116**.

Latterly, pancreatic cancer cell lines were treated with **116**,^[54] but it was found that the study on low hENT1 expression and adenocarcinoma of the pancreas (LEAP) demonstrated no difference in survival rates of patients treated with **116** in comparison to gemcitabine. The result would suggest that expression of hENT1 in cancer patients does not play a key role in effectiveness of gemcitabine as a chemotherapeutic agent and the survivability of patients.

1.2 – Positron emission tomography

Positron emission tomography (PET) is a non-invasive imaging technique, which allows for cross-sectional images of the subject to be taken and in turn used to construct 3D images. It has found extensive use in the field of diagnostic cancer treatment, with a range of radiopharmaceuticals employed towards neurodegenerative diseases,^[55] hypoxia^[56] and a variety of cancers such as lung,^[57] ovarian^[58] and breast.^[59] Due to the high sensitivity of PET imaging and concentrations required for image acquisition, typically in the nanomole to picomole range, it is the imaging modality of choice within clinical oncology.^[60]

1.2.1 – Principles of PET Imaging

The underpinning physical principle of PET imaging is dependent on the use of unstable radionuclides that undergo radioactive decay pathways, resulting in the emission of a positron (β^+) and a neutrino.^[61] The emission is the result of an unstable proton becoming a neutron within the radionuclide, with the total number of nucleons remaining constant. Typical β^+ decay is illustrated in Eqn. 1.01 in the context of ^{18}F .



The decay process is dependent upon the radionuclide, where the number of disintegrations per time unit is related to the number of radioactive nuclei, N , by the decay constant λ , shown in Eqn. 1.02:

$$\frac{dN}{dt} = -\lambda N \quad (\text{Eqn. 1.02})$$

The above equation is also the mathematical form of the activity, A_t , of a radionuclide, defined as “the number of nuclear decays occurring in a given quantity of material in a small time, interval, divided by that time interval”.

$$A_t = -\frac{dN}{dt} = \lambda N \quad (\text{Eqn. 1.03})$$

The unit of activity is the Becquerel (Bq), where 1 Bq is equal to one disintegration per second. It is more commonly noted with Curie (Ci) as the non-SI unit, where 1 Ci = 3.7×10^{10} Bq. Specific activity can also be defined as “the activity of a material

divided by the mass of the tracer”, the units of which are Bq mol⁻¹. Molar activity is the activity per mole, units of Bq g⁻¹ and is more commonly used (Eqn. 1.04).

$$A_t = \frac{\lambda N}{\left(\frac{m \cdot N}{N_A}\right)} = \frac{\lambda N_A}{m} \quad (\text{Eqn. 1.04})$$

Resolving Eqn. 1.03 leads to an expression for the number of radioactive nuclei at time t , if the initial number of nuclei is known, as shown in Eqn. 1.05. Indeed this expression is also true of the activity of a radionuclide (Eqn. 1.06):

$$N_t = N_0 e^{-\lambda t} \quad (\text{Eqn. 1.05})$$

$$A_t = A_0 e^{-\lambda t} \quad (\text{Eqn. 1.06})$$

The half-life of a radionuclide of a single radioactive decay process, is “the time required for the activity to decrease to half its value by that process”, the solution for which is illustrated in Eqns. 1.08 and 1.09:

$$\frac{N_{t_{1/2}}}{N_0} = 0.5 = e^{(-\lambda t_{1/2})} \quad (\text{Eqn. 1.08})$$

$$t_{1/2} = \frac{\ln(2)}{\lambda} \quad (\text{Eqn. 1.09})$$

In the case of fluorine-18, the half-life is 109.8 minutes, decaying to stable nuclide ¹⁸O (Eqn. 1.01). By contrast some (radio)nuclei may undergo alternative decay pathways, such as α -decay, isomeric transition (γ emission) or β^- decay, whereby an electron is emitted such as that seen in the decay of technetium-99 (Eqn. 1.10).



β^+ decay is a random decay pathway, which accounts for 97% of the emission profile of ¹⁸F. The emitted positron has an average energy of 250 keV but may be produced at energies as high as 630 keV. The remaining 3% of the emission profile is described by electron capture, the reverse process, where an electron from the radionuclide’s inner shell combines with a proton, forming a neutron and a neutrino (Eqn. 1.11).^[62]



Following emission from the radionuclide, the positron travels a distance from the point of emission – typically less than 1 mm, but has a maximum mean free path of 2.4 mm in H₂O – until colliding with an electron (Figure 1.06), annihilating both particles and producing two antiparallel gamma rays with an energy of 511 keV.^[63]

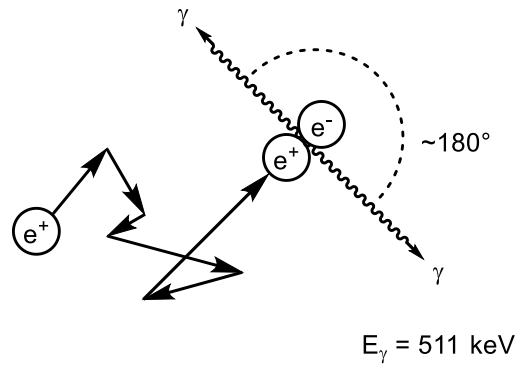


Figure 1.06: Principle of PET illustrating annihilation of a positron with an electron. Two collinear γ -rays are emitted of 511 keV, which are used to construct the image.

The emitted γ -rays are nearly antiparallel at approximately 180° - the deviation estimated at $\pm 0.25^\circ$ which is the cause of the loss in the spatial resolution of PET detectors.^[64] The γ -rays are detected using photoscintillators, whereby the origin of annihilation can be discerned along the line of response. Critically, the γ -rays need to be aligned with the scintillation crystal on the detector, otherwise no detection will be noted.

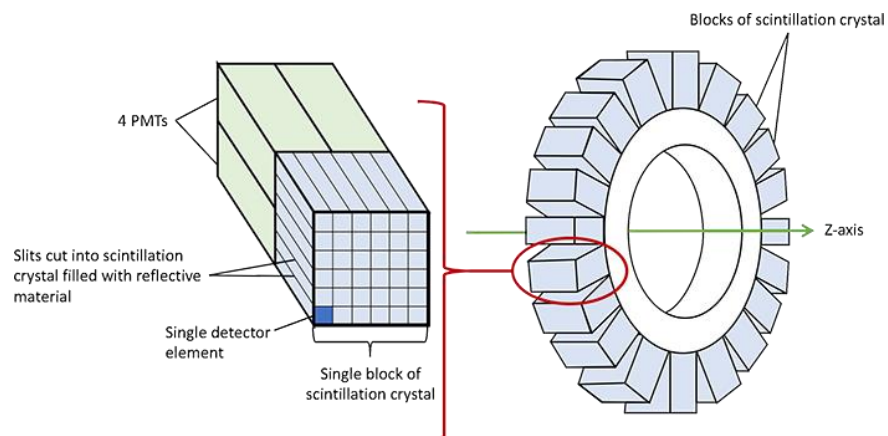


Figure 1.07: Detection of γ -rays using scintillator with photomultiplier tubes, and their arrangement on a PET scanner.

Photons of energy 511 keV are absorbed by the scintillation crystal, and subsequently reemitted as lower energy photons in the visible light region or UV.^[64] The lower energy photons are detected by the photomultiplier tubes and converted into an electrical signal which can be read by a computer, subsequently allowing for an image to be created. As shown in Figure 1.07, a typical PET scanner is constructed of several individual detectors, in perpendicular fashion to the scanner (z-axis) which allow for maximum spatial mapping and increased spatial resolution of the image acquired. The detector unit may also map along the z-axis by the patient bed moving, resulting in the construction of a cross-sectional image. The signals generated on opposite detectors by impact of the γ -rays must occur within a coincidence time window of 6 – 12.5 ns to be judged as coincident.^[65] If within the time frame, the coincidence event is denoted a line of response connecting the two detectors, allowing for positional information to be abstracted from the annihilation event.^[66]

Indeed, this is an ideal scenario – termed true coincidence – as all annihilation processes are unlikely to be behave in this fashion, due to many factors. The γ -photons may be absorbed by other matter before detection by the scintillator or scattered by another medium *en route*.

1.2.2 – ^{18}F production

Fluorine-18 is produced in a cyclotron, which accelerates particles using a magnetic current to bombard a sample. Selected examples for the production of fluorine-18 are listed in Table 1.03,^[62] and demonstrate the range of molar activities available depending on the irradiation method. If $[^{18}\text{F}]\text{F}_2$ is the desired target, bombardment of neon-20 gas (containing F_2) with deuterium ions delivers carrier added $[^{18}\text{F}]$ fluorine gas, containing a isotopic mixture of fluorine-18 and fluorine-19 in low molar activity.

Entry	Nuclear reaction	Target	Product	Molar activity (GBq μmol^{-1})
1	$^{20}\text{Ne}(\text{d},\alpha)^{18}\text{F}$	^{20}Ne (200 $\mu\text{mol F}_2$)	$[^{18}\text{F}]\text{F}_2$	0.04 – 0.40
2	$^{18}\text{O}(\text{p},\text{n})^{18}\text{F}$	$^{18}\text{O}_2$ (50 $\mu\text{mol F}_2$)	$[^{18}\text{F}]\text{F}_2$	0.36 – 2.00
3	$^{18}\text{O}(\text{p},\text{n})^{18}\text{F}$	H_2^{18}O	$[^{18}\text{F}]\text{F}^-$	4×10^4

Table 1.03: Methods of $[^{18}\text{F}]$ production.

Alternatively, the radioactive gas may also be produced via high energy proton bombardment of enriched oxygen-18 gas, again containing fluorine-19 gas, delivering $[^{18}\text{F}]\text{F}_2$ in increased specific activity. Both aforementioned production methods deliver electrophilic fluorine, which can be directly used or converted into less reactive equivalents or synthetically useful $N\text{-}[^{18}\text{F}]\text{F}$ reagents.^[67,68]

The greatest activity can be obtained by high energy proton irradiation of enriched H_2^{18}O , which delivers $[^{18}\text{F}]\text{F}^-$ as an aqueous solution. The process is depicted in Figure 1.08. The solution is eluted over a quaternary ammonium anion (QMA) exchange cartridge, which traps the fluoride-18. The QMA exchange resin is composed of polymer-bound R_4N^+ salts. The eluent, H_2^{18}O , is collected and disposed of. The bound $[^{18}\text{F}]\text{F}^-$ is eluted from the column using an acetonitrile/water mixture (4:1 v/v) containing potassium carbonate and Kryptofix 2.2.2 (K_{222}), as counterion source and chelator respectively, liberating $[^{18}\text{F}]\text{KF}$. The solution of $[^{18}\text{F}]\text{KF}$ in $\text{MeCN}/\text{H}_2\text{O}$ is then azeotropically dried, ready for radiochemistry. Different counterions have also been employed, leading to the development of alternative nucleophilic sources of $[^{18}\text{F}]\text{F}^-$, such as $[^{18}\text{F}]\text{TBAF}$ and $[^{18}\text{F}]\text{CsF}$.^[69,70]

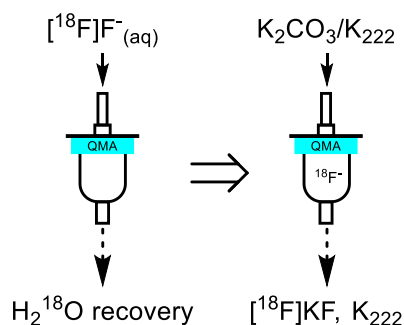


Figure 1.08: Catch and release procedure of fluoride-18 by a QMA cartridge.

The reactivity of the fluoride is highly dependent on its nature and environment. Typically, dissolved metal fluorides can act as good nucleophiles, but are rendered “inert” by hydration and the nucleophilicity of fluoride is outweighed by its basicity (Figure 1.09).

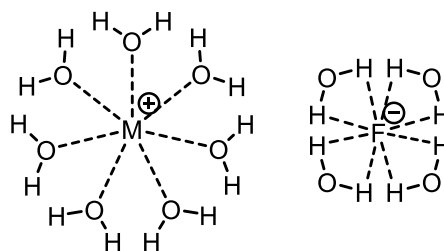


Figure 1.09: Hydration of dissolved metal fluorides.

The advent of phase transfer catalysts (PTC) as reagents, such as chelators like K_{222} or 18-crown-6 as shown in Figure 1.10, weaken the ion pairing of fluorides, accessing fluoride with greatly improved nucleophilicity hence reactivity, often termed “naked” fluoride.^[71] The chelator used can be changed to match the size of the cation used in the elution mixture to maximise encapsulation of the metal ion. Equally, tetraalkylammonium cations can be used without these chelators.

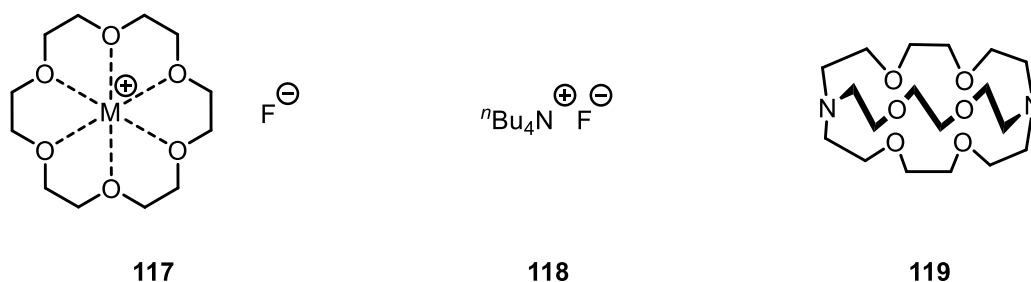


Figure 1.10: Examples of “naked” fluoride by chelator (18-crown-6) and metal cation (*left*, **117**) or tetrabutylammonium (*centre*). The structure of Kryptofix® 222 (**119**) is also shown for reference (*right*).

1.2.3 – Application and principles of radiotracers

A range of radionuclides that undergo β^+ decay can be utilised as contrast agents for PET imaging. A representative set of radionuclides is presented in Table 1.04.

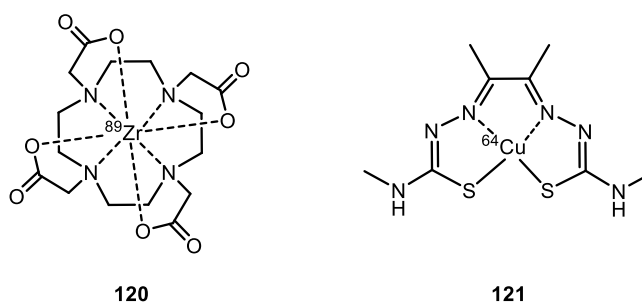


Figure 1.11: Example radiotracers using ^{89}Zr (**120**) and ^{64}Cu (**121**).

Entry	Isotope	Half-life	$E_{\max} \beta^+ / \text{keV}$	Decay pathway / %
1	^{89}Zr	78.4 h	897	23
2	^{64}Cu	12.7 h	653	18
3	^{18}F	109.8 min	633	97
5	^{11}C	20.4 min	960	>99
4	^{13}N	10.0 min	1199	>99
5	^{15}O	2.0 min	1735	>99%

Table 1.04: Selected examples of radionuclides that have found use within PET imaging.

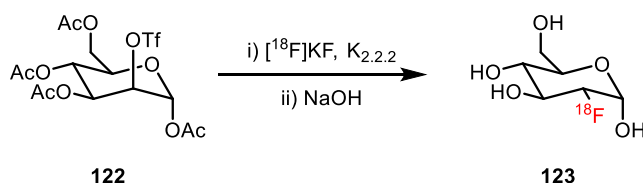
Depicted in Figure 1.11 is an example of a zirconium-89 radiotracer chelated to DOTA (**120**),^[72] can also be used for protein labelling via a targeting vector,^[73] while copper-64 has been used in combination with the ligand ATSM (**121**) for hypoxia imaging.^[74]

While both these metal-based radiotracers have long half-lives, which would allow for image acquisition over a longer time period, their decay pathway with respect to β^+ emission is inefficient (decay pathway, Table 1.04).

By contrast, ^{18}F has a more desirable half-life of approximately 110 minutes. As such, it makes it an ideal candidate within radiotracers as it would minimise radiation exposure to the patient, while also being appreciable on a biological timescale. Furthermore, fluorine is a commonly encountered bioisostere of the hydroxyl group, due to similar van der Waals radii and bond lengths to carbon.^[75] Alternatively, nitrogen-13 and carbon-11 also undergo β^+ decay, and could be incorporated into candidate radiotracers as they will likely contain one of the two nuclides, providing an appropriate labelling strategy were in place. Critically however, is their significantly shorter half-lives. If there were a deprotection step following radiosynthesis, potentially half of the radioactivity could be lost for both radionuclides.

In vivo tracking is the function of radiotracers, whereby a bioactive molecule mimicking its non-radiolabelled congener is introduced allowing for information regarding the biological system can be obtained. Incorporation of the radionuclide into the therapeutic agent should not significantly interfere or alter the pharmacokinetics of the metabolite.

This point is elegantly exploited by [^{18}F]fluorodeoxyglucose ([^{18}F]FDG, **123**, Scheme 1.49), one of the most used radiotracers within the oncology field



Scheme 1.49: General scheme for the radiosynthesis of [^{18}F]FDG, **123**.

It was first synthesised in 1973 using [^{18}F]F $_2$,^[76] but today it is more commonly synthesised using [^{18}F]KF. [^{18}F]FDG synthesis typically commences from mannose triflate (**122**), following by basic hydrolysis of the protecting acetate esters motifs (Scheme 1.01), in high yield and high molar activity. The precursor is produced from D-mannose in 16% yield over 5 steps,^[77] and typically administered as a saline solution to patients. The synthesis of **123** in clinical faculties is conducted using automated instruments and disposable cartridges, using equipment such as those displayed in Figure 1.12.



Figure 1.12: Commonly used instrument for the clinical production of [^{18}F]FDG, GE FASTlab 2 (*left*) and TRASIS AllinOne (*right*).

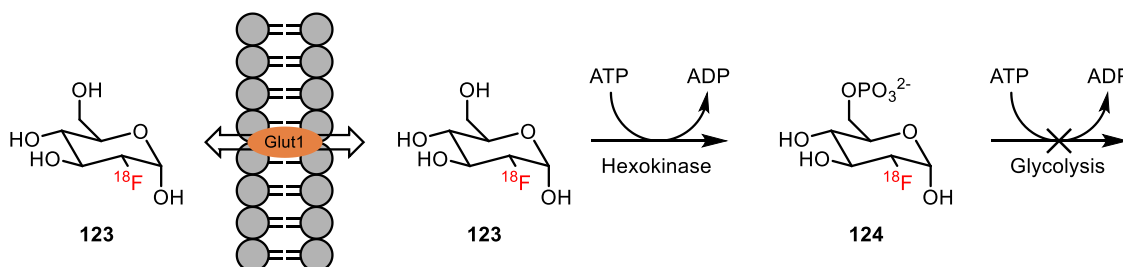


Figure 1.13: *In vivo* mode of action of [^{18}F]FDG (**123**).

The *in vivo* activity of [^{18}F]FDG is key to the widespread use, illustrated in Figure 1.13. Once administered, the sugar analogue will accumulate in areas with increased metabolic activity with increased glucose demand, such as fast-growing cancer cells. It is reversibly transported into cells by glucose transporters and subsequently phosphorylated at the 6-position by hexokinase and adenosine triphosphate (ATP), producing an equivalent of adenosine diphosphate (ADP) as by-product. Once **124** is formed, its anionic character means that it cannot be transported out of the cell, but equally cannot be metabolised further as it is lacking the requisite 2-OH- group for further glycolysis. As such, **124** will accumulate within the sugar hungry cell, hence the radiolabelled compound will highlight the cells and where within the body they are during a PET scan.^[78] Despite its extensive use within oncology, **123** lacks specificity, hence targeting towards particular organs or diseases is difficult. As such, the development of targeted radiotherapeutics would allow for imaging with improved specificity.

Given the sensitivity of the technique, the amount of radiotracer needed to be administered to the patient is incredibly low, typically picomolar. Because the physiological concentration is low, the toxicological concerns aren't as significant compared to the millimolar quantities required for therapeutic agents.

1.2.4 – ^{18}F radiochemistry

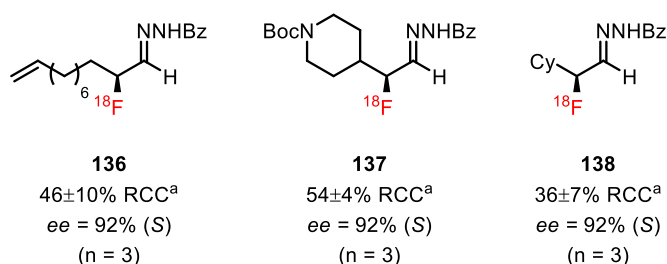
1.2.4.1 – Electrophilic fluorination

As previously discussed, one of the major pathways to access electrophilic fluorine-18 for radiochemistry is via [^{18}F]F₂ which is not widely available, nor conveniently handled or manipulated for chemistry. As such, multiple endeavours have surfaced attempting to use it indirectly for electrophilic fluorination.

Gouverneur and co-workers developed the radiosynthesis of [^{18}F]NFSI from the sodium dibenzenesulfonimide and [^{18}F]F₂ (Scheme 1.50),^[67] and its application towards fluorination of silylated latent nucleophiles such as enol ethers. The method of synthesis is comparable to that which produces NFSI commercially,^[79] and was shown to perform well in comparison to standard NFSI.

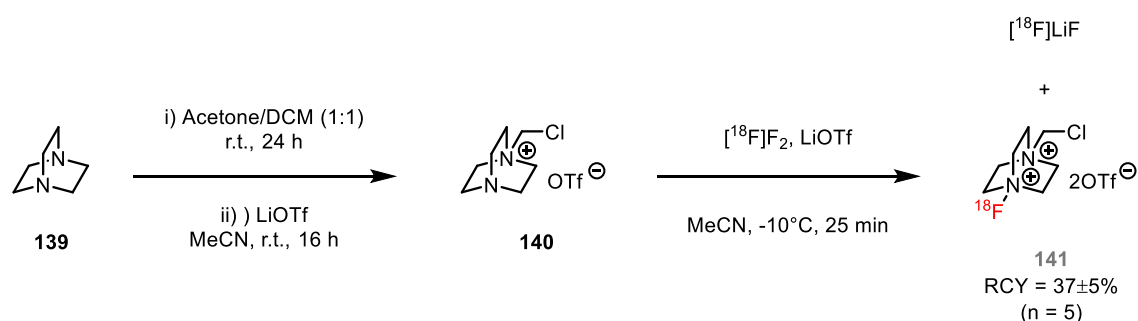
[^{18}F]NFSI was then successfully applied by Gouverneur to enantioselective fluorination of aldehydes (Schemes 1.50 and 1.51),^[80] based on previous organomediated fluorination by MacMillan.^[81]

This work effectively demonstrated a merger of radiochemistry with organomediated enantioselective processes, with good radiochemical conversions and very high *ee*. Interestingly, all substrates were derived as their hydrazone congener, to minimise racemisation (Scheme 1.52). Radiochemical conversion is commonly used within the field, and calculated referring to the radioactivity of the active agent, in this case [^{18}F]NFSI.



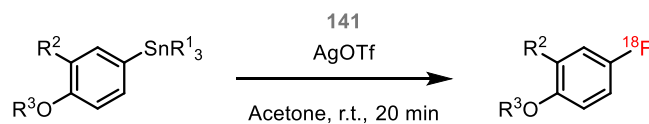
Scheme 1.52: The substrate scope of aldehydes explored with [^{18}F]NFSI. ^a RCC determined by radio-HPLC relative to [^{18}F]NFSI.

Following from this work, Teare *et al* successfully synthesised [^{18}F]Selectfluor bistriflate as an alternative electrophilic radiofluorination agent.^[68] It was synthesised in comparable fashion to its non-radioactive analogue (Scheme 1.53), but triflate counter anions were employed due to potential formation of [^{18}F]BF₄⁻. Alkylation of DABCO (**139**) by DCM followed by anion exchange yielded intermediate **140**, with no yield noted. Fluorination of **140** by [^{18}F]F₂ with lithium triflate delivered [^{18}F]Selectfluor bistriflate **141** in an average radiochemical yield of 37% across five runs.



Scheme 1.53: The synthesis of [^{18}F]Selectfluor bistriflate (**141**) from DABCO (**139**).

The authors demonstrated that silyl ether **127** could be fluorinated in RCY up to 50% (not shown), but also showed that **141** could be used towards electrophilic fluorodestannylation of electron rich aromatics, in combination with silver triflate, shown in Table 1.05.^[68]



Entry	Compound	R ¹	R ²	R ³	RCY ^[a]
1	142	Me	OMe	Me	18 (n = 3)
2	143	Me	H	Me	17 (n = 3)
3	144	^t Bu	H	H	14 (n = 3)

^[a] Decay corrected RCY after semi-preparative HPLC. Based on stock solution of **xx**, activity is 1:1 with [¹⁸F]LiF.

Table 1.05: The electrophilic radiofluorination of arylstannanes by **141**.

This application was illustrated for the synthesis of 6-[¹⁸F]fluoro-L-DOPA,^[55,82] a commonly used imaging agent in the diagnosis and treatment of Parkinson's disease,^[83] where it accumulates in neuroendocrine cells, allowing for imaging. Its mechanism of action is shown in Figure 1.14.

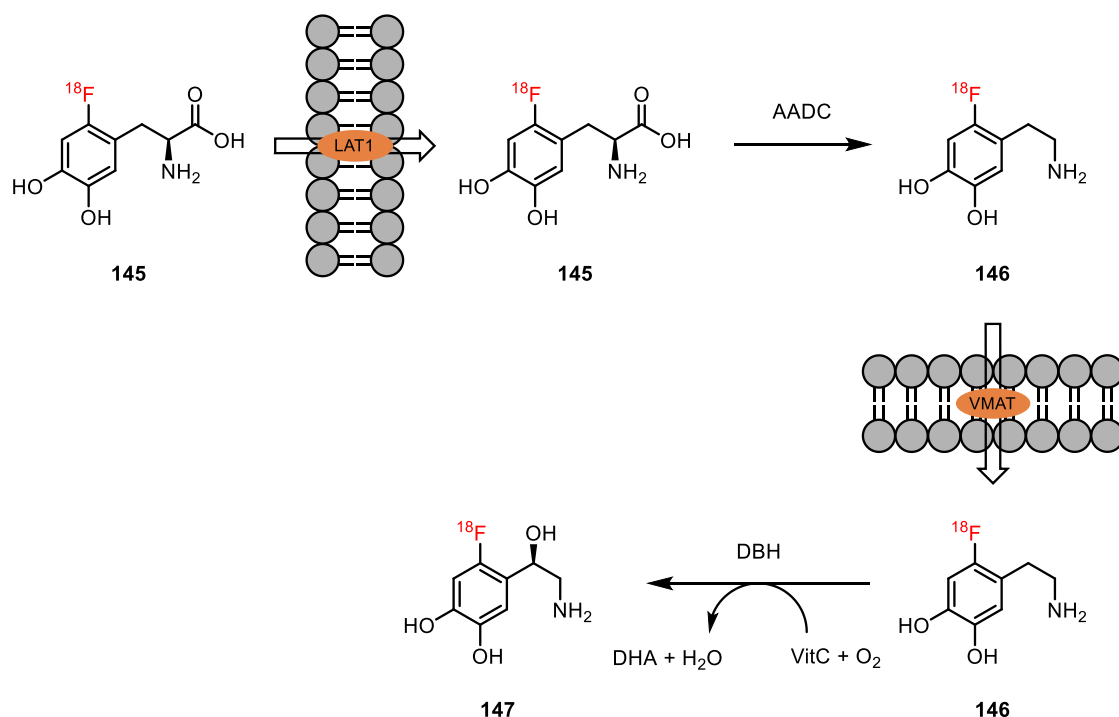
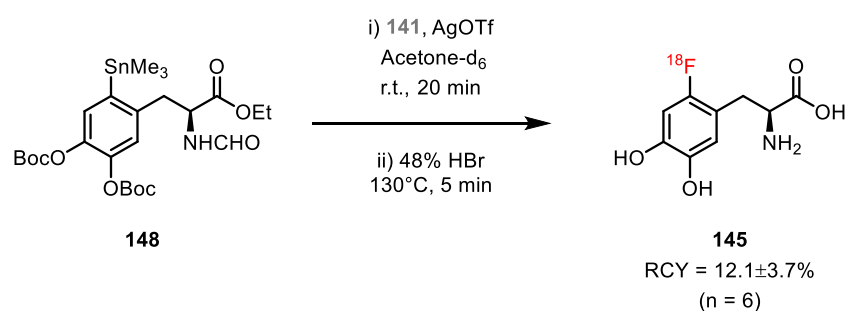


Figure 1.14: *In vivo* mode of action of 6-[¹⁸F]F-L-DOPA.

LAT1 = L-Type Amino Acid Transporter, AADC = Amino Acid Decarboxylase, VMAT = Vesicular Monoamine Transporter, DBH = Dopamine β-hydroxylase, DHA = Dehydroascorbic acid.

It is first transported across the cell barrier by L-type amino acid transporters, prior to decarboxylation by AADC. Further intracellular transport mediated by vesicular transporters allows storage in gastroenteropancreatic tumours,^[55] prior to hydroxylation by DBH to ¹⁸F-fluoronorepinephrine **147**. Unlike [¹⁸F]FDG, there is no mechanism which inhibits release of 6-[¹⁸F]F-L-DOPA from within cells, it is due to increased storage within neuroendocrine vesicles.^[84]

6-[¹⁸F]F-L-DOPA was prepared from precursor **148** – itself synthesised in 3 steps from L-DOPA at 21% yield^[82] – utilising the silver mediated methodology previously explored and [¹⁸F]Selectfluor bistriflate, before deprotection by aqueous hydrobromic acid (Scheme 1.54), in acceptable radiochemical yield.



Scheme 1.54: The radiosynthesis of **145** by silver mediated, electrophilic radiofluoro-destannylation and acidic deprotection.

1.2.4.2 – Nucleophilic fluorination

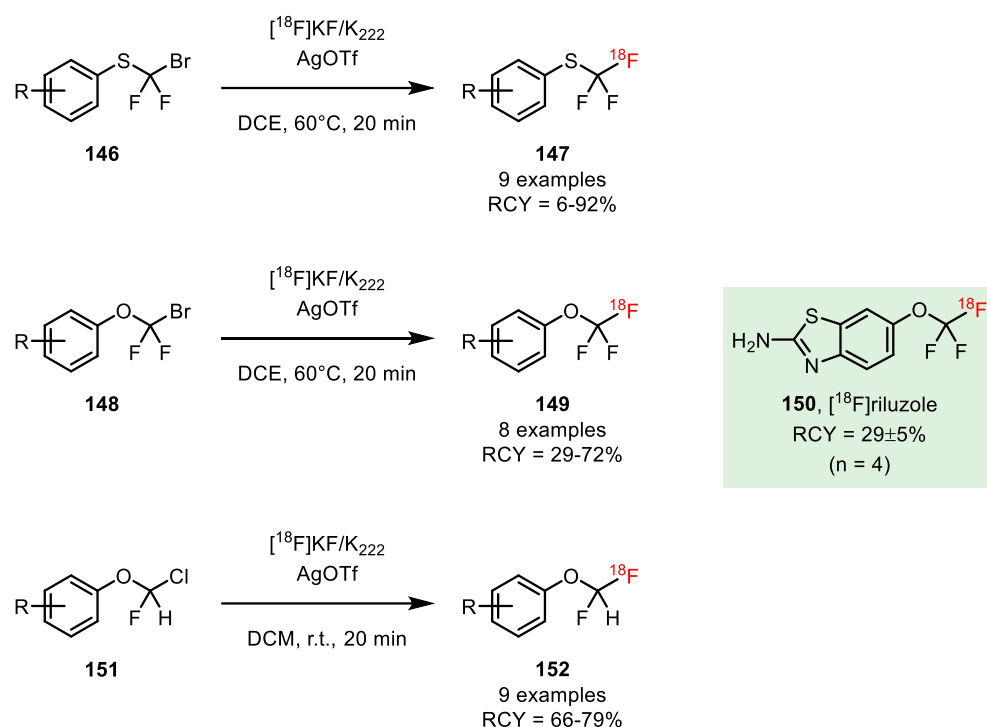
The primary method of fluorine-18 production is as fluoride-18, due to the increased molar activity. One drawback using fluoride – despite the apparent nucleophilicity^[85] – is the inherent basic nature of the anion (pK_a $\text{HF}_{[\text{DMSO}]} \approx 15$, $\text{HF}_{[\text{water}]} \approx 3.2$), which, upon hydration in the presence of water reduces the potency of $^{18}\text{F}^-$ as a nucleophile.^[71] As such, azeotropic drying of the aqueous dispensing solution is performed with acetonitrile and improvement of the nucleophilicity by chelators or tetraalkylammonium counterions are two methods targeted (Figures 1.09 and 1.10). Research into the functionalisation of chelators has been undertaken by Kim, which nicely demonstrates the dual capability of crown ethers to bind not only the counterion, but also dock the fluoride.^[86,87] Considerations to the eluting counterion also need to be applied, where commonly used anions such as carbonate, bicarbonate and oxalate are non-nucleophilic in nature.^[88]

Typical nucleophilic reactions using fluoride-18 utilise dipolar aprotic solvents such as DMSO, DMF and MeCN,^[89,90] proceeding with S_N2 like character. Tertiary alcohols such as *tert*-amyl alcohol have demonstrated application within nucleophilic (radio)fluorination,^[71,91] further demonstrating that some degree of hydrogen bonding may be beneficial.^[92,93]

The choice of leaving group can also be critical to effective nucleophilic displacement, with a balance between leaving group ability and stability of precursor of critical importance.^[94] Additionally, a better leaving group will also lead to competitive elimination under basic conditions.^[88] Jacobsen and Chen report the order of leaving group ability as $\text{Cl} < \text{Br} < \text{I} < \text{OTs} < \text{OMs} < \text{OpNs} < \text{OTf}$, with triflate being the most reactive, but greatest susceptibility to elimination.^[95] Sulfonates demonstrate a substantial subsection within the leaving groups available for fluoride displacement, with a range of reactivities accessible.

Other parameters that require careful modification to minimise deleterious pathways include obvious factors such as temperature, also less intuitive interactions such as the ratio of PTC to base and precursor.^[88]

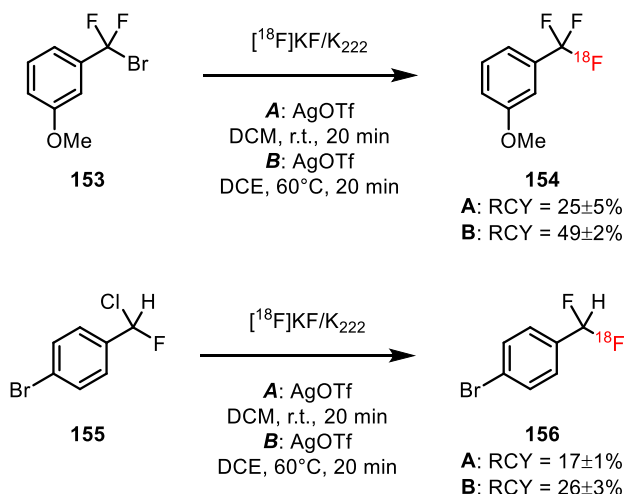
Additional reagents may be included to improve the efficiency of the displacement. Gouverneur and co-workers utilised silver triflate in their work which employed halogens as the leaving group of $-\text{CF}_2$ and $-\text{CHF}$ units attached to phenols and thiophenols (Scheme 1.55).^[96]



Scheme 1.55: Summary of radiofluorination of **146**, **148** and **151** mediated by AgOTf.

Their studies allowed access to [^{18}F]SCF₃ and [^{18}F]OCF₃ motifs, which are commonly found within pharma and agrochemicals as their fluorine-19 analogues, by late stage fluorination. The strategy was applied to the synthesis of [^{18}F]riluzole (**150**, Scheme 1.55), a drug used in the treatment of amyotrophic lateral sclerosis, more commonly known as motor neurone disease. The exploitation of the affinity of silver(I) for halides and their subsequent precipitation out of solution towards radiofluorination is an impressive strategy. Alternative metal triflates were unsuccessful in facilitating the reaction, while the silver counterion needed to be weakly coordinating such as triflate or triflimide. When concluding, they suggest that cationic intermediates are involved in the halogen exchange reaction.^[97]

The developed Ag^I methodology was later applied to benzylic systems, towards the formation of [^{18}F]CF₃ and [^{18}F]CHF₂ units.^[98] Two selected examples are shown in Scheme 1.56, demonstrating the two methods employed to effectively radiofluorinate the substrates. For more difficult examples, doubling the amount of AgOTf used, from 1 to 2 equivalents, in combination with DCE as higher boiling point solvent.



Scheme 1.56: Selected examples of benzylic radiofluorination using silver triflate.

1.2.5 – Radiofluorination of nucleosides

1.2.5.1 – Early-stage fluorination

$[^{18}\text{F}]$ -Fluorine labelled nucleosides have been successfully synthesised as predictive biomarkers,^[99] with varying strategies employed. One commonly utilised method is the fluorination of a ribofuranose derivative, prior to glycosylation. This strategy is termed early-stage fluorination, and has found extensive use in the synthesis of fluorinated nucleosides such as $[^{18}\text{F}]\text{FAC}$, $[^{18}\text{F}]\text{FMAC}$, $[^{18}\text{F}]\text{FAU}$ derivatives and $[^{18}\text{F}]\text{FLT}$ (**157**, **158** and **161** respectively, Figure 1.15).^[100,101]

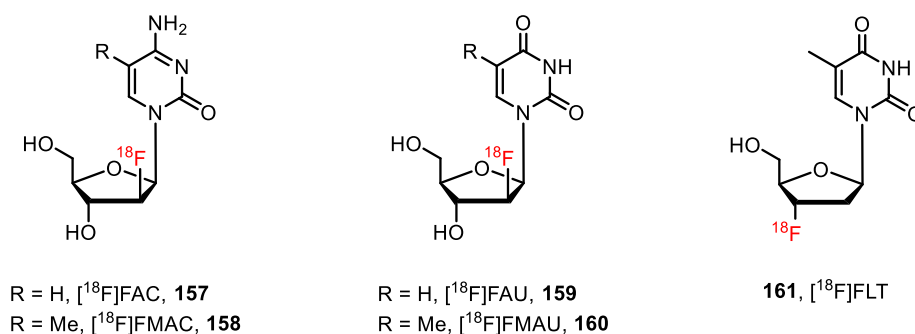
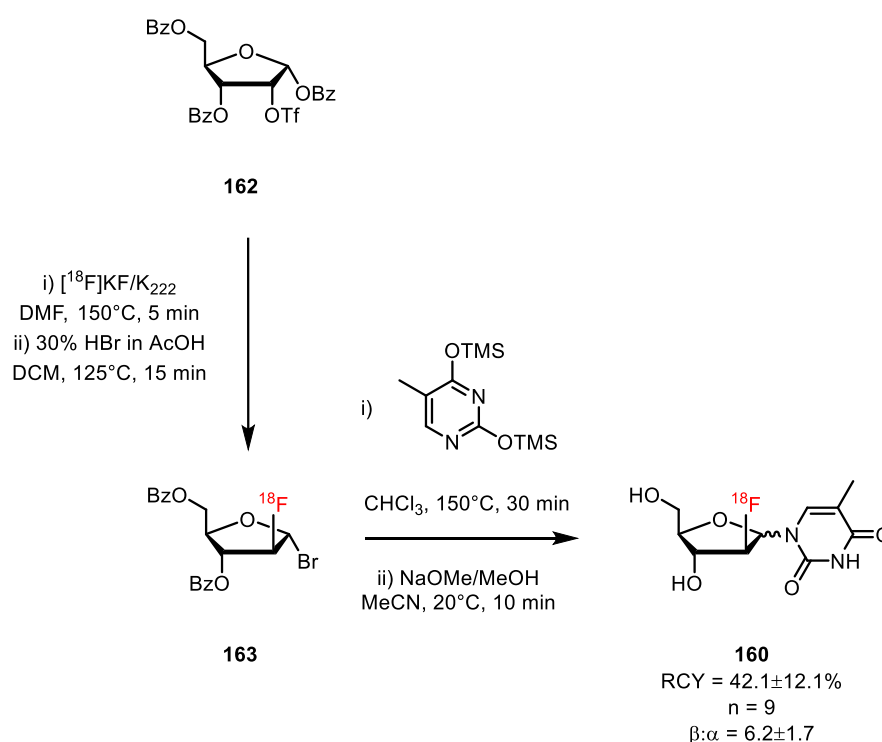


Figure 1.15: Selected structures of example $[^{18}\text{F}]$ nucleosides.

As depicted in Scheme 1.57, this strategy was applied in the synthesis of [^{18}F]FMAU by Shields and co-workers,^[100] based upon research by Howell.^[102] Ribofuranose **162** was subjected to radiofluorination in DMF for 5 minutes, and then converted to 1-bromo-ribofuranosyl intermediate **163**. Glycosylation was conducted in chloroform, which was found to improve the anomeric selectivity over other solvents like DCM and MeCN. Final deprotection by sodium methoxide in methanol afforded the target compound in an average radiochemical yield of 42.1% (decay corrected) over 9 runs, in >98% radiochemical purity (by radio-HPLC).



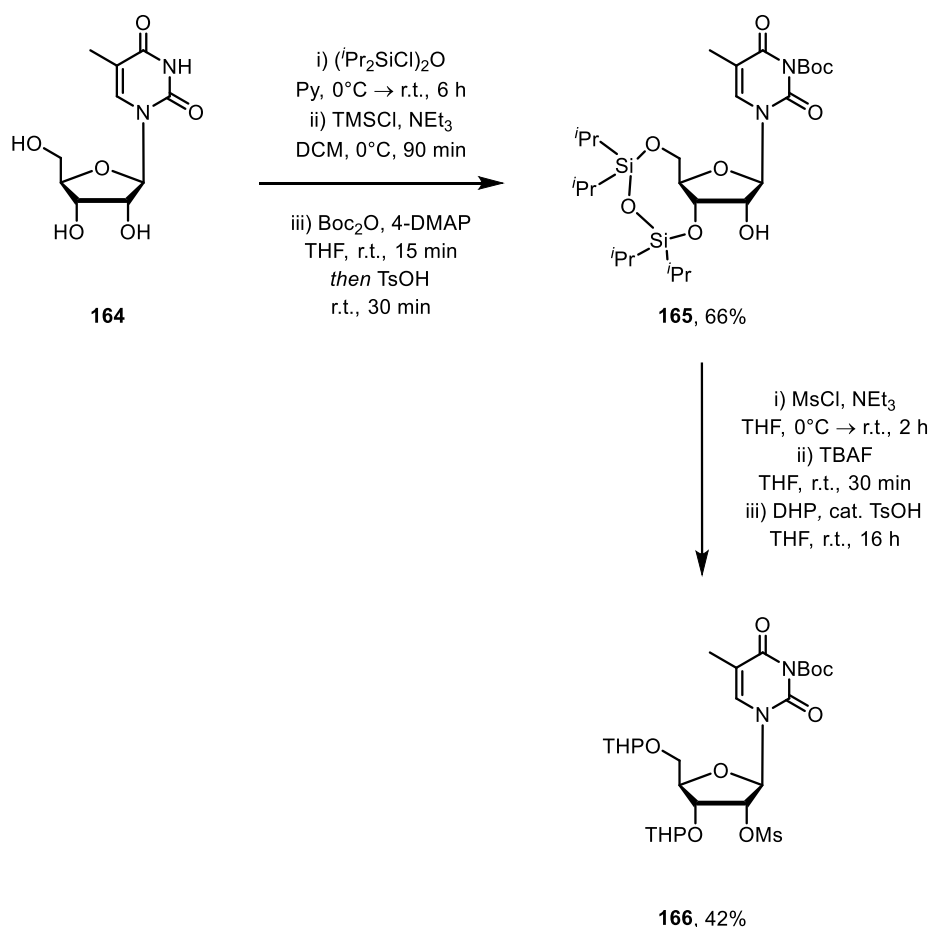
Scheme 1.57: The early stage fluorination strategy applied to [^{18}F]FMAU, **160**.

The method was also applied to other uridine nucleobases, demonstrating its applicability. From these results, the synthetic methodology can be viewed as highly appealing as a generic radiofluorination approach, given it may be applied to the precursor **162**, followed by selection of appropriate nucleobase prior to ring appendage. One issue surrounding the method may be the anomeric selectivity of the glycosylation, and subsequent separation of the anomers after deprotection. Due to the number of steps involved following radiofluorination, the timescale of this processes is of great importance, as the activity of the [^{18}F]-labelled material constantly decays and decreases. The authors claim that synthesis from initial [^{18}F]fluoride capture to isolated compound after HPLC purification is roughly 160 minutes, which would need to be accounted for when original [^{18}F]F⁻ dispensing.

1.2.5.2 – Late-stage fluorination

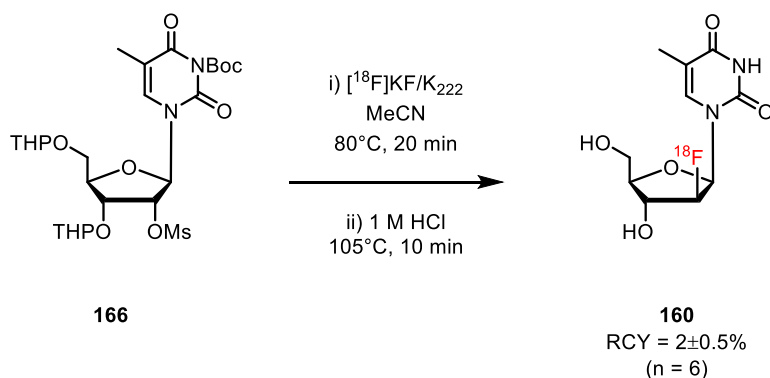
Because of the drawback surrounding the loss of activity of [^{18}F]fluoride associated with early-stage fluorination, late-stage fluorination offers the potential for radiopharmaceuticals with increased activity. As a result, bespoke starting materials require synthesising for the target molecule.

Alauddin and co-workers also synthesised [^{18}F]FMAU, but via late-stage fluorination.^[103,104] Radiolabelling precursor was constructed beginning from 5-methyluridine (**164**, Scheme 1.58) firstly by protecting the 3'- and 5'- hydroxyl groups with 1,3-dichloro-1,1,3,3-tetraisopropylidisiloxane and protection of the 2'-OH with TMSCl. Di-*tert*-butyl dicarbonate was used to protect the N³ position, before acid hydrolysis of 2'-O-TMS to afford intermediate **165**. Activation of the 2'-OH by methanesulfonyl chloride, followed by fluoride mediated silyl protecting group removal and subsequent re-protection of the 3' and 5' alcohols as their tetrahydropyranyl ethers, delivering **166** in 42% yield from **165**.



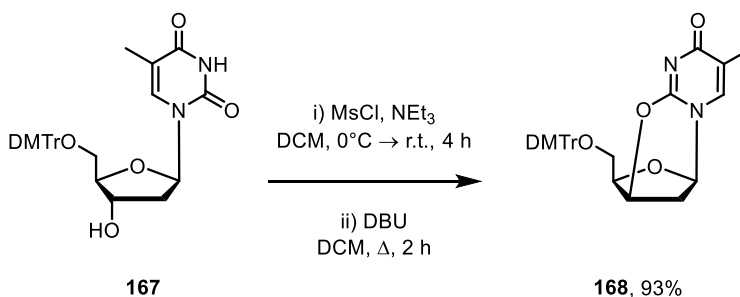
Scheme 1.58: Synthesis of radiolabelling precursor **166**.

166 was fluorinated by [^{18}F]KF with K_{222} in acetonitrile, followed by acid hydrolysis of the THP ethers and N^3 -Boc group (Scheme 1.59), in low radiochemical yield – lower than that of the early-stage fluorination – but high molar activities were achieved (*c.f.* $\geq 1.8 \text{ Ci mmol}^{-1}$)



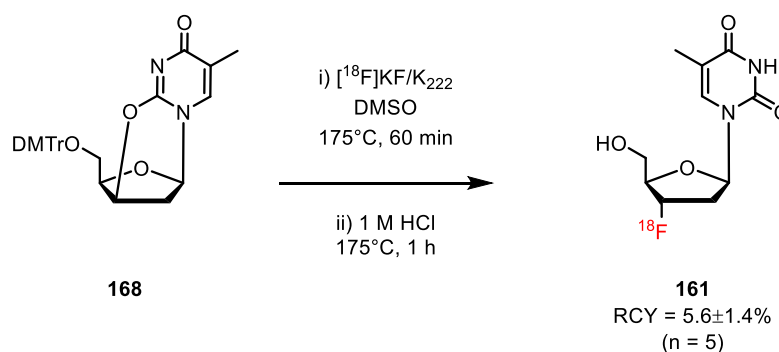
Scheme 1.59: Synthesis of [^{18}F]FMAU (**160**) by late-stage radiofluorination of **166**.

Eisenhut and co-workers reported the synthesis of 3'-deoxy-3'-[^{18}F]fluoro-thymidine in 2000,^[105] starting from commercially available 5-O-(4,4'-dimethoxytrityl)thymidine (**167**, Scheme 1.60). Treatment of **167** with methanesulfonyl chloride activated the 3'-hydroxyl group, such that upon reacting with DBU formed anhydro compound **168**.



Scheme 1.60: Synthesis of radiolabelling precursor **168**.

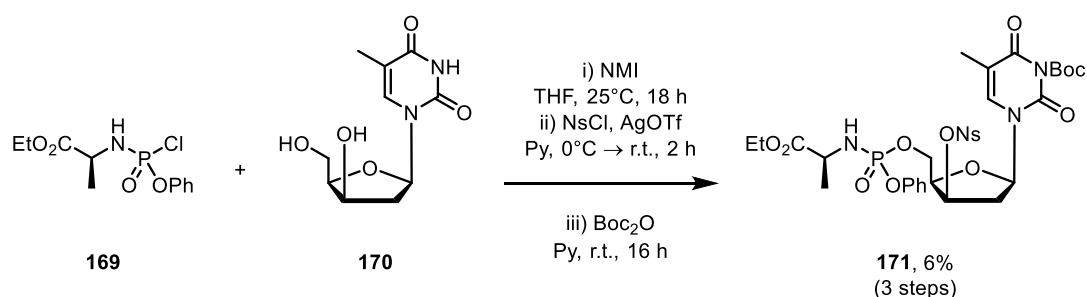
Sequential treatment of **168** with [^{18}F]KF with K_{222} in anhydrous DMSO and cleavage of 5'-O-(4,4'-dimethoxy)trityl protecting group furnished [^{18}F]FLT (**161**) in an average radiochemical yield of 5.6% over 5 runs (Scheme 1.61). The method cleverly manipulates the formation of anhydro intermediate **168** such that two nucleophilic displacements at the 3'- position deliver the desired configuration of the radiofluorinated product, and not its diastereomer. Simultaneously, the use of **168** requires no protecting group at the N^3 position.



Scheme 1.61: Synthesis of [^{18}F]FLT (**161**) by late-stage radiofluorination of **168**.

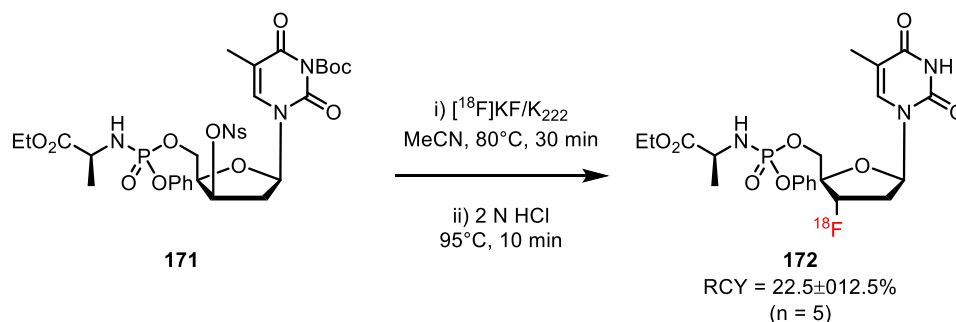
While Alauddin commented on the possible formation of the 2,2'-anhydro intermediate, they ruled it out as a competitive pathway during the radiofluorination as it was not detected by radio-HPLC, nor did it match the reference for its non-radioactive analogue.^[104]

Recently, Cavaliere *et al* demonstrated that late-stage fluorination may be applied to 5-O-phosphorylated precursors,^[106] despite the strength of P-F bonds.^[107] The authors also targeted [^{18}F]FLT, but as the ProTide derivative such that drug delivery may be quicker after radiofluorination, bypassing the rate limiting phosphorylation of 5'-OH. Combining 3- β -hydroxy thymidine congener with chlorophosphoramidate **169** in the presence of NMI in anhydrous THF, followed by sequential activation of the 3'-OH by *para*-nosylchloride and protection of N³ by Boc₂O to yield radiolabelling precursor **171**, in 6% yield over 3 steps (Scheme 1.62).



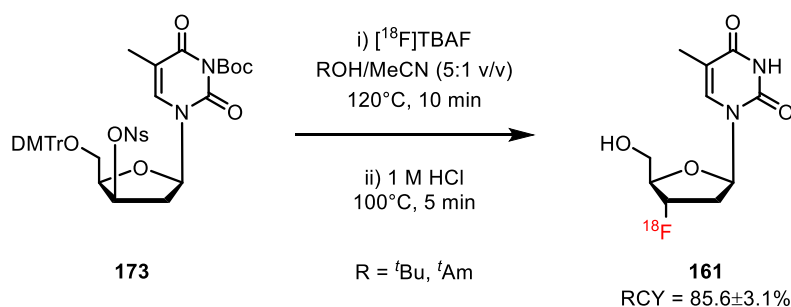
Scheme 1.62: Preparation of precursor **171** for radiolabelling.

The authors then investigated the [^{18}F]fluorination of **171** and found that [^{18}F]FLT ProTide **172** could be afforded in an average radiochemical yield of 22.5% over 5 runs (Scheme 1.63). High radiochemical purities ($\geq 97\%$) and specific activity of 56 GBq mol⁻¹ were obtained for **172**, with a total time of 130 minutes for synthesis.



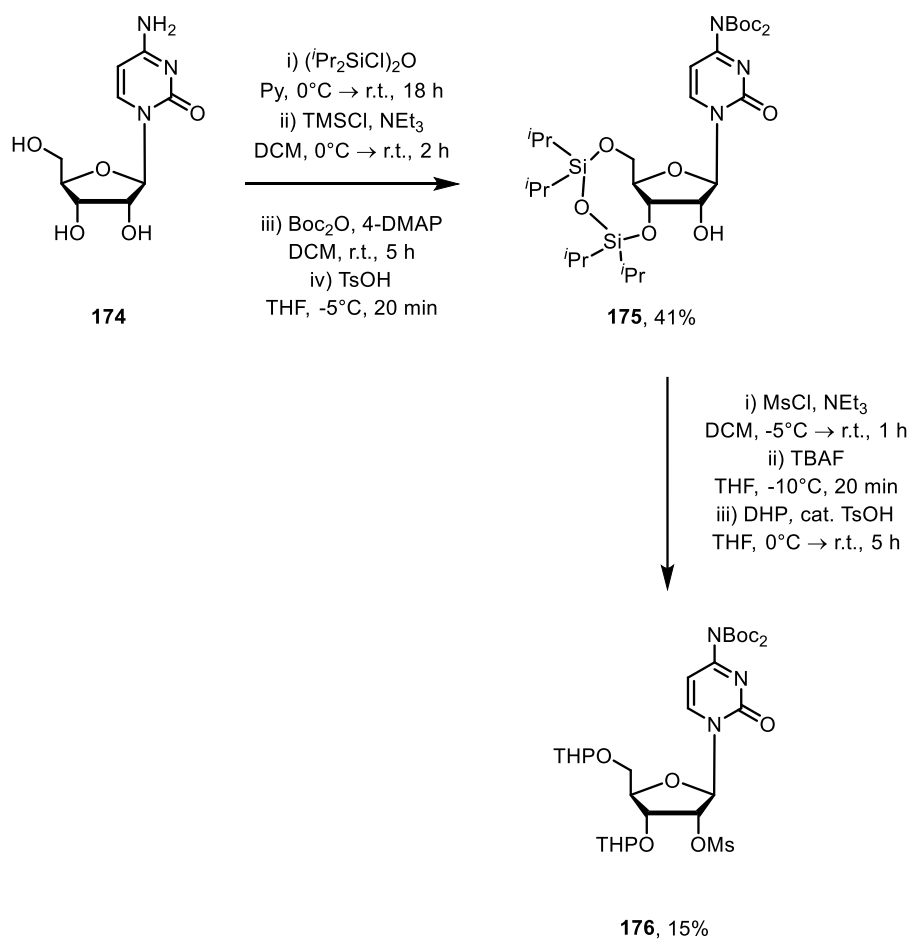
Scheme 1.63: [^{18}F]Radiolabelling of precursor towards the synthesis of [^{18}F]FLT ProTide **172**.

Investigators in Korea combined the aforementioned potential to execute nucleophilic fluorination substitution in protic media by synthesising [^{18}F]FLT, with different fluoride counterions. Shown in Scheme 1.64 is the radiosynthesis of **173** by [^{18}F]TBAF and use of *tert*-butanol or *tert*-amyl alcohol as cosolvent, followed by protecting group removal by acid treatment. [^{18}F]FLT was synthesised in high radiochemical yield and purity (98.5±1.2%), although the number of repeats was not noted in the report.^[108,109]



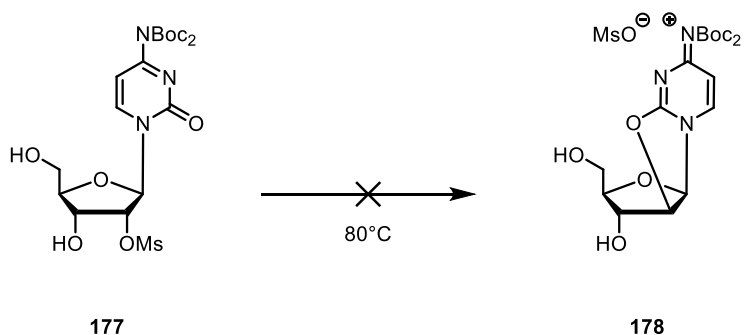
Scheme 1.64: Synthesis of [^{18}F]FLT from **173** using protic solvent and [^{18}F]TBAF.

Meyer *et al* employed a similar strategy to Alauddin in the construction of precursor **176** towards the synthesis of [^{18}F]FAC, shown in Scheme 1.65. The hydroxyl motifs of cytidine (**174**) were sequentially protected as the silyl ethers, using TIPSDCl₂ at the 3' and 5' alcohol positions and trimethylsilylchloride to protect the 2'-OH. Next, di-*tert*-butyl dicarbonate was utilised to mask the N⁴ position prior to 2'-O-TMS removal by *para*-toluene sulfonic acid to deliver intermediate **175** in 41% across 4 steps. Activation of the 2-OH by methanesulfonate chloride, tethered 3',5'-O-silyl ether removal by TBAF and reprotection by dihydropyran and catalytic TsOH yielded precursor **176** in 15% yield over 3 steps, ready for radiofluorination.



Scheme 1.65: Synthesis of radiolabelling precursor **176**.

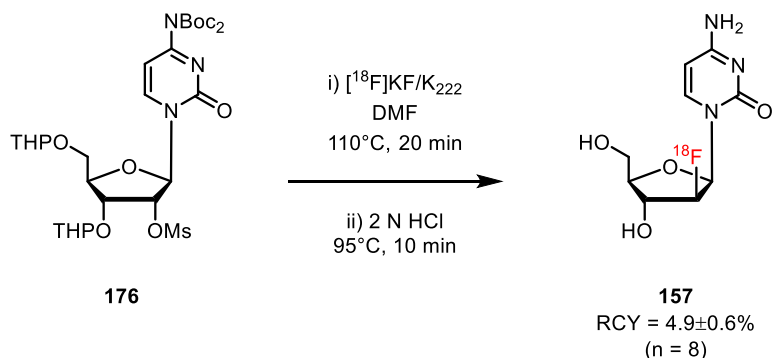
Noting the previous observations, the authors probe the potential formation of the 2,2'-anhydro product from precursor **176** (obtained after TBAF deprotection), by heating it to eliminate mesylate anion from the 2' position, shown in Scheme 1.66.



Scheme 1.66: Attempted formation of **178** by thermolysis of **177**.

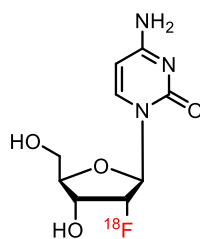
Notably, no thermolysis of the starting material was detected as analysed by ^1H NMR. This could be ascribed to the imide-like nature of the N^4 position, where the lone pair of the nitrogen is involved in both amide motifs hence is has increased delocalisation and is less able to participate in 2,2'-anhydro intermediate formation.

Optimisation of the radiofluorination of **176** identified heating the azeotropically dried $[\text{}^{18}\text{F}]\text{KF}$ at 110°C in DMF as the best conditions, delivering the intermediate in $9.4\pm 0.8\%$ ($n = 3$), by radio-TLC. Lower temperatures were less efficient in inducing the $[\text{}^{18}\text{F}]$ fluorination, while increasing temperature or length of reaction were deleterious to the intermediate production. Acid mediated removal of the 3',5'-O THP ethers and N^4 -Boc moieties successfully yielded $[\text{}^{18}\text{F}]\text{FAC}$ (**157**) in an overall radiochemical yield of $4.9\pm 0.6\%$ over 8 runs (Scheme 1.67). The authors note that shorter times were investigated for the deprotection step but returned decreased yields of **157**. Following isolation by semi-preparative HPLC, target compound **157** was isolated in high purity ($\geq 98\%$) with molar activity of $\geq 63 \text{ GBq mol}^{-1}$, delivering 0.75 – 0.86 Gbq of $[\text{}^{18}\text{F}]\text{FAC}$ after a total synthesis time of 168 minutes.



Scheme 1.67: Sequential $[\text{}^{18}\text{F}]$ fluorination and acid treatment of **176** to afford $[\text{}^{18}\text{F}]\text{FAC}$ (**157**).

The authors probed the reason for lower radionuclide incorporation upon increased reaction heating. It was determined to be due to competitive formation of the undesired stereoisomer **179** (Figure 1.68), which suggests *in situ* formation of 2,2'-anhydro intermediate at elevated temperatures, in agreement with other reports.^[104,105]



179

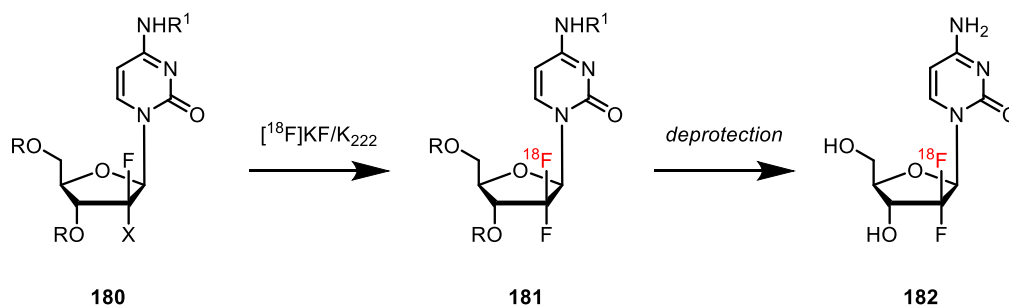
Figure 1.68: Formation of undesired stereoisomer of [¹⁸F]FAC during radiofluorination.

2 – Research aims and objectives

The ultimate aim of the research is to develop a robust, reliable synthetic method towards an appropriate radiolabelling precursor, for the synthesis of [^{18}F]gemcitabine (**182**, Scheme 2.01). The synthesis of [^{18}F]gemcitabine would offer critical *in vivo* data on patients with cancer and specifically pancreatic cancer, where the mortality rates are very high. Not only would **182** demonstrate the same pharmacokinetic characteristics as gemcitabine, but would also allow for patients to be screened to determine whether gemcitabine could be a viable treatment option. Additionally, such PET probes require significantly less material to be administered versus standard chemotherapeutics, putting the patient under less distress.

This is envisioned by fluorine-18 substitution of an appropriate leaving group from precursor **180**, followed by removal of any protecting groups. Careful consideration of the chosen leaving group is required, as improved ability to leave is cancelled out by side reactions such as elimination. Additionally, the precursor would ideally be stable to air and moisture, such that sufficient amounts may be synthesised at a given time. Critically, the collaborative nature of the project allowed access to [^{18}F]fluoride, such that nucleophilic fluorination was the method of incorporating fluorine-18.

Ideally, a late stage radiofluorination strategy would be employed, in order to capitalise on the amount of radioactive material produced, which would require a new synthetic route towards **180**. Radiofluorination at the 2' position is also challenging, given the targeted nucleophilic substitution at a tetra substituted carbon. As such, non-radioactive fluorination test reactions will also be conducted to evaluate the viability of the fluorination methods, along with synthesis of authentic, non-radioactive samples for comparison and method development.



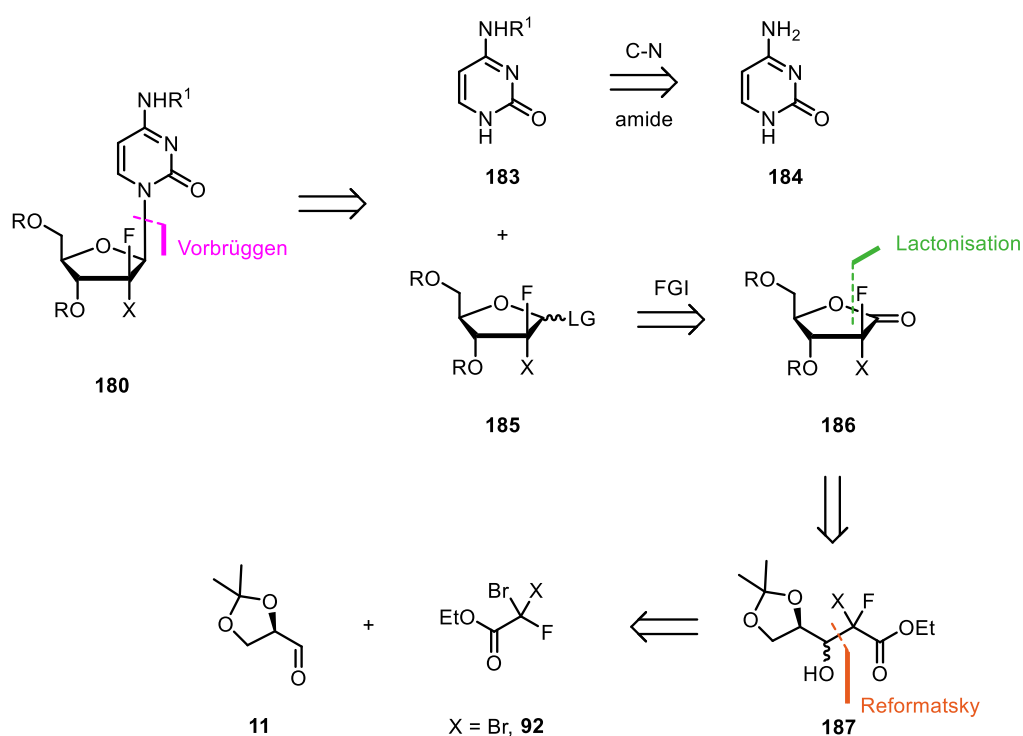
Scheme 2.01: Proposed radiofluorination and deprotection of precursor **180** towards [^{18}F]gemcitabine.

3 – Results and discussion

3.1 – Synthetic route 1

3.1.1 – Disconnection strategy

The retrosynthetic design (Scheme 3.01) for the radiolabelling precursor began by disconnecting the N^4 -functionalised cytosine nucleobase **183** – derived from cytosine (**184**) from the tetrahydrofuryl ring of **180**, which would require an activated lactol type compound (**185**), with the 3' and 5' hydroxyl moieties appropriately protected. **185** could be accessed from the lactone, which in turn may be achieved by ring closing lactonisation. The (protected) β -hydroxy ester **187** could then be synthesised akin to Hertel's original synthesis,^[8] beginning with 2,3-*O*-isopropylidene-D-glyceraldehyde^[110] (**11**) and combining with ethyl 2,2-dibromo-2-fluoro acetate (**92**) by way of a Reformatsky-type reaction.

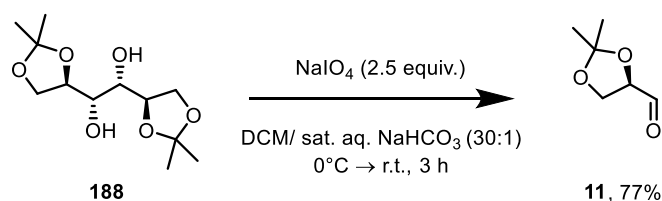


Scheme 3.01: Retrosynthesis and disconnection of **180**.

3.1.2 – Synthesis

Thus, drawing inspiration from Hertel's seminal work,^[8] initial investigations began with D-mannitol diacetonide **188**, which was treated with 2.5 equivalents sodium periodate in

a biphasic mixture of DCM and aqueous NaHCO₃, to furnish 2,3-*O*-isopropylidene-D-glyceraldehyde^[110] **11** in 77% yield. This reaction to cleave the vicinal diol was also scalable, producing 60 mmol after purification by distillation. It was noted that **11** was unstable when isolated and couldn't be stored long term (greater than one month), as degradation was observed by NMR, in accordance to the literature.^[110] The optical purity of the aldehyde was determined as $[\alpha] = +42^\circ$ in DCM, agreeing with that reported by Ryall and coworkers,^[111] confirming the correct stereochemistry was present prior to formation of lactone derivative **186**.

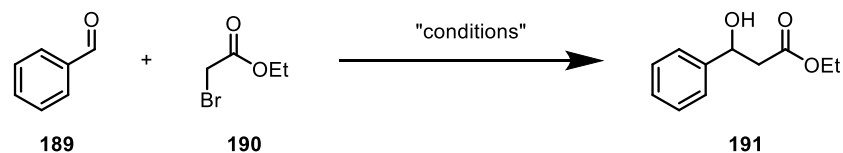


Scheme 3.02: The synthesis of **11** from D-mannitol diacetonide (**188**).

Strategies considered for the addition to **11**, such as the enolate of the corresponding functionalised ester were discounted due to competing addition reactions such as intermolecular Aldol reaction and condensation. Analogous to that described by Hertel, a Reformatsky reaction of **92** with **11** would furnish the desired β -hydroxy ester. Use of the *in-situ* generated organozinc intermediate would also retain the necessary ester functionality for later lactonisation. However, due to the synthetic design strategy, incorporation of the leaving group was required at this early stage. While chloride was initially mooted for the radiofluorination due to its enhanced stability, bromide would provide an improved leaving group. Moreover, iodo equivalents would be desired, allowing for easier oxidative addition of zinc, but such compounds are not commercially available and the synthesis is non-trivial.

To ensure that the active organozinc was being formed and consumed, the reaction was simplified to benzaldehyde as the electrophile and ethyl bromoacetate as the latent nucleophile. A screen of activation methods were undertaken, presented in Table 3.01.

Activation of the zinc by iodine in dioxane with sonication for 5 minutes did not produce **191** by ¹H NMR analysis (Entry 1). Pleasingly, using 1.6 equivalents of zinc with 12 mol % TMSCl in Et₂O furnished the β -hydroxy ester in 56% isolated yield (Table 3.01, Entry 3). The amount of TMSCl required was subsequently investigated (entries 4-8), but did not demonstrate any improvement, with increased amounts returning diminished yields of **191**.



Entry	Zn [equiv.]	Activator [equiv.]	Solvent	Time [h]	Yield 191 [%] ^[a]
1	1.8	I ₂ (0.20) ^[b]	Dioxane [0.5 M]	0.083	-
2	1.6 ^[b]	TMSCl (0.12)	Et ₂ O [0.4 M]	16	(54)
3	1.6^[c]	TMSCl (0.12)	Et₂O [0.4 M]	16	(56)
4	1.6	TMSCl (0.05)	Et ₂ O [0.2 M]	16	37
5	1.6	TMSCl (0.10)	Et ₂ O [0.2 M]	16	46
6	1.6	TMSCl (0.15)	Et ₂ O [0.2 M]	16	51
7	1.6	TMSCl (0.20)	Et ₂ O [0.2 M]	16	48
8	1.6	TMSCl (0.25)	Et ₂ O [0.2 M]	16	41
9 ^[d]	1.6 ^[b]	-	-	2	70

Reaction conditions: benzaldehyde (1 mmol), ethyl 2-bromoacetate (1.2 equiv.), zinc (as specified), activator (as specified). ^[a] Yield determined by ¹H NMR using mesitylene as internal standard. Isolated yield in parentheses. ^[b] Granular zinc used. ^[c] 20-30 mesh zinc used. ^[d] Reaction conducted in mixer mill, benzaldehyde (1 mmol), ethyl 2-bromoacetate (1.2 equiv.), 30 Hz.

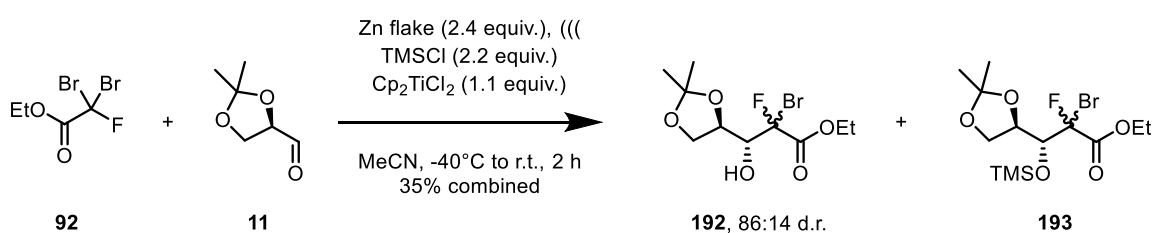
Table 3.01: Investigation on activators required for zinc activation for the production of **191**.

Interestingly, the reaction proceeded in the absence of external activator when the reagents were subjected to vibratory ball milling, delivering 70% NMR yield of the β -hydroxy ester.

Satisfied that active Zn⁰ was being produced, focus returned to the original substrates for the Reformatsky reaction. As such, taking commercially available ethyl dibromofluoroacetate (**92**) with the protected glyceraldehyde and zinc metal, and TMSCl as activator for zinc, delivered none of the target material after protic work up.

Organozinc reagents are known to be moisture sensitive and are commonly generated *in situ* and not isolated, so it was difficult to determine whether the active organozinc was being formed. Alternative activators such as 1,2-dibromoethane and acidic wash of the metal were also unsuccessful in making the reaction proceed.

Specifically focussing on aldehyde **11**, the lack of product formation would suggest it is not as reactive as benzaldehyde. This obstacle could be circumvented by a Lewis acid, akin to that used in the Mukaiyama aldol addition reaction.^[10] As such, employing 1.1 equivalents of bis(cyclopentadienyl) titanium (IV) dichloride with **11** to a sonicated suspension of zinc (2.4 equivalents), TMSCl (2.2 equivalents) and ethyl dibromoacetate (**92**, 2 equivalents) in MeCN at -40°C delivered a mixture of the β -hydroxy ester and the corresponding TMS protected ester in a combined 35% yield, separable by silica gel column chromatography. β -hydroxy ester **192** was isolated as a diastereomeric mixture, in a ratio of 86:14 by ^{19}F NMR.



Scheme 3.03 Optimised reaction of Cp_2TiCl_2 promoted Reformatsky of β -hydroxy ester derivatives **192** and **193**.

This observation suggests that TMSCl may serve a dual purpose here; both as activator of zinc and alcohol protecting group. It was also observed that an alkene by-product was being formed in the reaction, which was identified as **194**, resulting from a second oxidative addition of zinc and subsequent hydroxide elimination. A limitation of this approach is the diastereoselectivity of the nucleophile attack onto **11**, with both *syn* and *anti* isomers possible.

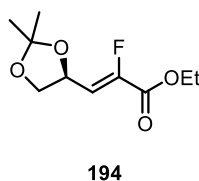
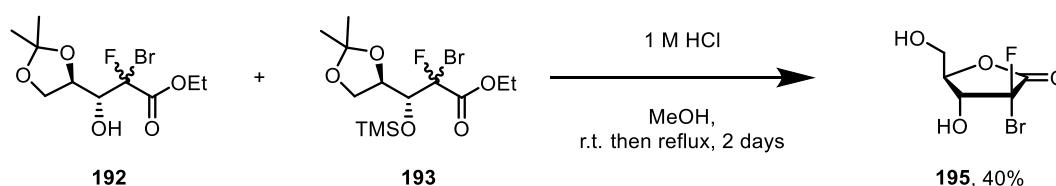


Figure 3.01: Structure of alkene **194** observed during crude ^1H NMR analysis of the reaction shown in Scheme 3.03.

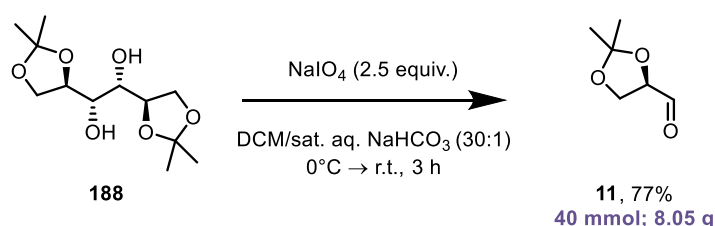
While the stereochemistry of the dihalo functionality does not need to be strictly defined, the configuration of the (silylated) alcohol is crucial given the need for the (*R*)-stereoisomer at the 3' position of gemcitabine. Yasuda and coworkers report that using Cp_2TiCl_2 enhances the selectivity of the diastereomer formation by way of facial discrimination.^[10] While a similar concept may be proposed here, it is worth noting that the incorporation of a larger bromine atom (vs fluorine) may reduce the selectivity imparted by the sterically incumbered Lewis acid, thus explaining the lower diastereoselectivity (86:14 d.r.) observed and yield compared to those reported. Additionally, the presence of alkene **194** demonstrates the potential reactivity of the α -bromo ester functionality with zinc – a classic example in the Reformatsky and Blaise reactions.

With the desired β -hydroxy ester in hand, concomitant deprotection of the acetonide functionality and cyclisation under acidic conditions of both **192** and **193** afforded lactone **195** in 40% isolated yield, depicted in Scheme 3.04. It was noted that the unprotected lactone was susceptible to decomposition, even when stored in the fridge.



Scheme 3.04: Concomitant acetal deprotection and lactonisation under acidic conditions.

Given the early stage nature of these reactions in the synthetic route, scale up reactions were undertaken. The oxidative cleavage of **188** was robust and could be successfully performed on 40 mmol scale yielding 8.05 g of pure aldehyde (Scheme 3.05), which was unsuitable for long-term storage. The Lewis acid aided Reformatsky reaction was unsuccessfully translated to larger scale reactions, with hydrolysis of the *in-situ* generated organozinc being observed by ^1H NMR. As such, an alternative synthetic strategy was explored to access the dihalogenated ribonolactone.

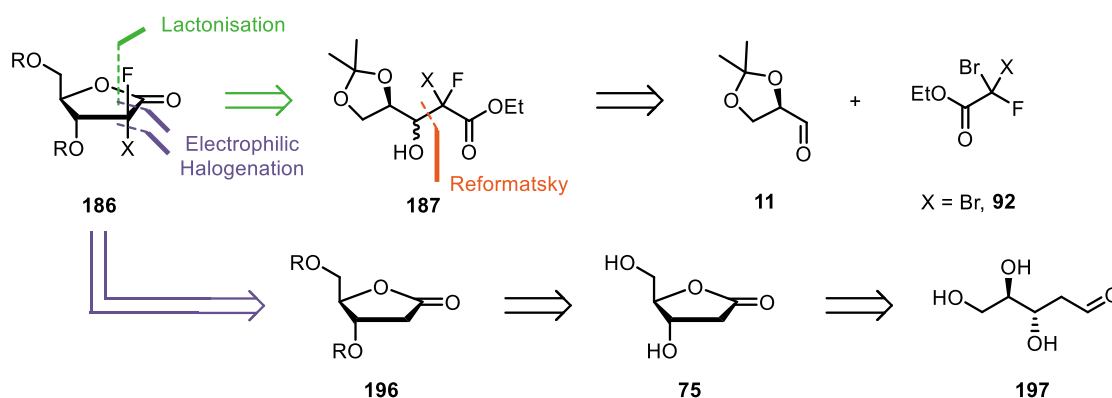


Scheme 3.05: Scale up of the oxidative cleavage of **188** by sodium periodate.

3.2 – Synthetic route 2

3.2.1 – Disconnection strategy

The initial disconnection strategy shown in Scheme 3.06 was based upon incorporating the geminal *di*-halo functionality from one of the starting materials (**92**) prior to formation of the lactone. Alternatively, formation of the 2-deoxy ribonolactone **75** would provide access to its halogenated congener via enolate chemistry using electrophilic sources of the halides, akin to the work demonstrated by Cen and Sauve.^[20] This approach could allow for improved diastereoselectivity at the 2-position, depending on the addition of the halogen electrophile, and increased potential for diversification and functionalisation by this step-wise, modular approach.

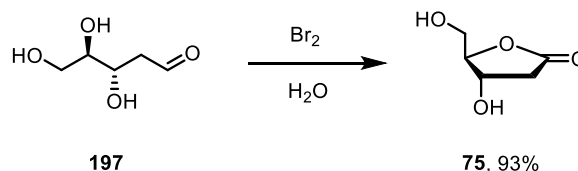


Scheme 3.06: Retrosynthesis and disconnection of **186**, by lactonisation (Synthetic route 1, green) or electrophilic halogenation (Synthetic route 2, purple).

3.2.2 – Synthesis

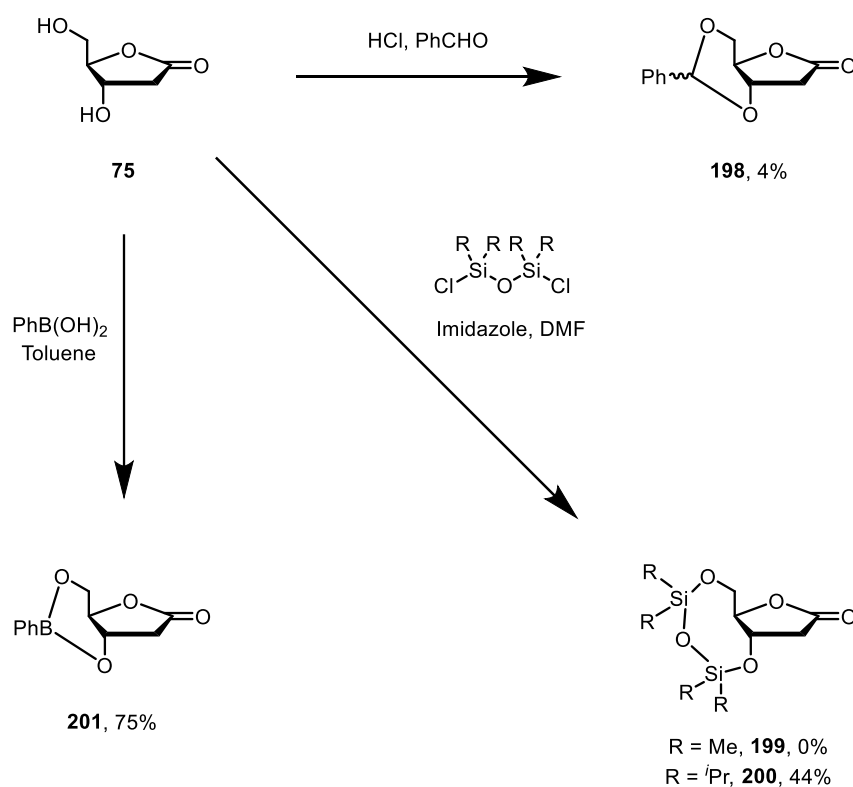
3.2.2.1 – Ring construction and protection

Beginning with commercially available 2-deoxy-D-ribose **197**, oxidative cyclisation with elemental bromine in the dark for 5 days furnished 2-deoxy-D-ribo-1,4-lactone **75** in 93% isolated yield, depicted in Scheme 3.07. Several previous syntheses in the literature use Ag_2CO_3 as an elegant choice of base during reaction work up – which acts to both neutralise the hydrobromic acid by-product and also precipitate AgBr , delivering pure product.^[112,113] It was found that using K_2CO_3 was just as effective, followed by purification of the crude mixture by silica gel column chromatography in 5% MeOH/EtOAc to afford pure **75**.



Scheme 3.07: Oxidative cyclisation of **197** by Br₂.

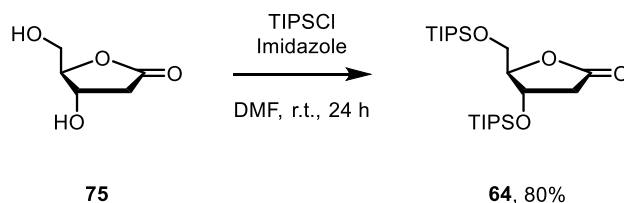
Next, appropriate protecting groups for the 3- and 5-hydroxyl groups needed to be selected. This could be conveniently achieved by capping both alcohols with the same protecting group, such as a boronate ester. As shown in Scheme 3.08, three different groups were employed: (i) boronate ester (**201**), from **75** with phenyl boronic acid in toluene at room temp; (ii) benzylidene acetal (**198**), and (iii) utilising 1,3-dichloro-1,1,3,3-tetraisopropylidisiloxane with γ -lactone **75** in DMF and imidazole to yield **200**. The synthesis of the analogous 1,1,3,3-tetramethyldisiloxane (**199**) was unsuccessful.



Scheme 3.08: Investigation of 3,5-O- capped protecting groups of **75**.

On balance and comparison of the three synthesised molecules it was decided that due to their low yield, continued synthesis of **198** and **199** would not be pursued.

In parallel, individual protecting groups for the hydroxyl moieties were investigated. As discussed previously, ester protecting groups have fallen foul of this ribonolactone α -functionalisation strategy due to competing elimination, rendering the requirement of bulky silanol-type protecting groups.^[114] Thus, drawing inspiration from Cen and Sauve's work,^[20] 2-deoxy-D-ribo-1,4-lactone **75** was protected as the silyl ether, from triisopropylsilyl chloride in DMF with imidazole as base, furnishing 80% of **64** after purification by column chromatography (Scheme 3.09).

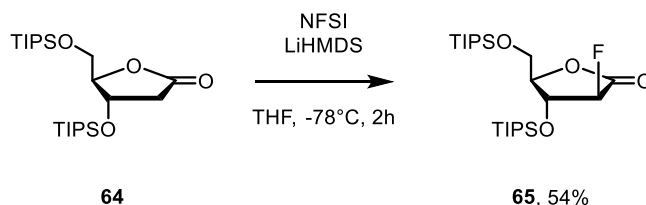


Scheme 3.09: The formation of **64** from **75** with TIPSCl under basic conditions.

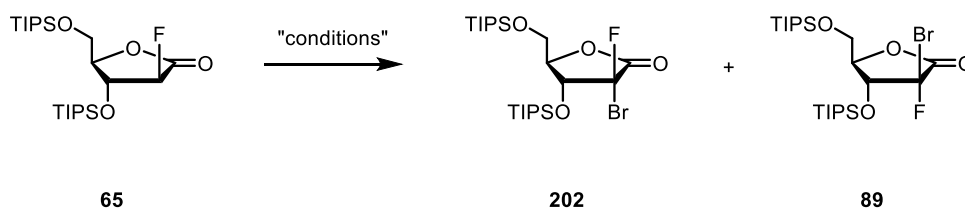
It was decided that due to the enhanced yield obtained for the *bis*-TIPS protection, in conjunction with literature precedent surrounding its use in the functionalisation of lactones that the disiloxane protection methodology would not be further investigated.^[20,23,24]

3.2.2.2 – α -halogenation

In the designed synthetic strategy, the introduction of an appropriate leaving group for ^{18}F displacement was targeted. As a start point, halides were focussed upon, as they should readily undergo the relevant substitution. As both fluoride and leaving group halide needed to be installed, it was decided that fluorination, followed by subsequent bromination would be a preliminary strategy. Depicted in Scheme 3.10 is reaction of **64** with NFSI and LiHMDS, which furnished mono-fluoro lactone **65** in 54% yield, as a single diastereomer, as previously reported.^[20]



Scheme 3.10: The electrophilic fluorination of **64** by NFSI and LiHMDS.



Entry	Conditions	Yield of 65 ^[a]	Yield of 202 ^[a]	Yield of 89 ^[a]
1	NEt ₃ (6 equiv.), TMSOTf (3 equiv.) then NBS (1.5 equiv.) DCM, 0°C → r.t., overnight	(>95%)	-	-
2	NBS (1.5 equiv.), LiHMDS (2 equiv.) THF, -78°C, 180 min	>95%	-	-
3	NBS (1.5 equiv.), KHMDS (2 equiv.) THF, -78°C, 15 min	67	15%	18%
4	NBS (1.5 equiv.), KHMDS (2 equiv.) THF, -78°C, 180 min	>95%	-	-

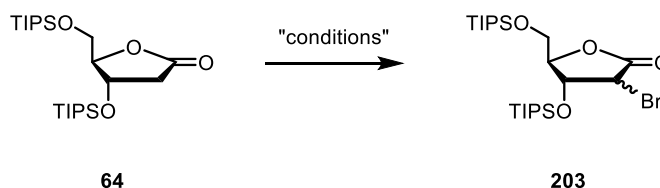
^[a] Yield measured by ¹⁹F NMR with α,α,α -trifluorotoluene.

Table 3.02: The screened bromination conditions of **65** by NBS.

From **65**, installation of bromine via electrophilic NBS was attempted, initial efforts proceeded *via* silyl enol ether formation by treatment with TMSOTf and NEt₃ (Table 3.02), only to return the starting material in quantitative amount. This result suggests that the pK_a of the α -proton is too high to be deprotonated by triethylamine, even in the presence of Lewis acidic TMSOTf. Next, stronger bases were probed. LiHMDS did not facilitate the bromination of **65** (Entry 2), potentially due to lithium-halogen exchange or bromine abstraction by LiHMDS.^[24,115] It is worth noting however in Voight's synthesis of ABBV-168 (**99**, Scheme 1.41), LiHMDS promoted bromination was achieved.^[24] Switching to KHMDS proved promising, with increased formation of the *gem*-dihalo lactone (Table 3.02, Entry 3). The lactone was formed in a diastereomeric ratio of 9:10 of (*R*):(*S*) at the 2-position by ¹⁹F NMR,^[24] although the configuration of the α position was unimportant at this point. Unfortunately, upon increasing the reaction time to 3 hours (Table 3.02, Entry 4), no product formation was observed.

These disappointing results forced a rethink of the α -halogenation strategy, suggesting it might be preferential to brominate first, and then fluorinate with an appropriate electrophilic agent.

Utilising previously explored brominating conditions, **64** was converted efficiently into the mono-Br lactone **203**, in a diastereomeric ratio of 2:1 of arabino (*S*)-**203** to ribono (*R*)-**203**, assigned by 2D NOESY and COSY ^1H NMR of each pure diastereomer. Conclusively, it was a through space interaction between H^a and H^b that allowed one of the diastereomers to be assigned as the (*R*)-ribo sugar, the major product. Allowing the reaction to run overnight provides increased yield of **203**, in a ratio of 1:0.7 arabino:ribo respectively (Entry 2).



Entry	Conditions	Yield of 203 ^[a]
1	NEt ₃ (6 equiv.), TMSOTf (3 equiv.) then NBS (1.5 equiv.) DCM, 0°C → r.t., 3 h	62%
2	NEt ₃ (6 equiv.), TMSOTf (3 equiv.) then NBS (1.5 equiv.) DCM, 0°C → r.t., overnight	70%
3	NEt ₃ (6 equiv.), TMSOTf (3 equiv.), then NBS (1.5 equiv.) DCM, 0°C → r.t., overnight ^[b]	45%
4	NEt ₃ (6 equiv.), TMSOTf (3 equiv.), then NBS (1.5 equiv.) DCM, 0°C → r.t., overnight ^[c]	55%
5	NEt ₃ (6 equiv.), TMSOTf (3 equiv.), then NBS (1.5 equiv.) DCM, 0°C → r.t., overnight ^[e]	<5% ^[d]
6	DBU (6 equiv.), TMSOTf (3 equiv.), then NBS (1.5 equiv.) DCM, 0°C → r.t., overnight	- (>95% 64)
7	(BrCl ₂ C) ₂ (1.3 equiv.), LiHMDS (1.5 equiv.) THF, -78°C, 4 h	19% (16% 64) (46% 206)

^[a] Isolated yield. ^[b] Stabilised DCM used. ^[c] Reaction ran in the dark. ^[d] Analysis of crude reaction mixture. ^[e] TMSOTf added first, then NEt₃

Table 3.03: The screened bromination conditions of **64**.

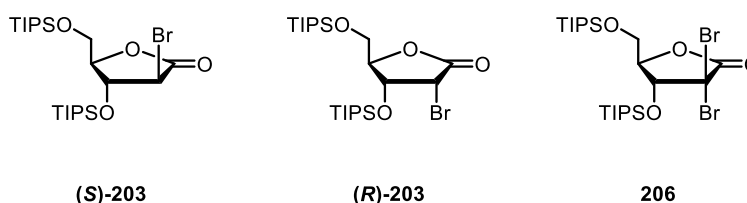
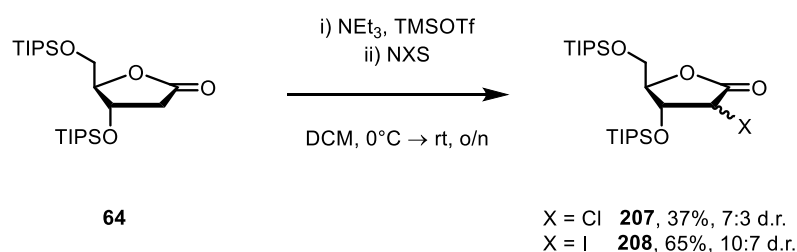


Figure 3.02: The structures of brominated products from the conditions screened in Table 3.03.

The excess of (*S*)-**203** could be rationalised by preferential *si* approach of NBS from the top face of the *trans* enolate, minimising any steric clash with the 3-*O*-TIPS group. Despite this, a large amount of the 2-deoxy 2-bromo ribonolactone (*R*)-**203** is formed, which may be attributed to the *re* addition of bromine to the enolate, as NBS would not be considered a bulky electrophile. Alternatively a potential radical mechanism may be in play, as NBS can split homolytically and is employed in radical reactions such as the Wohl-Ziegler reaction.^[116] It is noteworthy that when stabilised DCM was used (Table 3.03, Entry 3), which contains amylene as stabiliser, diminished yield of the brominated product was observed – the amylene may be acting as a bromine radical scavenger. As a control experiment, the reaction was also conducted in the dark (Entry 4) which would inhibit homolytic cleavage of NBS therefore the possibility of a radical reaction. Fortunately, this led to a good yield of the target material although lower than the optimal conditions of Entry 2 – again as a mixture of diastereomers. Markedly, adding TMSOTf before NEt₃ led to a complex mixture when the crude reaction mixture was analysed by ¹H NMR, with trace desired compound. This unwanted reactivity infers that initial exposure of **64** to Lewis acidic TMSOTf may lead to coordination across multiple Lewis basic sites within the starting material. Subsequent addition of base could then access a range of undesired products, such as those from ring opening of the lactone or elimination reactions.

After purification by column chromatography, the remaining isolated material is starting material **64**, indicating incomplete conversion. The lack of complete conversion may either be due to insufficient NBS equivalents or a low concentration of silyl enol ether formed *in situ*. To probe this hypothesis, DBU was employed as a stronger base (Entry 6). Unfortunately, this control did not improve the yield of **203**, returning near quantitative starting material. Use of 1,2-dibromotetrachloroethane with LiHMDS (Entry 7) successfully formed 19% isolated yield of desired compound **203** (1.5:1 arabino:ribo ratio), and 16% of starting material **64**. However, the yield was significantly diminished compared to the NEt₃/TMSOTf/NBS strategy, with the majority of the isolated material being the *gem*-dibromo lactone **206**, returned in 46% isolated yield.

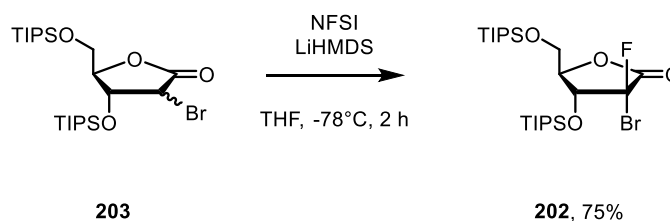
Satisfied that, of the explored conditions in Table 3.02, Entry 2 was optimal for α -bromination, alternative leaving groups were investigated. By using NBS, other halides may be targeted using their respective *N*-halo-succinimide, illustrated in Scheme 3.11. Employing the silyl enol ether formation conditions used previously, *N*-chlorosuccinimide was reacted with γ -lactone **64**, to form the α -chloro congener **207**, in 37% yield. Similarly, 2-deoxy-2-iodo-3,5-bis-*O*-TIPS- γ -lactone **208** was synthesised in good yield (65%).



Scheme 3.11: The halogenation of **64** by *N*-halosuccinimides

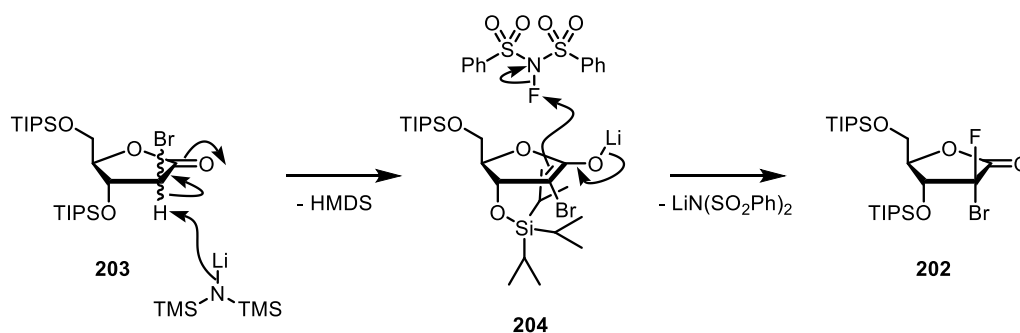
However, due to the lack of stability of alkyl iodides and their potential for decomposition, this synthetic pathway was discounted. Given that bromide is a better leaving group than chloride, and in the context of the goal of the project, it would potentially lead to a better candidate as a radiolabelling precursor for displacement by fluoride. Therefore, while α -chloro analogue **206** was a viable option in the designed synthesis, only bromo **203** was pursued for further development.

With appropriate conditions for the formation of **203**, attention then turned to fluorination. Adapting Liotta's conditions,^[117] reacting **203** with NFSI in THF at -78°C under basic conditions formed the desired ribonolactone in good yield, with no remaining starting material. (Scheme 3.12).



Scheme 3.12: The NFSI/LiHMDS mediated fluorination of **203**.

Remarkably, a single diastereomer is formed (determined by ^{19}F NMR) with the fluorine believed to be on the top face of the lactone. Due to the requirement of bulky TIPS-O protecting groups, the physical state of all but one of the functionalised lactones are sticky liquids or oils, thus absolute configuration by X-ray analysis has not been possible.



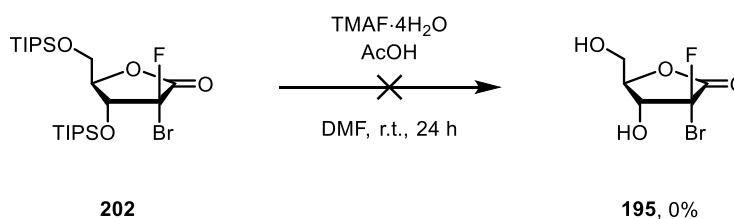
Scheme 3.13: The proposed reaction mechanism explaining the diastereoselective formation of **202**.

Considering the reaction mechanism (Scheme 3.13) one can rationalise the formation of the single diastereomer: Following α -deprotonation by LiHMDS, the lithium enolate could rationally be trapped by the electrophilic NFSI from both the *re* and *si* face of intermediate **204**. However, given the steric bulk 3-O-TIPS group which essentially blocks the *si* addition of fluorine, similar to what was observed for the α -bromination. In addition, the bulky nature of NFSI will likely play a role in reinforcing preference for *re* addition of the electrophile is the only outcome. By comparison, Voight's studies delivered the opposite diastereomer which had notably different ^{19}F NMR shift of -135.61 ppm, versus -127.53 ppm for **202**.^[24] Notably, no loss of the α -Br is observed, either by bromide elimination or bromine extraction by LiHMDS.

3.2.2.3 – Lactone deprotection

While confident in the assignment of relative stereochemistry after electrophilic fluorination, and agreement with other precedent literature data,^[24] absolute configuration by X-ray analysis would conclusively assign the configuration at the α -position. While protecting the 5- and 3- hydroxyl groups as their triisopropyl silyl ethers was necessary for the α functionalisation, downstream chemistry did not require such bulky groups. In addition to this, due to their lipophilic nature, most of the protected lactones discussed present themselves as viscous oils in physical appearance thus rendering them unsuitable for analysis by crystallographic methods. Deprotection of the silyl ethers and reprotection may allow for such analysis while not hindering further synthesis.

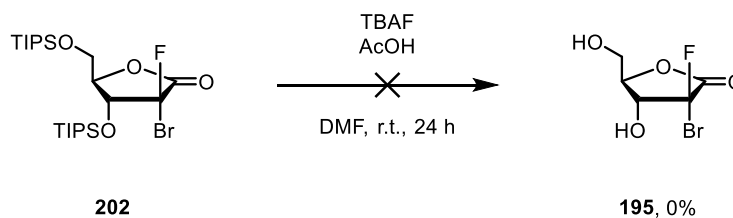
Subjecting **202** to tetramethylammonium fluoride tetrahydrate in combination with acetic acid in DMF consumed all starting material by $^{19}\text{F}\{^1\text{H}\}$ NMR with reference to α,α,α -trifluorotoluene as internal standard, reaction shown in Scheme 3.14. As expected, formation of triisopropyl silyl fluoride is observed, with a peak at -185.4 ppm,^[118] at 82% NMR yield. While the deprotection was successful, the only other environment of note was two singlets at -201.0 and -201.2 ppm, at 50% and 30% NMR yield respectively. Troublingly, this is a similar shift to that observed for the mono-fluorinated ribonolactone **65**, whereby the two singlets arise from the two possible diastereomers of the monofluorinated compound.



Scheme 3.14: The TMAF mediated deprotection of **202**.

This observation suggests that deprotection was successful but has potentially been accompanied by debromination. GC-MS analysis of the crude mixture revealed a peak corresponding to a mass of 230/231 m/z. This peak equates to the mass of target compound **195**, demonstrating that some degree of desired product formation may have occurred, in amounts detectable by GC-MS. Crucially, the ^{19}F NMR data didn't match that for the previously synthesised 2-deoxy-2-bromo-2-fluoro-ribose (195), therefore the current deprotection strategy was ultimately unsuccessful.

Changing to TBAF as the fluoride source (Scheme 3.15) resulted in an increased 94% NMR yield of TIPSF. Again, all starting material was consumed, returning 23% and 48% NMR yield of the suspected monofluorinated diastereomers.

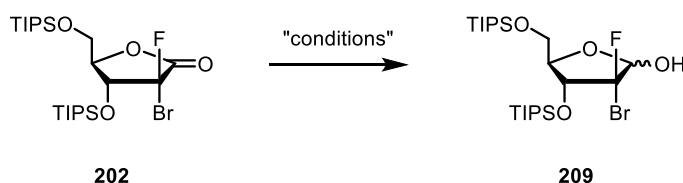


Scheme 3.15: The TBAF mediated deprotection of **202**.

Unfortunately, it seemed although the deprotection conditions were effective in removing the bulky silyl ether protecting groups, they were not compatible with the ribonolactone, possibly leading to degradation of the resulting *in situ* compounds. Therefore, changing to an alternative protecting group for later reactions – and potential crystallographic analysis – was not feasible at this stage and not pursued further.

3.2.2.4 – Mesityl-*O*-lactol formation

With the desired *gem*-dihalo functionality installed, reduction of the lactone to the γ -lactol was targeted. Mild reductants were required, as ring opening of the lactone could be envisaged and such side reactions would want to be avoided. As such, **202** was treated with DIBAL-H in toluene, producing **209** in 67% isolated yield. Although successful, this strategy seemed quite wasteful given the need to use 7 equivalents of reductant. Therefore in an attempt to be more economical, akin to Chou's synthesis,^[13] lithium tri-*tert*-butoxy aluminium hydride was utilised as the reducing agent of choice, forming lactol **209** in quantitative yield.



Entry	Conditions	Yield of 209 ^[a]
1	DIBAL-H (7 equiv.) Toluene, -78°C, 2 h	67%
2	LiAl(O ^{<i>t</i>} Bu) ₃ H (1.2 equiv.) THF/Et ₂ O, 0°C → r.t., 4 h	>95%

^[a] Isolated yield.

Table 3.04: The reduction of **202** to lactol **209**.

It was noted that the reaction proceeded more smoothly when conducted in a mixed solvent system of Et₂O/THF (4:1), resulting in a cleaner crude ¹H NMR. **209** was isolated as a 71:29 ratio of diastereomers by ¹⁹F NMR. The diastereomeric ratio remained the same even after months of storage in the fridge, despite the potential for anomerisation. Perhaps surprisingly, the diastereomeric ratio was the same using both DIBAL-H and LiAl(O^{*t*}Bu)₃H. The diastereomers – shown in Figure 3.03 – are inseparable by column chromatography, so both were carried forward for the next reaction.

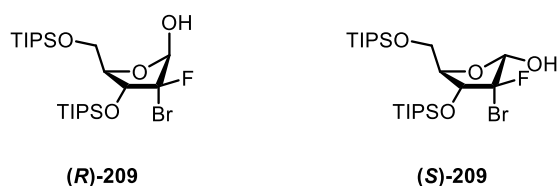
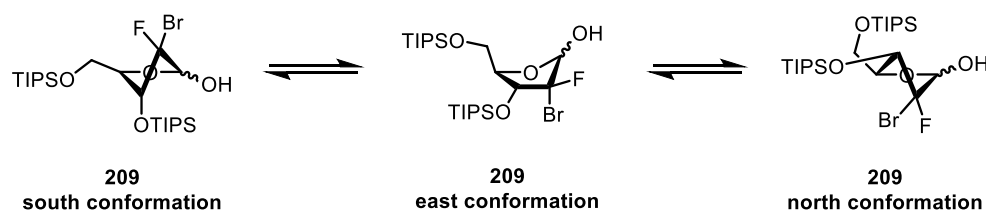
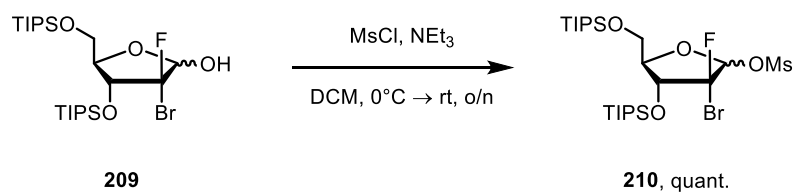


Figure 3.03: The configuration of the two diastereomers of **209**.

Interestingly, the multiplicity of ^{19}F shifts demonstrates that each diastereomer of lactol **209** has inherently different interactions with the neighbouring protons. One diastereomer exhibits a doublet of doublets at -120.62 ppm in the non-proton decoupled ^{19}F NMR, which is the expected multiplicity given two vicinal protons, resulting in two $^3J_{\text{F-H}}$ coupling constants of 11.1 and 5.8 Hz. Interestingly, the second diastereomer only demonstrates a doublet at -127.34 ppm, with a $^3J_{\text{F-H}}$ of 12.8 Hz. This suggests that the conformation of this diastereomer shows no detectable coupling between the fluorine atom and the vicinal hydrogen atoms, potentially stemming from a near 90° dihedral angle within the strained conformation, or that the magnitude of the coupling is beyond the sensitivity of the NMR spectrometer. The 2-deoxy furanose ring is unlikely to sit as depicted in general, in an east conformation (Scheme 3.16, centre **209**). The compound will preferentially sit in either a south (*C2-endo/C3-exo*) or north (*C2-exo/C3-endo*) conformation, depicted in Scheme 3.16. As a result, the fluorine at the 2-position may not interact with the vicinal hydrogen atoms, hence explaining the origin of the observed multiplicities.



Scheme 3.16: The potential extreme north/south conformations of **209**.

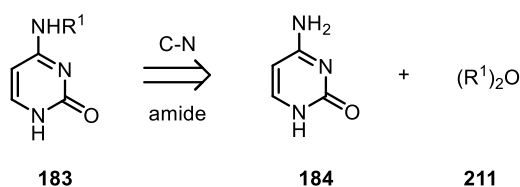


Scheme 3.17: The formation of **210** by basic mesylation of lactol **209**.

γ -lactol **209** was subsequently treated with methane sulfonyl chloride in DCM with NEt_3 as base, forming the mesylated lactol **210** in quantitative yield, without the need for purification (Scheme 3.17). It was found that washing with water during work up of the reaction resulted in decreased product yield, causing hydrolysis of **210** and returning undesired starting material. Again, the compound was formed in a diastereomeric mixture, on this occasion in a ratio of 59:41. This observation suggests increased anomerisation compared to lactol **209**, arising from the increased leaving group ability of the mesylate vs. hydroxide. Interestingly, the ratio of the diastereomers remains constant after long term storage in the fridge, demonstrating no change in equilibrium between the two diastereomers.

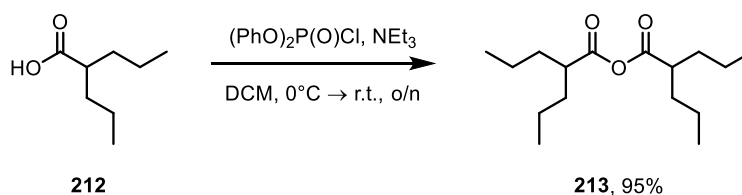
3.2.2.5 – Glycosylation

With mesylated lactol **210** in hand, attention turned towards the Vorbrüggen glycosylation reaction.^[119–122] With the observed selectivity in the developed ribonofuranose synthetic methodology, the procedure could well be applied towards the synthesis of a range of nucleosides. With the focus of gemcitabine in mind, the pyrimidine cytosine was targeted for ring appendage. In order to improve the efficiency of the ring appending reaction, the N^4 functionality of the cytosine nucleobase was protected as the amide (Scheme 3.18). At this point, considering the desire to improve the lipophilicity of these chemotherapeutic agents, cytosine was protected as both the N^4 -acetamide and N^4 -2-propylpentamide (henceforth referred to as N^4 -valproamide).



Scheme 3.18: The proposed synthesis of N^4 functionalised cytosines by reacting **184** with anhydride **211**.

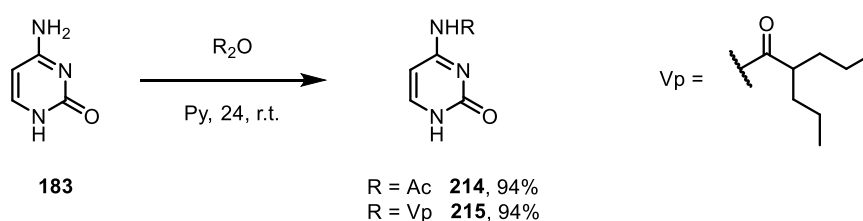
The use of valproic anhydride would provide a convenient reagent to functionalise cytosine at the N^4 -position, rendering synthesis of the anhydride. Use of EDC.HCl with valproic acid formed the desired anhydride in 31% NMR yield,^[123] while DCC mediated coupling yielded no target material. In order to improve the yield of the anhydride formation, phosphorous coupling reagents were subsequently targeted. Successful anhydride formation was finally realised by combining valproic acid with diphenyl phosphoryl chloride in the presence of triethylamine,^[124] yielding 95% of **213** (Scheme 3.19). A subtle shift in the ¹H NMR of the α -proton from 2.38 ppm (in valproic acid) to 2.44 ppm was observed upon anhydride formation.



Scheme 3.19: The formation of anhydride **213**.

Tellingly, IR spectroscopy revealed effective anhydride formation, with two carbonyl stretching frequencies observed, at 1809 and 1746 cm^{-1} (c.f. $\tilde{\nu}_{\text{C=O}}$ (valproic acid) = 1703 cm^{-1}). These stretches are indicative of an anhydride, representing the symmetric and asymmetric carbonyl stretching frequencies, respectively.

The anhydrides were each combined with cytosine in pyridine for 24 hours and precipitated from cold water to form their respective N^4 -amides in excellent yields, both isolated in 94% yield (Scheme 3.20). This simple approach would allow for a range of N^4 -amido cytosines to be constructed, depending on the target molecule. It also circumvents the use of valuable downstream material for selective N^4 functionalisation, such as those initially employed for the synthesis of LY2334737.^[25]

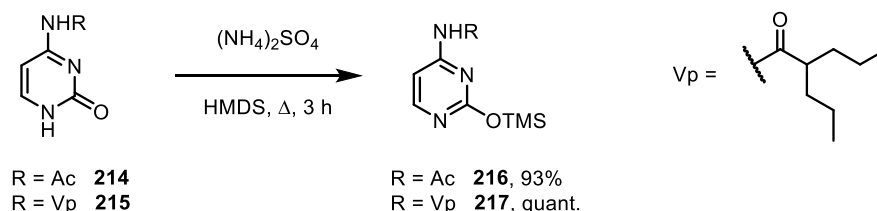


Scheme 3.20: The treatment of cytosine with acetic anhydride and valproic anhydride.

In line with previous literature, the Vorbrüggen reaction (also known as the silyl-Hilbert-Johnson reaction) employs nucleobases that are typically protected as their silyl ether equivalents and used directly for the subsequent reaction with a primed ribofuranose. Such protecting methodology minimises side reactions, such as those possible via the N^4 -position. Given the transient nature of the TMS protecting group, and its susceptibility to moisture, the intermediates of these reactions are not commonly isolated – which begs the question, can the conversion be trusted? The simple answer is yes, as the reaction has been proved to work. But it does question the exact nature of the intermediate.

Typical conditions^[125] employing TMSCl as silylating agent in the presence of triethylamine in toluene did not yield the silylated pyrimidine. Changing to using HMDS as solvent in the presence of catalytic TMSCl yielded **216** in 57%. Crucially, utilising ammonium sulfate in substoichiometric quantities as weak proton source with HMDS produced N -(2-(trimethylsilyloxy)pyrimidin-4-yl) acetamide **216** in 93% isolated yield (Scheme 3.21). Interestingly, the product was isolated as the *mono*-TMS protected cytosine – confirmed by HRMS – and not the often reported *bis*-TMS. N^4 -Valproyl cytosine was also subjected to the reaction conditions, isolating **217** in quantitative yield

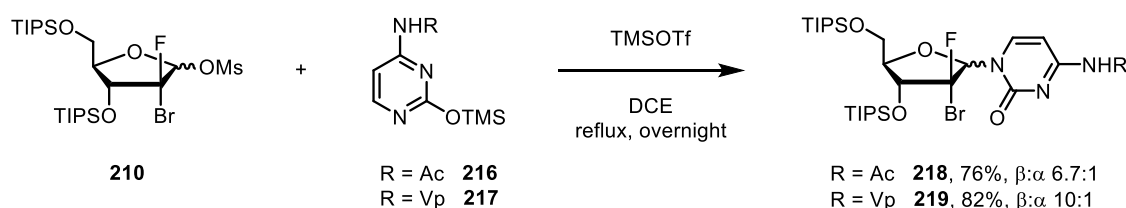
(also Scheme 3.21). Analogously, **218** was also isolated as the *mono*-TMS protected cytosine, which suggests that N^4 - functionalised cytosine nucleobases are silylated once – contrary to that commonly reported,^[13,16,126,127] but may still be true for unfunctionalised nucleobases.^[8,24]



Scheme 3.21: The protection of N^4 -amido cytosines **214** and **215** by ammonium sulfate and HMDS.

Having successfully synthesised TMS-protected N^4 - functionalised cytosines **216** and **217**, attention turned to developing its reaction with mesylated lactol **210**.

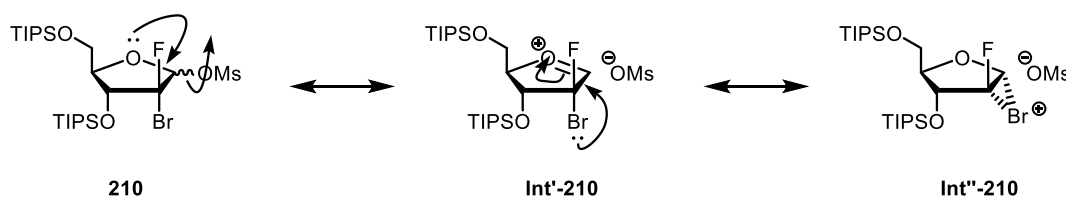
In the presence of TMSOTf as Lewis acid – sometimes described as Friedel-Crafts catalyst^[121] – at reflux in anhydrous DCE, **210** with **216** formed nucleoside **218** in an anomeric mixture of 6.7:1 of β : α in 76% yield (shown in Scheme 3.22). Comparably, **219** was produced from **217** and **210** in 82% but notably there is a considerable shift towards the formation of the desired β -anomer, in a ratio of 10:1. This suggests a subtle yet significant role of the amide moiety – its precise role and how the observed selectivity is imparted is unclear, and further clarification might be difficult. Upon work-up of the reaction, any unreacted N^4 - functionalised cytosine is precipitated and recovered, allowing for it to be reused for future glycosylation reactions.



Scheme 3.22: The glycosylation of **210** with of N^4 -amido-O-TMS-cytosines **216** and **217**.

The enhanced β selectivity observed in both cases may be explained by neighbouring group participation, when considering the reaction mechanism (Scheme 3.23). A resonance form of **210**, with a dissociated mesylate counter anion and an oxocarbenium

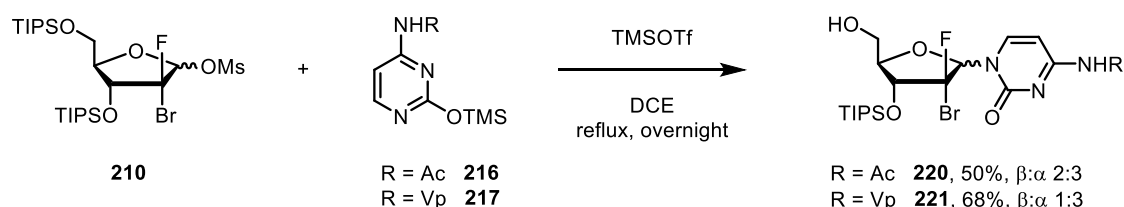
cation could be envisaged (**Int'-210**). This could be resonance stabilised by a lone pair of the bromine atom, thus leading to facial selectivity.



Scheme 3.23: The possible resonance forms of **210**.

If resonance form (**Int''-210**) were present during the reaction, the incoming nucleophile would display facial selectivity towards the top face of the cationic tetrahydrofuran ring, opposite the bromonium moiety – although attack of both faces could be attacked in S_N1 fashion. Straightforward displacement of the mesylate could be imagined which would allow for formation of both anomers, although because **Int'-210** is an activated form of **210**, this S_N2 character may be less likely. Similarly, in the case of **Int'-210** the size of the bromine atom could be envisaged to play a large role in negating *re* face attack to the oxocarbenium – which would form the α anomer – hence preferential *si* face addition leading to the β anomer is observed. It is also worth noting that the 3-*O*-TIPS group could be influencing the selectivity too, as it is a very large steric group and would negate nucleophilic attack from the lower face of ribofuranose **210** – all of which would aid in explaining a more pronounced β selectivity.

Notably on one occasion of the reaction of **210**, the products were the mono-deprotected compounds **220** and **221**, shown in Scheme 3.24, which allowed separation and isolation of each anomer following purification by column chromatography.

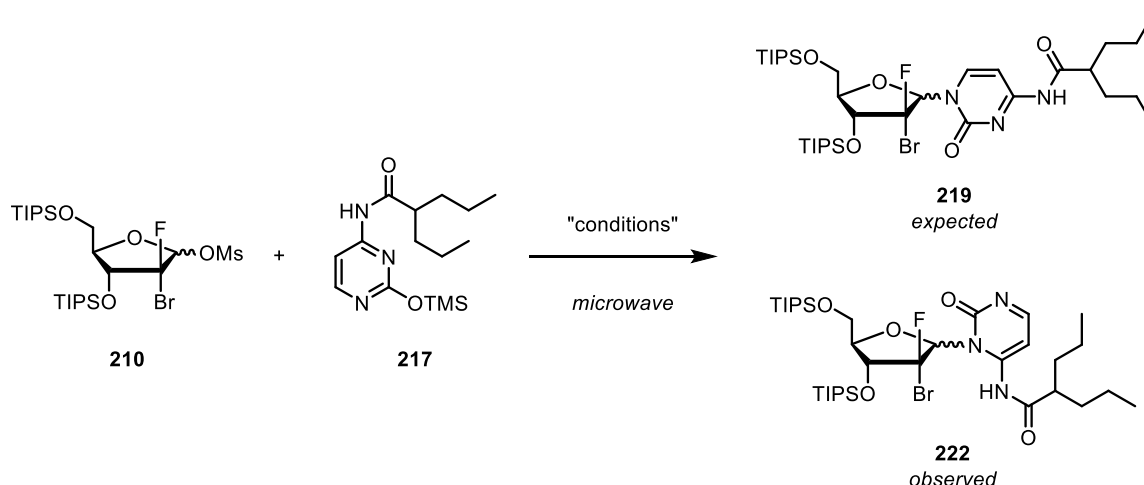


Scheme 3.24: The unexpected formation of **220** and **221** by glycosylation of **210** with of N^4 -amido-*O*-TMS-cytosines **216** and **217**.

The reason for this deprotection remain unclear, but has been observed in previous investigations.^[23] One possible explanation may be that the conditions are particularly forcing, resulting in loss of the more facile 5-O-TIPS group. In any case, with the next step of the synthesis being the TIPS deprotection, this unusual result ultimately delivers a desired intermediate.

Notably, the anomeric ratio is inverted compared to that observed under reaction conditions shown in Scheme 3.22. This was a highly unusual observation, potentially arising due to a purity issue in synthesising **216** and **217**, or due to anomerisation post-glycosylation,^[13] but would require further investigation to clarify.

In an attempt to develop a higher throughput methodology, use of microwave assisted synthesis was pursued, akin to that performed by Jamison and co-workers.^[128] As such, mesyl lactol **210** was irradiated at 150°C in acetonitrile, in the absence and presence of various Lewis and Brønsted acids (Table 3.05).



Entry	Conditions	Yield of 222 ^[a]	Ratio 222:219 ^[b]
1	TMSOTf (10 mol %) MeCN, 150°C, 10 min	30% (d.r. 61:39)	>200:1
2	Pyridinium triflate (10 mol %) MeCN, 150°C, 10 min	33% (d.r. 67.5:37.5)	>200:1
3	2,6-Lutidinium triflate (10 mol %) MeCN, 150°C, 10 min	38% (d.r. 68:32)	>200:1
4	2,4,6-Collidinium triflate (10 mol %) MeCN, 150°C, 10 min	37% (d.r. 64:36)	>200:1
5	No catalyst MeCN, 150°C, 10 min	36% (d.r. 69:33)	>200:1

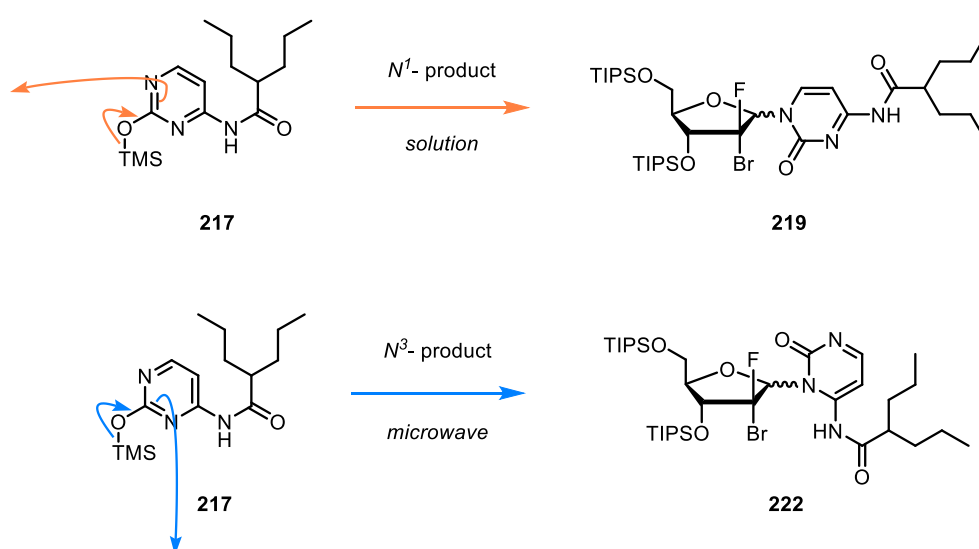
^[a] Isolated yield. Diastereomeric ratio determined by ¹⁹F NMR of crude mixture.

^[b] Regioisomeric ratio determined by ¹⁹F NMR of crude mixture.

Table 3.05: The glycosylation of **210** with **217** under microwave irradiation with various activators.

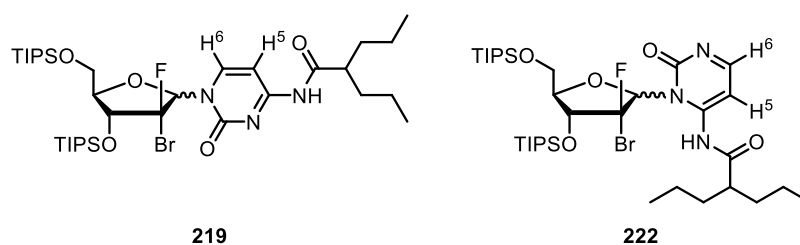
Utilising TMSOTf in 10 mol % as Lewis acid, **219** was not detected by ^{19}F NMR analysis. HRMS revealed the compound had the same mass as the targeted **219**, but analysis of the ^1H NMR of the isolated material revealed a different compound was formed, which was tentatively assigned as the N^3 - nucleoside, produced in an anomeric mixture of 61:39. Employing pyridinium triflate – easily accessed from combining pyridine with triflic acid in diethyl ether – as Brønsted acid yielded **222** in a slightly improved yield of 33%. Use of bulkier, substituted pyridines increased the yield marginally again to 38% and 37% for 2,6-lutidinium triflate and 2,4,6-collidinium triflate respectively (Entries 3 and 4). The reaction was also conducted in the absence of catalyst (Entry 5), which surprisingly delivered **222** in a comparable yield of 36%. This result infers that the abstraction/displacement of the mesylate anion does not require a catalyst, implying a different reactivity – such as $\text{S}_{\text{N}}1$ – may be active. Considering the anomeric selectivity discussed earlier, it is highly probable that some neighbouring group participation is indeed in effect, as per **Int''-210** in Scheme 3.24.

The preferential formation of the N^3 - product over the N^1 - is unusual, but microwave heating allows for alternative attack from the N^3 - position of pyrimidinone ring, as opposed to nucleophilic addition through N^1 - (illustrated in Scheme 3.25). This example suitably demonstrates the potential of enabling technologies such as microwave chemistry allowing for development of alternative nucleosides as potential active pharmaceutical ingredients (APIs).



Scheme 3.25: The comparison of the reactivity of **217**, depending on method employed. Formation of **219** is observed under conventional batch heating (*top*) and **222** is isolated when heating under microwave irradiation (*bottom*).

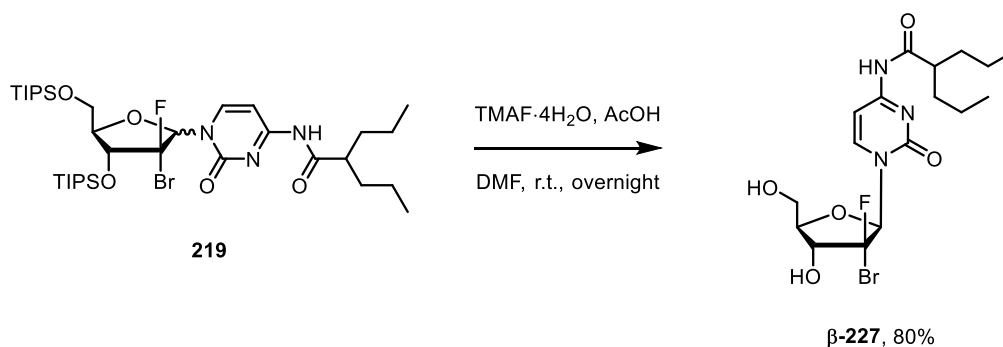
Determination of the product from the microwave glycosylation as **222** was achieved by comparison of the ^1H NMR spectra of the isolated β -anomer of each from their respective methods of synthesis (Table 3.06). The environment of the hydrogen atoms on the pyrimidinone ring demonstrate notable change, both in chemical shift and coupling constant, as their respective environments are inherently different. In **219**, the protons are *cis*-alkene in nature and in a fairly similar chemical environment, although H^6 is likely to be more deshielded due to its proximity to N^1 . By comparison in **222**, H^6 could be described as “imine-like”, explaining why it is significantly more deshielded, with a shift of 8.42 ppm. Significantly, the coupling constant between the protons is less pronounced, with $^3J_{\text{HH}} = 5.6$ Hz, perhaps due to the relationship between H^5 and H^6 , which may be described as *s-cis* diene, in a locked orientation.



Entry	Compound	H^5 shift / ppm	H^6 shift / ppm	$^3J_{\text{HH}}$ / Hz
1	219	7.45	7.88	7.6
2	222	7.89	8.42	5.6

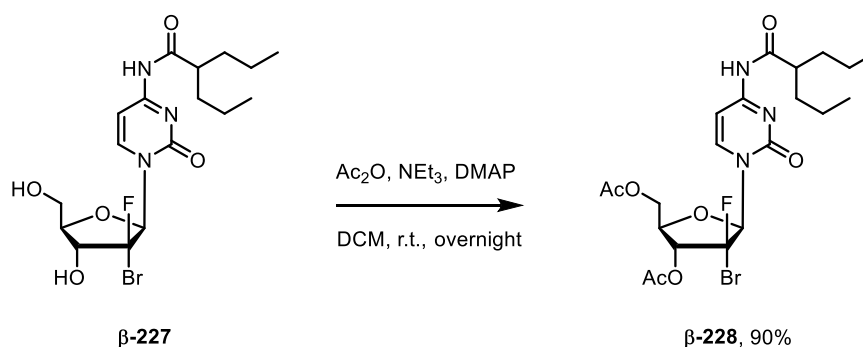
Table 3.06: The ^1H NMR shifts and 3J values of **219** and **222**.

In the case of **220**, while possible to partially separate the anomers during purification, it was simpler to combine the mixture and subject to TMAF mediated deprotection conditions in DMF, in combination with acetic acid (likely forming HF *in situ*), yielding the desired β -anomer in 80% yield after purification by column chromatography, shown in Scheme 3.28.



Scheme 3.28: The sequential deprotection of **219** and acetylation for the synthesis of **β -227**.

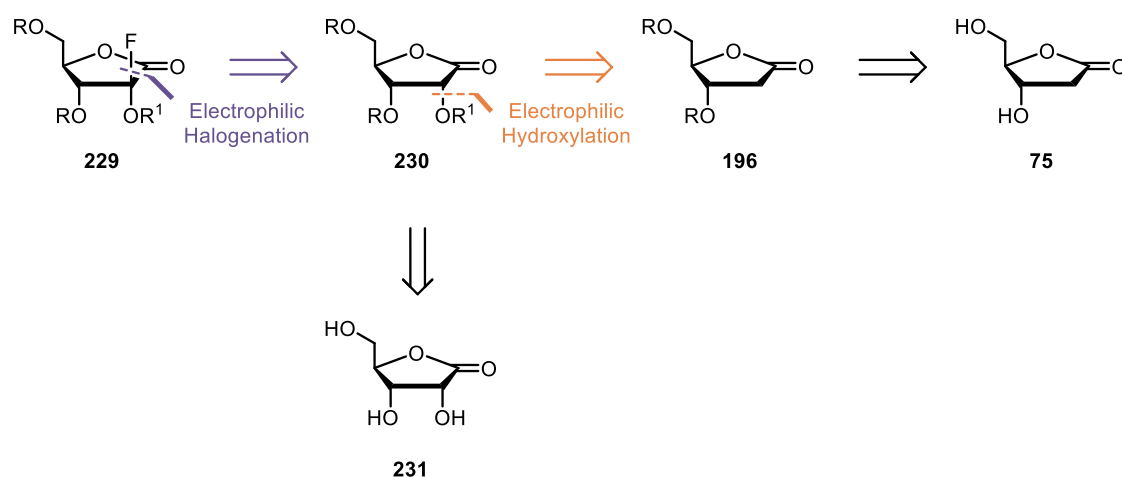
Acetylation of intermediate **β -227** was effective in affording radiolabelling precursor **β -228** in 90% yield by treatment with acetic anhydride with 4-DMAP and triethylamine in DCM (Scheme 3.29). Investigation of (radio)labelling and related studies of **β -228** is discussed in Section 3.4 (Page 107).



Scheme 3.29: The synthesis of radiolabelling precursor **β -228** acetylation of **β -227**.

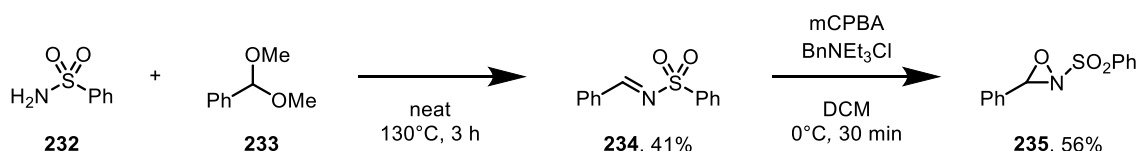
3.2.3 – α -hydroxy lactone formation

Halides represent a strong option as a leaving group for the targeted radiofluorination, with their installation via a range of electrophilic halogen sources, such as *N*-halosuccinimides. However, alternative moieties with enhanced leaving group properties exist, which may allow for greater ease of displacement by [^{18}F]fluoride. Leaving groups such as mesylate, 4-nosylate and triflate have found use in aliphatic nucleophilic fluorination,^[88,129] which could be accessed through a 2'-fluoro-cytidine analogue. Despite the lack of literature precedent surrounding the fluorohydrin moiety that would be required, it was an interesting thought process to investigate, illustrated by the disconnection strategy shown in Scheme 3.30. Additionally, such improved leaving group ability may increase the potential for disfavoured elimination to form an α,β -unsaturated- γ -lactone or other byproducts.



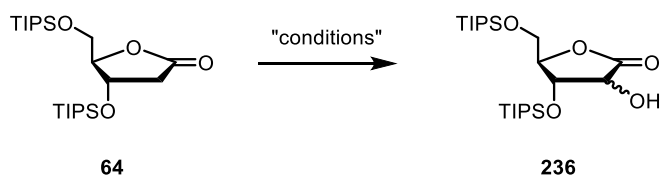
Scheme 3.30: Disconnection of **229**.

Given that a robust method for forming **64** ($\text{R}^1 = \text{TIPS}$) was in hand, formation of α -hydroxy lactone moiety was initially targeted by electrophilic hydroxylation, using Davis' oxaziridine as an electrophilic source of oxygen.^[130] As such, **235** was synthesised (Scheme 3.31); firstly by formation of imine **234** from benzene sulphonamide (**232**) and neat benzaldehyde dimethyl acetal (**233**), and subsequent oxidation by mCPBA using benzyl triethyl ammonium chloride as phase transfer catalyst.^[131]



Scheme 3.31: The synthesis of oxaziridine **235**.

As α -hydroxylation would be achieved *via* the enolate of lactone **64**, it was treated with LiHMDS and oxaziridine **235** in the presence of TMSOTf as Lewis acid, which led to no observable desired product formation (Table 3.07, Entry 1). Omitting the Lewis acid, thereby accessing the more reactive enolate led to a different crude ^1H NMR from the reaction, with new proton environments observed at 28% NMR yield – potentially corresponding to an adjacent proton of an alcohol group. Notably, much of the oxaziridine was returned (*c.f.* 66% NMR yield) despite the consumption of starting material **64**, with mass balance ruling out the effective formation of **236**. This result also suggests that **235** may not be sufficiently electrophilic.



Entry	Conditions	Rec. of 64 ^[a]	Yield of 236 ^[a]
1	LiHMDS (1.5 equiv.), TMSOTf (1.6 equiv.) then 235 (1.7 equiv.) THF, -78°C, 2 h	33% (66% 235)	-
2	LiHMDS (1.5 equiv.), 235 (1.7 equiv.) THF, -78°C, 2 h	9% (81% 235)	-
3	LiHMDS (1.5 equiv.), TMSOTf (1.6 equiv.) then mCPBA (1.7 equiv.) THF, -78°C, 2 h	32%	14%
4	LiHMDS (1.5 equiv.), mCPBA (1.7 equiv.) THF, -78°C, 2 h	38%	-

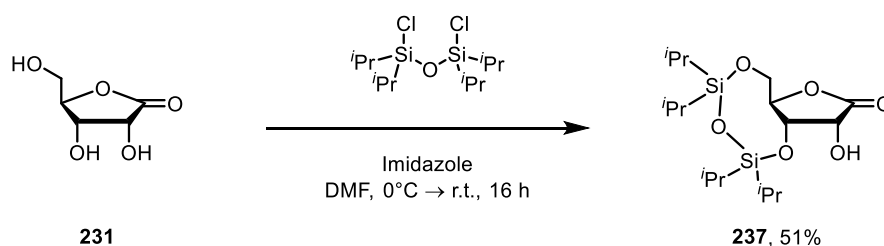
^[a] ^1H NMR yield using mesitylene as internal standard.

Table 3.07: The conditions screened for the α -hydroxylation of **64**.

As an alternative, the Rubottom oxidation (Entries 3 and 4) was investigated. Exclusion of TMSOTf (Entry 4) – required for the formation of the silyl enol ether intermediate – did not yield **236**. Interestingly, examination of the crude ^1H NMR of Entry 3 showed a new peak at 6.17 ppm (dd, $J = 5.7, 2.0$ Hz) [and another at 5.41 ppm (tt, $J = 2.3, 1.6$ Hz)], which may be attributed to the proton adjacent to the newly installed hydroxyl group and alpha to the lactone moiety (potentially coupling to the *OH*). With an encouraging 14% NMR yield, attempted isolation by column chromatography yielded no desired product.

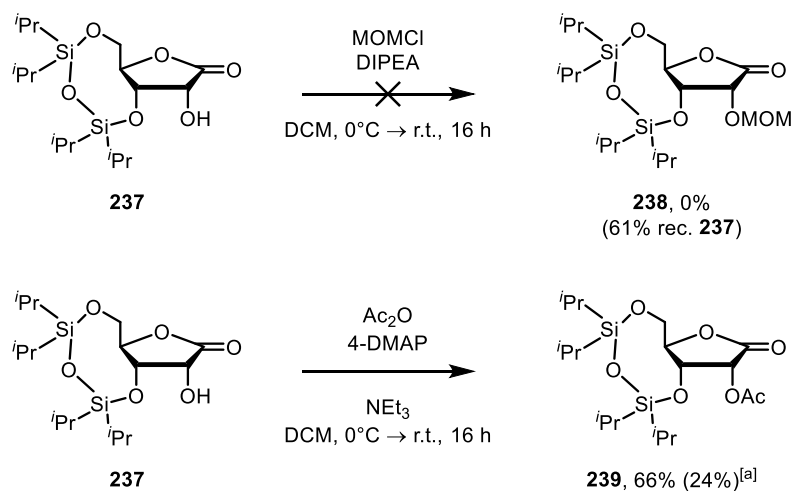
It is worth noting that the hydroxylation may have been performed on the mono-fluorinated lactone **65**, as opposed to hydroxylation and subsequent fluorination, but this strategy was not explored.

Alternatively, the desired functionality may be conveniently accessed by beginning from D-ribonic- γ -lactone (**231**); and subsequent protection and fluorination *via* the previously explored enolate chemistry. As shown in Scheme 3.32, studies commenced by protecting commercially available **231** with 1,3-dichloro-1,1,3,3-tetraisopropyldisiloxane to afford **237** in 51%.^[132]



Scheme 3.32: The protection of **231**.

An orthogonal protecting group to the disiloxy ether moiety was deemed highly desirable for the α -hydroxy functionality. Additionally, a non-eliminating functionality would be ideal, given the basic conditions of the electrophilic fluorination. Shown in Scheme 3.33 is the 2-O-functionalisation of **237**; firstly, treatment with methoxymethyl chloride in DCM was unsuccessful in delivering protected lactone **238**, returning the starting material in 61% isolated yield. Alternatively, Ac_2O was used and furnished **239** in 66% NMR yield and a diminished 24% isolated yield.



^[a] ¹H NMR yield using mesitylene as internal standard. Isolated yield in parentheses.

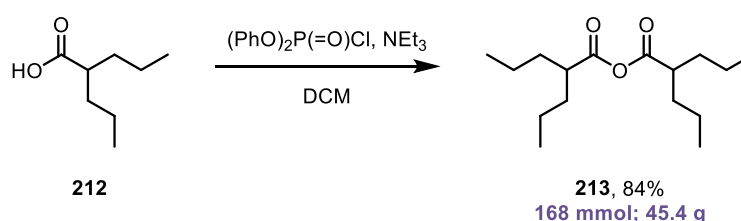
Scheme 3.33: The attempted 2-O- derivatisation of **237**.

With an appropriately functionalised lactone in hand, fluorination of **239** would be targeted as the next step in this synthetic strategy.

3.3 – Scale-up of synthetic route 2

Given the target precursor for radiolabelling is chemically very similar to LY2334737 (**100**, Scheme 1.42), there is sufficient scope for the unprotected analogue to be investigated as a potential anticancer agent itself. Due to the amount of chemotherapeutics required during a course of treatment – 1000 mg m⁻² of gemcitabine is administered weekly for up to 7 weeks^[133] – a scalable method of producing the key 2-bromo-2-fluoro-lactol **209** would be required, along with *N*⁴-valproyl cytosine (**215**).

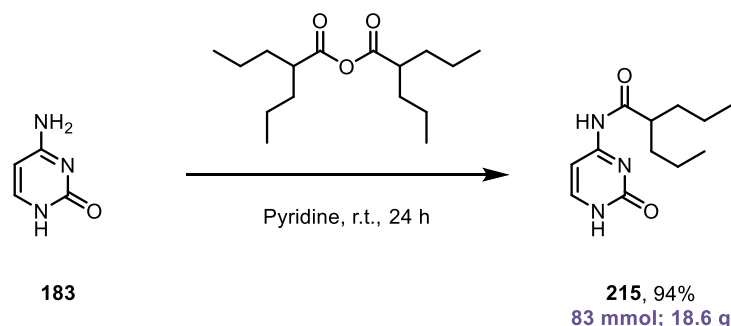
The previously explored method of anhydride formation from reacting valproic acid with diphenylphosphoryl chloride was successfully translated to a 400 mmol scale (with respect to **212**, yielding 45.4 g of anhydride at 84% yield (Scheme 3.36).



Scheme 3.36: The scale up synthesis of valproic anhydride, **213**.

The only modification required for the reaction was further washing with saturated aqueous NaHCO₃ to remove an acidic by-product, likely a phosphoric acid type compound, without deleterious effect on the anhydride.

Utilising valproic anhydride with cytosine in anhydrous pyridine on 83 mmol scale (with respect to cytosine) effectively afforded **215** as an impure mixture. After precipitation from cold water, the crude product contained a mixture of valproic acid as by-product and unreacted cytosine.

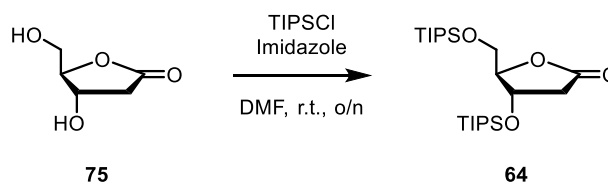


Scheme 3.37: The combination of cytosine with valproic anhydride to form **215** on scale.

Each of these impurities were removed by selective trituration – saturated aqueous NaHCO_3 was used to quench remaining acid, and cytosine was removed by 0.5 M HCl – finally yielding 18.6 g of **215** at 94% yield after purification (Scheme 3.37).

As previously discussed, oxidative cyclisation of 2-deoxy-ribose was investigated and was quickly found to be scale dependent – if the reactions were conducted on a scale greater than 40 mmol, they would become inefficient, resulting in lower product yield and increased formation of undesired by-products. As such, multiple reactions could be run in parallel and then combined for work-up and purification, again utilising K_2CO_3 as neutralising agent.

Once sufficient **75** had been synthesised, different scale reactions were investigated for its protection as **64**. The results are summarised in Table 3.09, but it can be seen that irrespective of scale, the reaction is highly repeatable delivering decagrams of **64**.

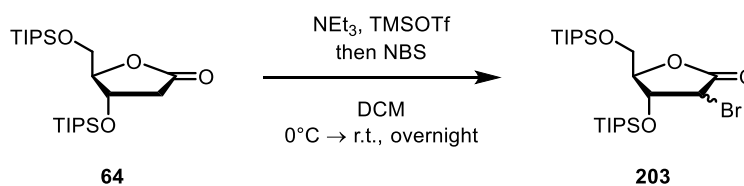


Entry	Scale / mmol	Yield of 64 ^[a]	Mass of 64 / g
1	38	75	12.73
2	86.8	80	31.00
3	137.3	78	47.51
4	75.8	80	26.90

^[a] Isolated yield.

Table 3.09: The investigation of the effect of scale upon formation of **64**.

By comparison, when scaling up the α -bromination reaction of **64**, the process was found to be more inconsistent, delivering a range of yields ranging from 35% to 70%. The reason for this variation is difficult to pinpoint conclusively, although there is somewhat of an inverse correlation between scale and yield. Alternative work up methods were also found to impair the reaction, as filtering the reaction over a plug of silica returned only 16% yield of the desired compound. Therefore, this reaction requires further refinement in order to ensure it is reproducibility and independent of scale.

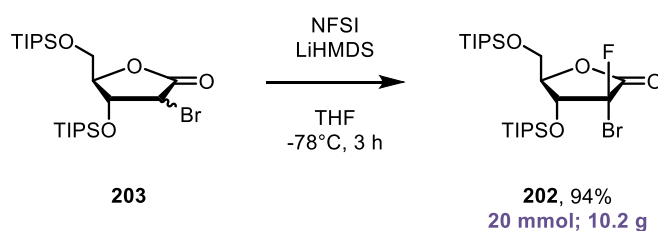


Entry	Scale / mmol	Yield of 203 ^[a]	Mass of 203 / g
1	7.72	70	2.85
2	28.6	51	7.67
3	69.7	35	12.60
4 ^[b]	67.5	16	5.50
5	4.8	69	1.74

^[a] Isolated yield. ^[b] Crude mixture filtered over Si plug.

Table 3.10: The scale-up of α -bromination reaction of **64**.

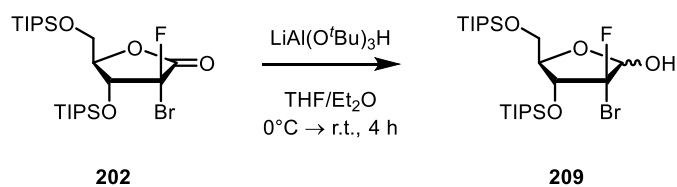
Focussing on the electrophilic fluorination (Scheme 3.38), altering the stoichiometries of reagents for the reaction – increasing to 1.7 equiv. of LiHMDS and 1.9 equiv. of NFSI – allowed the reaction yield to increase to 94% when conducted on a 20 mmol scale. This result suggests that previous conditions were not forming sufficient *in situ* lithium enolate to react with NFSI. Even upon increasing scale, only one diastereomer is formed during this reaction.



Scheme 3.38: The improved fluorination of **203** when scaled-up with increased equivalents of LiHMDS and NFSI.

Due to the necessity of the triisopropyl silyl protecting groups, the majority of the resulting compounds are thick, viscous oils with high boiling points. As such, purification by distillation is not possible – even when using forcing conditions such as 220°C at 10 mbar of pressure, the compounds co-distill. Kugelrohr distillation was attempted to purify crude mixtures of **202** and **203**, and in both instances the reaction mixtures were not resolved.

Remarkably the compounds were stable under these conditions, with no observable degradation by ^1H NMR analysis. As such, the purification of the intermediates by column chromatography is a drawback of the developed methodology.



Entry	Scale / mmol	Yield of 209 ^[a]	Mass of 209 / g
1 ^[b]	3.9	70	1.49
2 ^[b]	6.7	42 (32% 202)	1.54
3 ^[b]	8.8	81	3.84
4 ^[c]	10.6	quant.	5.62
5 ^[c]	12.3	91	6.08
6 ^[c]	16.3	87	7.74

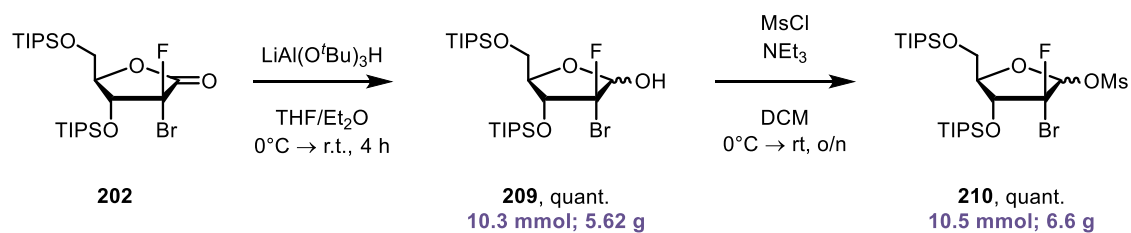
^[a] Isolated yield. ^[b] 1.2 equiv. of $\text{LiAl(O}^t\text{Bu)}_3\text{H}$ used. ^[c] 1.1 equiv. of $\text{LiAl(O}^t\text{Bu)}_3\text{H}$ used.

Table 3.11: The reduction of **202** when performed on scale.

Table 3.11 examines the varying scale and subsequent effect on the reduction of **202**, and it can be seen that the results demonstrate a scale dependency of the reaction – the exception being Entry 2, potentially due to use of lithium *tert*-butoxyaluminium hydride that had degraded. The optimum conditions appear to be when the reaction is conducted on ~10 mmol scale (Entry 4), returning 5.62 g of lactol **209** quantitatively. Increasing scale further reveals a slight reduction in isolated yield (Entries 5 and 6).

Another issue upon increasing the scale of this process was the removal of the aluminium salts; which could be circumvented by use of Rochelle salts, washing with 0.5 M HCl or employing the Fieser work-up method^[134] – but the former returned lower yields of **209**.

As previously, mesylation of lactol **209** proceeded smoothly independent of scale to afford 6.6 g of **210** (Scheme 3.39).

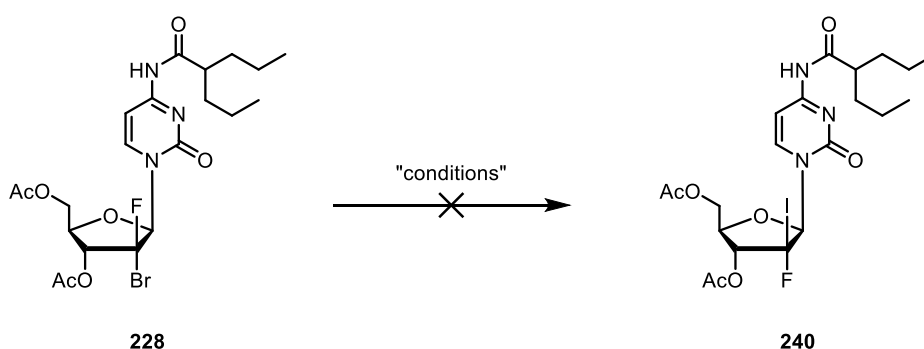


Scheme 3.39: The sequential scale up reactions towards **210** by reduction and mesylation.

3.4 – Fluorination

3.4.1 – Cold ^{19}F fluorination

In preparation for the attempted fluorination, performing the substitution reaction with non-radioactive fluorine was targeted in order to generate & characterise a sample of the target cold material. Derivatisation of **228** was attempted, in order to access more reactive compounds that may better serve the fluorination reaction. As such, **228** was subjected to typical Finkelstein reaction conditions, to obtain the 2'-fluoro-2'-iodo congener (**240**). Acetone was initially employed as reaction solvent (Table 3.12, Entry 1), with an excess of potassium iodide at room temperature for 24 hours yielding none of the desired material (**240**), only returning **228** quantitatively. Switching to 2-butanone at reflux, as higher boiling point solvent also did not produce **240** (Entry 2), nor did changing from potassium iodide to sodium iodide (Entry 3) with both attempts returning starting material, confirmed by MS and ^{19}F NMR.



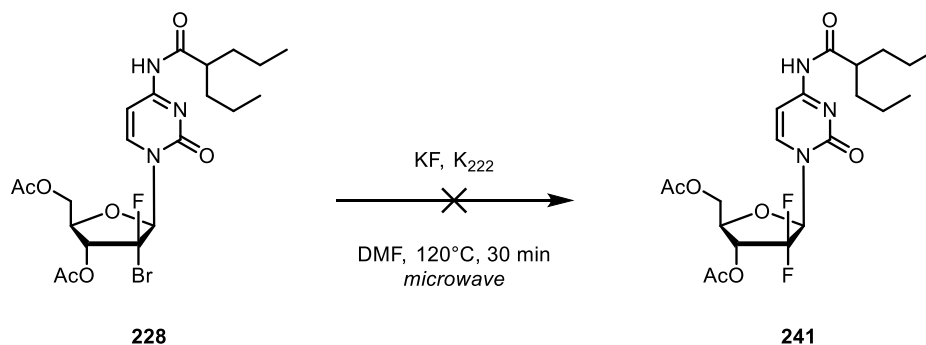
Entry	Conditions	Yield of 240 ^[a]
1	KI (5 equiv.) Acetone, r.t., 24 h	- (quant. 228)
2	KI (5 equiv.) 2-Butanone, reflux, 46 h	- (quant. 228)
3	NaI (5 equiv.) 2-Butanone, reflux, 24 h	- (quant. 228)

^[a] Isolated yield.

Table 3.12: The reaction of **228** under Finkelstein-like conditions.

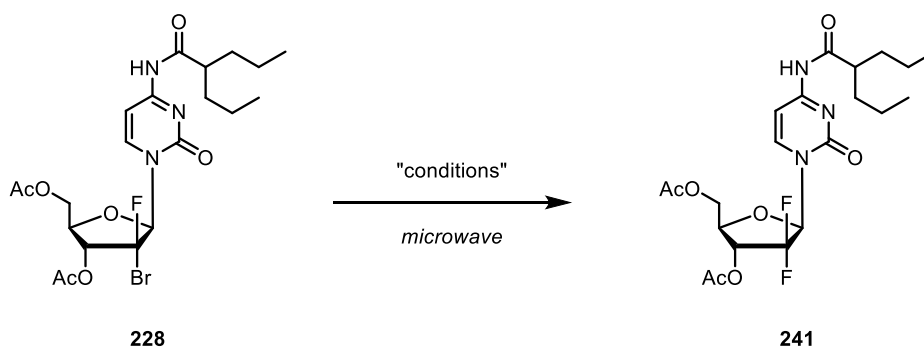
From the results presented in Table 3.12, it can be seen that highly forcing conditions would be required to facilitate the substitution reaction, even with the aid of by-product precipitation as employed in the Finkelstein reaction. Utilising microwave chemistry could allow for this process take place, allowing for elevated temperatures to be reached in

appreciable time, given the desired application to ^{18}F labelling and the half-life of fluorine-18.



Scheme 3.40: The fluorination of **228** under ^{18}F -like conditions.

Initially, precursor **228** was reacted with potassium fluoride with phase transfer catalyst K_{222} in DMF, irradiated at 120°C for 30 min (Scheme 3.40) but did not successfully yield compound **241** after work up. Instead, the use of silver fluoride was tested with a two-fold target – as fluoride source and to aid with bromide abstraction, precipitating out insoluble AgBr as by-product. Replacing KF with AgF resulted in consumption of starting material **228**, but no desired product formation (Table 3.13, Entry 1). Omitting chelator K_{222} only returned **228** (Entry 2), while increasing time or not performing azeotropic drying of KF and K_{222} (to mimic radiofluorination conditions) did not furnish **241** (Entries 3 and 4 respectively).



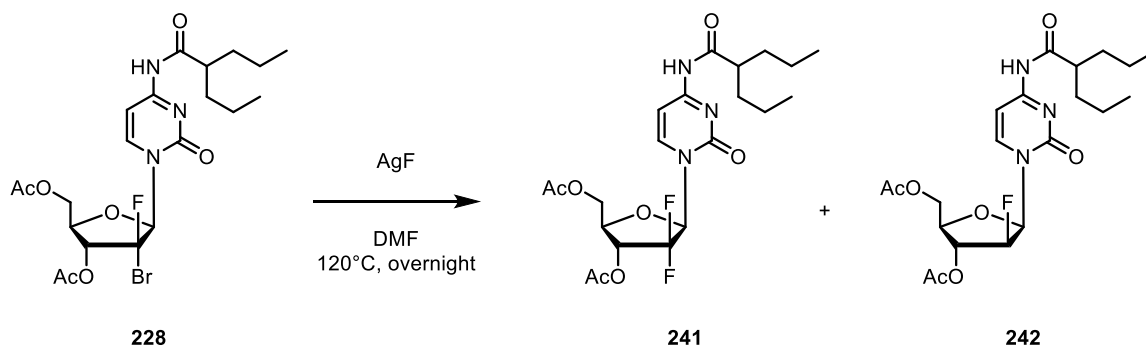
Entry	Conditions	Yield of 241 ^[a]
1	AgF (5 equiv.), K ₂₂₂ (1 equiv.) DMF, 120°C, 30 min	- (60% 228)
2	AgF (5 equiv.) DMF, 120°C, 30 min	- (quant. 228)
3	AgF (5 equiv.), K ₂₂₂ (1 equiv.) DMF, 120°C, 60 min	- (9% 228)
4 ^[b]	AgF (5 equiv.), K ₂₂₂ (1 equiv.) DMF, 120°C, 30 min	-

^[a] ¹⁹F NMR yield, using α,α,α -trifluorotoluene as internal standard. ^[b] No azeotropic drying.

Table 3.13: The fluorination of **228** using silver(I) fluoride under microwave irradiation.

Returning to conventional solution chemistry, precursor **228** was reacted with silver fluoride in the presence and absence of phase transfer catalyst Kryptofix® 222 (Scheme 3.40 and 3.41 respectively). Qualitative analysis of the crude reaction mixture by HRMS revealed that, pleasingly, **241** was successfully formed under both sets of reaction conditions.

Examination of the HRMS spectrum of the fluorination reaction in the absence of K₂₂₂ (Figure 3.04, reaction of Scheme 3.41) reveals a fragment at 536.1251 m/z, which equates to unreacted starting material, [**228**+H]⁺ – and can be identified from the splitting pattern of bromine – while the signal at 238.1556 m/z arises from *N*⁴-valproyl cytosine (**215**).



Scheme 3.41: The fluorination reaction of **228** by silver(I) fluoride.

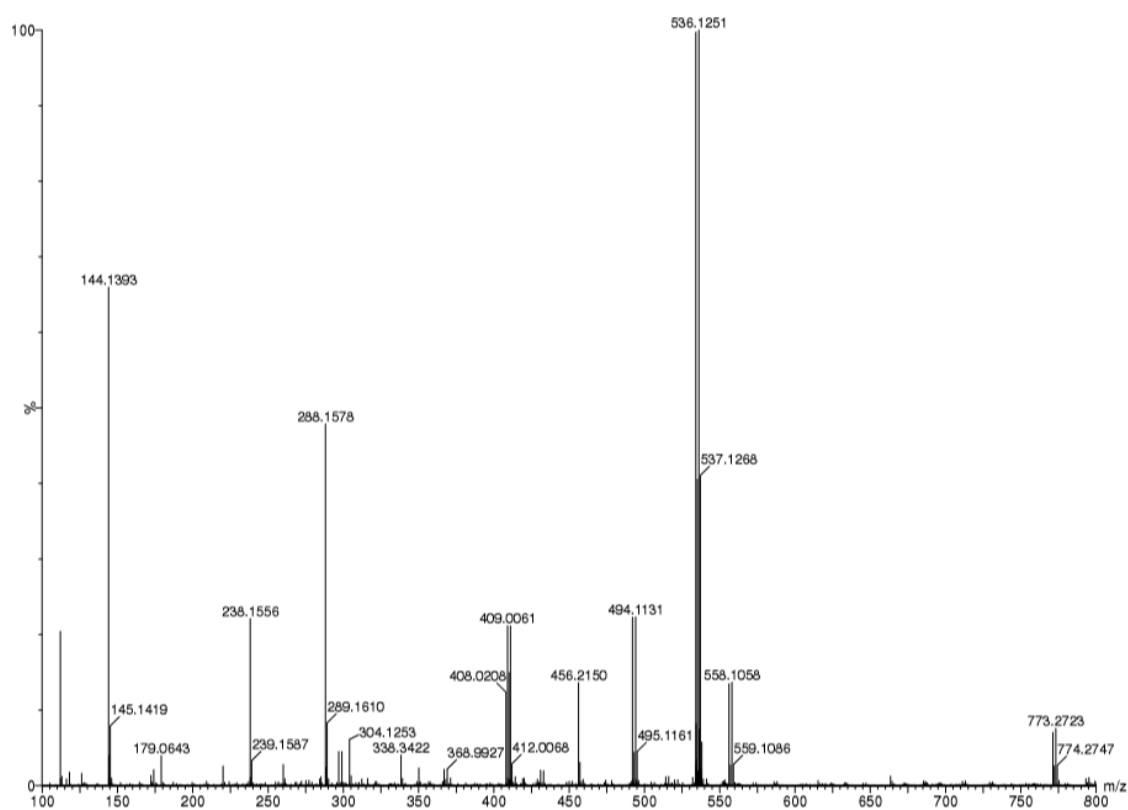
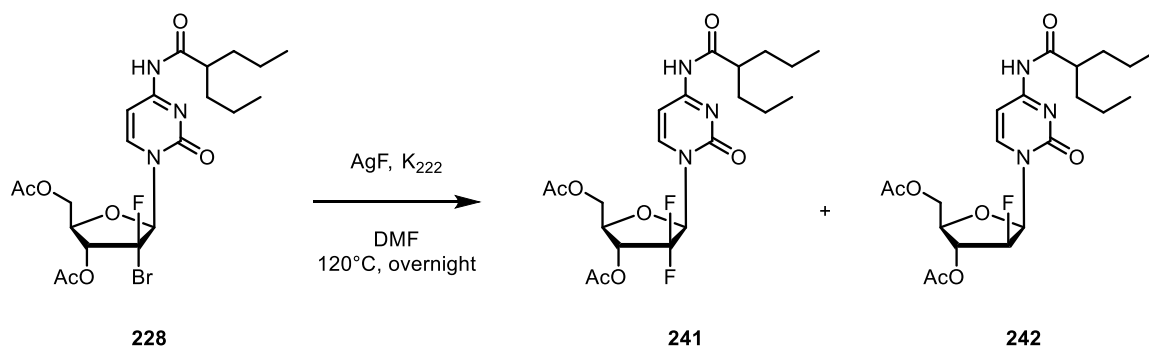


Figure 3.04: HRMS spectrum of the reaction mixture of that shown in Scheme 3.41.

The fragment observed at 456.2150 m/z is calculated to be from a debromohydrofluorinated derivative of the **228** (i.e. **242**, $[\text{M}+\text{H}]^+$). Formation of **242** may be rationalised by silver mediated bromine abstraction from **228**, potentially by a radical based mechanism.^[135]



Scheme 3.42: The fluorination reaction of **228** by silver(I) fluoride with K_{222} .

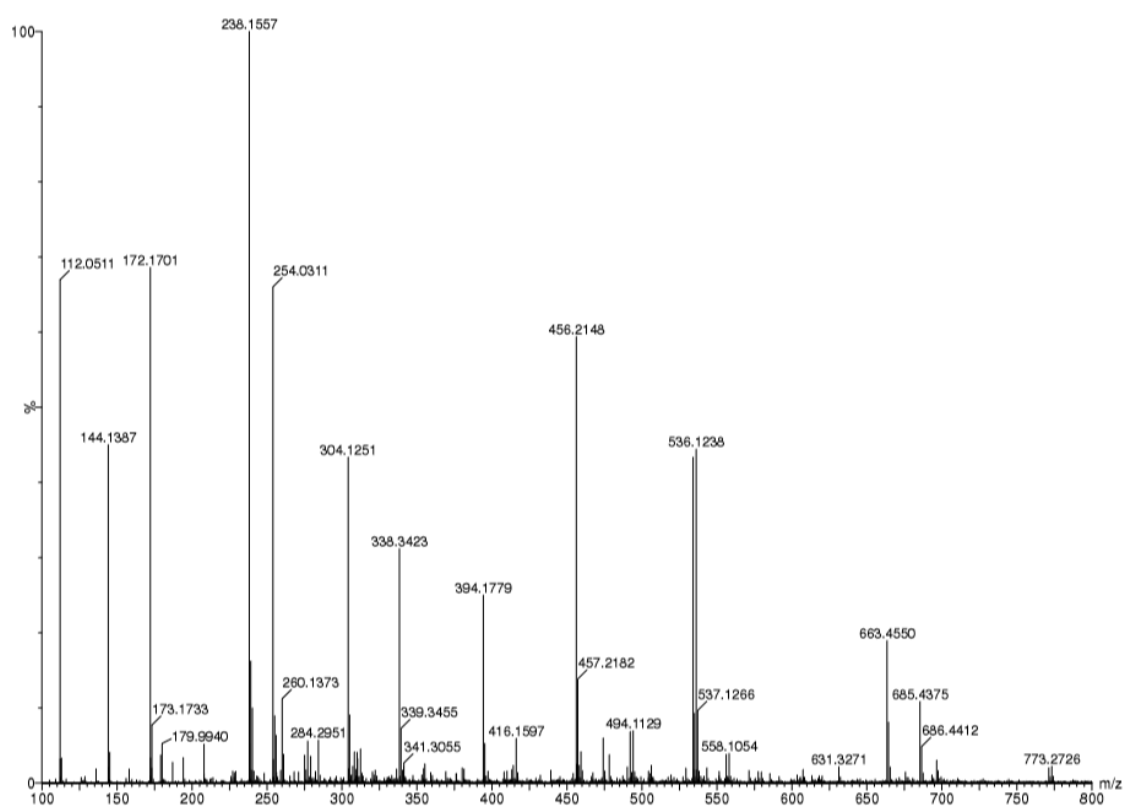


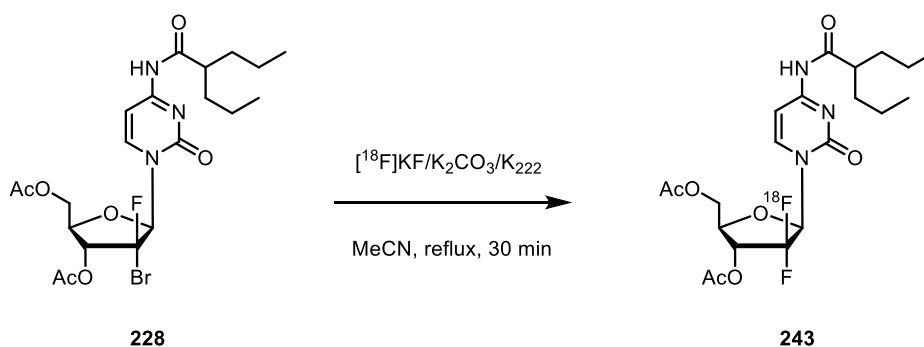
Figure 3.05: HRMS spectrum of the reaction mixture of that shown in Scheme 3.42.

The reaction was also conducted with K_{222} , the HRMS spectrum of which (Figure 3.05) paints a similar picture, despite apparent increased fragmentation (which might not necessarily reflect reaction conditions). Again, fragments at 238.1557 and 536.1238 m/z correspond to N^t -valproyl cytosine and **228** respectively.

Again, the debromohydrofluorinated motif is presented as the fragment at 456.2148 m/z (calculated 455.1844 m/z, **242**), along with a detectable amount of the fully protected difluorinated compound **241** ($[M+H]^+$ calc 474.2052 found 474.2055, see Appendix 6.3). These positive results demonstrate that fluorination is possible on the synthesised precursor **228**, and that the protecting group strategy employed is also compatible.

3.4.2 – Radiofluorination

Having explored the fluorination reaction, the challenge then turned to performing the reaction radiochemically. Studies commenced by reacting **228** with azeotropically dried $[^{18}\text{F}]\text{KF}/\text{K}_2\text{CO}_3/\text{K}_{222}$ in acetonitrile at reflux, with an initial activity of 13.9 MBq (Scheme 3.43).



Scheme 3.43: The attempted radiofluorination reaction of **228** by $[^{18}\text{F}]\text{KF}$ with K_{222} .

Analysis of the crude reaction mixture by radio-TLC (Figure 3.06) using 70% EtOAc/hexanes as eluent showed that in addition to the free fluoride signal (Figure 3.06, Region 1), a new radioactive signal was present (Region 2). Relative to the free fluoride, 37.5% of the radioactive count was from the new signal, equating to an activity of roughly 3.8 MBq from a total activity of 10.25 MBq in the crude reaction mixture post-reaction. Unfortunately, the radio-HPLC trace of the reaction media did not correspond to that of the non-radioactive sample, indicating that the reaction was not successful in forming **243**, but another product. Despite the R_f (radio-TLC) and retention time (radio-HPLC) having similarities to the analogous ^{19}F target compound, there is not sufficient evidence that the radioactive compound formed is **243**. Due to insufficient time, further investigation into the radiofluorination reaction was not possible.

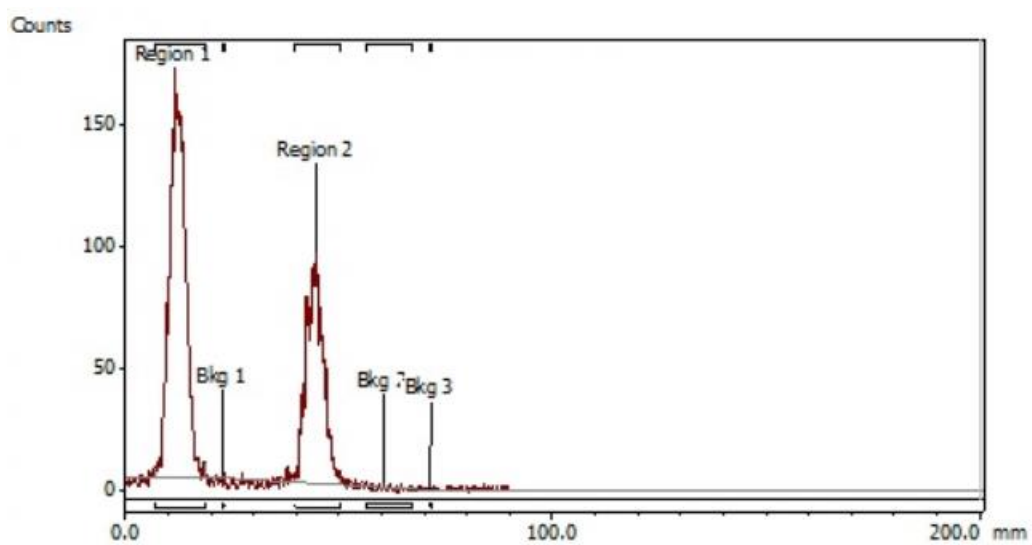
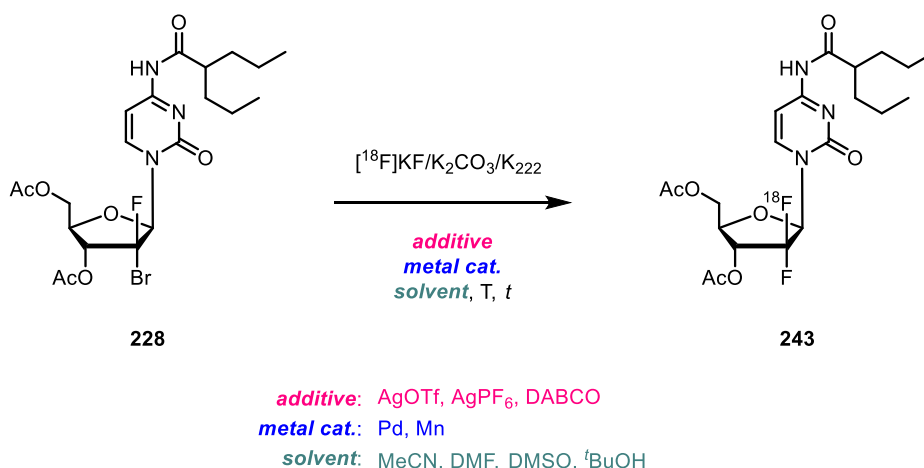


Figure 3.06: Radio-TLC trace reaction shown in Scheme 3.42.

3.4.3 – Conclusions and outlook

Radiofluorination of **228** was briefly investigated, under typical conditions employed for ^{18}F reaction, using K_{222} and MeCN to form gemcitabine prodrug **243**. Results demonstrate that a new radioactive peak was detected by radio-TLC with a similar R_f to the target compound, although the identity of the product could not be determined.

There is significant scope to further investigate and develop the radiofluorination chemistry applied to this system, illustrated within Scheme 3.44. With a suitable precursor in hand, besides temperature (T) and time (t), investigation of alternative solvents such as DMF and $^t\text{BuOH}$ may yield the desired compound.^[71] Similarly, utilising reagents to aid with bromine abstraction such as silver triflate or alternative Lewis acids may aid the process by increasing the $\text{S}_{\text{N}}1$ character of the reaction, given the forcing conditions required for potential $\text{S}_{\text{N}}2$ reaction to occur. Additionally a Lewis base like DABCO could be included, which may promote the formation of an activated intermediate more susceptible to radiofluorination.

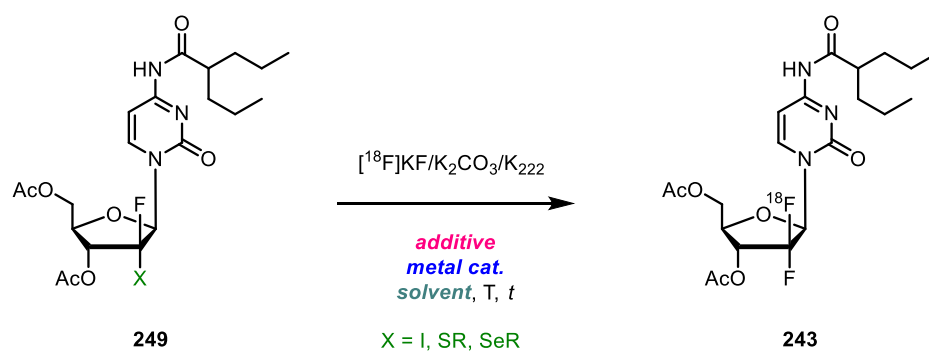


Scheme 3.44: Potential radiofluorination conditions that could be explored to synthesise **243** from **228**.

Modern approaches would potentially involve the use of transition metal catalysts, such as palladium^[136] or porphyrin ligated manganese.^[137,138] Recent elegant developments from the Ritter lab have employed a thianthrenation strategy on aromatic substrates.^[139]

Reconsideration of the design of precursor **228** could also allow access to alternative leaving groups. Installation of an iodine at the 2' position would not only improve the leaving group ability, but access to more oxidisable motif which may further improve

radiofluorination. Similarly, sulfur and selenium groups could be introduced as these may also be oxidised, but could lead to competitive elimination reactions.



Scheme 3.45: Potential radiofluorination conditions that could be explored to synthesise **243** from **249**.

Compound **228** has a great deal of potential as a precursor for radiofluorination and achieving the target of an ^{18}F -labelled gemcitabine prodrug, while also demonstrating potential as a chemotherapeutic agent itself and will no doubt be a good platform for further work to be based from.

3.5 – Tissue culture work

Due to the structural similarity between the targeted radiolabelling precursor and LY2334737 (**100**), it is conceivable that **227** would also demonstrate anti-cancer properties – the *gem*-dihalo functionality, believed to be the source of the chemotherapeutic properties, could still induce apoptosis *in vivo*.

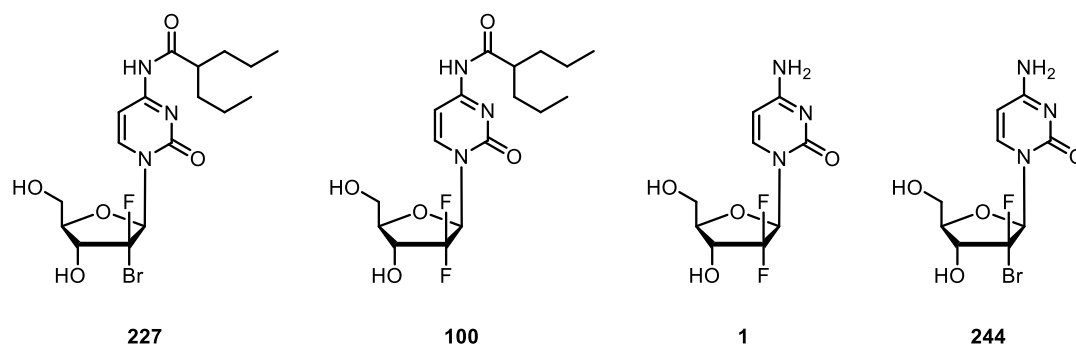


Figure 3.07: Structure of compounds evaluated for cytotoxicity.

Based on previous in-house work, Panc 10.05 cell lines were chosen to screen **227** against, as they were found to be most sensitive cell lines to treatment with gemcitabine, as opposed to other pancreatic cancer cell lines such as Capan-2 and HPAF-II. In order to ascertain the cytotoxicity of **227**, LY2334737 (**100**) and gemcitabine (**1**) were also ran against Panc 10.05 as control samples. Unfortunately, synthesis of the 2'-bromo-2'-fluoro analogue of gemcitabine (**244**) was elusive and could not be obtained.

Each tested compound was initially dissolved in DMSO, and then diluted to the appropriate concentration. As DMSO is known to present a low risk of cytotoxicity, control samples of the respective diluted DMSO concentrations were also screened against the Panc10.05 lines.

In order to visualise the cell death, an IncuCyte S3 was used as it allowed automatic live imaging of the cell plates at specified time intervals, visualised by fluorescence microscopy. As such, Incucyte Cytotox Red Reagent was used as a fluorescent probe, which binds to the DNA of an unhealthy, permeable plasma membrane, staining the cell red (from blue) when cell death occurs. This staining is in turn detected by the microscope within the instrument. When the reagent dye is administered, a background reading of the red area is required in order to highlight the cells that have undergone apoptosis, hence the red area vs normal area.

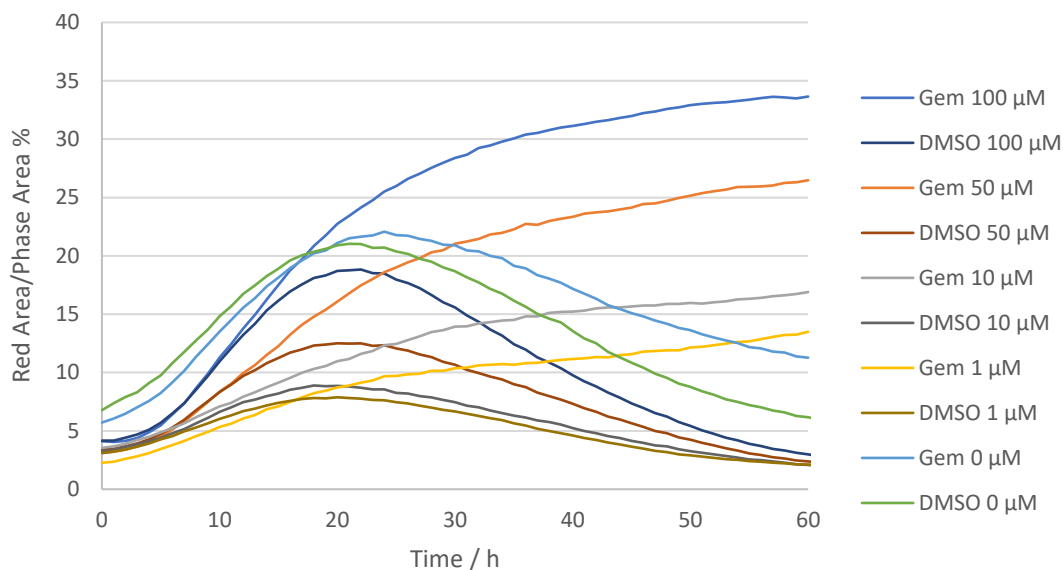


Figure 3.08: Red area normalised to phase area (%) as a function of time for gemcitabine and DMSO control against Panc10.05.

The cell lines were cultured in growth medium after defrosting and split appropriately, and seeded in 96-well plates at a density of 2×10^5 cells mL^{-1} . As such, the data obtained for the tested compounds isn't completely quantitative due to the competing growth of cells and death by cytotoxic agent.

Gemcitabine was screened as a control sample, at concentrations of 100 μM , 50 μM , 10 μM and 1 μM , and the experiment was monitored for over 2 days. It can be observed that there is a positive correlation between increasing gemcitabine concentration and cell death, indicated by amount of red area observed (Figure 3.09). Also, the rate of cell death is greater at higher dosages of gemcitabine, notably so between the higher control limits of 100 μM and 50 μM . It can also be seen that increasing concentrations of control DMSO samples induces a mild degree of apoptosis initially, before peaking at 20 hours for DMSO 100 μM sample, which implies cell growth.

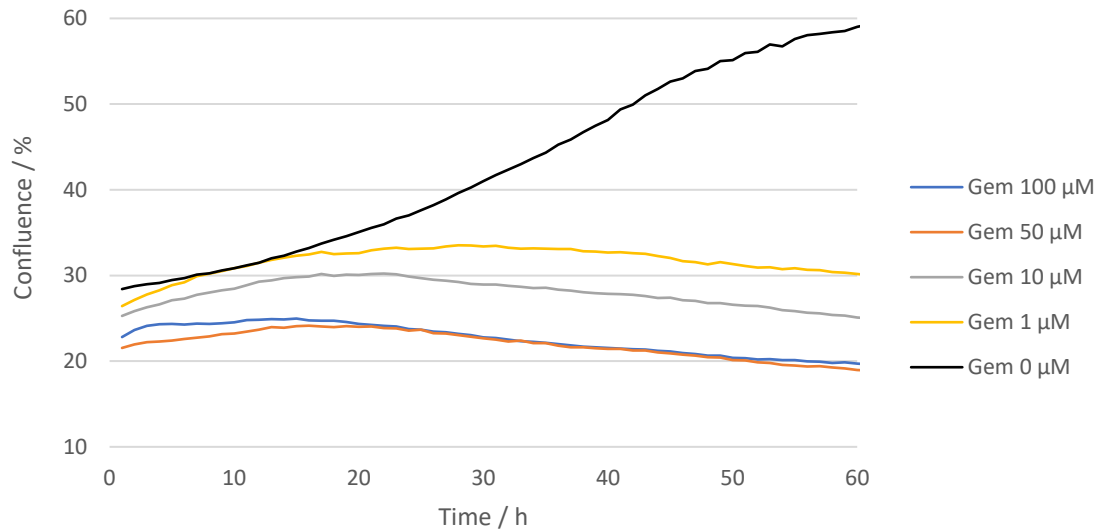


Figure 3.09: Confluence (%) as a function of time for gemcitabine against Panc10.05.

This is reinforced upon examination of the confluency (%) vs time (h) graph, which clearly displays an increase in confluency – the degree or amount of cells present – of the untreated sample (Gem 0 μM), indicating cell growth and that the cells weren't sufficiently confluent before the beginning of the experiment. However even when Gem 1 μM is employed, it is sufficiently cytotoxic to overcome cell growth over the course of the experiment.

Satisfied that the conditions employed for gemcitabine were suitable, **100** and **227** were also screened at the same concentrations.

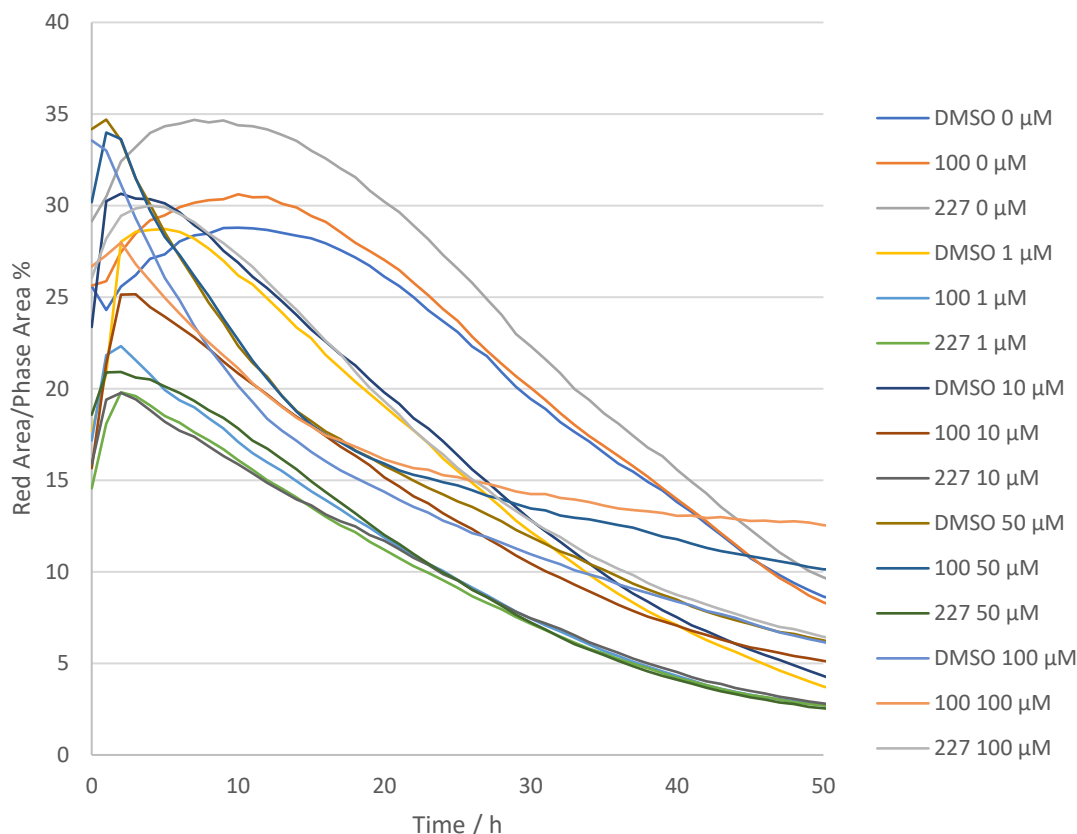


Figure 3.10: Red area normalised to phase area (%) as a function of time for LY2334737 (**100**), **227** and DMSO control against Panc10.05.

As with gemcitabine, area of red dye normalised against background fluorescence was measured as a function of time, shown in Figure 3.10. With the inconsistent data trends at the beginning of the experiment, likely associated with equilibration and introduction to the instrument environment, it is difficult to interpret. In general for all the data sets presented in Figure 3.10, there are no clear indications of an increase in red dye – hence cell death – as time increases. One of few conclusions that can be drawn is that come the end of the experiment, the two data sets demonstrating the greatest degree of apoptosis are the 100 μM and 50 μM of **227**, inferring that these are the most cytotoxic conditions explored. Analysis of cell confluence as a function of time demonstrates clearly that during the period of the experiment that cell growth continues (confluence increases), even in the presence of cytotoxic agents **100** and **227**. This infers that the cells weren't incubated for long enough prior to the beginning of the experiment, or that insufficient cells were seeded prior to initial incubation – the latter being more likely. After a period of equilibration (*cf.* 2 hours), the higher concentrations of LY2334737 (50 μM and 100 μM) slowly decrease below a confluency of around 30% over the duration of the experiment. These two sample sets demonstrate marked inhibited cell growth, hence inferred cytotoxicity, compared with the remaining sample set given cell growth.

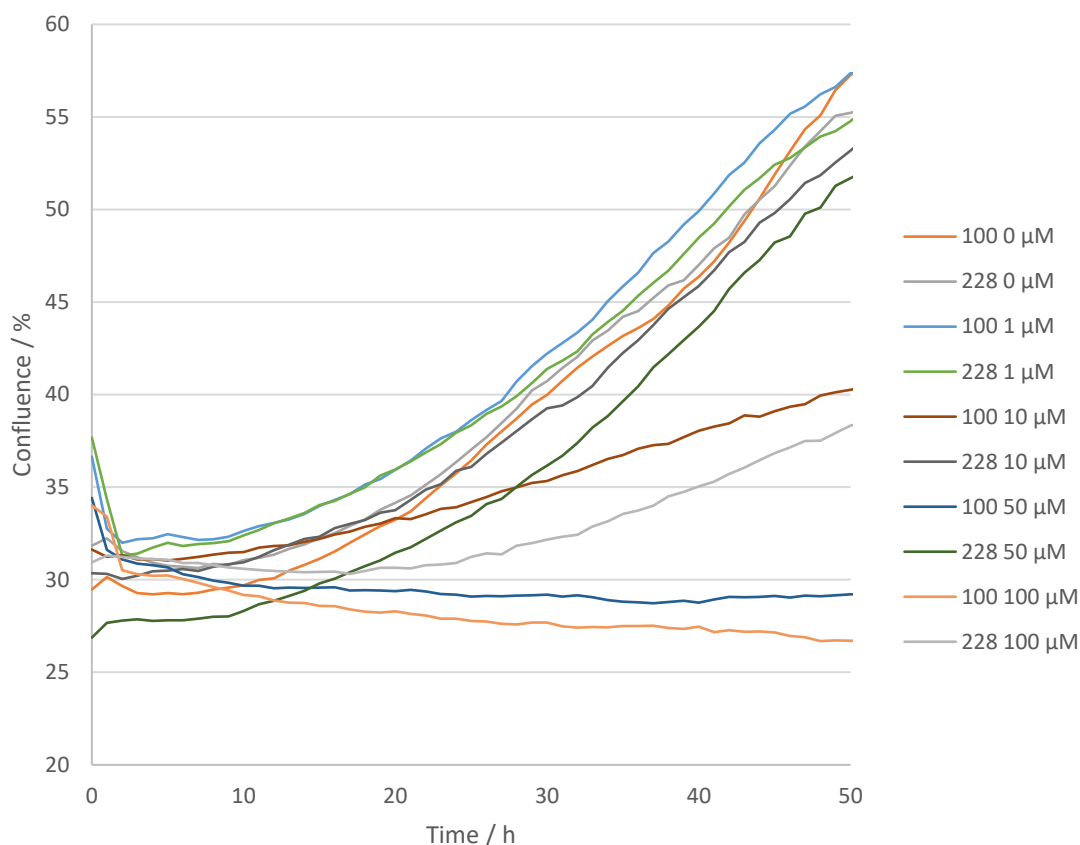


Figure 3.11: Confluence (%) as a function of time for LY2334737 (**100**) and **227** against Panc10.05.

Pleasingly, the next best performer can be seen to be the 100 μM sample of **227**, over the course of the experiment. Under these conditions, the compound performs comparably, if slightly poorer, than the 50 μM Lilly (LY2334737) data set up until 20 hours or so. At that point, the trend plateaus and confluency increases, indicating that cell growth is greater than cell death. This data set comes between 50 μM and 10 μM of LY2334737, indicates a fair degree of cytotoxicity. Marginal cytotoxicity for 50 μM 2'-Br-LY2334737 may also be observed, between the beginning of the experiment and 10 hours, but thereafter cell growth is clearly visible as confluency increases dramatically. Analysis of the confluence percentage shows that the 10 μM LY2334737 follows a similar trend to the 100 μM 2'-Br-LY2334737 data set, but at a greater percentage of confluence. This infers that the sample sets may be of similar cytotoxicity, but also that 100 μM 2'-Br-LY2334737 may demonstrate enhanced apoptosis than 10 μM LY2334737 and be a viable alternative as a chemotherapeutic. Unfortunately, due to the experiment conditions, no further meaningful conclusions may be drawn from the data set, with increasing confluency overwhelming the data set.

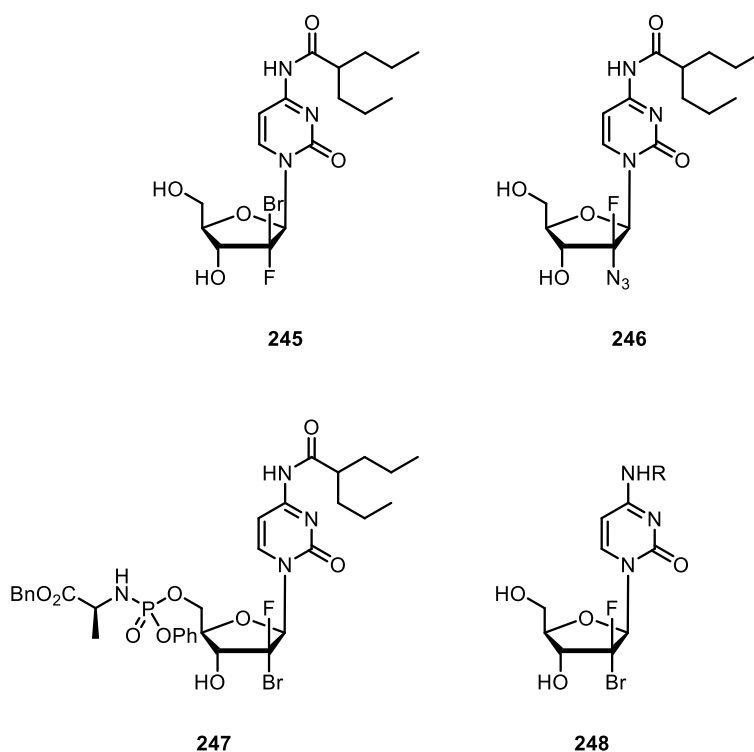


Figure 3.13: Structures of compounds of interest that may be synthesised for possible cytotoxic activity against Panc10.05.

ribonolactone functionality, introducing a different moiety with known biological activity, such as an azido analogue (**246**) or carboxylates, could influence the hydrogen bonding network within DNA and lead to a change in cytotoxicity. Similarly, modifying the amide functionality at the N^4 position will likely alter the cytotoxic properties of the compound and could be manipulated to further increase the lipophilic nature of the drug hence improve efficacy. An alternative approach would utilise the proside strategy developed by McGuigan and co-workers,^[32] incorporating a phosphoramidate moiety at the 5' position to overcome the rate limiting phosphorylation.^[40] This tactic could allow for either the non-functionalised or N^4 functionalised (**248**) compound to be used to improve the chances of incorporation and uptake into cancer cells.

4 – Conclusion

The objective of the research undertaken was to develop a synthetic route towards an appropriate precursor for radiofluorination and the production of [^{18}F]gemcitabine (**182**) by late-stage fluorination. Initial modification of Hertel's original synthesis^[8] was unsuccessfully translated to a synthetically useful scale (>1 mmol). As such, the synthetic strategy was revised, targeting installation of the leaving group by enolate chemistry of lactone **64**.^[12,20] A scalable, diastereoselective synthetic route towards 2-bromo-2-fluoro-ribonolactone **202** has been described, being produced on decagram scale in 49% yield over 4 steps from 2-deoxy-D-ribose. The observed selectivity is attributed to the use of NFSI as fluorinating agent, in conjunction with sterically bulky TIPS protected alcohol groups, which invokes facial selectivity and promotes single diastereomer formation. This methodology is complementary to recently published research.^[24] Exploration of alternative oxygen-based leaving groups was also investigated.

Glycosylation of **210** with cytosine derivatives **214** and **215** proceeded with high anomeric selectivity, which were in turn successfully transformed into radiolabelling precursors **226** and **228**. The multigram synthesis of **202** and **228** demonstrates notable stability, a desirable characteristic when designing precursors for radiofluorination, but hints at potential difficulty when targeting hot fluorination. Additionally, use of microwave heating allowed access to **222**, a different class of nucleosides, which could themselves be tested for radiofluorination and cytotoxicity.

In preparation of fluorination, authentic cold samples were synthesised for method development and characterisation. Non-radioactive ^{19}F labelling studies were conducted on precursor **228**, and it was found that **228** underwent fluorination, as detected by HRMS analysis. Initial radiofluorination studies were also investigated, reacting **228** with [^{18}F]KF delivered a radioactive compound following analysis by radio-TLC, which unfortunately did not match the target compound. Future work would further investigate the radiofluorination of **228** (in conjunction with **226**) towards [^{18}F]gemcitabine, in order to ascertain the suitability of **226/228** as radiolabelling precursors. Parameters to investigate may include protic solvent,^[71] and additives such as AgOTf to promote fluorination of **228**.^[98] Synthetically, alternative leaving groups or protecting groups may also be explored for the hot fluorination if **226** and **228** are unsuitable substrates.

Cytotoxic studies were also undertaken to evaluate the bioactivity of **227**, in comparison to gemcitabine (**1**) and LY2334737 (**100**). These preliminary results demonstrated anti-cancer properties, but further testing is required to determine criteria such as IC_{50} of the synthesised compounds.

5 – Experimental

5.1 – General information

Unless stated otherwise, all reactions were performed in oven-dried glassware sealed with rubber septa under a nitrogen atmosphere and were stirred with teflon-coated magnetic stirrer bars. Dry THF, acetonitrile, toluene, DCM and diethyl ether were obtained after passing these previously degassed solvents through activated alumina columns (Mbraun, SPS-800). Dry DMF was obtained from Acros Organics. All other solvents and commercial reagents were used as supplied without further purification unless stated otherwise.

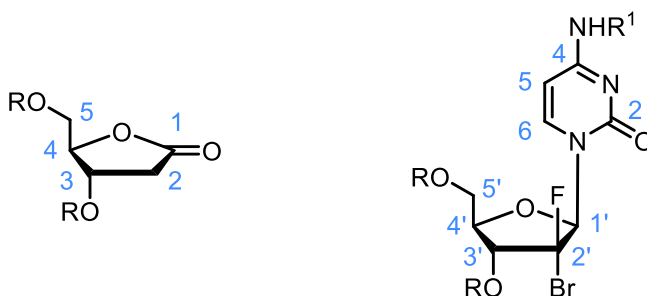
Room temperature (r.t.) refers to 20-25 °C. Temperatures of 0°C and -78°C were obtained using ice/water and CO₂ (s)/acetone baths respectively. All reactions involving heating were carried out using DrySyn blocks and a contact thermometer. In vacuo refers to the use of a rotary evaporator under reduced pressure. Microwave synthesis was carried out using a Biotage® Initiator+ Robot 60 Microwave Synthesizer.

Analytical thin layer chromatography was carried out using aluminium plates coated with silica (Kieselgel 60 F254 silica) and visualization was achieved using ultraviolet light (254 nm), followed by staining with a 1% aqueous KMnO₄ solution. Column chromatography used Kieselgel 60 silica in the solvent system stated.

Infrared spectra were recorded on a Shimadzu IRAffinity-1 Fourier Transform ATIR spectrometer as thin films using a pike miracle ATR accessory. Characteristic peaks are quoted (ν_{\max} / cm⁻¹).

¹H, ¹³C{¹H}, ¹⁹F{¹H} and ¹⁹F NMR spectra were obtained on either a Bruker Avance 400 (400 MHz ¹H, 101 MHz ¹³C, 377 MHz ¹⁹F) or a Bruker Avance 500 (500 MHz ¹H, 126 MHz ¹³C, 471 MHz ¹⁹F) spectrometer at 25 °C in the stated solvent. Chemical shifts are reported in parts per million (ppm) relative to the residual solvent signal or to internal standard (¹⁹F: α,α,α -trifluorotoluene, -62.61 ppm). All coupling constants, *J*, are quoted in Hz. Multiplicities are reported with the following symbols: s = singlet, d = doublet, t = triplet, q = quartet, m = multiplet and multiples thereof. The abbreviation Ar is used to denote aromatic, br to denote broad and app. to denote apparent signals. Carbon shifts are reported to the nearest 0.1 ppm and the number of signals rounded to the same value is indicated in brackets. Carbons in an identical environment giving one signal are not indicated further.

The structures below denote the numbering system used when assigning ^1H and ^{13}C environments:



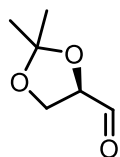
High resolution mass spectrometry (HRMS, m/z) data was acquired either at Cardiff University on a Micromass LCT spectrometer or at the EPSRC UK National Mass Spectrometry Facility at Swansea University.

Radiochemistry was conducted at the Wales Research and Diagnostic Positron Emission Tomography Imaging Centre (PETIC), University Hospital Wales, on a Trasis ALLINONE unit.

Fluorescence microscopy was conducted using a Sartorius Incucyte® S3 Live-Cell Analysis System, in conjunction with Incucyte® Cytotox Red Reagent for counting dead cells as fluorescent imaging probe.

5.2 – Synthetic route 1

2,3-O-Isopropylidene-D-glyceraldehyde (**11**)^[9]



1,2:5,6-di-O-isopropylidene-D-mannitol (10.49 g, 40.0 mmol) was dissolved in DCM (150 mL), to which saturated aqueous NaHCO₃ (5 mL) was added, maintaining the temperature below 25°C. NaIO₄ (21.39 g, 100 mmol, 2.5 equiv.) was subsequently added portion-wise over 20 minutes, and solution was stirred for 3 hours at room temperature. Solids generated during the reaction were filtered off and washed with additional DCM, and the filtrate dried over MgSO₄. The solvent was removed under reduced pressure and purified by distillation (25 mbar, 72-74°C) to yield **11** (8.05 g, 77% yield) as colourless oil.

¹H NMR (400 MHz, CDCl₃) δ 9.71 (d, *J* = 1.9 Hz, 1H, CHO), 4.38 (ddd, *J* = 7.3, 4.7, 1.9 Hz, 1H, CH(CHO)), 4.17 (dd, *J* = 8.8, 7.5 Hz, 1H, CH₂), 4.10 (dd, *J* = 8.8, 4.7 Hz, 1H, CH₂), 1.48 (s, 3H, CH₃), 1.41 (s, 3H, CH₃).

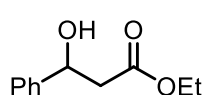
¹³C{¹H} NMR (101 MHz, CDCl₃) δ 202.0 (CHO), 111.4 (C(CH₃)₂), 80.0 (-CH(CHO)), 65.7 (CH₂), 26.4 (CH₃), 25.3 (CH₃).

IR (cm⁻¹): 3424, 2986, 1736, 1456, 1371, 1256, 1209, 1150, 1065, 843.

HRMS (TOF ES⁺): [C₆H₁₀O₄+H]⁺ calc. 131.0708, found 131.0714

[α]_D = +42° (*c* = 0.5, DCM, 23 °C).

Ethyl 3-hydroxy-3-phenylpropanoate (**191**)



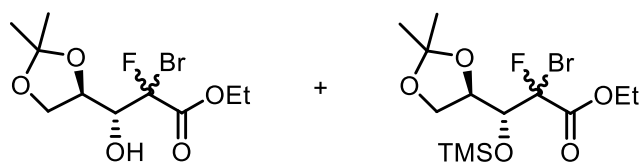
To a 10 mL Retsch stainless steel jar was added zinc (2 mmol, 0.131 g), aldehyde (1 mmol), α-bromo ester (1.2 mmol) under air atmosphere. A stainless steel ball of mass 4.0 g was added and the mixture was milled at 30 Hz for 2 hours. The resulting black/grey paste mixture was transferred into a flask and the jar was rinsed with ethyl acetate (2 x 10 mL), before quenching with 2 M HCl solution (10 mL). The quenched solution was then washed and extracted with EtOAc. The combined organic layers were dried over MgSO₄ and concentrated *in vacuo*. The crude mixture was purified by column chromatography (20% Ethyl Acetate/Petroleum ether) to yield **191** (140 mg, 72%) as a light yellow oil.

¹H NMR (500 MHz, CDCl₃) δ 7.43 - 7.35 (m, 4H, ArH), 7.34 - 7.27 (m, 1H, ArH), 5.16 (dd, *J* = 8.9, 3.9 Hz, 1H, PhCHOH), 4.21 (q, *J* = 7.1 Hz, 2H, OCH₂CH₃), 2.85 - 2.65 (m, 2H, CH₂), 1.29 (t, *J* = 7.1 Hz, 3H, OCH₂CH₃).

¹³C NMR (126 MHz, CDCl₃) δ 172.6 (C=O), 142.6 (ArC), 128.7 (ArC), 128.0 (ArC), 125.8 (ArC), 70.5 (PhCHOH), 61.0 (OCH₂), 43.5 (CH₂), 14.3 (CH₃).

HRMS (EI) calcd for [M] = C₁₁H₁₄O₃: 194.0943, found: 194.0944.

Ethyl 2-bromo-3-((R)-2,2-dimethyl-1,3-dioxolan-4-yl)-2-fluoro-3-hydroxypropanoate (192) and ethyl 2-bromo-3-((R)-2,2-dimethyl-1,3-dioxolan-4-yl)-2-fluoro-3-((trimethylsilyl)oxy)propanoate (193)*



To a suspension of sonicated zinc powder (157.1 mg, 2.4 mmol, 2.4 equiv., [325 mesh]) in anhydrous MeCN (3 mL) was added ethyl dibromofluoroacetate (280 μ L, 2 mmol, 2 equiv.) at room temperature. After stirring for 10 minutes, TMSCl (280 μ L, 2.2 mmol, 2.2 equiv.) was added at 0°C and stirred for a further 10 minutes. After cooling to -40°C, a solution of compound **11** (130.1 mg, 1 mmol) in MeCN (1 mL) and Cp₂TiCl₂ (273.2 mg, 1.1 mmol, 1.1 equiv.) were added to the mixture. The mixture was stirred at -40°C for 1.5 h, then allowed to warm to r.t. and stirred for 1 h. Diethyl ether (10 mL) and saturated aqueous NaHCO₃ (10 mL) were added at 0°C, stirred for 5 min and filtered through celite. The filtrate was separated, washed with brine and dried over MgSO₄. Flash chromatography on silica gel (40% EtOAc/Hexane) provided a mixture of **192** (63.2 mg, 86:14 d.r.) and **193** (56.9 mg, combined 35% yield) as a colourless oil.

192: ¹H NMR (400 MHz, CDCl₃) δ 4.69 (td, J = 6.7, 3.0 Hz, 1H, CH), 4.51 (ddd, J = 25.1, 5.2, 3.0 Hz, 1H, CHOH), 4.35 (q, J = 7.1 Hz, 2H, EtCH₂), 4.07 – 4.04 (m, 2H, CH₂), 3.16 (d, J = 5.4 Hz, 1H, OH), 1.42 (s, 3H, CH₃), 1.38 (s, 3H, CH₃), 1.34 (t, J = 7.1 Hz, 3H, EtCH₃).

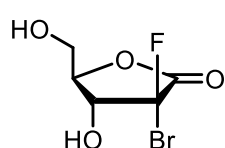
¹³C{¹H} NMR (101 MHz CDCl₃): δ 165.0 (d, J = 27.1 Hz, C=O), 109.0 (CH₂), 96.7 (d, J = 270.0 Hz, CFB), 74.5 (d, J = 20 Hz, CHOH), 74.4 (C(CH₃)₂), 64.1 (d, J = 7.1 Hz, CH), 63.6 (EtCH₂), 26.2 (CH₃), 25.4 (CH₃), 13.8 (EtCH₃).

¹⁹F{¹H} NMR (376.5 MHz, CDCl₃): δ -133.8 (s, *major*), -133.1 (s, *minor*).

193: ¹H NMR (CDCl₃, 400 MHz): 4.75 (ddd, J = 7.6, 6.7, 2.0 Hz, 1H, CH), 4.63 (dd, J = 25.7, 2.0 Hz, 1H, CH), 4.51 (q, J = 8 Hz, 2H, EtCH₂), 3.98-3.96 (m, 2H, CH₂), 1.42 (s, 3H, CH₃), 1.38 (s, 3H, CH₃), 1.34 (t, J = 8 Hz, 3H, EtCH₃), 0.14 (s, 9H, Si(CH₃)₃).

* In the absence of MS, the structural identities of **192** and **193** cannot be conclusively assigned hence the structures proposed are tentative.

(3R,4R,5R)-3-bromo-3-fluoro-4-hydroxy-5-(hydroxymethyl)dihydrofuran-2(3H)one (195)



To a solution of **192** and **193** (0.35 mmol) in MeOH (6 mL) was added aqueous HCl (1 M, 3.8 mL, 19.0 equiv.) at room temperature. The solution was then refluxed for overnight. After cooling to room temperature, the reaction

mixture was extracted with ethyl acetate (3 x 25 mL). The organic layers were collected, dried over MgSO₄. The crude material was purified by column chromatography (100% EtOAc) to give **195** (32.0 mg, 40% yield) as a clear oily liquid.

¹H NMR (400 MHz, CDCl₃) δ 4.60 (ddd, *J* = 15.3, 8.0, 7.4 Hz, 1H, *H*^β), 4.16 – 4.08 (m, 2H, *H*^{βa} and *H*^{βb}), 3.92 – 3.85 (m, 1H, O⁵*H*), 2.97 (dd, *J* = 7.3, 3.8 Hz, 1H, *H*^α), 2.02 (dd, *J* = 8.0, 4.7 Hz, 1H, O³*H*).

¹³C{¹H} NMR (101 MHz, CDCl₃) δ 165.0 (d, *J* = 27.7 Hz, C¹), 99.0 (d, *J* = 279.7 Hz, C²), 80.0 (d, *J* = 7.5 Hz, C⁴), 72.0 (d, *J* = 21.3 Hz, C³), 58.5 (C⁵).

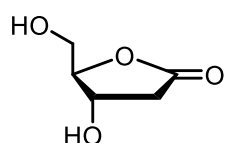
¹⁹F{¹H} NMR (376 MHz, CDCl₃) δ -128.16 (s).

¹⁹F NMR (376 MHz, CDCl₃) δ -128.17 (dd, *J* = 14.5, 1.7 Hz).

* In the absence of MS, the structural identity of **195** cannot be conclusively assigned hence the structure proposed is tentative.

5.3 – Synthetic route 2

(4S,5R)-4-hydroxy-5-(hydroxymethyl)dihydrofuran-2(3H)-one (**75**)



Bromine (4.8 mL, 95.5 mmol, 2.5 equiv.) was added dropwise to a solution of 2-deoxy-D-ribose (5.097 g, 38 mmol) in water (50 mL), and stirred in the dark at room temperature for 5 days. The reaction was neutralised with K_2CO_3 . Excess bromine and solvent were removed under reduced pressure (fitted with $Na_2S_2O_3$ (aq) trap). The crude mixture was purified by column chromatography (0% → 5% MeOH/EtOAc) to yield **75** (4.671 g, 93% yield) as a light yellow oil.

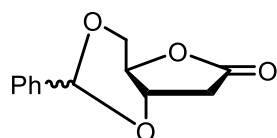
1H NMR (500 MHz, DMSO- d_6) δ 5.48 (d, J = 4.1 Hz, O^3H), 5.06 (t, J = 5.4 Hz, O^5H), 4.26 (m, 2H, H^6 and H^4), 3.56 (dd, J = 12.2, 3.7 Hz, 1H, H^{6a}), 3.52 (dd, J = 12.2, 3.8 Hz, 1H, H^{6b}), 2.81 (dd, J = 17.7, 6.4 Hz, 1H, H^{2a}), 2.22 (dd, J = 17.7, 2.3 Hz, 1H, H^{2b}).

$^{13}C\{^1H\}$ NMR (126 MHz, DMSO- d_6) δ 176.2 (C^1), 88.3 (C^4), 67.8 (C^3), 60.8 (C^5), 38.0 (C^2).

IR (cm^{-1}): 3389, 2934, 1744, 1364, 1169, 1051.

HRMS (CI): $[C_5H_{12}O_4+NH_4]^+$ calc. 150.0761, found 150.0760.

(4aR,7aS)-2-phenyltetrahydro-6H-furo[3,2-d][1,3]dioxin-6-one (**198**)

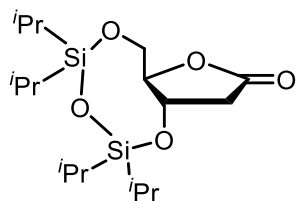


A solution of **75** (663.9 mg, 5.0 mmol) with HCl (12 M, 600 μ L, 7 mmol, 1.4 equiv.) in benzaldehyde (10 mL) was stirred overnight at room temperature. The mixture was concentrated *in vacuo* to deliver a brown solid, which was collected and washed with EtOH to deliver **198** (40.5 mg, 4% yield) as a white solid, in a diastereomeric mixture.

1H NMR (500 MHz, $CDCl_3$) δ 7.50 – 7.46 (m, 2H, ArH), 7.45 – 7.36 (m, 3H, ArH), 6.24 (s, 0.2H, PhCH), 5.76 (s, 1H, PhCH), 4.79 (ddd, J = 8.3, 3.7, 2.5 Hz, 1H, H^6), 4.75 (ddd, J = 7.5, 4.0, 2.7 Hz, 0.2H, $H^{6'}$), 4.63 – 4.55 (m, 2H, H^4 , H^{6a} and $H^{4'}$), 4.61 (dd, J = 13.0, 1.7 Hz, 0.2H, $H^{6'}$), 4.24 (dd, J = 13.0, 2.2 Hz, 0.2H, $H^{6b'}$), 4.23 (dd, J = 13.2, 2.1 Hz, 1H, H^{6b}), 3.05 (dd, J = 16.0, 2.5 Hz, 1H, H^{2a}), 3.01 (obs. d, J = 2.6 Hz, 0.2H, $H^{2a'}$), 2.64 (dd, J = 16.0, 3.8 Hz, 1H, H^{2b}), 2.64 – 2.59 (m, 0.2H, $H^{2b'}$).

HRMS (EI $^+$): $[C_{12}H_{12}O_4]$ calc. 220.0736 found 220.0734.

Data is consistent with the literature.^[140]

(6aR,9aS)-2,2,4,4-tetraisopropyltetrahydro-8H-furo[3,2-f][1,3,5,2,4]trioxadisilocin-8-one (200)

To a solution of **75** (1.3392 g, 10.1 mmol) and imidazole (1.7423 g, 25.6 mmol, 2.5 equiv.) in anhydrous DMF (25 mL) was added 1,3-dichloro-1,1,3,3-tetraisopropylidisiloxane (4.8 mL, 15 mmol, 1.49 equiv.) dropwise at room temperature. After complete addition, the reaction was then stirred at r.t. for

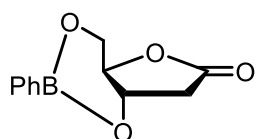
24 h before being poured onto water (50 mL), and extracted into Et₂O (3 x 50 mL). The combined organics were washed with water, saturated aqueous NaHCO₃ and brine (3 x 40 mL each), then dried over MgSO₄ and concentrated *in vacuo*. The crude mixture was purified by column chromatography (20% Et₂O/Hexane) to deliver **200** (1.6323 g, 44% yield) as a thick, colourless oil.

¹H NMR (500 MHz, CDCl₃) δ 4.63 (dd, *J* = 16.3, 7.9 Hz, 1H, *H*^β), 4.21 (td, *J* = 6.7, 3.6 Hz, 1H, *H*^α), 4.14 (dd, *J* = 12.3, 3.5 Hz, 1H, *H*^{6a}), 3.93 (dd, *J* = 12.3, 6.6 Hz, 1H, *H*^{6b}), 2.86 (dd, *J* = 17.3, 8.0 Hz, 1H, *H*^{7a}), 2.71 (dd, *J* = 17.3, 9.2 Hz, 1H, *H*^{7b}), 1.12 – 1.01 (m, 28H, SiCH(CH₃)₂ and SiCH(CH₃)₂).

¹³C{¹H} NMR (126 MHz, CDCl₃) δ 173.1 (C¹=O), 85.0 (C⁴), 69.8 (C³), 62.5 (C⁵), 38.0 (C²), 17.6 (SiCH(CH₃)₂), 17.5 (SiCH(CH₃)₂), 17.4 (2C, SiCH(CH₃)₂), 17.3 (SiCH(CH₃)₂), 17.1 (SiCH(CH₃)₂), 17.0 (2C, SiCH(CH₃)₂), 13.4 (SiCH(CH₃)₂), 13.3 (SiCH(CH₃)₂), 13.0 (SiCH(CH₃)₂), 12.7 (SiCH(CH₃)₂).

Data is consistent with the literature.^[141]

The same method was attempted synthesis of **199**, but no target material was detected/synthesised.

(4aR,7aS)-2-phenyltetrahydro-6H-furo[3,2-d][1,3,2]dioxaborinin-6-one (201)

To a flame dried flask containing **75** (277.4 mg, 2.1 mmol) and phenyl boronic acid (488.1 mg, 4 mmol, 2 equiv.), was added toluene (10 mL) and the solution stirred at room temperature

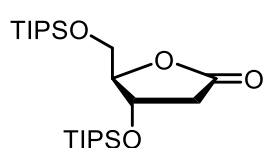
overnight. The reaction mixture was filtered and dried *in vacuo* to deliver **201** (328.8 mg, 75% yield) as an off-white solid.

¹H NMR (500 MHz, CDCl₃) δ 7.78 (d, *J* = 7.2 Hz, 2H, ArH), 7.49 (t, *J* = 7.3 Hz, 1H, ArH), 7.38 (t, *J* = 7.4 Hz, 2H, ArH), 5.17 – 5.09 (m, 1H), 4.91 (d, *J* = 8.3 Hz, 1H), 4.59 (d, *J* = 12.9 Hz, 1H), 4.31 (d, *J* = 13.2 Hz, 1H), 3.07 (dd, *J* = 16.2, 2.1 Hz, 1H, *H*^{7a}), 2.72 (dd, *J* = 16.2, 3.9 Hz, 1H, *H*^{7b}).

¹³C NMR (126 MHz, CDCl₃) δ 169.0 (C¹), 135.2 (ArC), 132.2 (ArC), 128.0 (ArC), 73.3 (C⁵), 73.2 (C⁴), 69.4 (C³), 35.7 (C²).

HRMS (EI+): [C₁₁H₁₁O₄¹¹B] calc 218.0750 found 218.0756

(4S,5R)-4-((triisopropylsilyl)oxy)-5-(((triisopropylsilyl)oxy)methyl)dihydrofuran-2(3H)-one (64)



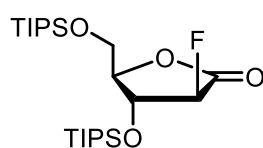
To a solution of **75** (11.4727 g, 86.84 mmol) and imidazole (35.4697 g, 521 mmol, 6 equiv.) in anhydrous DMF (100 mL) was added triisopropylsilyl chloride (75 mL, 350 mmol, 4 equiv.) dropwise *via* dropping funnel at 0°C. After complete addition, further DMF (75 mL) was added and the solution was warmed to room temperature and stirred for 24 h. The reaction was quenched by pouring onto water (100 mL) and extracted with ethyl acetate (3 x 150 mL). The combined organic layers were washed successively with saturated aqueous NaHCO₃, H₂O and brine (2 x 100 mL each), dried over MgSO₄ and concentrated *in vacuo*. The crude mixture was purified by column chromatography (5% Et₂O/Hexane) to yield **64** (30.9951 g, 80% yield) as a colorless oil. ¹H NMR (500 MHz, CDCl₃) δ 4.67 (dt, *J* = 6.6, 1.9 Hz, 1H, *H^β*), 4.41 (dd, *J* = 4.2, 2.8 Hz, 1H, *H^α*), 3.93 (dd, *J* = 11.3, 3.1 Hz, 1H, *H^{δa}*), 3.88 (dd, *J* = 11.3, 2.4 Hz, *H^{δb}*), 2.88 (dd, *J* = 17.6, 6.6 Hz, 1H, *H^{2a}*), 2.44 (dd, *J* = 17.6, 2.0 Hz, 1H, *H^{2b}*), 1.14 – 1.03 (m, 42H, SiCH(CH₃)₂ and SiCH(CH₃)₂).

¹³C{¹H} NMR (126 MHz, CDCl₃) δ 176.1 (C¹), 88.9 (C⁴), 70.1 (C³), 63.4 (C⁵), 39.7 (C²), 18.0 (3C, SiCH(CH₃)₂), 12.0 (2C, SiCH(CH₃)₂).

IR (film) cm⁻¹: 2943, 2866, 2359, 1788, 1460, 1385, 1165, 1125, 1098, 1067, 1013, 966, 880, 683.

HRMS (TOF AP+): [C₂₃H₄₉O₄Si₂]⁺ calc 445.3169 found 445.3177.

(3S,4R,5R)-3-fluoro-4-((triisopropylsilyl)oxy)-5-(((triisopropylsilyl)oxy)methyl)-dihydrofuran-2(3H)-one (65)



To a solution of **64** (791.6 mg, 1.78 mmol) and NFSI (842.3 mg, 2.67 mmol, 1.5 equiv.) in anhydrous THF (10 mL) at -78°C was added LiHMDS (2.4 mL, 1 M in THF, 1.3 equiv.) dropwise. After complete addition, the mixture was stirred at -78°C for 2 h and then quenched by saturated aqueous NH₄Cl (10 mL). The mixture was warmed to room temperature, extracted with EtOAc (3 x 10 mL), and the combined organic layers successively washed with saturated aqueous NaHCO₃ and brine (1 x 20 mL each), dried over MgSO₄, and concentrated *in vacuo*. The crude product was purified by flash chromatography (2.5% → 7.5% EtOAc/Hexane) to afford **65** (450.2 mg, 54%) as a colourless solid.

^1H NMR (500 MHz, CDCl_3) δ 5.14 (dd, $J = 51.3, 7.4$ Hz, 1H, H^f), 4.94 (dt, $J = 18.8, 7.2$ Hz, 1H, H^g), 4.19 (dt, $J = 7.0, 2.2$ Hz, 1H, H^h), 4.11 (dt, $J = 12.1, 2.1$ Hz, 1H, H^{6a}), 3.94 (dd, $J = 12.2, 2.3$ Hz, 1H, H^{6b}), 1.16 – 1.04 (m, 42H, $\text{SiCH}(\text{CH}_3)_2$ and $\text{SiCH}(\text{CH}_3)_2$).

$^{13}\text{C}\{^1\text{H}\}$ NMR (126 MHz, CDCl_3) δ 168.9 (d, $J = 23.2$ Hz, C^1), 92.9 (d, $J = 198.8$ Hz, C^2), 82.0 (d, $J = 10.3$ Hz, C^4), 71.9 (d, $J = 20.8$ Hz, C^3), 60.4 (C^5), 18.0 (2C, $\text{SiCH}(\text{CH}_3)_2$), 17.9 (2C, $\text{SiCH}(\text{CH}_3)_2$), 12.3 ($\text{SiCH}(\text{CH}_3)_2$), 12.0 ($\text{SiCH}(\text{CH}_3)_2$).

^{19}F NMR $\{^1\text{H}\}$ (376 MHz, CDCl_3) δ -200.84 (s).

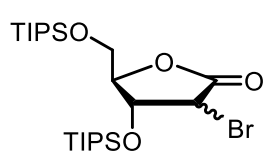
^{19}F NMR (471 MHz, CDCl_3) δ -200.78 (dd, $J = 51.5, 18.9$ Hz).

IR (cm^{-1}): 2943, 2864, 1809, 1464, 1236, 1142, 1107, 1070, 1040, 881, 799, 683.

HRMS (ES): $[\text{C}_{23}\text{H}_{47}\text{FO}_4\text{Si}_2+\text{H}]^+$ calc. 463.3075 found 463.3076.

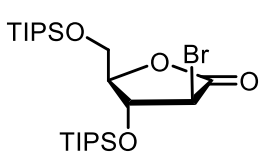
Data is consistent with the literature.^[20]

(4R,5R)-3-bromo-4-((triisopropylsilyl)oxy)-5-(((triisopropylsilyl)oxy)methyl)-dihydrofuran-2(3H)-one (**203**)



To a solution of **64** (3.4353 g, 7.72 mmol) and triethylamine (6.5 mL, 46.3 mmol, 6 equiv.) in anhydrous DCM (60 mL) was added TMSOTf (4.0 mL, 23.16 mmol, 3 equiv.) slowly over 10 minutes at 0°C . After complete addition, the reaction was stirred at 0°C for a further 30 minutes. NBS (2.0615 g, 11.58 mmol, 1.5 equiv.) was then added in a single portion, and the reaction stirred for 2 hours at 0°C , before warming to room temperature and stirred overnight. The reaction mixture was poured onto saturated aqueous NaHCO_3 (100 mL) and extracted with DCM (3 x 50 mL). The combined organics were washed successively with water and brine (3 x 50 mL each), dried over MgSO_4 and concentrated *in vacuo*. The residue was purified by column chromatography (5% Et_2O /Hexane) to afford **203** (2.8497 g, 70% yield) as a mixture of diastereomers as a colourless oil (arabino:ribono 2:1). Further purification by column chromatography separated the diastereomers for further analysis, and configuration assignment based on ^1H COSY and NOESY NMR. Strong spatial correlation observed between H^f and H^g of *ribono* diastereomer.

Arabino/ β **204** (major diastereomer):



^1H NMR (500 MHz, CDCl_3) δ 4.88 (t, $J = 4.3$ Hz, 1H, H^g), 4.38 (app. dd, $J = 8.4, 3.9$ Hz, 1H, H^h), 4.33 (d, $J = 4.6$ Hz, 1H, H^f), 4.06 (dd, $J = 11.4, 4.7$ Hz, 1H, H^{6a}), 3.97 (dd, $J = 11.4, 3.6$ Hz, 1H, H^{6b}), 1.15 – 1.03 (m, 42H, $\text{SiCH}(\text{CH}_3)_2$ and $\text{SiCH}(\text{CH}_3)_2$).

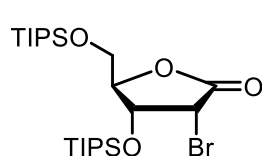
$^{13}\text{C}\{^1\text{H}\}$ NMR (126 MHz, CDCl_3) δ 171.1 (C^1), 87.1 (C^4), 76.0 (C^3), 61.7 (C^5), 45.0 (C^2), 18.1 (2C, $\text{SiCH}(\text{CH}_3)_2$), 18.0 (2C, $\text{SiCH}(\text{CH}_3)_2$), 12.4 ($\text{SiCH}(\text{CH}_3)_2$), 12.0 ($\text{SiCH}(\text{CH}_3)_2$).

IR (cm⁻¹): 2943, 2866, 1800, 1460, 1140, 1067, 881, 683.

Appearance: Colourless oil

HRMS (TOF AP⁺): [C₂₃H₄₇O₄Si₂Br+H]⁺ calc. 523.2275 found 523.2278

Ribono/ α **205** (minor diastereomer):



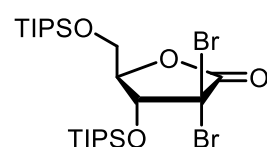
¹H NMR (500 MHz, CDCl₃) δ 4.62 (dd, J = 5.6, 4.7 Hz, 1H, H^{β}), 4.57 (d, J = 5.6 Hz, 1H, H^{β}), 4.39 (dt, J = 4.5, 2.1 Hz, 1H, H^{α}), 4.10 (dd, J = 12.0, 2.3 Hz, 1H, H^{6a}), 3.94 (dd, J = 12.0, 2.1 Hz, 1H, H^{6b}), 1.13 – 1.02 (m, 42H, SiCH(CH₃)₂ and SiCH(CH₃)₂).

¹³C{¹H} NMR (126 MHz, CDCl₃) δ 171.2 (C¹), 85.6 (C⁴), 69.2 (C³), 61.1 (C⁵), 46.9 (C²), 18.1 (SiCH(CH₃)₂), 18.0 (2C, SiCH(CH₃)₂), 12.5 (SiCH(CH₃)₂), 12.0 (SiCH(CH₃)₂).

IR (cm⁻¹): 2945, 2866, 1796, 1464, 1150, 1065, 881, 685.

Appearance: Low melt white solid.

(4R,5R)-3,3-dibromo-4-((triisopropylsilyl)oxy)-5-(((triisopropylsilyl)oxy)methyl)-dihydrofuran-2(3H)-one (206)



To a solution of 2-deoxy-3,5-di-*O*-(isopropylsilyl)-*D*-ribonolactone (904.0 mg, 2.0 mmol) and dibromotetrachloroethane (848.5 mg, 2.6 mmol, 1.3 equiv) in anhydrous THF (10 mL, [0.2 M]) at -78°C was added LiHMDS (3 mL, 3 mmol, 1.5 equiv.) slowly as to maintain $T < -75^{\circ}\text{C}$. After complete addition, the reaction was stirred at -78°C for 4 hours, before quenching with saturated aqueous NH₄Cl and warming to r.t.. The golden reaction mixture was extracted with Et₂O (3 x 20 mL) and successively washed with saturated aqueous NaHCO₃, water and brine (3 x 20 mL each). The crude mixture was dried over MgSO₄ and concentrated *in vacuo*. The crude mixture was purified by column chromatography (2%→3% Et₂O in Petroleum ether), affording a mixture of the *arabino* (S) (**204**) and *ribo* (R) (**205**) diastereomers (3:2 ratio, 196.4 mg, 19% yield) and **206** (556.4 mg, 46% yield)

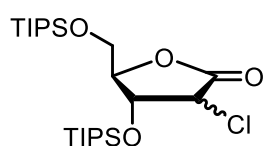
¹H NMR (400 MHz, CDCl₃) δ 4.91 (d, J = 7.3 Hz, 1H, H^{β}), 4.18 – 4.14 (m, 2H, H^{α} and H^{6a}), 3.95 (dd, J = 12.9, 2.4 Hz, 1H, H^{6b}), 1.10 (m, 42H, SiCH(CH₃)₂ and SiCH(CH₃)₂).

¹³C{¹H} NMR (126 MHz, CDCl₃) δ 167.2 (C¹), 83.92 (C⁴), 77.80 (C³), 59.27 (C²), 58.15 (C⁵), 18.2 (2C, SiCH(CH₃)₂), 18.0 (SiCH(CH₃)₂), 17.9 (SiCH(CH₃)₂), 12.9 (SiCH(CH₃)₂), 12.1 (SiCH(CH₃)₂).

IR (cm⁻¹): 2945, 2868, 1803, 1462, 1190, 1169, 1146, 1063, 885, 785, 685.

HRMS (TOF ES⁺): [C₂₃H₄₆O₄Si₂Br₂+H]⁺ calc. 601.1380 found 601.1392.

(4R,5R)-3-chloro-4-((triisopropylsilyl)oxy)-5-(((triisopropylsilyl)oxy)methyl)-dihydrofuran-2(3H)-one (207)



To a solution of **64** (409.5 mg, 0.92 mmol) and triethylamine (770 μ L, 5.52 mmol, 6 equiv.) in anhydrous DCM (10 mL) was added TMSOTf (480 μ L, 2.76 mmol, 3 equiv.) slowly over 10 minutes at 0°C. After complete addition, the reaction was stirred at 0°C for a further 30 minutes. NCS (185.2 mg, 1.38 mmol, 1.5 equiv.) was then added in a single portion, and the reaction stirred for 1 hours at 0°C, before warming to room temperature and stirred overnight. The reaction mixture was poured onto saturated aqueous NaHCO₃ (20 mL) and extracted with DCM (3 x 20 mL). The combined organics were washed successively with water and brine (3 x 20 mL each), dried over MgSO₄ and concentrated *in vacuo*. The residue was purified by column chromatography (3% Et₂O/Hexane) to afford **207** (164.9 mg, 37% yield) as a mixture of diastereomers as a colourless oil (d.r. = 7:3). Assignment of diastereomers was not possible from 2D NOESY NMR. The data presented is of the separated diastereomers.

¹H NMR (400 MHz, CDCl₃) δ 4.71 (dd, J = 5.5, 2.3 Hz, 1H, H^{β}), 4.68 (d, J = 5.5 Hz, 1H, H^{γ}), 4.44 (app. q, J = 2.3 Hz, 1H, H^{α}), 4.05 (dd, J = 11.8, 2.5 Hz, 1H, H^{6a}), 3.92 (dd, J = 11.8, 2.0 Hz, 1H, H^{6b}), 1.12 (m, 42H, SiCH(CH₃)₂ and SiCH(CH₃)₂).

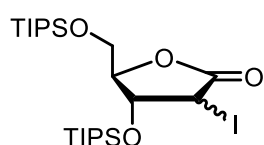
¹³C NMR (126 MHz, CDCl₃) δ 171.5 (C¹), 86.4 (C⁴), 70.9 (C³), 62.2 (C²), 56.3 (C⁵), 18.0 (4C, SiCH(CH₃)₂), 12.4 (SiCH(CH₃)₂), 11.9 (SiCH(CH₃)₂).

¹H NMR (400 MHz, CDCl₃) δ 4.83 (dd, J = 6.2, 5.4 Hz, 1H, H^{β}), 4.38 (d, J = 6.2 Hz, 1H, H^{γ}), 4.29 (dt, J = 5.4, 3.1 Hz, 1H, H^{α}), 4.08 (dd, J = 11.8, 3.4 Hz, 1H, H^{6a}), 3.94 (dd, J = 11.8, 3.0 Hz, 1H, H^{6b}), 1.12 (m, 42H, SiCH(CH₃)₂ and SiCH(CH₃)₂).

¹³C{¹H} NMR (126 MHz, CDCl₃) δ 170.3 (C¹), 85.3 (C⁴), 75.5 (C³), 60.9 (C²), 58.9 (C⁵), 18.1 (2C, SiCH(CH₃)₂), 18.00 (SiCH(CH₃)₂), 17.9 (SiCH(CH₃)₂), 12.4 (SiCH(CH₃)₂), 12.0 (SiCH(CH₃)₂).

HRMS (TOF AP⁺): [C₂₃H₄₇O₄Si₂³⁵Cl+H]⁺ calc. 479.2780 found 479.2783.

(4R,5R)-3-iodo-4-((triisopropylsilyl)oxy)-5-(((triisopropylsilyl)oxy)methyl)-dihydrofuran-2(3H)-one (208)



To a solution of **64** (423.0 mg, 0.95 mmol) and triethylamine (800 μ L, 5.7 mmol, 6 equiv.) in anhydrous DCM (10 mL) was added TMSOTf (495 μ L, 2.85 mmol, 3 equiv.) slowly over 10 minutes at 0°C. After complete addition, the reaction was stirred at 0°C for a further 30 minutes. NIS (321.9 mg, 1.43 mmol, 1.5 equiv.) was then added

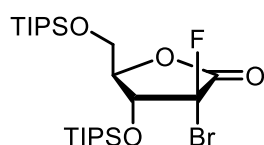
in a single portion, and the reaction stirred for 1 hours at 0°C, before warming to room temperature and stirred overnight. The reaction mixture was poured onto saturated aqueous NaHCO₃ (25 mL) and extracted with DCM (3 x 20 mL). The combined organics were washed successively with water and brine (3 x 25 mL each), dried over MgSO₄ and concentrated *in vacuo*. The residue was purified by column chromatography (3% Et₂O/Hexane) to afford **208** (349.5 mg, 65% yield) as a mixture of diastereomers as a colourless solid (d.r. = 0.7:1).

¹H NMR (500 MHz, CDCl₃) δ 4.90 (t, *J* = 2.8 Hz, 0.7H, *H*^β), 4.67 (d, *J* = 6.0 Hz, 1H, *H*^ρ), 4.49 (td, *J* = 5.2, 2.6 Hz, 0.7H, *H*^α), 4.43 (d, *J* = 2.9 Hz, 0.7H, *H*^{ρ'}), 4.23 (dt, *J* = 5.9, 2.0 Hz, 1H, *H*^α), 4.12 (dd, *J* = 12.1, 1.8 Hz, 1H, *H*^{βa}), 4.07 (d, *J* = 5.2 Hz, 1.3H, *H*^β and *H*^{βa}), 3.98 (app. t, *J* = 6.0 Hz, 1H, *H*^{βb}), 3.94 (dd, *J* = 12.1, 2.1 Hz, 1H, *H*^{βb}), 1.16 – 1.03 (m, 72H, SiCH(CH₃)₂ and SiCH(CH₃)₂).

HRMS (TOF AP⁺): [C₂₃H₄₇O₄²⁸Si₂¹²⁷I+H]⁺ calc. 571.2136 found 571.2137.

No ¹³C{¹H} NMR recorded.

(3R,4R,5R)-3-bromo-3-fluoro-4-((triisopropylsilyloxy)-5-(((triisopropylsilyloxy)-methyl)dihydrofuran-2(3H)-one (202)



To a solution of **203** (5.4385 g, 10.4 mmol) and NFSI (5.7408 g, 18.2 mmol, 1.75 equiv.) in anhydrous THF (20 mL) at -78°C was added LiHMDS (15.6 mL, 1 M in THF, 1.5 equiv.) dropwise. After complete addition, the mixture was stirred at -78°C for 4 h and then quenched by saturated aqueous NH₄Cl (20 mL). The mixture was warmed to room temperature, extracted with Et₂O (3 x 50 mL), and the combined organic layers successively washed with saturated aqueous NaHCO₃ and brine (3 x 20 mL each), dried over MgSO₄, and concentrated *in vacuo*. The crude product was purified by flash chromatography (5% Et₂O/Hexane or 40% DCM/Hexane) to afford **202** (4.525 g, 75%) as a colourless oil.

¹H NMR (500 MHz, CDCl₃) δ 4.79 (dd, *J* = 14.6, 7.7 Hz, 1H, *H*^β), 4.16 (dt, *J* = 12.5, 2.0 Hz, 1H, *H*^{βa}), 4.05 (dt, *J* = 7.7, 1.6 Hz, 1H, *H*^α), 3.97 (dd, *J* = 12.5, 1.8 Hz, 1H, *H*^{βb}), 1.12 (m, 42H, SiCH(CH₃)₂ and SiCH(CH₃)₂).

¹³C{¹H} NMR (126 MHz, CDCl₃) δ 165.8 (d, *J* = 27.9 Hz, C¹), 100.0 (d, *J* = 278.5 Hz, C²), 81.5 (d, *J* = 8.4 Hz, C⁴), 72.5 (d, *J* = 20.5 Hz, C³), 59.1 (C⁵), 18.0 (2C, SiCH(CH₃)₂), 17.9 (2C, SiCH(CH₃)₂), 12.6 (SiCH(CH₃)₂), 12.1 (SiCH(CH₃)₂).

¹⁹F{¹H} NMR (376 MHz, CDCl₃) δ -127.53 (s).

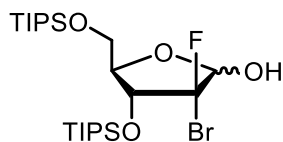
¹⁹F NMR (376 MHz, CDCl₃) δ -127.53 (dd, *J* = 14.8, 1.5 Hz).

IR (cm⁻¹): 2943, 2870, 1813, 1462, 1192, 1134, 1065, 957, 922, 883, 795, 687, 660.

HRMS (ES): [C₂₃H₄₆BrFO₄Si₂+H]⁺ calc. 541.2180 found 541.2174.

Data is consistent with the literature.^[142]

(3R,4R,5R)-3-bromo-3-fluoro-4-((triisopropylsilyl)oxy)-5-(((triisopropylsilyl)oxy)-methyl)tetrahydrofuran-2-ol (209**)**



To a solution of lithium tri-*tert*-butoxyaluminium hydride (2.97 g, 11.7 mmol, 1.1 equiv.) in anhydrous diethyl ether (90 mL) was added dropwise **202** (5.75 g, 10.62 mmol) in anhydrous THF (20 mL) over 10 minutes at 0°C. After addition, the reaction was warmed to room temperature and stirred for 3 hours. The reaction was quenched with methanol and stirred at room temperature for a further hour, before filtering over a short silica pad. The filtrate was extracted with diethyl ether (3 x 25 mL), and the combined organics washed with saturated aqueous NaHCO₃, water and brine (1 x 50 mL each), dried over MgSO₄ and concentrated *in vacuo* to afford **209** (5.6244 g, 97% yield) as a colourless oil. The crude product was used for the next reaction without purification. The anomers were inseparable by column chromatography and used as a mixture for the next reaction.

¹H NMR (500 MHz, CDCl₃) δ 5.34 (dd, *J* = 9.2, 0.9 Hz, 1H, *H*¹), 5.17 (ddd, *J* = 12.7, 5.9, 0.6 Hz, 0.4H, *H*¹), 4.72 (dd, *J* = 12.8, 6.6 Hz, 1H, *H*^β), 4.67 (ddd, *J* = 11.6, 4.6, 0.6 Hz, 0.4H, *H*^β), 4.08 (td, *J* = 4.6, 0.8 Hz, 0.4H, *H*^α), 3.96 – 3.93 (app. td, *J* = 7.0, 1.5 Hz, 1H, *H*^α), 3.91 – 3.86 (m, 2H, -CH₂OTIPS and CHOH), 3.84 – 3.79 (m, 1.6H, *H*^δ), 3.48 (d, *J* = 12.7 Hz, 0.4H, O¹*H*), 1.21 – 1.05 (m, 59H, SiCH(CH₃)₂ and SiCH(CH₃)₂).

¹³C{¹H} NMR (126 MHz, CDCl₃) δ 115.6 (d, *J* = 265.0 Hz, C²), 112.8 (d, *J* = 277.3 Hz, C²), 100.0 (d, *J* = 21.5 Hz, C¹), 98.8 (d, *J* = 31.3 Hz, C¹), 83.8 (d, *J* = 3.8 Hz, C⁴), 83.1 (d, *J* = 8.7 Hz, C⁴), 74.6 (d, *J* = 24.3 Hz, C³), 72.3 (d, *J* = 21.8 Hz, C³), 62.4 (C⁵), 61.4 (H^δ), 18.1 (2C, SiCH(CH₃)₂ and SiCH(CH₃)₂), 18.0 (2C, SiCH(CH₃)₂), 12.6 (SiCH(CH₃)₂), 12.5 (SiCH(CH₃)₂), 12.1 (SiCH(CH₃)₂), 12.0 (SiCH(CH₃)₂).

¹⁹F {¹H} NMR (376 MHz, CDCl₃) δ -120.68 (s), -127.37 (s).

¹⁹F NMR (471 MHz, CDCl₃) δ -120.62 (dd, *J* = 10.8, 5.6 Hz), -127.34 (d, *J* = 12.8 Hz).

IR (cm⁻¹): 2945, 2897, 2868, 2363, 2342, 1464, 1391, 1234, 1186, 1159, 1121, 1090, 1061, 1013, 997, 957, 883, 829, 791, 739, 685.

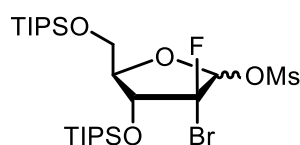
HRMS (ES): [C₂₃H₄₈⁷⁹BrFO₄Si₂+Na]⁺ calc. 565.2156 found 565.2140.

DIBAL-H reduction: To a solution of **202** (6.6015 g, 12.2 mmol) in anhydrous toluene (50 mL) at -78°C was added DIBAL-H (1 M in hexanes, 86 mL, 85.4 mmol, 7 equiv.). The solution was stirred at -78°C for 2 hours, before quenching with MeOH (75 mL) and warming to rt. The mixture was then filtered over a pad of silica before washing with 0.1 M HCl. The solution was extracted with Et₂O (3 x 250 mL), and successively washed

with saturated aqueous NaHCO₃, water and brine (3 x 150 mL each), dried over MgSO₄ and concentrated *in vacuo*. Purification by column chromatography (8% Et₂O/Hexanes) gave an impure product, which was purified again by column chromatography (50% DCM/Hexane) to yield **209** (4.4197 g, 67%) as a colourless oil, isolated as a mix of diastereomers (71:29).

Analytical data for both the products of both methods were identical.

(3R,4R,5R)-3-bromo-3-fluoro-4-((triisopropylsilyl)oxy)-5-(((triisopropylsilyl)oxy)methyl)tetrahydrofuran-2-yl methanesulfonate (210)



To a solution of **209** (4.4197 g, 8.1 mmol), NEt₃ (1.60 mL, 11.34 mmol, 1.4 equiv.) in dry DCM (50 mL) was added methane sulfonyl chloride (760 μL, 9.82 mmol, 1.2 equiv.) slowly at 0°C. After complete addition, the reaction was warmed to room temperature and stirred overnight. The reaction mixture was then concentrated *in vacuo* and redissolved in EtOAc (50 mL), before washing with saturated aqueous NaHCO₃ and brine (3 x 50 mL). The solution was dried over MgSO₄ and concentrated *in vacuo*, to afford **210** (4.79 g, 95% yield) as a colourless oil, isolated as a diastereomeric mixture (59:41).

¹H NMR (400 MHz, CDCl₃) δ 6.19 (d, *J* = 1.6 Hz, 1H, *H*¹OMs), 6.04 (d, *J* = 7.4 Hz, 0.7H, *H*¹OMs), 4.63 – 4.52 (m, 2H, *H*⁸ and *H*⁹), 4.26 (dd, *J* = 8.5, 4.2 Hz, 0.7H, *H*^{6a}), 4.03 (dt, *J* = 11.7, 1.8 Hz, 1.3H, *H*⁴ and *H*^{6b}), 3.94 – 3.88 (m, 2.5H, *H*^{6a} and *H*⁴), 3.84 (dd, *J* = 11.8, 4.2 Hz, 1H, *H*^{6b}), 3.11 (s, 2H, MsCH₃), 3.07 (s, 3H, MsCH₃), 1.16 – 1.03 (m, 72H, SiCH(CH₃)₂ and SiCH(CH₃)₂).

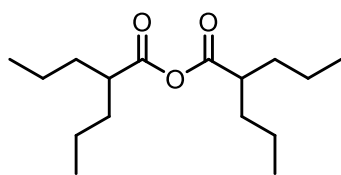
¹³C{¹H} NMR (126 MHz, CDCl₃) δ 111.9 (d, *J* = 253.8 Hz, C²), 109.2 (d, *J* = 281.8 Hz, C²), 104.4 (d, *J* = 21.5 Hz, C¹), 103.4 (d, *J* = 40.5 Hz, C¹), 88.0 (d, *J* = 1.9 Hz, C⁴), 84.4 (d, *J* = 7.6 Hz, C⁴), 75.2 (d, *J* = 29.1 Hz, C³), 72.3 (d, *J* = 20.7 Hz, C³), 62.1 (C⁵), 61.8 (C⁵), 40.3 (MsCH₃), 40.1 (MsCH₃), 18.1 (3C, SiCH(CH₃)₂ and SiCH(CH₃)₂), 18.0 (4C, SiCH(CH₃)₂ and SiCH(CH₃)₂), 12.7 (SiCH(CH₃)₂), 12.6 (SiCH(CH₃)₂), 12.0 (SiCH(CH₃)₂ and SiCH(CH₃)₂).

¹⁹F {¹H} NMR (376 MHz, CDCl₃) δ -114.85 (s), -125.37 (s).

¹⁹F NMR (471 MHz, CDCl₃) δ -114.82 (dd, *J* = 16.8, 7.3 Hz, minor diastereomer), -125.34 (d, *J* = 12.0 Hz, major diastereomer).

IR (cm⁻¹): 2945, 2868, 2363, 1464, 1375, 1184, 1144, 1103, 1070, 951, 881, 856, 818, 681, 523.

HRMS (ES): [C₂₄H₅₀⁷⁹BrFO₆Si₂S+Na]⁺ calc. 643.1932 found 643.1931

2-Propylpentanoic/Valproic anhydride (213)

To a solution of valproic acid (**212**, 17.7162 g, 123 mmol, 2 equiv.), and NEt_3 (17.5 mL, 125 mmol, 2.0 equiv.) in anhydrous DCM (125 mL) was added diphenylphosphoryl chloride (12.8 mL, 61.75 mmol) dropwise at 0°C . Once

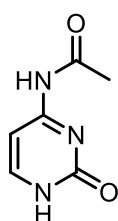
addition was complete, the reaction was warmed to room temperature and stirred overnight. The reaction was quenched with cold water, organic separated and aqueous extracted with DCM (3 x 50 mL). The combined organics were with saturated aqueous NaHCO_3 (5 x 50 mL) and brine (3 x 50 mL), dried over MgSO_4 and concentrated to yield **213** (15.7978 g, 95% yield) as a colourless liquid ($\rho = 0.9156 \text{ g L}^{-1}$)

^1H NMR (500 MHz, CDCl_3) δ 2.44 (tt, $J = 8.7, 5.3$ Hz, 2H, CH^{Pr}), 1.68 – 1.60 (m, 4H, CHCH_2), 1.50 – 1.32 (m, 12H, CHCH_2 and $\text{CH}_2\text{CH}_2\text{CH}_3$), 0.91 (app. t, $J = 7.3$ Hz, 12H, $-\text{CH}_2\text{CH}_3$).

$^{13}\text{C}\{^1\text{H}\}$ NMR (126 MHz, CDCl_3) δ 172.1 (VpC=O), 46.4 (CH), 34.1 (CHCH_2), 20.6 (CH_2CH_2), 14.1 (CH_3).

IR (cm^{-1}): 2955, 2934, 2361, 1809, 1746, 1462, 1024.

HRMS (ES): $[\text{C}_{16}\text{H}_{30}\text{O}_3 + \text{CH}_3\text{CN} + \text{Na}]^+$ calc. 334.2358, found 334.2360.

***N*-(2-oxo-1,2-dihydropyrimidin-4-yl)acetamide (214)**

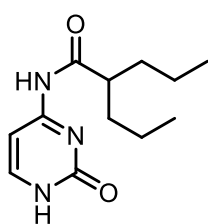
Cytosine (**184**, 1.111 g, 10.0 mmol) and acetic anhydride (1.94 mL, 20.6 mmol) were dissolved in anhydrous pyridine (20 mL) and stirred at room temperature for 24 h. The reaction mixture was precipitated in cold water and filtered. The precipitate was washed with further cold water and dried to afford **214** (1.19 g, 78% yield) as a white solid.

^1H NMR (400 MHz, $\text{DMSO}-d_6$) δ 11.52 (s, 1H, N^4H), 10.75 (s, 1H, N^1H), 7.80 (d, $J = 7.0$ Hz, 1H, H^6), 7.09 (d, $J = 7.0$ Hz, 1H, H^5), 2.08 (s, 3H, AcCH_3).

$^{13}\text{C}\{^1\text{H}\}$ NMR (126 MHz, $\text{DMSO}-d_6$) δ 170.9 ($\text{AcC}=\text{O}$), 163.3 (C^2), 156.2 (C^4), 147.1 (C^6), 94.5 (C^5), 24.3 (AcCH_3).

IR (cm^{-1}): 2972, 1703, 1609, 1593, 1501, 1460, 1427, 1371, 1308, 1211, 682, 853, 812, 779, 679, 594.

HRMS (TOF ASAP⁺): $[\text{C}_6\text{H}_7\text{N}_3\text{O}_2 + \text{H}]^+$ calc. 154.0617, found 154.0617.

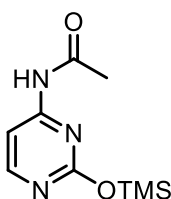
N-(2-oxo-1,2-dihydropyrimidin-4-yl)-2-propylpentanamide (215)

Cytosine (**183**, 1.111 g, 10.0 mmol) and valproic anhydride (1.94 mL, 20.6 mmol) were dissolved in anhydrous pyridine (15 mL) and stirred at room temperature for 24 h. The reaction mixture was cooled and precipitated with cold water and filtered. The precipitate was washed with further cold water and dried to afford **215** (1.66 g, 70% yield) as a white solid.

^1H NMR (400 MHz, DMSO- d_6) δ 11.55 (s, 1H, N^4H), 10.78 (s, 1H, N^1H), 7.81 (d, $J = 7.0$ Hz, 1H, H^6), 7.16 (d, $J = 7.0$ Hz, 1H, H^5), 2.60 (ddd, $J = 13.9, 9.2, 4.8$ Hz, 1H, CH^nPr), 1.51 (m, 2H, CH_2), 1.36 – 1.15 (m, 6H, CH_2), 0.85 (app. t, $J = 7.2$ Hz, 6H, 2CH_3). $^{13}\text{C}\{^1\text{H}\}$ NMR (101 MHz, DMSO- d_6) δ 177.1 (VpC=O), 163.3 (C^2), 156.2 (C^4), 147.3 (C^6), 94.7 (C^5), 45.7 (CH), 34.6 (CH_2), 20.1 (CH_2), 14.0 (CH_3).

IR (cm^{-1}): 2957, 2934, 1705, 1614, 1497, 1449, 1418, 1296, 1219, 1136, 1096, 924, 812, 584.

HRMS (FTMS + p NSI): $[\text{C}_{12}\text{H}_{19}\text{O}_2\text{N}_3+\text{H}]^+$ calc. 238.1550 found 238.1548

N-(2-((trimethylsilyl)oxy)pyrimidin-4-yl)acetamide (216)

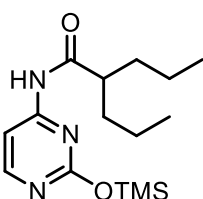
To a mixture of **214** (766 mg, 5 mmol) and ammonium sulfate (33.1 mg, 0.25 mmol, 0.05 equiv.) was added hexamethyldisilazane (3.14 mL, 15 mmol, 3 equiv.) and heated to reflux until a golden colour persisted (*c.f.* 3 hours). The mixture was then cooled to r.t. and concentrated *in vacuo* to afford **216** (1.05 g, 93% yield) as a white solid.

^1H NMR (500 MHz, DMSO- d_6) δ 7.80 (d, $J = 7.0$ Hz, 1H, H^6), 7.09 (d, $J = 7.0$ Hz, 1H, H^5), 5.28 (s, 1H, N^4H), 2.08 (s, 3H, AcCH_3), 0.01 (s, 9H, $\text{Si}(\text{CH}_3)_3$).

Unable to obtain $^{13}\text{C}\{^1\text{H}\}$ NMR.

IR (cm^{-1}): 2978, 1697, 1686, 1607, 1501, 160, 1373, 1310, 1217, 810, 681, 564.

HRMS (TOF ASAP⁺): $[\text{C}_9\text{H}_{15}\text{N}_3\text{O}_2\text{Si}+\text{H}]^+$ calc. 226.1012 found 226.1009

2-propyl-N-(2-((trimethylsilyl)oxy)pyrimidin-4-yl)pentanamide (217)

To a mixture of **215** (1.1865 g, 5 mmol) and ammonium sulfate (33.1 mg, 0.25 mmol, 0.05 equiv.) was added hexamethyldisilazane (3.14 mL, 15 mmol, 3 equiv.) and heated to reflux until a golden colour persisted (*c.f.* 3 hours). The mixture was then cooled to r.t. and concentrated *in vacuo* to afford **217** as a white solid (1.55 g, quant. yield).

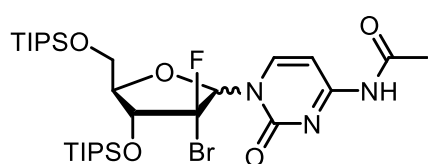
^1H NMR (500 MHz, DMSO- d_6) δ 7.80 (d, $J = 7.0$ Hz, 1H, H^6), 7.16 (d, $J = 7.0$ Hz, 1H, H^6), 2.64 – 2.56 (m, 1H, CH), 1.56 – 1.46 (m, 2H, CH_2), 1.36 – 1.28 (m, 2H, CH_2), 1.26 – 1.17 (m, 4H, CH_2), 0.85 (app. t, $J = 7.3$ Hz, 6H, 2CH_3), 0.01 (s, 9H, $\text{Si}(\text{CH}_3)_3$).

$^{13}\text{C}\{^1\text{H}\}$ NMR (126 MHz, DMSO- d_6) δ 177.0 (VpC=O), 163.2 (C^2), 156.2 (C^4), 147.3 (C^6), 94.7 (C^5), 45.7 (CH), 34.6 (CH_2), 20.1 (CH_2), 13.9 (CH_3), 1.8 ($\text{Si}(\text{CH}_3)_3$).

IR (cm^{-1}): 2980, 2363, 1690, 1614, 1497, 1456, 1396, 1300, 1217, 1155, 1080, 810, 611, 581.

HRMS (TOF ASAP⁺): $[\text{C}_{15}\text{H}_{27}\text{N}_3\text{O}_2\text{Si}+\text{H}]^+$ calc. 310.1951 found 310.1944

***N*-(1-((3R,4R,5R)-3-bromo-3-fluoro-4-((triisopropylsilyl)oxy)-5-(((triisopropylsilyl)oxy)methyl)tetrahydrofuran-2-yl)-2-oxo-1,2-dihydropyrimidin-4-yl)acetamide (218)**



A slurry of **216** (288.2 mg, 1.28 mmol, 1.5 equiv.) and trimethylsilyl trifluoromethanesulfonate (260 μL , 1.39 mmol, 1.63 equiv.) in anhydrous 1,2-dichloroethane (10 mL) was stirred at room

temperature for 1 hour. **210** (458.5 mg, 0.853 mmol) in anhydrous 1,2-dichloroethane (8 mL) was added and the reaction was heated at reflux overnight. The mixture was then cooled to room temperature, diluted with DCM and quenched with saturated aqueous NaHCO_3 (10 mL). The organic phase was washed with water (3 x 10 mL) and brine (2 x 10 mL), dried over MgSO_4 and concentrated *in vacuo*. The residue was purified by column chromatography (60% EtOAc/Hexane) to yield **218** (1.53 g, 76% yield) as a foamy solid, in an anomeric mixture (6.7:1 β : α anomer).

β -218

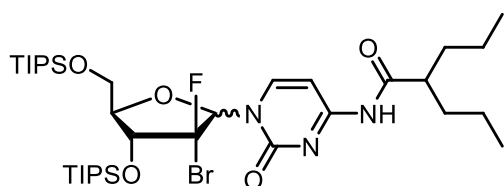
^1H NMR (500 MHz, CDCl_3) δ 9.05 (bs, 1H, N^4H), 7.86 (d, $J = 7.6$ Hz, 1H, H^6), 7.42 (d, $J = 7.6$ Hz, 1H, H^6), 6.57 (d, $J = 8.9$ Hz, 1H, H^1), 4.83 (dd, $J = 12.9, 5.7$ Hz, 1H, H^5), 4.22 (dd, $J = 9.2, 4.4$ Hz, 1H, H^4), 3.94 (ddd, $J = 11.2, 4.6, 2.3$ Hz, 1H, $H^{5'a}$), 3.90 (dd, $J = 11.4, 2.2$ Hz, 1H, $H^{5'b}$), 2.26 (s, 3H, AcCH_3), 1.08 (m, 42H, $\text{SiCH}(\text{CH}_3)_2$ and $\text{SiCH}(\text{CH}_3)_2$).

$^{13}\text{C}\{^1\text{H}\}$ NMR (125 MHz, CDCl_3) δ 170.6 ($\text{AcC}=\text{O}$), 162.9 (C^2), 155.0 (C^4), 145.1 (C^6), 116.3 (d, $J = 267.5$ Hz, $\text{C}^{2'}$), 96.2 (C^5), 88.6 (d, $J = 35$ Hz, C^1), 85.0 (C^4), 75.3 (d, $J = 25$ Hz), 61.7 (C^5), 25.2 (AcCH_3), 18.2 ($\text{SiCH}(\text{CH}_3)_3$), 18.1 (2C, $\text{SiCH}(\text{CH}_3)_3$), 18.0 ($\text{SiCH}(\text{CH}_3)_3$), 12.8 ($\text{SiCH}(\text{CH}_3)_3$), 12.6 ($\text{SiCH}(\text{CH}_3)_3$), 12.1 ($\text{SiCH}(\text{CH}_3)_3$), 12.0 ($\text{SiCH}(\text{CH}_3)_3$).

^{19}F NMR (CDCl_3 , 376.5 MHz) δ -111.7 (t, $J = 8.6$ Hz, β), -122.1 (dd, $J = 16.8, 5.0$ Hz, α).
IR (cm^{-1}): 2943, 2866, 1680, 1626, 1558, 1493, 1464, 1387, 1317, 1238, 1188, 1098, 1078, 1075, 999, 953, 883, 787, 683.

HRMS (ES): $[\text{C}_{29}\text{H}_{53}\text{BrFN}_3\text{O}_5\text{Si}_2+\text{H}]^+$ calc. 678.2769 found 678.2758.

***N*-1-((3*R*,4*R*,5*R*)-3-bromo-3-fluoro-4-((triisopropylsilyl)oxy)-5-(((triisopropylsilyl)oxy)methyl)tetrahydrofuran-2-yl)-2-oxo-1,2-dihydropyrimidin-4-yl)-2-propylpentanamide (**219**)**



A slurry of **217** (1.81 g, 4.76 mmol, 1.5 equiv.) and trimethylsilyl trifluoromethanesulfonate (940 μ L, 5.17 mmol, 1.63 equiv.) in anhydrous 1,2-dichloroethane (15 mL) was stirred at room temperature for 1 hour. **210** (2.08 g, 3.17 mmol) in anhydrous 1,2-dichloroethane (10 mL) was added and the reaction was heated to reflux overnight. The mixture was then cooled to room temperature, diluted with DCM and quenched with saturated aqueous NaHCO_3 (10 mL). The organic phase was washed with water (3 x 10 mL), brine (2 x 10 mL), then dried over MgSO_4 and concentrated *in vacuo*. The residue was purified by column chromatography (60% EtOAc/Hexane) to yield **219** (2.11 g, 87% yield) as a foamy solid, in an anomeric mixture (10:1 β : α anomer).

β -219

^1H NMR (500 MHz, CDCl_3) δ 7.96 (s, 1H, N^4H), 7.88 (d, $J = 7.6$ Hz, 1H, H^f), 7.45 (d, $J = 7.6$ Hz, 1H, H^f), 6.58 (d, $J = 8.6$ Hz, 1H, H^i), 4.84 (dd, $J = 12.7, 5.9$ Hz, 1H, H^g), 4.21 (dd, $J = 9.5, 3.9$ Hz, 1H, H^i), 3.95 (ddd, $J = 11.4, 4.4, 2.4$ Hz, 1H, H^{f^a}), 3.90 (dd, $J = 11.5, 2.3$ Hz, 1H, H^{f^b}), 2.30 – 2.22 (m, 1H, CH), 1.69 – 1.59 (m, 2H, CH_2), 1.52 – 1.42 (m, 2H, CH_2), 1.39 – 1.29 (m, 4H, CH_2), 1.11 (m, 42H), 0.91 (overlapping t, $J = 7.3$ Hz, 6H).

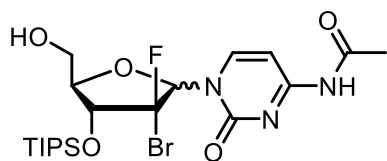
$^{13}\text{C}\{^1\text{H}\}$ NMR (125 MHz, CDCl_3) δ 176.5 (VpC=O), 162.5 (C^2), 155.1 (C^4), 145.3 (C^6), 116.3 (d, $J = 269.8$ Hz, C^2'), 96.0 (C^5), 88.5 (d, $J = 34.8$ Hz, C^1), 84.9 (d, $J = 4.7$ Hz, C^4), 75.2 (d, $J = 24.5$ Hz, C^3), 61.6 (C^5), 49.0 (CH), 35.0 (2C, CH_2), 20.8 (2C, CH_2), 18.1 (2C, $\text{SiCH}(\text{CH}_3)_3$), 18.0 (2C, $\text{SiCH}(\text{CH}_3)_3$), 14.2 (2C, CH_3), 12.5 ($\text{SiCH}(\text{CH}_3)_3$), 12.1 ($\text{SiCH}(\text{CH}_3)_3$).

^{19}F NMR (376.5 MHz, CDCl_3) δ -112.0 (t, $J = 8.1$ Hz, β), -121.9 (dd, $J = 17.2, 5.6$ Hz, α).

IR (cm^{-1}): 1674, 1622, 1557, 1489, 1460, 1400, 1317, 1103, 1069, 883, 783, 683.

HRMS (TOF ES $^+$): $[\text{C}_{35}\text{H}_{65}\text{N}_3\text{O}_5\text{FSi}_2\text{Br}+\text{H}]^+$ calc. 764.3688 found 764.3694.

***N*-1-((3*R*,4*R*,5*R*)-3-bromo-3-fluoro-5-(hydroxymethyl)-4-((triisopropylsilyl)oxy)-tetrahydrofuran-2-yl)-2-oxo-1,2-dihydropyrimidin-4-yl)acetamide (**220**)**



To a solution of **216** (assumed 5 mmol) in anhydrous DCE (20 mL) was added TMSOTf (780 μ L, 4.5 mmol, 1.5 equiv.). The mixture was stirred at room temperature for an hour, before addition of a solution of **210** in anhydrous DCE (stock solution of 3.7354 g, 6 mmol in 10 mL; 5 mL used). After complete addition, the mixture was heated to reflux overnight. After 16 hours, the mixture was cooled to room temperature and left to stir for 48 hours. The reaction mixture was filtered to remove precipitates, and the filtrate subsequently diluted with DCM (100 mL) and washed with H₂O (3 x 100 mL), saturated aqueous NaHCO₃ and brine (1 x 100 mL each). Combined aqueous washes were back-washed with further DCM (1 x 50 mL). The combined organics were dried over MgSO₄ and concentrated *in vacuo*. The crude mixture was purified by column chromatography (60% EtOAc/hexanes \rightarrow 100% EtOAc) to yield **220** (775.0 mg, 49% yield) as an anomeric mixture (~2:3 β : α). The anomers were separated and isolated, both as white solids, and individually analysed by NMR.

β -220

¹H NMR (500 MHz, CDCl₃) δ 9.73 (s, 1H, N⁴H), 8.22 (d, J = 7.3 Hz, 1H, H⁶), 7.46 (d, J = 7.4 Hz, 1H, H⁶), 6.69 (d, J = 3.7 Hz, 1H, H¹), 4.52 (dd, J = 15.2, 6.8 Hz, 1H, H⁸), 4.11 (d, J = 12.0 Hz, 1H, H^{5a}), 3.97 (d, J = 6.8 Hz, 1H, H⁴), 3.89 (d, J = 12.1 Hz, 1H, H^{5b}), 2.27 (s, 3H, AcCH₃), 1.20 – 1.05 (m, 21H, SiCH(CH₃)₃ and SiCH(CH₃)₃).

¹³C{¹H} NMR (126 MHz, CDCl₃) δ 171.2 (AcC=O), 163.3 (C²), 155.3 (C⁴), 145.1 (C⁶), 110.72 (d, J = 273.2 Hz, C^{2'}), 97.3 (C⁵), 90.0 (C⁴), 82.2 (d, J = 6.5 Hz, C¹), 73.6 (d, J = 24.8 Hz, C³), 59.7 (C⁵), 25.1 (AcCH₃), 18.0 (2C, SiCH(CH₃)₃), 12.6 (SiCH(CH₃)₃).

¹⁹F NMR (471 MHz, CDCl₃) δ -121.73 (s).

α -220

¹H NMR (500 MHz, CDCl₃) δ 9.37 (s, 1H, N⁴H), 7.85 (d, J = 7.4 Hz, 1H, H⁶), 7.47 (d, J = 7.3 Hz, 1H, H⁶), 6.74 (d, J = 7.3 Hz, 1H, H¹), 4.78 (dd, J = 12.8, 7.1 Hz, 1H, H⁸), 4.19 (d, J = 4.3 Hz, 1H, H⁴), 3.94 (d, J = 12.4 Hz, 1H, H^{5a}), 3.78 (d, J = 11.8 Hz, 1H, H^{5b}), 2.27 (s, 3H, AcCH₃), 1.21 – 1.06 (m, 21H, SiCH(CH₃)₃ and SiCH(CH₃)₃).

¹³C{¹H} NMR (126 MHz, CDCl₃) δ 170.9 (AcC=O), 163.1 (C²), 155.3 (C⁴), 145.0 (C⁶), 116.3 (d, J = 272.0 Hz, C^{2'}), 96.4 (C⁵), 88.0 (d, J = 34.1 Hz, C¹), 84.2 (d, J = 5.7 Hz, C⁴), 74.9 (d, J = 23.6 Hz, C³), 60.5 (C⁵), 25.2 (AcCH₃), 18.0 (SiCH(CH₃)₃), 12.5 (SiCH(CH₃)₃).

¹⁹F NMR (471 MHz, CDCl₃) δ -113.68 (app. t, J = 9.2 Hz).

¹H NMR (500 MHz, DMSO) δ 11.01 (s, 1H, N⁴H), 8.05 (d, J = 7.6 Hz, 1H, H⁶), 7.28 (d, J = 7.6 Hz, 1H, H⁶), 6.47 (d, J = 8.1 Hz, 1H, H¹), 5.24 (dd, J = 6.4, 4.6 Hz, 1H, O⁵H),

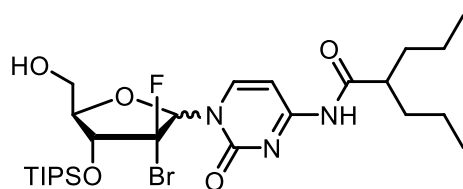
4.77 (dd, $J = 14.2, 7.3$ Hz, 1H, H^{β}), 4.14 (dt, $J = 7.0, 3.4$ Hz, 1H, H^{α}), 3.71 (d, $J = 11.8$ Hz, 1H, H^{6a}), 3.58 (ddd, $J = 12.1, 6.4, 4.0$ Hz, 1H, H^{6b}), 2.11 (s, 3H, AcCH₃), 1.17 – 1.04 (m, 21H).

¹³C NMR (126 MHz, DMSO) δ 171.2 (AcC=O), 162.9 (C²), 154.2 (C⁴), 145.3 (C⁶), 117.0 (d, $J = 269.4$ Hz, C^{2'}), 95.3 (C⁵), 87.3 (d, $J = 34.4$ Hz, C¹), 83.6 (d, $J = 5.6$ Hz, C⁴), 74.6 (d, $J = 23.6$ Hz, C³), 59.3 (C⁵), 24.5 (AcCH₃), 17.7 (SiCH(CH₃)₃), 11.9 (SiCH(CH₃)₃).

¹⁹F NMR (471 MHz, DMSO) δ -112.45 (dd, $J = 13.5, 8.5$ Hz).

HRMS (TOF AP⁺): [C₂₀H₃₃N₃O₅FSiBr+H]⁺ calc. 522.1435 found 522.1440.

***N*-(1-((3R,4R,5R)-3-bromo-3-fluoro-5-(hydroxymethyl)-4-((triisopropylsilyl)oxy)-tetrahydrofuran-2-yl)-2-oxo-1,2-dihydropyrimidin-4-yl)-2-propylpentanamide (221)**



To a solution of **217** (assumed 5 mmol) in anhydrous DCE (15 mL) was added TMSOTf (780 μ L, 4.5 mmol, 1.5 equiv.). The mixture was stirred at room temperature for an hour, before addition of a solution of **210** in anhydrous DCE

(stock solution of 3.7354 g, 6 mmol in 10 mL; 5 mL used). After complete addition, the mixture was heated to reflux overnight. After 16 hours, the mixture was cooled to room temperature and left to stir for 48 hours. The reaction mixture was diluted with DCM (100 mL) and washed with H₂O (3 x 100 mL), saturated aqueous NaHCO₃ and brine (1 x 100 mL each). Combined aqueous washes were back-washed with further DCM (1 x 50 mL). The combined organics were dried over MgSO₄ and concentrated *in vacuo*. The crude mixture was purified by column chromatography (80% Et₂O/hexanes \rightarrow 100% Et₂O) to yield **221** (1.0622 g, 58% yield) as an anomeric mixture (1:3 β : α). The anomers were separated and isolated, both as white solids, and individually analysed by NMR.

β -221

¹H NMR (500 MHz, CDCl₃) δ 8.19 (s, 1H, N⁴H), 8.15 (d, $J = 7.1$ Hz, 1H, H^{β}), 7.46 (d, $J = 7.6$ Hz, 1H, H^{β}), 6.70 (d, $J = 5.6$ Hz, 1H, H^{α}), 4.54 (dd, $J = 16.0, 7.0$ Hz, 1H, H^{β}), 4.10 (dt, $J = 12.2, 2.3$ Hz, 1H, H^{6a}), 4.01 – 3.95 (m, 1H, H^{α}), 3.91 (dd, $J = 12.2, 2.9$ Hz, 1H, H^{6b}), 2.30 (td, $J = 8.9, 4.5$ Hz, 1H), 1.68 – 1.58 (m, 4H), 1.51 – 1.43 (m, 2H), 1.38 – 1.28 (m, 4H), 1.19 – 1.06 (m, 21H, SiCH(CH₃)₂ and SiCH(CH₃)₂), 0.90 (overlapping t, $J = 7.3$ Hz, 6H, CH₃).

¹³C{¹H} NMR (126 MHz, CDCl₃) δ 176.4 (VpC=O), 162.5 (C²), 155.2 (C⁴), 145.2 (C⁶), 96.9 (C⁵), 82.2 (d, $J = 6.3$ Hz, C³), 73.7 (d, $J = 25.0$ Hz, C¹), 59.9 (C⁵), 49.1 (CH), 35.0 (d, $J = 2.3$ Hz, C⁴), 20.8 (CH₂), 18.0 (2C, SiCH(CH₃)₃), 14.2 (SiCH(CH₃)₃), 12.6 (CH₃).

N.B. C^{2'} missing

^{19}F NMR (471 MHz, CDCl_3) δ -121.86 (s).

^1H NMR (500 MHz, DMSO) δ 11.08 (s, 1H, N^4H), 8.43 (d, $J = 7.6$ Hz, 1H, H^6), 7.32 (d, $J = 7.6$ Hz, 1H, H^6), 6.56 (d, $J = 4.5$ Hz, 1H, H^1), 5.57 (s, 1H, O^5H), 4.46 (dd, $J = 15.3$, 7.5 Hz, 1H, H^6), 3.92 – 3.84 (m, 2H, H^1 and $\text{H}^{6\text{a}}$), 3.66 (d, $J = 12.3$ Hz, 1H, $\text{H}^{6\text{b}}$), 2.63 – 2.59 (m, 1H, CH), 1.52 (app. td, $J = 13.7$, 8.4 Hz, 2H, CH_2), 1.38 – 1.29 (m, 2H, CH_2), 1.27 – 1.18 (m, 4H, CH_2), 1.15 – 1.04 (m, 21H, $\text{SiCH}(\text{CH}_3)_2$ and $\text{SiCH}(\text{CH}_3)_2$), 0.85 (t, $J = 7.0$ Hz, 6H, CH_3).

$^{13}\text{C}\{^1\text{H}\}$ NMR (126 MHz, DMSO) δ 177.4 (VpC=O), 162.9 (C^2), 154.3 (C^4), 144.5 (C^6), 111.0 (d, $J = 273.3$ Hz, $\text{C}^{2'}$), 95.9 (C^5), 88.6 (d, $J = 19.1$ Hz, C^1), 81.7 (d, $J = 6.5$ Hz, C^4), 72.8 (d, $J = 23.7$ Hz, C^3), 58.1 (C^5), 45.8 (CH), 34.5 (CH_2), 20.0 (CH_2), 17.7 (2C, $\text{SiCH}(\text{CH}_3)_3$), 13.9 (2C, $\text{SiCH}(\text{CH}_3)_3$), 11.9 (CH_3).

^{19}F NMR (471 MHz, DMSO) δ -121.85 (s).

α -221

^1H NMR (500 MHz, DMSO) δ 11.04 (s, 1H, N^4H), 8.05 (d, $J = 7.6$ Hz, 1H, H^6), 7.34 (d, $J = 7.6$ Hz, 1H, H^6), 6.47 (d, $J = 8.1$ Hz, 1H, H^1), 5.23 (dd, $J = 6.5$, 4.6 Hz, 1H, O^5H), 4.77 (dd, $J = 14.1$, 7.2 Hz, 1H, H^6), 4.15 (dt, $J = 6.9$, 3.4 Hz, 1H, H^1), 3.72 (d, $J = 12.5$ Hz, 1H, $\text{H}^{6\text{a}}$), 3.58 (ddd, $J = 12.2$, 6.4, 3.8 Hz, 1H, $\text{H}^{6\text{b}}$), 2.67 – 2.59 (m, 1H, CH), 1.58 – 1.46 (m, 2H, CH_2), 1.39 – 1.29 (m, 2H, CH_2), 1.28 – 1.19 (m, 4H, CH_2), 1.18 – 1.03 (m, 21H, $\text{SiCH}(\text{CH}_3)_3$ and $\text{SiCH}(\text{CH}_3)_3$), 0.86 (overlapping t, $J = 7.3$ Hz, 6H, CH_3).

$^{13}\text{C}\{^1\text{H}\}$ NMR (126 MHz, DMSO) δ 177.4 (VpC=O), 162.9 (C^2), 154.2 (C^4), 145.4 (C^6), 116.9 (d, $J = 268.9$ Hz, $\text{C}^{2'}$), 95.4 (C^5), 87.3 (d, $J = 34.2$ Hz, C^1), 83.7 (C^4), 74.7 (d, $J = 23.4$ Hz, C^3), 59.3 (C^5), 45.8 (CH), 34.5 (CH_2), 20.1 (CH_2), 17.7 ($\text{SiCH}(\text{CH}_3)_3$), 14.0 ($\text{SiCH}(\text{CH}_3)_3$), 11.9 (CH_3).

^{19}F NMR (471 MHz, DMSO) δ -112.42 (dd, $J = 13.1$, 8.8 Hz).

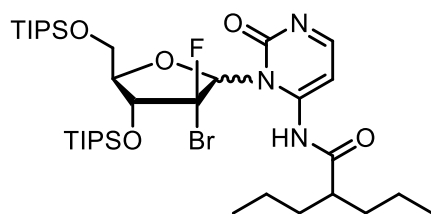
^1H NMR (500 MHz, CDCl_3) δ 8.18 (s, 1H, N^4H), 7.86 (d, $J = 7.6$ Hz, 1H, H^6), 7.49 (d, $J = 7.6$ Hz, 1H, H^6), 6.70 (d, $J = 7.7$ Hz, 1H, H^1), 4.77 (dd, $J = 13.0$, 7.1 Hz, 1H, H^6), 4.20 (dt, $J = 6.7$, 3.3 Hz, 1H, H^1), 3.93 (d, $J = 12.6$ Hz, 1H, $\text{H}^{6\text{a}}$), 3.82 – 3.76 (m, 1H, $\text{H}^{6\text{b}}$), 2.35 – 2.26 (m, 1H, CH), 2.17 (app. dd, $J = 7.1$, 5.2 Hz, 1H), 1.68 – 1.60 (m, 2H), 1.48 (ddd, $J = 13.7$, 8.9, 5.9 Hz, 2H), 1.37 – 1.30 (m, 1H), 1.11 (m, 21H, $\text{SiCH}(\text{CH}_3)_3$ and $\text{SiCH}(\text{CH}_3)_3$), 0.91 (overlapping t, $J = 7.3$ Hz, 6H, 2CH_3).

$^{13}\text{C}\{^1\text{H}\}$ NMR (126 MHz, CDCl_3) δ 176.4 (VpC=O), 162.5 (C^2), 145.1 (C^6), 96.1 (C^5), 88.0 (d, $J = 34.5$ Hz, C^1), 84.2 (C^4), 74.9 (d, $J = 23.8$ Hz, C^3), 60.6 (C^5), 49.1 (CH), 35.0 (2C, CH_2), 29.9 (CH_2), 20.8 (2C, CH_2), 18.0 ($\text{SiCH}(\text{CH}_3)_3$), 14.2 (2C, $\text{SiCH}(\text{CH}_3)_3$), 12.5 (CH_3).
N.B. C^4 and $\text{C}^{2'}$ missing.

^{19}F NMR (471 MHz, CDCl_3) δ -113.79 (dd, $J = 12.0$, 8.2 Hz).

HRMS (TOF AP⁺): $[\text{C}_{26}\text{H}_{45}\text{N}_3\text{O}_5\text{FSiBr}+\text{H}]^+$ calc. 606.2374 found 606.2372.

***N*-3-((3*R*,4*R*,5*R*)-3-bromo-3-fluoro-4-((triisopropylsilyl)oxy)-5-(((triisopropylsilyl)oxy)methyl)tetrahydrofuran-2-yl)-2-oxo-2,3-dihydropyrimidin-4-yl)-2-propylpentanamide (**222**)**



General method: To a flame dried microwave vial with **210** (130 mg, 0.2 mmol) and catalyst (if solid, 10 mol%) was added a solution of **217** in anhydrous MeCN (0.25 M, 1 mL, 1.25 equiv.) (and catalyst, if TMSOTf, 10 mol%). The microwave vial was

irradiated with a temperature gradient from 110°C to 150°C and held at 150°C for 10 minutes. After cooling to room temperature, the reaction mixture was diluted with EtOAc (10 mL), washed with H₂O (3 x 10 mL) and brine (10 mL), dried over MgSO₄ and concentrated under reduced pressure. The crude material was purified by column chromatography (10% Et₂O/Petrol) to deliver **222**.

Data for **β-222**, isolated from Entry 5 (no catalyst)

¹H NMR (400 MHz, CDCl₃) δ 8.42 (d, *J* = 5.6 Hz, 1H, *H*⁶), 7.89 (d, *J* = 5.6 Hz, 1H, *H*⁶), 7.85 (s, 1H, *N*⁴*H*), 6.69 (d, *J* = 1.6 Hz, 1H, *H*¹), 4.80 (dd, *J* = 12.2, 7.7 Hz, 1H, *H*⁶), 4.00 – 3.90 (m, 2H, *H*⁴ and *H*^{5a}), 3.84 (dd, *J* = 11.5, 3.3 Hz, 1H, *H*^{5b}), 2.29 – 2.21 (m, 1H, *CH*), 1.71 – 1.63 (m, 2H, *CH*₂), 1.48 (m, 2H, *CH*₂), 1.37 – 1.27 (m, 4H, *CH*₂), 1.17 – 1.07 (m, 21H, SiCH(CH₃)₃ and SiCH(CH₃)₃), 0.97 – 0.87 (m, 27H, *CH*₃ and SiCH(CH₃)₃ and SiCH(CH₃)₃).

¹³C NMR (126 MHz, CDCl₃) δ 175.8 (VpC=O), 162.9 (*C*²), 160.7 (*C*⁶), 158.9 (*C*⁴), 110.7 (d, *J* = 282.9 Hz, *C*²), 105.1 (*C*⁵), 100.2 (d, *J* = 19.0 Hz, *C*¹), 83.4 (d, *J* = 7.9 Hz, *C*⁴), 72.8 (d, *J* = 20.6 Hz, *C*³), 61.8 (*C*⁵), 49.1 (*CH*), 35.2 (2*C*, *CH*₂), 20.9 (*CH*₂), 18.1 (2*C*, SiCH(CH₃)₃), 17.9 (2*C*, SiCH(CH₃)₃), 14.2 (2*C*, SiCH(CH₃)₃), 12.7 (SiCH(CH₃)₃), 11.9 (*CH*₃).

¹⁹F NMR (471 MHz, CDCl₃) δ -125.50 (d, *J* = 12.1 Hz).

HRMS (TOF AP⁺): [C₃₅H₆₆N₃O₅FSi₂Br+H]⁺ calc. 764.3688 found 764.3691.

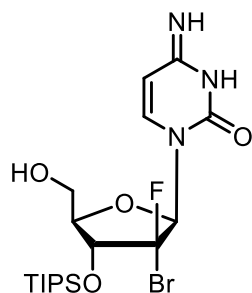
α-222

¹⁹F NMR (471 MHz, CDCl₃) δ -113.90 (dd, *J* = 18.3, 8.8 Hz).

Entry	Reaction	210 / mg	Catalyst (10 mol%)	Isolated mass and yield	β : α ratio
1	A	131.8	TMSOTf 3.5 μ L	46.4 mg 30%	61:39
2	B	127.4	Pyridinium triflate 4.8 mg	49.7 mg 33%	62.5:37.5 (5:3)
3	C	130.8	2,6-Lutidinium triflate 5.2 mg	57.5 mg 38%	68:32
4	D	126.9	2,4,6-Collidinium triflate 5.5 mg	56.7 mg 37%	64:36
5	E	133.1	-	54.6 mg 36%	67:33

Table 5.01: The conditions explored for the microwave-mediated glycosylation of **210** with **217**, with amount of reactants, yields and anomer selectivity noted. Anomer ratio determined by ^{19}F NMR analysis of the crude reaction mixture.

1-((2R,3R,4R,5R)-3-bromo-3-fluoro-5-(hydroxymethyl)-4-((triisopropylsilyl)oxy)-tetrahydrofuran-2-yl)-4-imino-3,4-dihydropyrimidin-2(1H)-one (β -223)



A solution of compound **218** (2.29 g, 3.37 mmol) in MeOH (22 mL) was treated with 12 M HCl (5.3 mL, 64.0 mmol, 19.0 equiv.), and stirred at room temperature over two days. White precipitate formed, which was collected by filtration and dried under high vacuum to yield **β -223** (1.01 g, 63%) as a colourless solid.

^1H NMR (500 MHz, DMSO- d_6) δ 9.38 (broad s, 1H, N^4H), 8.46 (broad s, 1H, N^3H), 7.91 (d, $J = 7.9$ Hz, 1H, H^6), 6.40 (d, $J = 8.1$ Hz, 1H, H^5), 6.12-6.08 (m, 1H, H^1), 4.77 (dd, $J = 14.0, 7.2$ Hz, 1H, H^3), 4.14 (app. dt, $J = 7.1, 3.4$ Hz, 1H, H^4), 3.70 (d, $J = 11.9$ Hz, 1H, H^{5a}), 3.59 (dd, $J = 12.4, 4.1$ Hz, 1H, H^{5b}), 1.17-1.07 (m, 21H, $\text{SiCH}(\text{CH}_3)_2$ and $\text{SiCH}(\text{CH}_3)_2$).

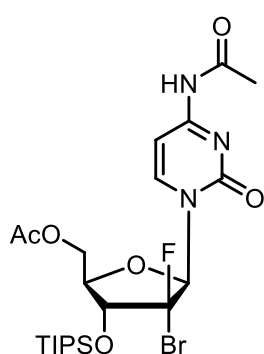
$^{13}\text{C}\{^1\text{H}\}$ NMR (125 MHz, DMSO- d_6) δ 159.8 (C^2), 147.6 (C^4), 143.8 (C^6), 116.5 (d, $J = 266.3$ Hz, C^2), 93.9 (C^5), 87.1 (d, $J = 35$ Hz, C^1), 83.9 (d, $J = 5$ Hz, C^4), 74.3 (d, $J = 22.5$ Hz, C^3), 59.3 (C^5), 17.7 ($\text{SiCH}(\text{CH}_3)_2$), 11.8 ($\text{SiCH}(\text{CH}_3)_2$).

^{19}F NMR (376.5 MHz, DMSO- d_6) δ -113.5 (dd, $J = 11.9, 8.5$ Hz).

IR (cm^{-1}): 3354, 2976, 2899, 2363, 2334, 1734, 1653, 1558, 1508, 1456, 1418, 1339, 1277, 1192, 1086, 1043, 880, 669, 519, 465, 444.

HRMS (ES): $[\text{C}_{18}\text{H}_{31}\text{BrFN}_3\text{O}_4\text{Si}+\text{H}]^+$ calc. 480.1329 found 480.1321.

((2R,3R,4R,5R)-5-(4-acetamido-2-oxopyrimidin-1(2H)-yl)-4-bromo-4-fluoro-3-((triisopropylsilyl)oxy)tetrahydrofuran-2-yl)methyl acetate (β -224)



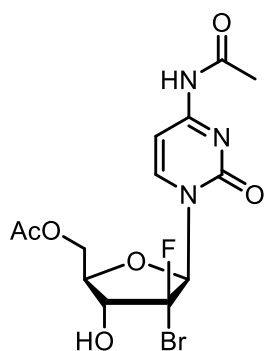
To a solution of **β -223** (145.1 g, 0.3 mmol), DMAP (7.4 mg, 0.06 mmol, 0.2 equiv.) and NEt_3 (252 μL , 1.8 mmol, 6 equiv.) in anhydrous DCM (4.5 mL) was added Ac_2O (69 μL , 0.72 mmol, 2.4 equiv.) and stirred at room temperature overnight. The reaction was quenched and washed with H_2O (3 x 30 mL) and brine (30 mL), dried over MgSO_4 and concentrated *in vacuo* to yield **β -224** (154.0 mg, 91%) as a colourless solid.

^1H NMR (500 MHz, CDCl_3) δ 10.09 (broad s, 1H, N^4H), 7.83 (d, $J = 7.7$ Hz, 1H, H^6), 7.48 (d, $J = 7.7$ Hz, 1H, H^5), 6.66 (d, $J = 9.0$ Hz, 1H, H^1), 4.65 (dd, $J = 12.4, 5.7$ Hz, 1H, H^{5a}), 4.24-4.38 (m, 2H, H^3 and H^4), 4.22-4.19 (m, 1H, H^{5b}), 2.30 (s, 3H, AcCH_3), 2.11 (s, 3H, AcCH_3), 1.19-1.09 (m, 21H, $\text{SiCH}(\text{CH}_3)_2$ and $\text{SiCH}(\text{CH}_3)_2$).

$^{13}\text{C}\{^1\text{H}\}$ NMR (125 MHz, DMSO- d_6) δ 170.5 (AcC=O), 166.2 (C^2), 155.8 (C^4), 141.0 (C^6), 115.8 (d, $J = 265$ Hz, C^2), 95.1 (C^5), 87.9 (d, $J = 35$ Hz, C^1), 76.1 (d, $J = 26.3$ Hz, C^3), 62.3 (C^5), 20.9 (AcCH_3), 18.0 ($\text{SiCH}(\text{CH}_3)_2$), 12.5 ($\text{SiCH}(\text{CH}_3)_2$).

HRMS (ES): [C₂₂H₃₆BrFN₃O₆Si+H]⁺ calc. 564.1541 found 564.1548.

((2R,3R,4R,5R)-5-(4-acetamido-2-oxopyrimidin-1(2H)-yl)-4-bromo-4-fluoro-3-hydroxytetrahydrofuran-2-yl)methyl acetate (β -225)



To a pre-stirred solution of tetramethylammonium fluoride tetrahydrate (297 mg, 1.8 mmol, 2 equiv.) and acetic acid (103 μ L, 1.8 mmol, 2.0 equiv.) was added dropwise a solution of **β -224** in anhydrous DMF (3 mL) at room temperature and stirred overnight. The reaction was quenched with H₂O (10 mL), extracted with EtOAc (3 x 20 mL), dried over MgSO₄ and concentrated *in vacuo* to yield **β -225** (289.2 mg, 78%) as a colourless solid.

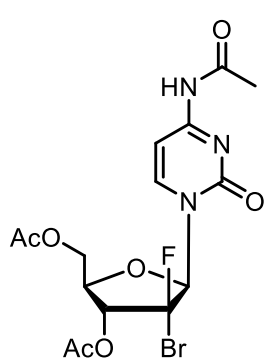
¹H NMR (500 MHz, DMSO-*d*₆) δ 11.0 (broad s, 1H, N⁴H), 8.1 (d, *J* = 7.6 Hz, 1H, H⁶), 7.27 (d, *J* = 7.6 Hz, 1H, H⁶), 6.86 (d, *J* = 5.7 Hz, 1H, O³H), 6.52 (d, *J* = 8.6 Hz, 1H, H¹), 4.50-4.45 (m, 1H, H⁸), 4.35 (dd, *J* = 12.1, 2.7 Hz, 1H, H^{6b}), 4.30 (m, 1H, H⁴), 4.19 (dd, *J* = 12.1, 6.1 Hz, 1H, H^{5a}), 2.12 (s, 3H, AcCH₃), 2.07 (s, 3H, AcCH₃).
¹³C{¹H} NMR (125 MHz, DMSO-*d*₆) δ 171.1 (AcC=O), 170.2 (AcC=O), 162.8 (C²), 154.2 (C⁴), 145.4 (C⁶), 116.9 (d, *J* = 266.7 Hz, C²), 95.3 (C⁵), 87.6 (d, *J* = 34.4 Hz, C¹), 80.4 (d, *J* = 6.3 Hz, C⁴), 74.0 (d, *J* = 23.6 Hz, C³), 62.4 (C⁵), 24.4 (AcCH₃), 20.6 (AcCH₃).

¹⁹F{¹H} NMR (376.5 MHz, DMSO-*d*₆) δ -113.0 (s).

IR (cm⁻¹): 3364, 3275, 2361, 2261, 2133, 1967, 1906, 1867, 1748, 1651, 1558, 1543, 1508, 1458, 1396, 1339, 1277, 1211, 1045, 1022, 988, 823, 764, 667.

HRMS (EI): [C₁₃H₁₅BrFN₃O₆+H]⁺ calc. 408.0207 found 408.0208.

(2R,3R,4R,5R)-5-(4-acetamido-2-oxopyrimidin-1(2H)-yl)-2-(acetoxymethyl)-4-bromo-4-fluorotetrahydrofuran-3-yl acetate (β -226)



To a solution of **β -223** (358.7 g, 0.88 mmol), DMAP (10.8 mg, 0.088 mmol, 0.1 equiv.) and NEt₃ (370 μ L, 2.64 mmol, 3 equiv.) in anhydrous DCM (4.5 mL) was added Ac₂O (105 μ L, 1.1 mmol, 1.2 equiv.) and stirred at room temperature overnight. The reaction was quenched and washed with H₂O (3 x 30 mL) and brine (1 x 30 mL), dried over MgSO₄ and concentrated *in vacuo* to yield **β -226** (288.6 mg, 73%) as a colourless solid.

¹H NMR (500 MHz, CDCl₃) δ 10.24 (s, 1H, N⁴H), 7.76 (d, *J* = 7.7 Hz, 1H, H⁶), 7.56 (d, *J* = 7.7 Hz, 1H, H⁶), 6.74 (d, *J* = 10.3 Hz, 1H, H¹), 5.65 (d,

$J = 14.5, 4.9$ Hz, 1H, H^{β}), 4.60 (app. q, $J = 5.2$ Hz, 1H, H^{α}), 4.32 (app. d, $J = 5.1$ Hz, 2H, H^{δ}), 2.31 (s, 3H, AcCH₃), 2.18 (s, 3H, AcCH₃), 2.13 (s, 3H, AcCH₃).

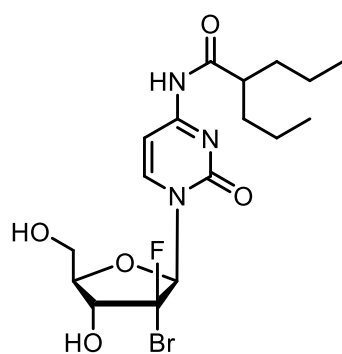
¹³C{¹H} NMR (125 MHz, CDCl₃) δ 171.5 (AcC=O) 170.5 (AcC=O), 168.5 (AcC=O), 163.7 (C⁴), 155.0 (C²), 144.0 (C⁶), 111.6 (d, $J = 264.8$ Hz, C^{2'}), 97.0 (C⁵), 89.7 (d, $J = 37.1$ Hz, C^{1'}), 80.6 (d, $J = 2.6$ Hz, C⁴), 74.9 (d, $J = 29.6$ Hz, C^{3'}), 62.2 (d, $J = 2.4$ Hz, C^{5'}), 25.1 (AcCH₃), 20.8 (2C, AcCH₃).

¹⁹F NMR (376.5 MHz, CDCl₃) δ -111.32 (app. t, $J = 9.4$ Hz).

IR v(cm⁻¹): 1744, 1667, 1620, 1555, 1489, 1435, 1381, 1315, 1207, 1107, 1042, 953, 899, 806, 783, 733, 664, 594, 521, 478.

HRMS (EI): [C₁₅H₁₇BrFN₃O₇+H]⁺ calc. 450.0312 found 450.0316.

***N*-(1-((2R,3R,4R,5R)-3-bromo-3-fluoro-4-hydroxy-5-(hydroxymethyl)tetrahydrofuran-2-yl)-2-oxo-1,2-dihydropyrimidin-4-yl)-2-propylpentanamide (β -227)**



To a solution of **219** (120 mg, 0.157 mmol) in anhydrous DMF (0.2M) were added acetic acid (4.0 eq) and tetramethylammonium fluoride tetrahydrate (103.9 mg, 0.629 mmol, 4 equiv.). The reaction was stirred at room temperature overnight and then was concentrated and purified by column chromatography (4% EtOH/EtOAc) to afford compound **β -227** (2.11 g, 80% yield) as a white foaming solid.

¹H NMR (500 MHz, DMSO-*d*₆) δ 11.0 (broad s, 1H, N⁴H), 8.05 (d, $J = 7.6$ Hz, 1H, H^{δ}), 7.35 (d, $J = 7.6$ Hz, 1H, H^{δ}), 6.71 (d, $J = 5.7$ Hz, 1H, H^{α}), 6.43 (d, $J = 8.4$ Hz, 1H, O³H), 5.11 (dd, $J = 6.4, 5.2$ Hz, 1H, O⁵H), 4.45 (ddd, $J = 14.9, 7.4, 6.0$ Hz, 1H, H^{β}), 4.11 (dt, $J = 7.4, 3.6$ Hz, 1H, H^{α}) 3.68 (app. d, $J = 12.4$, 1H, $H^{\delta'a}$), 3.60 – 3.54 (m, 1H, $H^{\delta'b}$) 2.64-2.61 (m, 1H, CH), 1.57-1.47 (m, 2H, CH₂), 1.38-1.29 (m, 2H, CH₂), 1.28 – 1.17 (m, 4H, CH₂), 0.86 (app. dt, $J = 1.8, 7.2$ Hz, 6H, CH₃).

¹³C NMR (125 MHz, CDCl₃) δ 177.3 (VpC=O), 162.8 (C²), 154.3 (C⁴), 145.5 (C⁶), 117.6 (d, $J = 266.3$ Hz, C^{2'}), 95.4 (C⁵), 87.7 (d, $J = 35$ Hz, C^{1'}), 83.2 (C⁴), 73.4 (d, $J = 22.5$ Hz, C^{3'}), 59.6 (C^{5'}), 45.8 (CH), 34.5 (CH₂), 20.1 (CH₂), 13.9 (CH₃).

¹⁹F{¹H} NMR (376.5 MHz, CDCl₃) δ -112.0 (s).

IR (cm⁻¹): 3234, 2959, 2932, 2872, 2363, 1701, 1653, 1612, 1580, 1487, 1431, 1393, 1312, 1269, 1242, 1217, 1161, 1134, 1107, 1065, 1043, 997, 880, 808, 787, 561, 525.

HRMS (ES⁺): [C₁₇H₂₅BrFN₃O₅+H]⁺ calc. 450.1040, found 450.1033.

Via deprotection routes of **β -228**:

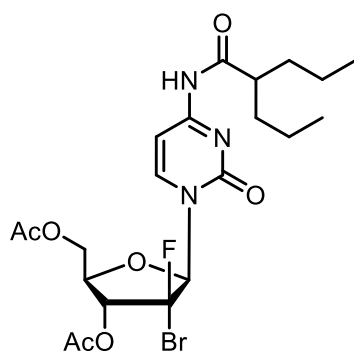
A) To a solution of guanidine hydrochloride (96.0 mg, 1 mmol) in EtOH (1 mL) was added sodium ethoxide (68.1 mg, 1 equiv.) and diluted with further EtOH. The mixture was stirred at r.t. for 1 hour, filtered and collected.

To a solution of **β -228** (53.1 mg, 0.1 mmol) in EtOH/DCM (500 μ L, 9:1) [in an oven dried microwave vial] was slowly added the guanidine solution (200 μ L, 1 M, 1 equiv.) at r.t.. The reaction was stirred at r.t. for 3 hours, concentrated *in vacuo* and purified by column chromatography to yield **β -227** (32.1 mg, 71%) as a colourless solid.

B) To an oven dried microwave vial, **β -228** (106.9 mg, 0.2 mmol) was dissolved in MeOH (1 mL) and cooled to 0°C. NH₃ (7N MeOH, 170 μ L, 6 equiv) was added slowly to cooled solution and warmed to r.t.. When the reaction was complete (3 h), monitored by TLC, the reaction was concentrated *in vacuo* and purified by column chromatography (EtOAc) to yield **β -227** (52.2 mg, 58%) as a colourless solid.

Spectroscopic data is identical for **β -227** when desilylated or deacetylated.

((2R,3R,4R,5R)-3-acetoxy-4-bromo-4-fluoro-5-(2-oxo-4-(2-propylpentanamido)-pyrimidin-1(2H)-yl)tetrahydrofuran-2-yl)methyl acetate (β -228)



To a solution of **β -227** (2.3138 g, 5.2 mmol), DMAP (126.0 mg, 0.1 mmol, 0.2 equiv.) in anhydrous DCM (26 mL) was added NEt₃ (4.3 mL, 30.8 mmol, 6 equiv.) and Ac₂O (1.25 mL, 13 mmol, 2.5 equiv.) sequentially, and stirred at room temperature overnight. The reaction was quenched and washed with H₂O (3 x 30 mL) and brine (1 x 30 mL), dried over MgSO₄ and concentrated *in vacuo*. Purification by column chromatography (100% EtOAc) gave **β -228** (2.1399 g, 78%) as a foaming white solid.

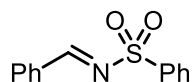
¹H NMR (500 MHz, CDCl₃) δ 8.12 (broad s, 1H, N⁴H), 7.73 (d, *J* = 7.7 Hz, 1H, H ^{δ}), 7.52 (d, *J* = 7.6 Hz, 1H, H ^{δ}), 6.75 (d, *J* = 10.2 Hz, 1H, H ^{ϵ}), 5.67 (dd, *J* = 12.4, 5.0 Hz, 1H, H ^{δ}), 4.56 (app. q, *J* = 4.9 Hz, 1H, H ^{ϵ}), 4.35 - 4.26 (m, 2H, H ^{δ} a and H ^{δ} b), 2.30 (tt, *J* = 8.9, 5.3 Hz, 1H, CH), 2.19 (s, 3H, AcCH₃), 2.14 (s, 3H, AcCH₃), 1.68 - 1.61 (m, 2H, CH₂), 1.53 - 1.45 (m, 2H, CH₂), 1.38 - 1.30 (m, 4H, CH₂), 0.92 (overlapping t, *J* = 7.3 Hz, 6H, CH₃).

¹³C NMR (125 MHz, CDCl₃) δ 176.4 (VpC=O), 170.5 (AcC=O), 168.5 (AcC=O), 162.6 (C²), 154.9 (C⁴), 144.1 (C⁶), 111.6 (d, *J* = 265 Hz, C²), 96.3 (C⁵), 89.5 (d, *J* = 36.3 Hz, C¹), 80.4 (d, *J* = 3.8 Hz, C⁴), 74.9 (d, *J* = 27.5 Hz, C³), 62.2 (C⁵), , 49.1 (CH), 35.0 (2C, CH₂), 31.1 (CH₂), 20.8 (3C, AcCH₃ and CH₂), 14.2 (2C, CH₃).

^{19}F NMR (376.5 MHz, CDCl_3) δ -111.5 (app. t, $J = 8.3$ Hz)

IR $\nu(\text{cm}^{-1})$: 3333, 2972, 2880, 1751, 1663, 1624, 1560, 1489, 1454, 1381, 1317, 1273, 1225, 1086, 1045, 880, 804, 787, 594, 432, 413.

HRMS (ES): $[\text{C}_{21}\text{H}_{29}\text{BrFN}_3\text{O}_7+\text{H}]^+$ calc. 534.1251 found 534.1241.

(E)-N-benzylidenebenzenesulfonamide (234)

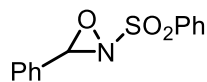
A mixture of benzenesulfonamide (1.5721 g, 10.0 mmol) and benzaldehyde dimethyl acetal (1.5 mL, 10.0 mmol) was heated for 3 hours to remove methanol from the reaction by distillation. The reaction was cooled to room temperature and concentrated *in vacuo*. The resulting slurry mixture was dissolved in the minimum amount of DCM, and upon addition of hexane a precipitate formed. The mixture was cooled overnight to aid precipitation, and filtered to furnish **234** (999.8 mg, 41% yield) as a white solid.

^1H NMR (500 MHz, DMSO- d_6) δ 9.19 (s, 1H, -CH=N), 8.06 – 8.02 (m, 2H, ArH), 7.99 – 7.95 (m, 2H, ArH), 7.79 – 7.70 (m, 2H, ArH), 7.67 (t, J = 7.8 Hz, 2H, ArH), 7.58 (t, J = 7.7 Hz, 2H, ArH).

$^{13}\text{C}\{^1\text{H}\}$ NMR (126 MHz, DMSO- d_6) δ 172.5 (CH=N), 138.5 (ArC), 136.0 (ArC), 134.5 (ArC), 132.5 (ArC), 132.0 (ArC), 130.0 (2C, ArC), 128.0 (ArC).

IR (cm^{-1}): 1595, 1571, 1447, 1312, 1157, 1088, 795, 750, 683, 629, 583

HRMS (ES): $[\text{C}_{13}\text{H}_{11}\text{NO}_2\text{S}]^+$ calc. 245.0511 found 245.0511.

3-phenyl-2-(phenylsulfonyl)-1,2-oxaziridine [Davis' oxaziridine] (235)

To a cooled solution of **234** (492 mg, 2 mmol), benzyltriethylammonium chloride (45.7 mg, 0.2 mmol, 0.1 equiv.) in $\text{CH}_2\text{Cl}_2/\text{NaHCO}_3$ (7 mL, 1:1 v/v) was added slowly a solution of mCPBA (548 mg, 70% active, 2.2 mmol, 1.1 equiv.) in CH_2Cl_2 (6 mL) under vigorous stirring. The biphasic mixture was stirred at 0°C for 30 minutes, warmed to room temperature and partitioned. The organic phase was washed with H_2O (2 x 10 mL), NaSO_3 (1 x 10 mL), H_2O and brine (2 x 10 mL each), dried over MgSO_4 and concentrated *in vacuo*. The mother liquor was dissolved in the minimum amount of DCM and precipitated out by slow addition to hexane. The solids were collected by filtration to give **235** (294 mg, 56% yield) as a white solid.

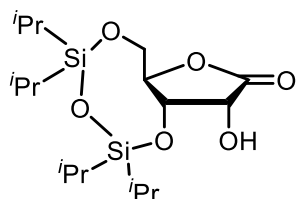
^1H NMR (500 MHz, CDCl_3) δ 8.09 – 8.03 (m, 2H, ArH), 7.79 – 7.74 (m, 1H, ArH), 7.68 – 7.62 (m, 2H, ArH), 7.50 – 7.38 (m, 5H, ArH), 5.49 (s, 1H, CHN).

$^{13}\text{C}\{^1\text{H}\}$ NMR (126 MHz, CDCl_3) δ 135.16 (ArC), 134.89 (ArC), 131.60 (ArC), 130.61 (ArC), 129.54 (ArC), 129.53 (ArC), 128.91 (ArC), 128.41 (ArC), 76.45 (C-N).

IR (cm^{-1}): 2980, 2363, 1445, 1389, 1346, 1319, 1294, 1231, 1169, 1084, 827, 787, 760, 727, 689.

HRMS (ASAP⁺): $[\text{C}_{13}\text{H}_{12}\text{NO}_3\text{S}+\text{H}]^+$ Calc. 262.0538 Found 262.0537

(6a*R*,9*R*,9a*S*)-9-hydroxy-2,2,4,4-tetraisopropyltetrahydro-8*H*-furo[3,2-*f*][1,3,5,2,4]trioxadisilocin-8-one (237)^[132]



To a solution of D-ribonic- γ -lactone (**231**, 593.2 mg, 4 mmol) and imidazole (1.3609, 20 mmol, 5 equiv.) in anhydrous DMF (30 mL) at 0°C was added dropwise a solution of 1,3-dichloro-1,1,3,3-tetraisopropyldisiloxane (1.54 mL, 4.8 mmol, 1.2 equiv.) in anhydrous DMF (10 mL) via dropping funnel.

After complete addition, the reaction mixture was stirred at 0°C for 10 minutes before warming to r.t. with stirring overnight. The reaction was quenched with H₂O (40 mL) and extracted into EtOAc (3 x 30 mL). The combined organics were washed with H₂O and brine (2 x 30 mL), dried over MgSO₄ and concentrated *in vacuo*. Purification by column chromatography yielded **237** (789.7 mg, 51% yield) as a colourless solid.

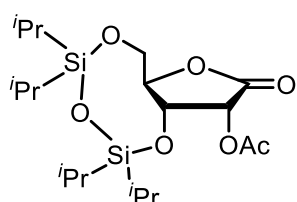
¹H NMR (500 MHz, CDCl₃) δ 4.54 – 4.49 (m, 1H, *H*^f), 4.43 (td, *J* = 6.4, 3.7 Hz, 1H, *H*^A), 4.24 (dd, *J* = 5.9, 2.2 Hz, 1H, *H*^f), 4.15 (dd, *J* = 12.5, 3.7 Hz, 1H, *H*^f_a), 3.98 (dd, *J* = 12.5, 6.2 Hz, 1H, *H*^f_b), 2.93 (d, *J* = 2.5 Hz, 1H, OH), 1.11 – 1.03 (m, 28H, SiCH(CH₃)₂ and SiCH(CH₃)₂).

¹³C{¹H} NMR (126 MHz, CDCl₃) δ 171.8 (C¹), 82.8 (C²), 70.0 (C⁴), 68.6 (C³), 61.8 (C⁵), 17.5 (SiCH(CH₃)₂), 17.4 (3C, SiCH(CH₃)₂), 17.2 (SiCH(CH₃)₂), 17.0 (2C, SiCH(CH₃)₂), 16.9 (SiCH(CH₃)₂), 13.4 (SiCH(CH₃)₂), 13.3 (SiCH(CH₃)₂), 13.0 (SiCH(CH₃)₂), 12.7 (SiCH(CH₃)₂).

IR (cm⁻¹): 2945, 2868, 2361, 1734, 1464, 1111, 1063, 1026, 885, 691.

HRMS (TOF AP⁺): [C₁₇H₃₄O₆Si₂+H]⁺ calc. 391.1972 found 391.1975.

(6a*R*,9*R*,9a*R*)-2,2,4,4-tetraisopropyl-8-oxotetrahydro-6*H*-furo[3,2-*f*][1,3,5,2,4]-trioxadisilocin-9-yl acetate (239)



To a solution of **237** (98.7 mg, 0.25 mmol), DMAP (3.5 mg, 0.025 mmol, 0.1 equiv.) in anhydrous DCM (1 mL) was added NEt₃ (50 μ L, 0.35 mmol, 1.4 equiv.) at 0°C, followed by dropwise addition of Ac₂O (28.5 μ L, 0.3 mmol, 1.2 equiv.). The reaction mixture was stirred at 0°C for 30 minutes before

warming to r.t. with stirring overnight. The reaction was quenched saturated aqueous NaHCO₃ (1 mL), extracted with DCM (3 x 5 mL), dried over MgSO₄ and concentrated *in vacuo*. Purification by column chromatography (10% EtOAc/Hexanes) yielded **239** (25.6 mg, 24% yield) as a colourless solid. **237** recovered (18.7 mg, 19%).

^1H NMR (400 MHz, CDCl_3) δ 5.34 (d, $J = 6.4$ Hz, 1H, H^f), 4.51 (dd, $J = 7.2, 6.6$ Hz, 1H, H^g), 4.40 (ddd, $J = 7.4, 5.6, 3.4$ Hz, 1H, H^d), 4.13 (dd, $J = 12.7, 3.4$ Hz, 1H, H^{6a}), 4.02 (dd, $J = 12.7, 5.6$ Hz, 1H, H^{6b}), 2.15 (s, 3H, CH_3), 1.11 – 0.97 (m, 28H, $\text{SiCH}(\text{CH}_3)_2$ and $\text{SiCH}(\text{CH}_3)_2$).

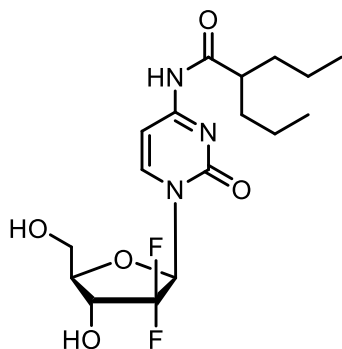
$^{13}\text{C}\{^1\text{H}\}$ NMR: (101 MHz, CDCl_3) δ 170.1 (C^1), 169.1 ($\text{AcC}=\text{O}$), 83.6 (C^2), 69.0 (C^4), 68.9 (C^3), 61.5 (C^5), 20.4 (CH_3), 17.5 ($\text{SiCH}(\text{CH}_3)_2$), 17.4 (3C, $\text{SiCH}(\text{CH}_3)_2$), 17.0 ($\text{SiCH}(\text{CH}_3)_2$), 16.9 (2C, $\text{SiCH}(\text{CH}_3)_2$), 13.4 ($\text{SiCH}(\text{CH}_3)_2$), 13.2 ($\text{SiCH}(\text{CH}_3)_2$), 13.0 ($\text{SiCH}(\text{CH}_3)_2$), 12.8 ($\text{SiCH}(\text{CH}_3)_2$).

IR (cm^{-1}): 2945, 2868, 2361, 1749, 1464, 1231, 1030, 883, 692.

HRMS (TOF AP⁺): [$\text{C}_{19}\text{H}_{36}\text{O}_7\text{Si}_2+\text{H}$]⁺ calc. 433.2078 found 433.2080.

5.4 – Synthesis of reference compounds

N-(1-((2*R*,4*R*,5*R*)-3,3-difluoro-4-hydroxy-5-(hydroxymethyl)tetrahydrofuran-2-yl)-2-oxo-1,2-dihydropyrimidin-4-yl)-2-propylpentanamide [**100**]^[25]



Method A: To a solution of gemcitabine hydrochloride (299.4 mg, 1 mmol) in DMF/DMSO (3:1 v/v, 10 mL) were added NMM (110 μ L, 1 equiv.), HOBT (153.9 mg, 1 equiv.), valproic acid (175 μ L, 1.1 equiv.) and EDC.HCl (250.3 mg, 1.3 equiv.) in order. The mixture was diluted with more DMF/DMSO (3:1 v/v, 10 mL), and heated to 55°C for 17 hours. The mixture was cooled to room temperature, and 10% NaCl solution (5 mL) and water (3 mL) were added while stirring. The mixture was subsequently extracted with EtOAc (3 x 10 mL), and the combined organic layers were washed with 15% LiCl solution (2 x 5 mL), saturated NaHCO₃ solution (10 mL) and brine (5 mL). The mixture was then concentrated *in vacuo*, and purified by flash column chromatography (80% EtOAc/Petroleum Ether 40-60) to afford **100** (97.5 mg, 25% yield) as an off-white solid.

Method B: To a cooled solution of gemcitabine hydrochloride (299.4 mg, 3.64 equiv.) in pyridine (6 mL) and acetonitrile (2 mL), was added TMSCl (580 μ L, 4.55 equiv.) dropwise as to maintain T < 10°C. The solution was stirred at 5°C for 2.5 hours. In a second flask, valproic acid (146.6 mg, 1.0 mmol) and CDI (162.7 mg, 1.0 mmol) were dissolved in MeCN (3 mL) and stirred for 1 hour at room temperature, before adding to the cooled gemcitabine solution. The mixture was then heated to 60°C for 40 hours. The mixture was cooled to 40°C before quenching with EtOH (6mL) and stirred for 30 mins prior to dilution with water (5 mL) and heating at 50°C for a further 5 hours. The solution was then concentrated *in vacuo* yielding a golden oil, and then dissolved with EtOAc (10 mL) and water (10 mL). The pH was adjusted to 2 using H₃PO₄, before extracting with EtOAc (3 x 10 mL), and the combined organic layers were washed with saturated aqueous NaHCO₃ (2 x 20 mL) and brine (2 x 20 mL). The solution was dried over MgSO₄, and concentrated under reduced pressure, yielding the crude reaction mixture, which was purified by flash column chromatography (80→90% EtOAc/Petroleum Ether 40-60) to afford **100** (275.5 mg, 70% yield) as a white foam.

^1H NMR (500 MHz, DMSO- d_6) δ 11.05 (s, 1H, N^4H), 8.25 (d, $J = 7.6$ Hz, 1H, H^6), 7.33 (d, $J = 7.6$ Hz, 1H, H^6), 6.32 (d, $J = 6.5$ Hz, 1H, OH^6), 6.17 (t, $J = 7.4$ Hz, 1H, $\text{H}^{1'}$), 5.29 (t, $J = 5.4$ Hz, 1H, H^6), 4.24 – 4.14 (m, 1H, OH^6), 3.89 (dt, $J = 8.5, 3.0$ Hz, 1H, $\text{H}^{4'}$), 3.84 – 3.77 (m, 1H, $\text{H}^{6'b}$), 3.65 (ddd, $J = 12.7, 5.7, 3.6$ Hz, 1H, $\text{H}^{6'a}$), 2.66 – 2.59 (m, 1H, CH), 1.57 – 1.48 (m, 2H, CH_2), 1.39 – 1.19 (m, 6H, CH_2), 0.85 (t, $J = 7.1$ Hz, 6H, CH_3).

$^{13}\text{C}\{^1\text{H}\}$ NMR (126 MHz, DMSO- d_6) δ 177.4 (Vp-C=O), 162.9 (C^2), 154.2 (C^4), 144.9 (C^6), 123.0 (t, $J = 258.3$ Hz, C^2), 96.0 (C^5), 84.1 (t, $J = 32.8$ Hz, C^1), 81.0 (C^4), 68.4 (t, $J = 22.2$ Hz, C^3), 58.8 (C^5), 45.8 (CH), 34.5 (CH_2), 20.0 (CH_2), 13.9 (CH_3).

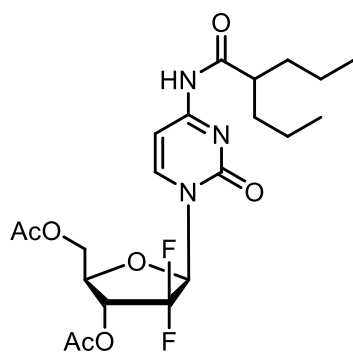
$^{19}\text{F}\{^1\text{H}\}$ NMR (471 MHz, DMSO- d_6) δ -116.87 (s).

IR (cm^{-1}): 2961, 2930, 2870, 2367, 2322, 1699, 1653, 1614, 1558, 1485, 1393, 1312, 1260, 1196, 1062, 806.

HRMS(ES^+): [$\text{C}_{17}\text{H}_{25}\text{N}_3\text{O}_5\text{F}_2+\text{H}$] $^+$ calc. 390.1841 found 390.1854.

Data is consistent with the literature.^[25]

((2R,3R,5R)-3-acetoxy-4,4-difluoro-5-(2-oxo-4-(2-propylpentanamido)pyrimidin-1(2H)-yl)tetrahydrofuran-2-yl)methyl acetate [LY2334737 3',5'-O-diacetate] (241)



Method: To a stirred solution of LY2334737 (96.8 mg, 0.25 mmol) and 4-DMAP (6.4 mg, 0.05 mmol, 0.2 equiv.) in anhydrous DCM (10 mL) was added NEt_3 (210 μL , 1.5 mmol, 6 equiv.) and Ac_2O (60 μL , 0.625 mmol, 2.5 equiv.). The reaction was stirred overnight at r.t. and quenched with H_2O . The mixture was extracted with DCM (3 x 10 mL), washed with H_2O and brine (3 x 20 mL each), dried over MgSO_4 and concentrated *in vacuo* to yield **241**

(105.5 mg, 89% yield) as a white solid.

^1H NMR (500 MHz, CDCl_3) δ 8.42 (s, 1H, N^4H), 7.77 (dd, $J = 7.6, 1.5$ Hz, 1H, H^6), 7.53 (d, $J = 7.6$ Hz, 1H, H^6), 6.46 (dd, $J = 10.9, 6.1$ Hz, 1H, $\text{H}^{1'}$), 5.28 (ddd, $J = 13.2, 5.4, 3.7$ Hz, 1H, H^6), 4.42 (app. d, $J = 4.1$ Hz, 2H, $\text{H}^{4'}$ and $\text{H}^{6'a}$), 4.34 (dd, $J = 9.5, 4.0$ Hz, 1H, $\text{H}^{6'b}$), 2.34 (tt, $J = 7.9, 4.8$ Hz, 1H, CH), 2.19 (s, 3H, Ac- CH_3), 2.13 (s, 3H, Ac- CH_3), 1.68 – 1.58 (m, 2H, CH_2), 1.51 – 1.42 (m, 2H, CH_2), 1.36 – 1.28 (m, 4H, CH_2), 0.90 (overlapping t, $J = 7.3$, 6H, CH_3).

$^{13}\text{C}\{^1\text{H}\}$ NMR (126 MHz, CDCl_3) δ 176.6 (Vp-C=O), 170.4 (Ac-C=O), 169.1 (Ac-C=O), 162.8 (C^2), 154.8 (C^4), 144.7 (C^6), 120.6 (dd, $J = 267.0, 259.9$ Hz, C^2), 97.2 (C^5), 84.1 (dd, $J = 39.5, 19.0$ Hz, C^1), 78.2 (d, $J = 3.4$ Hz, C^4), 70.8 (dd, $J = 34.1, 17.2$ Hz, C^3),

62.0 (s, C⁵), 48.9 (CH), 35.0 (2C, CH₂), 20.8 (AcCH₃), 20.7 (AcCH₃) 20.5 (CH₂), 14.2 (CH₃), 14.1 (CH₃).

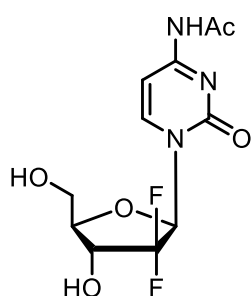
¹⁹F{¹H} NMR (376 MHz, CDCl₃) δ -116.35 (d, *J* = 246.2 Hz), -120.55 (d, *J* = 249.6 Hz).

¹⁹F NMR (471 MHz, CDCl₃) δ -115.93 (dt, *J* = 246.1, 11.2 Hz), -119.98 (d, *J* = 226.3 Hz).

IR (cm⁻¹): CDCl₃ (film): 1753, 1676, 1624, 1555, 1483, 1389, 1315, 1215, 1125, 1055.

HRMS (TOF AP⁺): [C₂₁H₂₉N₃O₇F₂+H]⁺ calc. 474.2052 found 474.2057.

***N*-(1-((2*R*,4*R*,5*R*)-3,3-difluoro-4-hydroxy-5-(hydroxymethyl)tetrahydrofuran-2-yl)-2-oxo-1,2-dihydropyrimidin-4-yl)acetamide [Gemcitabine *N*⁴-acetate] (**249**)**



To a solution of gemcitabine (263.7, 1 mmol) in water (1 mL) was added a solution of acetic anhydride (150 μ L, 1.5 mmol, 1.5 equiv.) in anhydrous dioxane (5 mL) at r.t.. The reaction was subsequently heated to 90 °C for 4 h. The mixture was then concentrated *in vacuo*, and the crude mixture purified by column chromatography (10% EtOH/EtOAc) to yield **249** (291.3 mg, 95% yield) as a white/colourless solid.

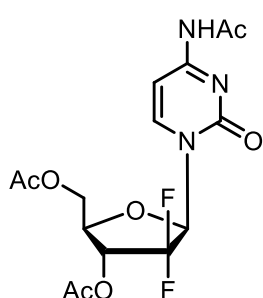
¹H NMR (500 MHz, DMSO-*d*₆) δ 11.00 (s, 1H), 8.24 (d, *J* = 7.6 Hz, 1H), 7.25 (d, *J* = 7.6 Hz, 1H), 6.35 (d, *J* = 6.4 Hz, 1H), 6.17 (t, *J* = 7.3 Hz, 1H), 5.33 (s, 1H), 4.24 – 4.14 (m, 1H), 3.89 (d, *J* = 8.5 Hz, 1H), 3.80 (d, *J* = 12.5 Hz, 1H), 3.69 – 3.62 (m, 1H), 2.11 (s, 3H).

¹³C{¹H} NMR (126 MHz, DMSO-*d*₆) δ 171.7 (Ac-C=O), 163.3 (C²), 154.7 (C⁴), 145.2 (C⁶), 125.84 – 120.95 (app. t, *J* = 259 Hz, C²), 96.3 (C⁵), 84.6 (C¹), 81.5 (C⁴), 68.8 (t, *J* = 22.7 Hz, C³), 59.2 (C⁵), 24.9 (AcCH₃).

¹⁹F NMR (471 MHz, DMSO-*d*₆) δ -116.96 (app. s).

* In the absence of MS, the structural identity of **249** cannot be conclusively assigned hence the structure proposed is tentative.

(2*R*,3*R*,5*R*)-5-(4-acetamido-2-oxopyrimidin-1(2*H*)-yl)-2-(acetoxymethyl)-4,4-difluorotetrahydrofuran-3-yl acetate [Gemcitabine *N*⁴,3',5'-*O*-triacetate] (250**)**



To a solution of gemcitabine (263.0 mg, 1 mmol), 4-DMAP (3.7 mg, 0.03 equiv.) in pyridine (20 mL) was added acetic anhydride (570 μ L, 6 mmol, 6 equiv.). The reaction mixture was stirred for 24 h at r.t., quenched with sat. aq. NaHCO₃ (25 mL). The mixture was extracted with Et₂O (3 x 30 mL), and the combined organics were washed with water (2 x 20 mL). The

organics were concentrated *in vacuo*, and purified by column chromatography (2% MeOH/DCM) to yield **250** (74.0 mg, 19% yield) as a foaming solid.

^1H NMR (500 MHz, CDCl_3) δ 10.14 (s, 1H, N^4H), 7.77 (d, $J = 7.6$ Hz, 1H, H^{f}), 7.53 (d, $J = 7.7$ Hz, 1H, H^{f}), 6.47 – 6.40 (m, 1H, H^{l}), 5.27 (dd, $J = 16.5, 5.2$ Hz, 1H, H^{f}), 4.41 (app. d, $J = 3.9$ Hz, 2H, H^{a} and H^{b}), 4.35 (dd, $J = 9.4, 4.0$ Hz, 1H, H^{b}), 2.28 (s, 3H, AcCH_3), 2.18 (s, 3H, AcCH_3), 2.13 (s, 3H, AcCH_3).

$^{13}\text{C}\{^1\text{H}\}$ NMR (126 MHz, CDCl_3) δ 171.0 (Ac-C=O), 170.4 (Ac-C=O), 169.1 (Ac-C=O), 163.5 (C^2), 154.8 (C^4), 144.7 (C^6), 120.6 (dd, $J = 267.1, 259.7$ Hz, C^2), 97.5 (C^5), 78.35 – 78.21 (app. t, $J = 3.5$ Hz, C^1), 70.8 (dd, $J = 34.1, 17.2$ Hz, C^3), 62.0 (C^4), 53.6 (C^5), 25.1 (AcCH_3), 20.8 (AcCH_3), 20.5 (AcCH_3).

^{19}F NMR (376 MHz, CDCl_3) δ -116.23 (d, $J = 246.4$ Hz).

IR (cm^{-1}): 1748, 1672, 1622, 1555, 1487, 1437, 1389, 1312, 1211, 1123, 1049, 912.

HRMS (ES^+): $[\text{C}_{15}\text{H}_{17}\text{F}_2\text{N}_3\text{O}_7+\text{H}]^+$ calc. 390.1113 found 390.1124.

5.5 – Fluorination

Finkelstein

Method A

An oven dried flask containing **228** (106.7 mg, 0.2 mmol), KI (171.1 mg [KI] or NaI], 5 equiv.) and acetone (10 mL) was stirred for 24 hours at room temperature. The reaction mixture was filtered, washed with further acetone and concentrated *in vacuo*.

Method B

An oven dried flask containing **228** (107.9 mg, 0.2 mmol), KI (167.3 mg, 5 equiv.) and 2-butanone (10 mL) was heated to reflux for 46 hours. The reaction mixture was cooled to r.t. filtered and concentrated *in vacuo*.

Method C

An oven dried flask containing **228** (53.4 mg, 0.1 mmol), NaI (77.8 mg, 5 equiv.) and 2-butanone (4 mL) was heated to reflux for 24 hours. The reaction was quenched with H₂O (5 mL), extracted into EtOAc (10 mL) and washed with H₂O (3 x 10 mL). The organic phase was dried over MgSO₄ and concentrated *in vacuo*.

Non-radioactive ¹⁹F fluorination

To an oven dried microwave vial containing KF (14.7 mg, 5 equiv) and K₂₂₂ (18.8 mg, 1 equiv.) was added MeCN (200 μL) and azeotropically dried at 100°C under vacuum. Drying was repeated four further times. **228** (26.9 mg, 0.05 mmol) in solvent (300 μL) was introduced to dried KF/K₂₂₂ mixture at r.t. and heated to 50°C for 15 hours. Product mixture was analysed by TLC and ¹⁹F NMR.

To an oven dried microwave vial containing metal fluoride (14.7 mg [KF], 32.0 mg [AgF], 5 equiv) and K₂₂₂ (18.8 mg, 1 equiv.) was added MeCN (200 μL) and azeotropically dried at 100°C under vacuum. Drying was repeated four further times. **228** (26.9 mg, 0.05 mmol) in solvent (500 μL) was introduced to dried KF/K₂₂₂ mixture at r.t. and heated at 120°C for 30/60 minutes. Product mixture was analysed by TLC and ¹⁹F NMR.

5.6 – Cell culture details

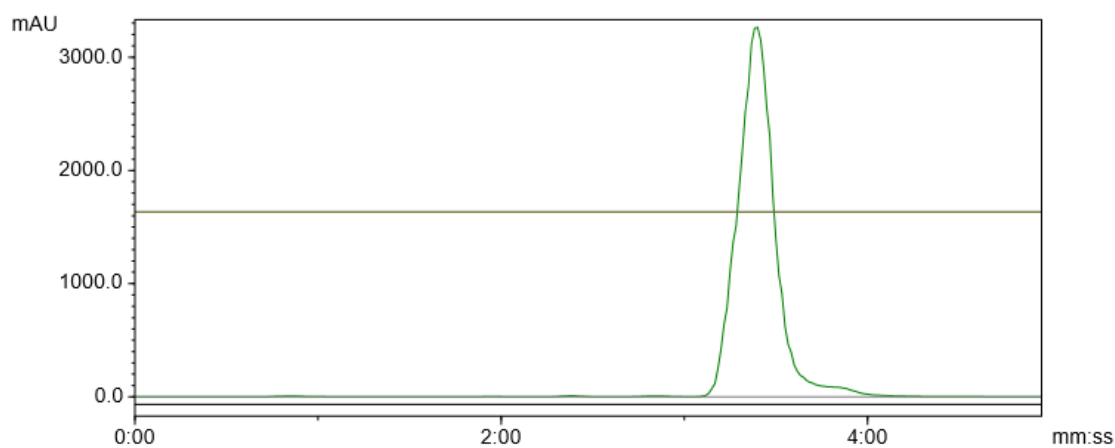
Panc 10.05 cell lines were donated by Dr. Catherine Hogan's research group, and grown in RPMI Medium with 10% FBS. The cells were maintained in an incubator at 37°C containing 5% CO₂. The cells were split every 2-4 days (when appropriate) and medium changed at ratios of 1:1, 1:2, 1:3 or 1:5 with respect master cell stock. Growth medium was changed additionally when necessary, PBS used for washing vessels and 0.25% Trypsin-EDTA solution used to remove cells from culture vessel.

For the tested compounds, a master stock of each was prepared by dissolving an appropriate amount in 500 µL of DMSO (Cat. No. D2650-5X5ML; Hybri-Max™, sterile-filtered, BioReagent, suitable for hybridoma, ≥99.7%) prior to diluting with growth medium to create stock concentrations of 200 µM, 100 µM, 20 µM and 2 µM. (LY2334737 = 2.0 mg, 2'Br-LY2334737 = 2.3 mg, Gemcitabine = 1.3 mg). Stock solutions of tested compounds in media were stored at -20°C. Corresponding DMSO control samples were also prepared.

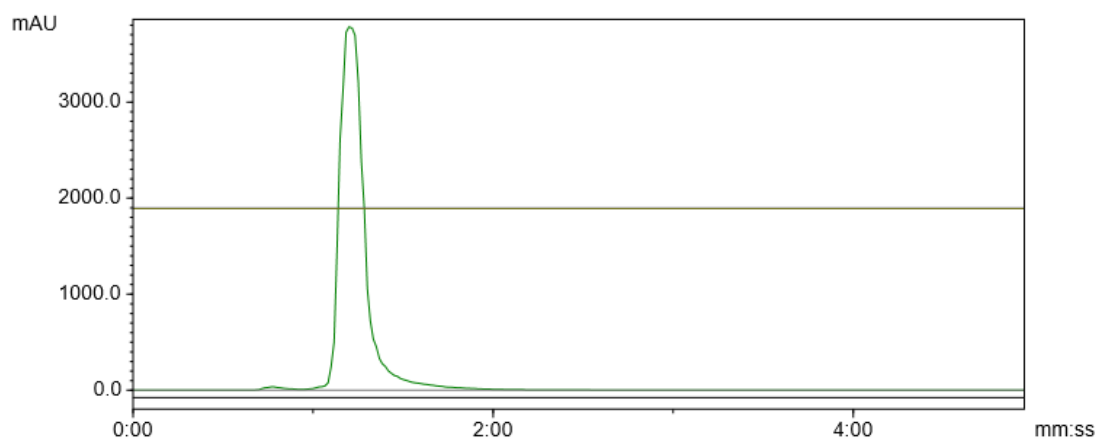
For experiments, cells were seeded in 96-well plates at a seeding density of 2x10⁵ cells mL⁻¹ and incubated for 24 hours after seeding to allow for adhesion to vessel surface. For each experiment, three wells were used per condition and each experiment repeated. Subsequently, each well was drained of its growth medium and resuspended in 75 µL of 500 nM IncuCyte® Cytotox Red Reagent (Cat. No. 4632) as imaging agent, and 75 µL of cytotoxic agent of known concentration introduced, resulting in an effective half concentration for both imaging and cytotoxic agent. Wells containing untreated cells were also screened as untreated controls. Plates were then incubated in IncuCyte® S3 Live-Cell Analysis System at 37°C containing 5% CO₂ for the duration of the experiment, monitored and imaged over the course of the experiment at 4 images per well per hour.

6 – Appendix

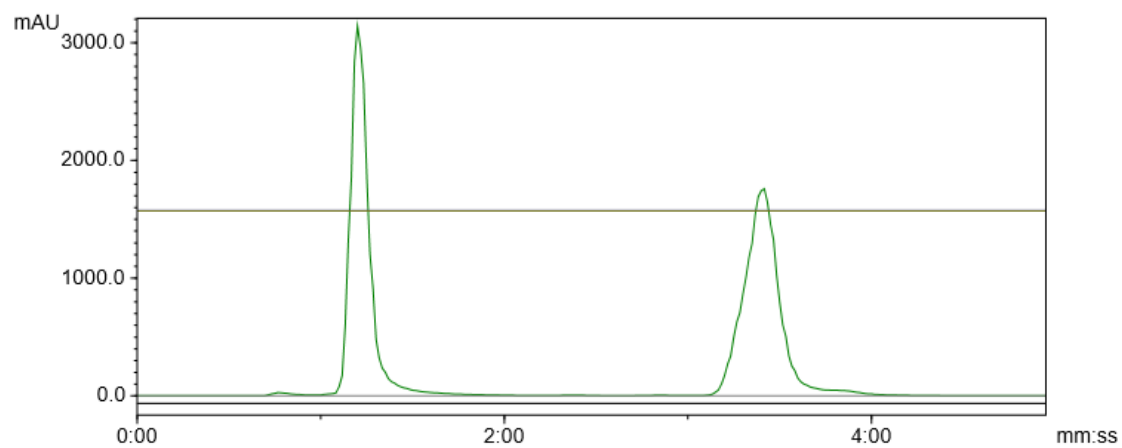
6.1 – HPLC traces of selected compounds



Precursor in 50/50 MeCN/H₂O with 0.1% HCO₂H at 40°C in a C₁₈ Agilent (150 mm) column. Retention time of 3 min 20 s.



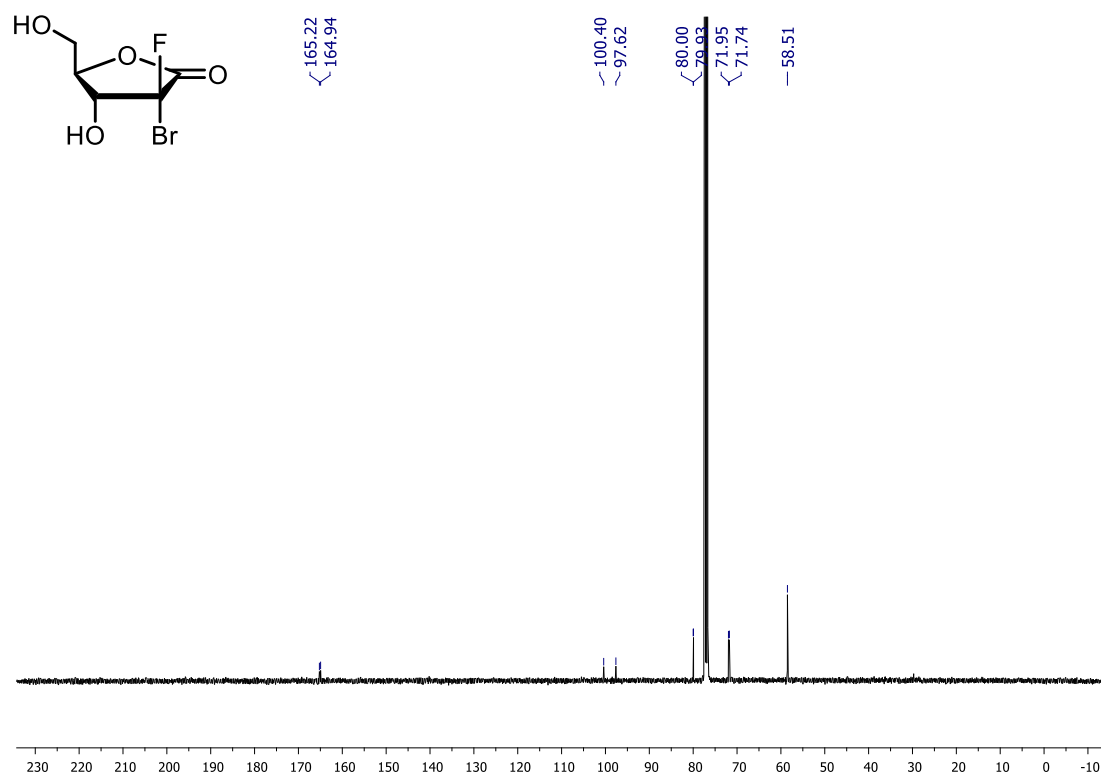
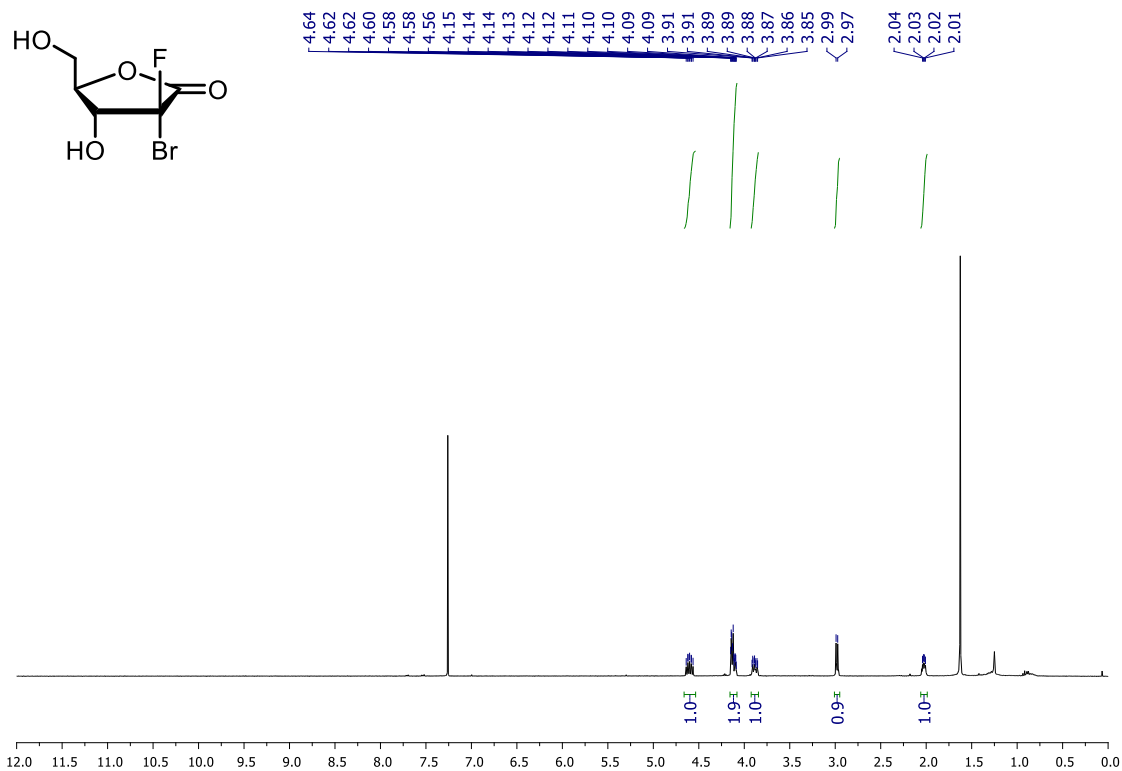
Product in 50/50 MeCN/H₂O with 0.1% HCO₂H at 40°C in a C₁₈ Agilent (150 mm) column. Retention time of 1 min 10 s.

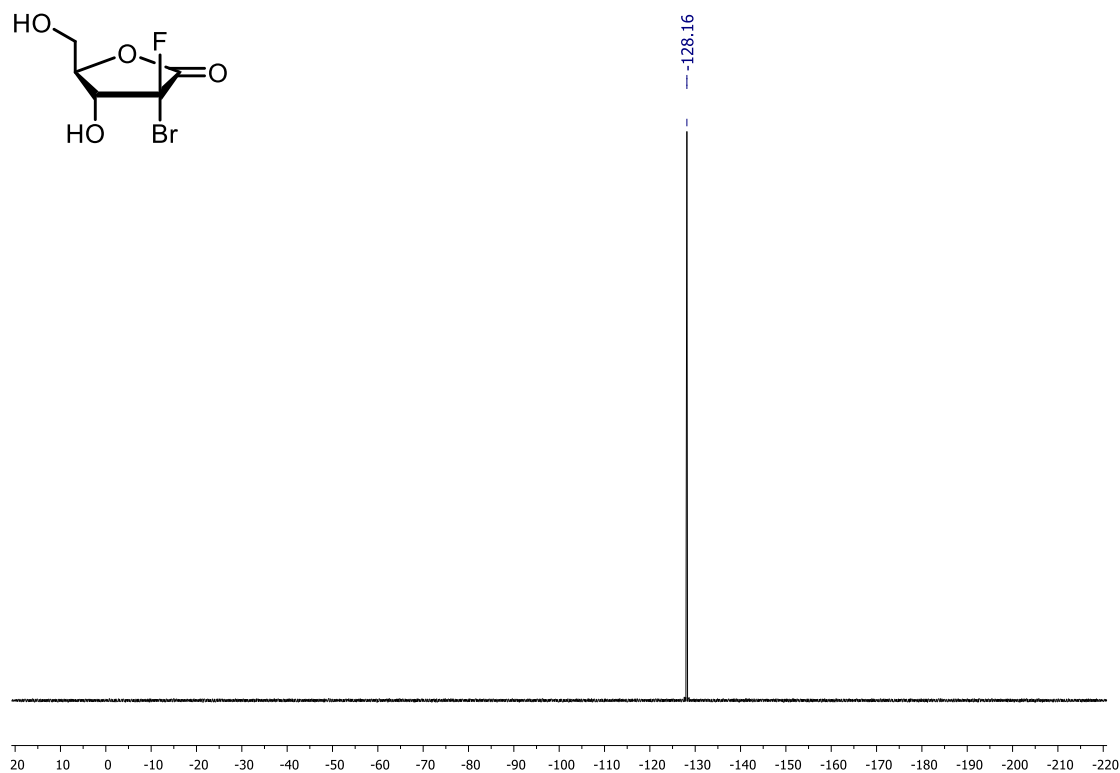


Product/precursor overlay trace in 50/50 MeCN/H₂O with 0.1% HCO₂H at 40°C in a C₁₈ Agilent (150 mm) column.

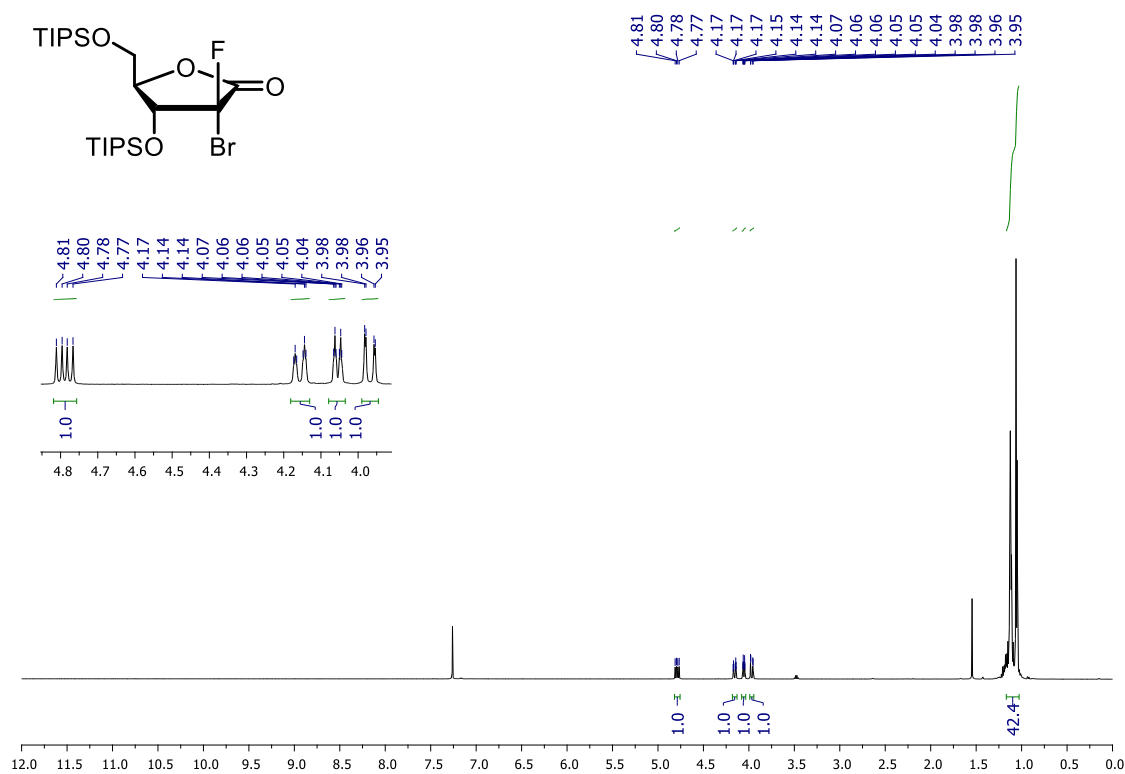
6.2 – Selected NMR spectra

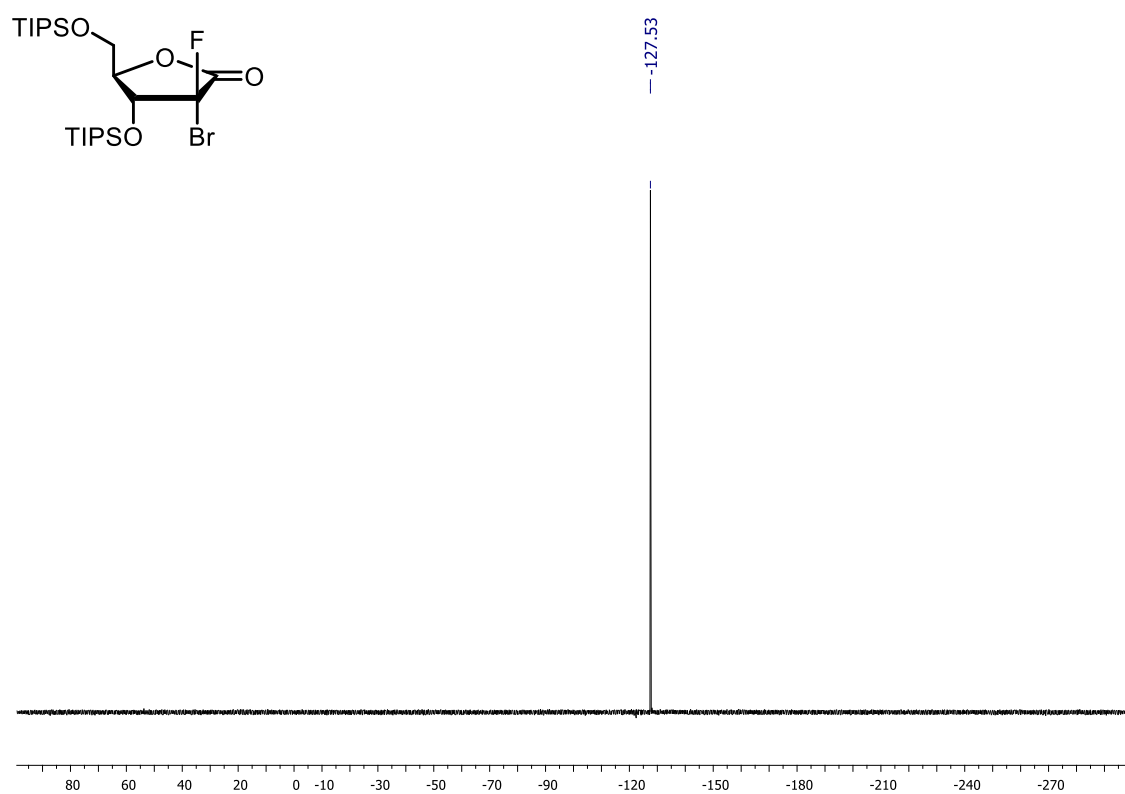
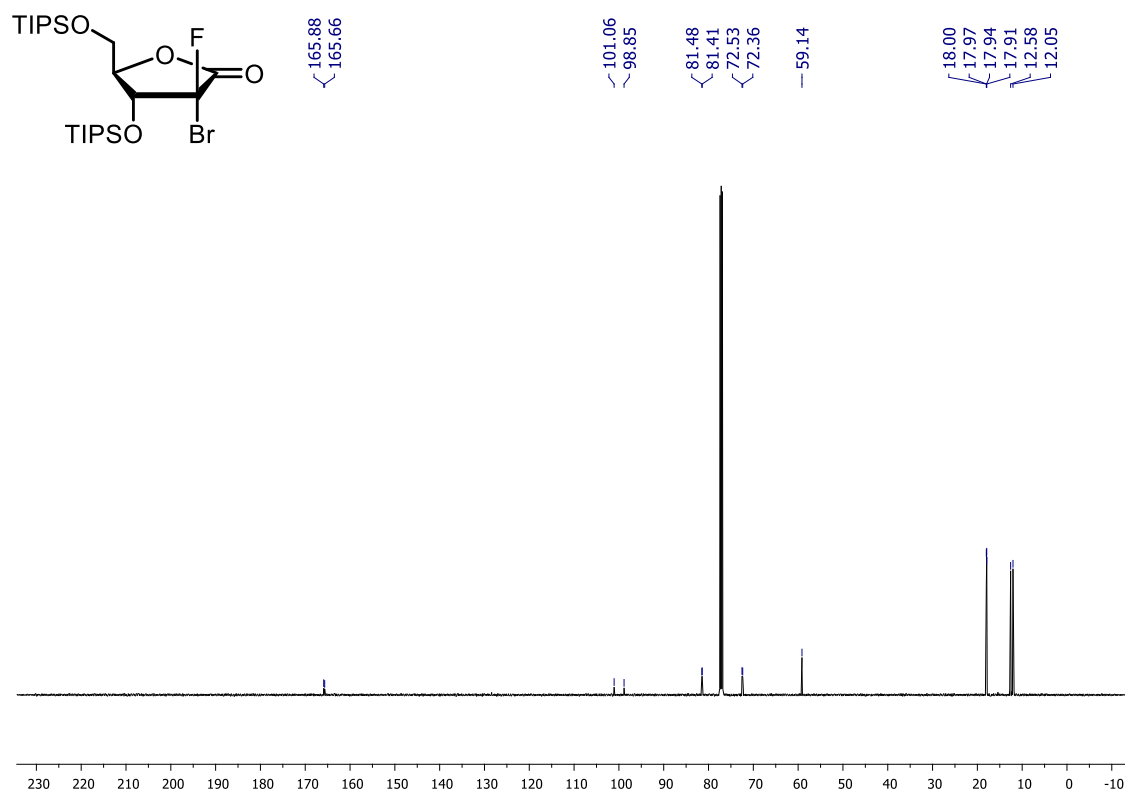
(3R,4R,5R)-3-bromo-3-fluoro-4-hydroxy-5-(hydroxymethyl)dihydrofuran-2(3H)-one (195)



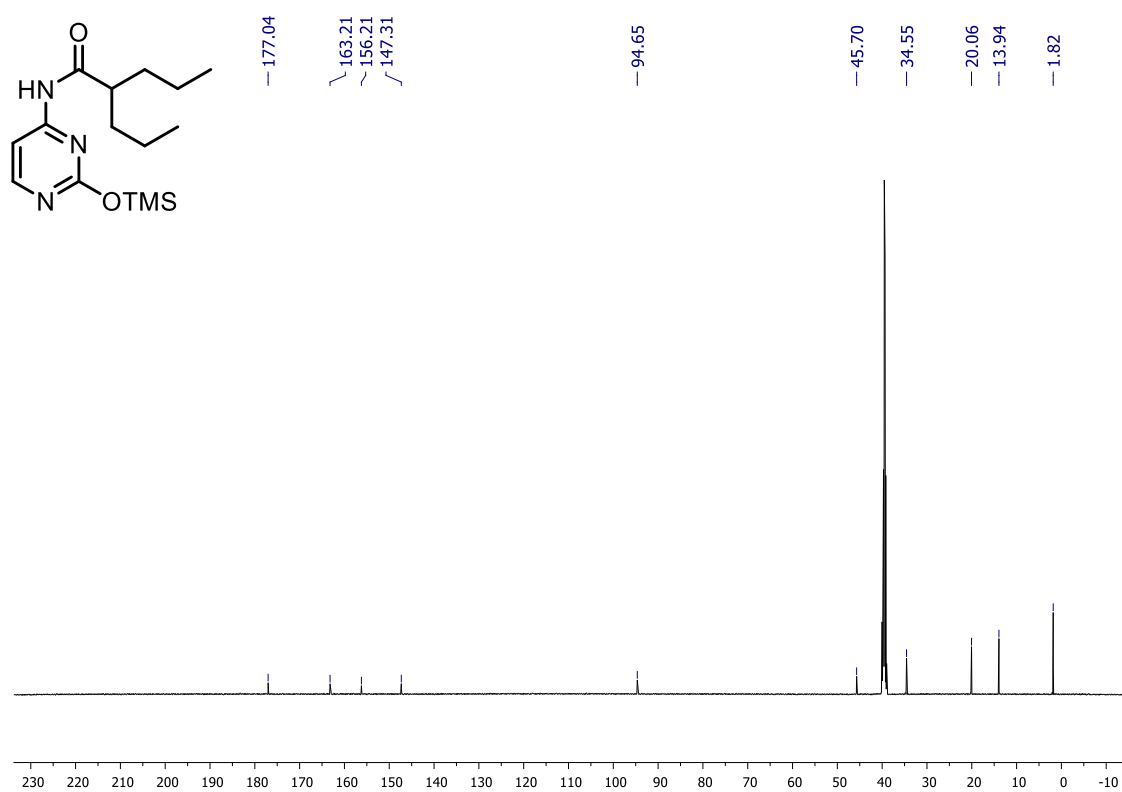
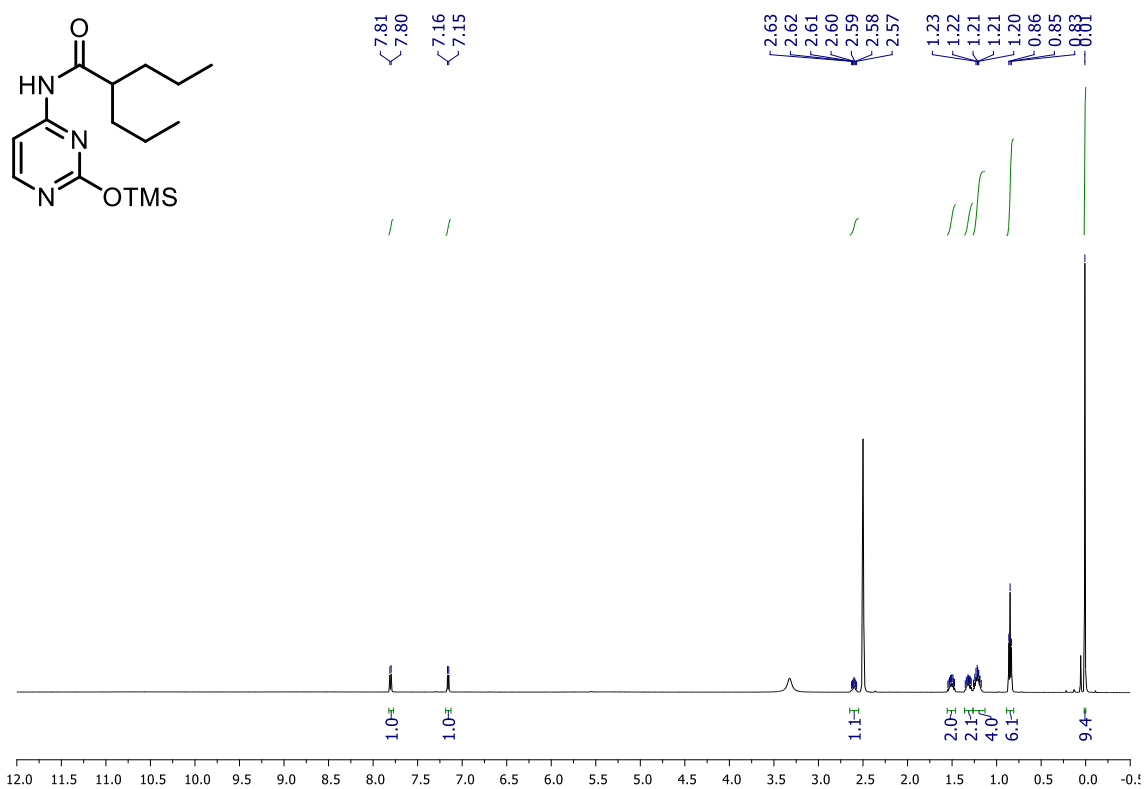


(3R,4R,5R)-3-bromo-3-fluoro-4-((triisopropylsilyloxy)methyl)dihydrofuran-2(3H)-one (202)

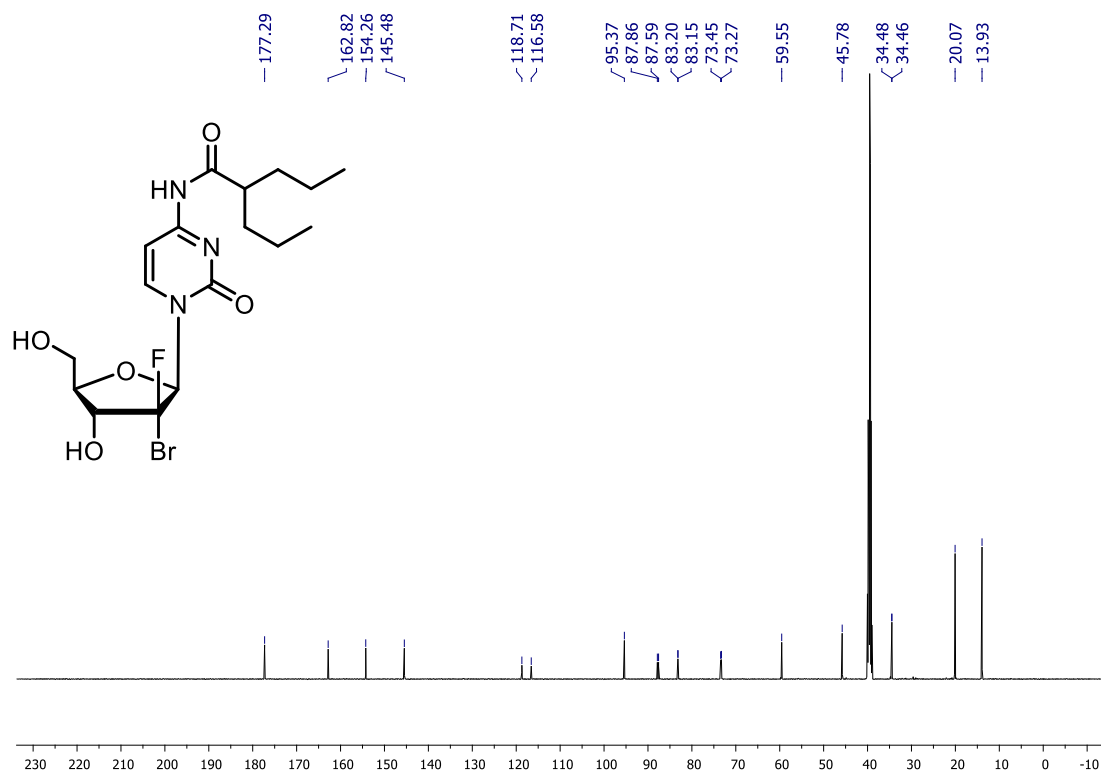
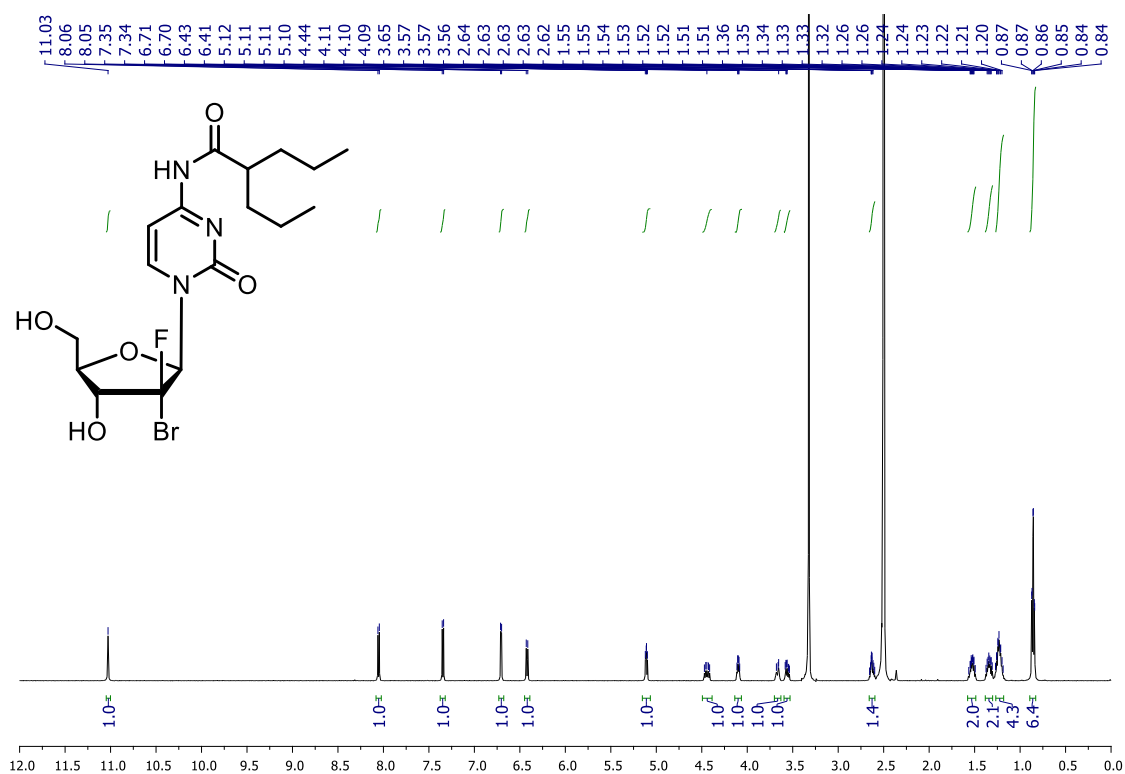


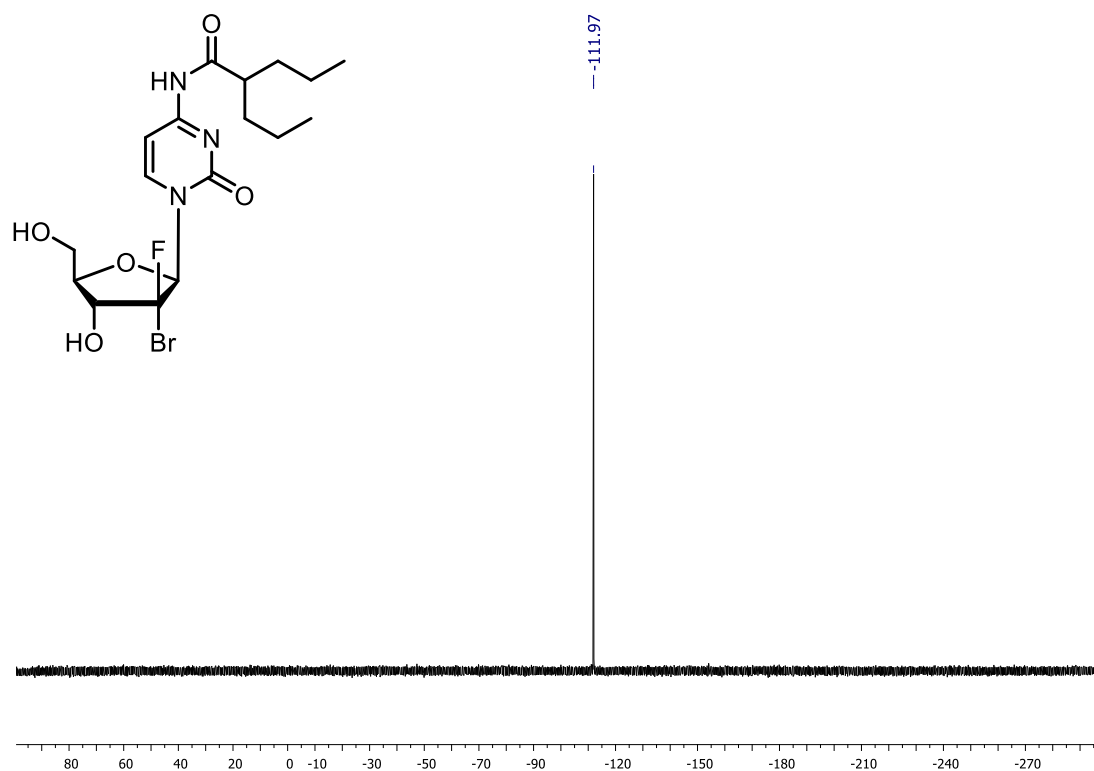


2-propyl-N-(2-((trimethylsilyl)oxy)pyrimidin-4-yl)pentanamide (217)

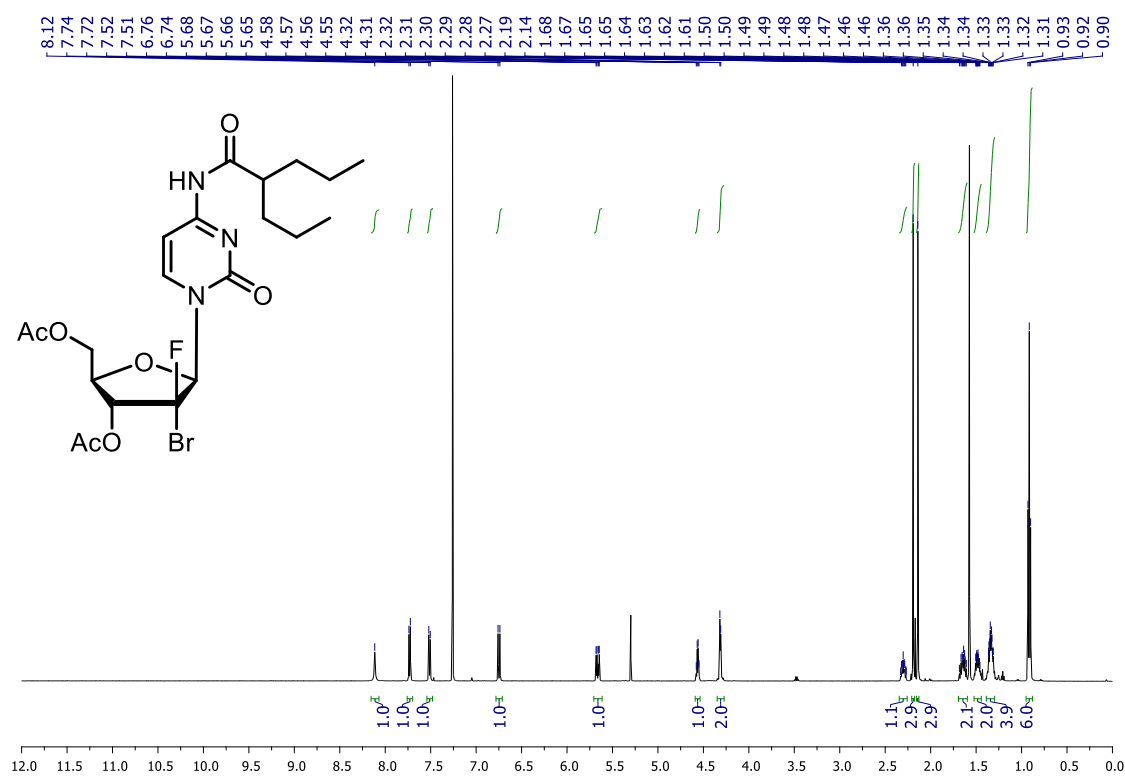


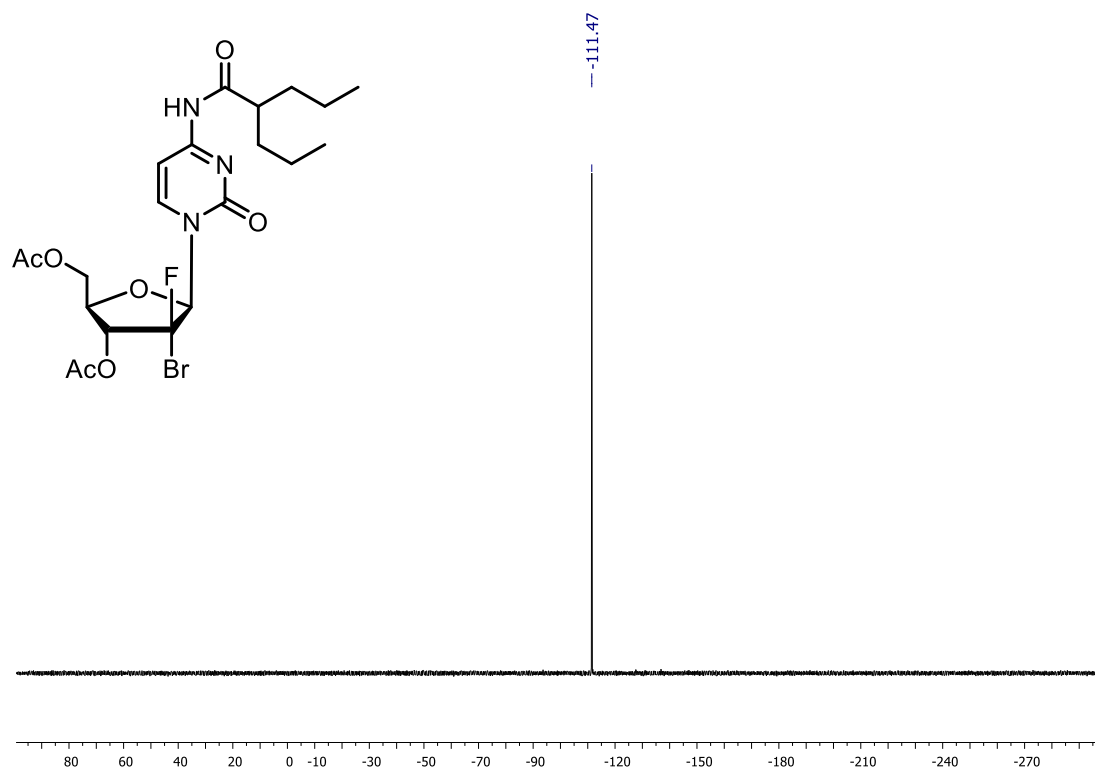
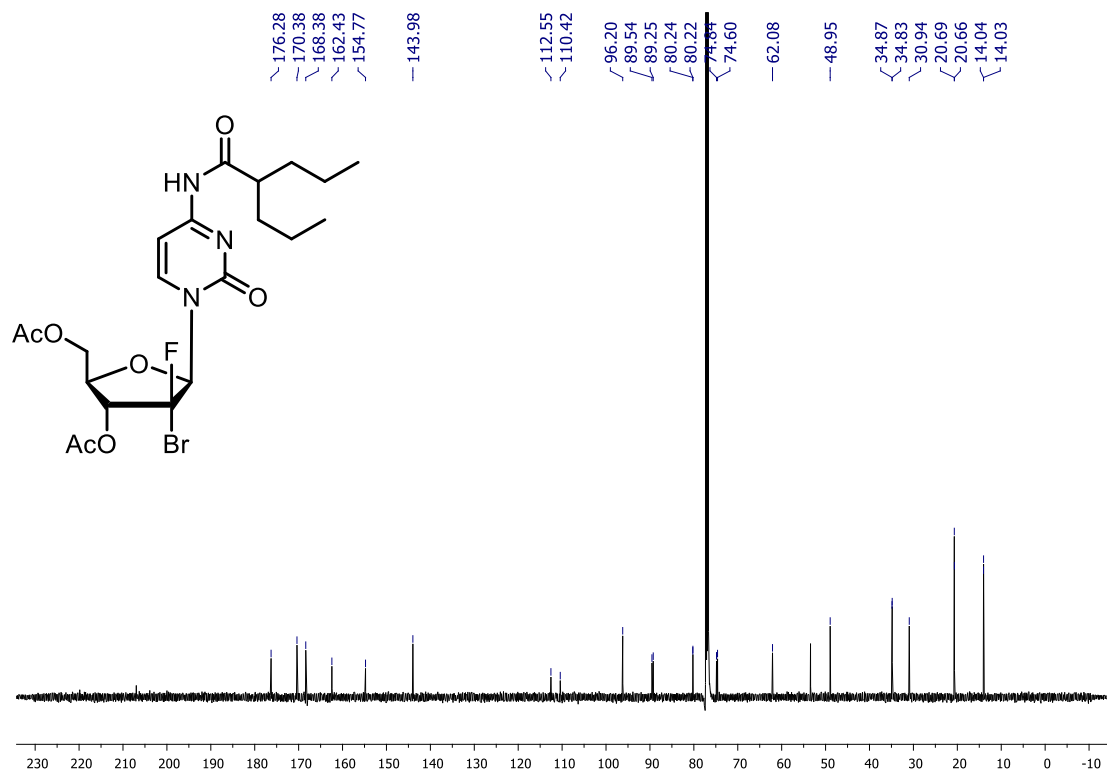
***N*-1-((2*R*,3*R*,4*R*,5*R*)-3-bromo-3-fluoro-4-hydroxy-5-(hydroxymethyl)-tetrahydrofuran-2-yl)-2-oxo-1,2-dihydropyrimidin-4-yl)-2-propylpentanamide (227)**





((2R,3R,4R,5R)-3-acetoxy-4-bromo-4-fluoro-5-(2-oxo-4-(2-propylpentanamido)pyrimidin-1(2H)-yl)tetrahydrofuran-2-yl)methyl acetate (228)





6.3 – HRMS report

Elemental Composition Report

Single Mass Analysis

Tolerance = 5.0 PPM / DBE: min = -1.5, max = 100.0

Element prediction: Off

Number of isotope peaks used for i-FIT = 3

Monoisotopic Mass, Odd and Even Electron Ions

93 formula(e) evaluated with 1 results within limits (up to 50 best isotopic matches for each mass)

Elements Used:

C: 0-21 H: 0-30 N: 0-3 O: 0-7 F: 0-2

Minimum:				-1.5					
Maximum:		5.0	5.0	100.0					
Mass	Calc. Mass	mDa	PPM	DBE	i-FIT	Norm	Conf (%)	Formula	
474.2055	474.2052	0.3	0.6	7.5	617.2	n/a	n/a	C21 H30 N3 O7 F2	

References

- [1] J. Spratlin, R. Sangha, D. Glubrecht, L. Dabbagh, J. D. Young, C. Dumontet, C. Cass, R. Lai, J. R. Mackey, *Clin Cancer Res* **2004**, *10*, 6956–6961.
- [2] J. H. Beumer, J. L. Eiseman, R. A. Parise, E. Joseph, J. M. Covey, M. J. Egorin, *Clin Cancer Res* **2008**, *14*, 3529–3535.
- [3] J. R. Kroep, C. J. A. van Moorsel, G. Veerman, D. A. Voorn, R. M. Schultz, J. F. Worzalla, L. R. Tanzer, R. L. Merriman, H. M. Pinedo, G. J. Peters, in *Purine and Pyrimidine Metabolism in Man IX* (Eds.: A. Griesmacher, M.M. Müller, P. Chiba), Springer US, Boston, MA, **1998**, pp. 657–660.
- [4] V. W. T. Ruiz van Haperen, G. Veerman, J. B. Vermorken, G. J. Peters, *Biochemical Pharmacology* **1993**, *46*, 762–766.
- [5] N. M. F. S. A. Cerqueira, P. A. Fernandes, M. J. Ramos, *Chem. Eur. J.* **2007**, *13*, 8507–8515.
- [6] M. Slusarczyk, M. H. Lopez, J. Balzarini, M. Mason, W. G. Jiang, S. Blagden, E. Thompson, E. Ghazaly, C. McGuigan, *J. Med. Chem.* **2014**, *57*, 1531–1542.
- [7] C. McGuigan, R. N. Pathirana, N. Mahmood, A. J. Hay, *Bio. Med. Chem. Lett.* **1992**, *2*, 701–704.
- [8] L. W. Hertel, J. S. Kroin, J. W. Misner, J. M. Tustin, *J. Org. Chem.* **1988**, *53*, 2406–2409.
- [9] D. Y. Jackson, *Synth. Commun.* **1988**, *18*, 337–341.
- [10] Y. Matsumura, H. Fujii, T. Nakayama, Y. Morizawa, A. Yasuda, *J. Fluorine Chem.* **1992**, *57*, 203–207.
- [11] J. A. Weigel, *J. Org. Chem.* **1997**, *62*, 6108–6109.
- [12] Y. Cen, A. A. Sauve, *Nucleosides, Nucleotides & Nucleic Acids* **2010**, *29*, 113–122.
- [13] T. S. Chou, P. C. Heath, L. E. Patterson, L. M. Poteet, R. E. Lakin, A. H. Hunt, *Synthesis* **1992**, 1992, 565–570.
- [14] X. Jiang, J. Li, R. Zhang, Y. Zhu, J. Shen, *Org. Process Res. Dev.* **2008**, *12*, 888–891.
- [15] D. P. Kjell, *Catalytic Stereoselective Glycosylation Process for Preparing 2'-Deoxy-2',2'-Difluoronucleosides and 2'-Deoxy-2'-Fluoronucleosides*, **1995**, US5426183A.
- [16] T. Liu, J. Tang, J. Liang, Y. Chen, X. Wang, J. Shen, D. Zhao, B. Xiong, J.-D. Cen, Y.-L. Chen, *Tetrahedron* **2019**, *75*, 1203–1213.
- [17] Y.-K. Chang, J. Lee, G.-S. Park, M. Lee, C. H. Park, H. K. Kim, G. Lee, B.-Y. Lee, J. Y. Baek, K. S. Kim, *Tetrahedron* **2010**, *66*, 5687–5691.
- [18] C. Chien, P.-S. Chien, C.-K. Hwang, *Stereoselective Synthesis of Beta-Nucleosides*, **2012**, EP2508528A1.
- [19] K. Brown, A. Weymouth-Wilson, B. Linclau, *Carbohydr. Res.* **2015**, *406*, 71–75.
- [20] Y. Cen, A. A. Sauve, *J. Org. Chem.* **2009**, *74*, 5779–5789.
- [21] R. Damrauer, R. Simon, M. Krempp, *J. Am. Chem. Soc.* **1991**, *113*, 4431–4435.
- [22] S. Mengshetti, L. Zhou, O. Sari, C. De Schutter, H. Zhang, J. H. Cho, S. Tao, L. C. Bassit, K. Verma, R. A. Domaoal, M. Ehteshami, Y. Jiang, R. Ovadia, M. Kasthuri, O. Ollinger Russell, T. McBrayer, T. Whitaker, J. Pattassery, M. L. Pascual, L. Uher, B. Y. Lin, S. Lee, F. Amblard, S. J. Coats, R. F. Schinazi, *J. Med. Chem.* **2019**, *62*, 1859–1874.
- [23] R. Ovadia, A. Khalil, H. Li, C. De Schutter, S. Mengshetti, S. Zhou, L. Bassit, S. J. Coats, F. Amblard, R. F. Schinazi, *Bioorg. Med. Chem.* **2019**, *27*, 664–676.
- [24] E. A. Voight, B. S. Brown, S. N. Greszler, G. T. Halvorsen, G. Zhao, A. W. Kruger, J. Hartung, K. A. Lukin, S. R. Martinez, E. G. Moschetta, M. T. Tudesco, N. D. Ide, *J. Org. Chem.* **2019**, *84*, 4723–4734.
- [25] D. M. Bender, J. Bao, A. H. Dantzig, W. D. Diseroad, K. L. Law, N. A. Magnus, J. A. Peterson, E. J. Perkins, Y. J. Pu, S. M. Reutzel-Edens, D. M. Remick, J. J. Starling, G. A. Stephenson, R. K. Vaid, D. Zhang, J. R. McCarthy, *J. Med. Chem.* **2009**, *52*, 6958–6961.
- [26] Z. Guo, J. M. Gallo, *J. Org. Chem.* **1999**, *64*, 8319–8322.

- [27] S. L. W. Koolen, P. O. Witteveen, R. S. Jansen, M. H. G. Langenberg, R. H. Kronemeijer, A. Nol, I. Garcia-Ribas, S. Callies, K. A. Benhadji, C. A. Slapak, J. H. Beijnen, E. E. Voest, J. H. M. Schellens, *Clin Cancer Res* **2011**, *17*, 6071–6082.
- [28] S. J. Faivre, A. J. Olszanski, K. Weigang-Köhler, H. Riess, R. B. Cohen, X. Wang, S. P. Myrand, E. R. Wickremsinhe, C. L. Horn, H. Ouyang, S. Callies, K. A. Benhadji, E. Raymond, *Invest New Drugs* **2015**, *33*, 1206–1216.
- [29] N. Yamamoto, H. Nokihara, Y. Yamada, K. Uenaka, R. Sekiguchi, T. Makiuchi, C. A. Slapak, K. A. Benhadji, T. Tamura, *Cancer Chemother Pharmacol* **2013**, *71*, 1645–1655.
- [30] J. R. Infante, K. A. Benhadji, G. K. Dy, G. Fetterly, W. W. Ma, J. Bendell, S. Callies, A. A. Adjei, *Invest New Drugs* **2015**, *33*, 432–439.
- [31] Y. Yu, X. Xu, Z. Du, M. Shi, *Cancer Chemother Pharmacol* **2012**, *69*, 1265–1275.
- [32] Y. Mehellou, J. Balzarini, C. McGuigan, *Chem. Med. Chem* **2009**, *4*, 1779–1791.
- [33] C. McGuigan, P. Sutton, D. Cahard, K. Turner, G. O’Leary, Y. Wang, M. Gumbleton, E. De Clercq, J. Balzarini, *Antiviral Chem. Chemother.* **1998**, *9*, 473–479.
- [34] G. Birkus, R. Wang, X. Liu, N. Kutty, H. MacArthur, T. Cihlar, C. Gibbs, S. Swaminathan, W. Lee, M. McDermott, *Antimicrob Agents Chemother* **2007**, *51*, 543–550.
- [35] G. Birkus, N. Kutty, G.-X. He, A. Mulato, W. Lee, M. McDermott, T. Cihlar, *Mol Pharmacol* **2008**, *74*, 92–100.
- [36] C. McGuigan, H.-W. Tsang, D. Cahard, K. Turner, S. Velazquez, A. Salgado, L. Bidois, L. Naesens, E. De Clercq, J. Balzarini, *Antiviral Res.* **1997**, *35*, 195–204.
- [37] S. Chang, G. W. Griesgraber, P. J. Southern, C. R. Wagner, *J. Med. Chem.* **2001**, *44*, 223–231.
- [38] C. McGuigan, S. R. Nicholls, T. J. O’Connor, D. Kinchington, *Antiviral Chem. Chemother.* **1990**, *1*, 25–33.
- [39] A. Q. Siddiqui, C. Ballatore, C. McGuigan, E. De Clercq, J. Balzarini, *J. Med. Chem.* **1999**, *42*, 393–399.
- [40] Y. Mehellou, H. S. Rattan, J. Balzarini, *J. Med. Chem.* **2018**, *61*, 2211–2226.
- [41] B. M. Anderson, E. H. Cordes, W. P. Jencks, *J. Biol. Chem.* **1961**, *236*, 455–463.
- [42] E. Murakami, T. Tolstykh, H. Bao, C. Niu, H. M. M. Steuer, D. Bao, W. Chang, C. Espiritu, S. Bansal, A. M. Lam, M. J. Otto, M. J. Sofia, P. A. Furman, *J. Biol. Chem.* **2010**, *285*, 34337–34347.
- [43] X. Song, P. L. Lorenzi, C. P. Landowski, B. S. Vig, J. M. Hilfinger, G. L. Amidon, *Mol. Pharmaceutics* **2005**, *2*, 157–167.
- [44] W. Xiao, J. Wei, C.-Y. Zhou, C.-M. Che, *Chem. Commun.* **2013**, *49*, 4619–4621.
- [45] C. McGuigan, *Chemical Compounds*, **2005**, WO2005012327 (A2).
- [46] B. Simmons, Z. Liu, A. Klapars, A. Bellomo, S. M. Silverman, *Org. Lett.* **2017**, *19*, 2218–2221.
- [47] U. Pradere, E. C. Garnier-Amblard, S. J. Coats, F. Amblard, R. F. Schinazi, *Chem. Rev.* **2014**, *114*, 9154–9218.
- [48] C. A. Roman, J. Balzarini, C. Meier, *J. Med. Chem.* **2010**, *53*, 7675–7681.
- [49] M. J. Sofia, D. Bao, W. Chang, J. Du, D. Nagarathnam, S. Rachakonda, P. G. Reddy, B. S. Ross, P. Wang, H.-R. Zhang, S. Bansal, C. Espiritu, M. Keilman, A. M. Lam, H. M. M. Steuer, C. Niu, M. J. Otto, P. A. Furman, *J. Med. Chem.* **2010**, *53*, 7202–7218.
- [50] “Success still eludes pancreatic cancer pipeline,” can be found under <https://www.evaluate.com/vantage/articles/analysis/spotlight/success-still-eludes-pancreatic-cancer-pipeline>, **2019**.
- [51] G. W. Camiener, *Biochem. Pharmacol.* **1967**, *16*, 1691–1702.
- [52] F. Myhren, B. Boerretzen, A. Dalen, M. L. Sandvold, *Gemcitabine Derivatives*, **1998**, WO9832762 (A1).
- [53] M. L. Sandvold, C. Galmarini, F. Myhren, G. Peters, *Nucleosides, Nucleotides & Nucleic Acids* **2010**, *29*, 386–393.

- [54] “Another pancreatic cancer drug hits the dust - Clavis/Clovis’ CP-4126,” can be found under <https://www.thepharmaletter.com/article/another-pancreatic-cancer-drug-hits-the-dust-clavis-clovis-cp-4126>, n.d.
- [55] H. Minn, S. Kauhanen, M. Seppänen, P. Nuutila, *J. Nucl. Med.* **2009**, *50*, 1915–1918.
- [56] E. Lopci, I. Grassi, A. Chiti, C. Nanni, G. Cicoria, L. Toschi, C. Fonti, F. Lodi, S. Mattioli, S. Fanti, *Am. J. Nucl. Med. Mol. Imaging* **2014**, *4*, 365–384.
- [57] A. Al-Sugair, R. E. Coleman, *Seminars in Nuclear Medicine* **1998**, *28*, 303–319.
- [58] P. Prakash, C. G. Cronin, M. A. Blake, *American Journal of Roentgenology* **2010**, *194*, W464–W470.
- [59] S. K. Yang, N. Cho, W. K. Moon, *Korean J. Radiol.* **2007**, *8*, 429–437.
- [60] A. Gallamini, C. Zwarthoed, A. Borra, *Cancers (Basel)* **2014**, *6*, 1821–1889.
- [61] E. L. Cole, M. N. Stewart, R. Littich, R. Hoareau, P. J. H. Scott, *Curr. Top. Med. Chem.* **2014**, *14*, 875–900.
- [62] S. Preshlock, M. Tredwell, V. Gouverneur, *Chem. Rev.* **2016**, *116*, 719–766.
- [63] S. M. Ametamey, M. Honer, P. A. Schubiger, *Chem. Rev.* **2008**, *108*, 1501–1516.
- [64] M. E. Phelps, *PET: Molecular Imaging and Its Biological Applications*, Springer-Verlag, New York, **2004**.
- [65] G. Ariño, M. Chmeissani, G. De Lorenzo, C. Puigdemengoles, E. Cabruja, Y. Calderón, M. Kolstein, J. G. Macias-Montero, R. Martinez, E. Mikhaylova, D. Uzun, *J Instrum* **2013**, *8*, DOI 10.1088/1748-0221/8/02/C02015.
- [66] T. G. Turkington, *J. Nucl. Med. Technol.* **2001**, *29*, 4–11.
- [67] H. Teare, E. G. Robins, E. Årstad, S. K. Luthra, V. Gouverneur, *Chem. Commun.* **2007**, 2330–2332.
- [68] H. Teare, E. G. Robins, A. Kirjavainen, S. Forsback, G. Sandford, O. Solin, S. K. Luthra, V. Gouverneur, *Angew. Chem. Int. Ed.* **2010**, *49*, 6821–6824.
- [69] D. E. Olberg, J. M. Arukwe, D. Grace, O. K. Hjelstuen, M. Solbakken, G. M. Kindberg, A. Cuthbertson, *J. Med. Chem.* **2010**, *53*, 1732–1740.
- [70] K. S. Jang, Y.-W. Jung, G. Gu, R. A. Koeppe, P. S. Sherman, C. A. Quesada, D. M. Raffel, *J. Med. Chem.* **2013**, *56*, 7312–7323.
- [71] D. W. Kim, Jeong, S. T. Lim, M.-H. Sohn, J. A. Katzenellenbogen, D. Y. Chi, *J. Org. Chem.* **2008**, *73*, 957–962.
- [72] D. N. Pandya, N. Bhatt, H. Yuan, C. S. Day, B. M. Ehrmann, M. Wright, U. Bierbach, T. J. Wadas, *Chem. Sci.* **2017**, *8*, 2309–2314.
- [73] Y. Zhang, H. Hong, W. Cai, *Curr Radiopharm* **2011**, *4*, 131–139.
- [74] A. L. Våvere, J. S. Lewis, *Dalton Trans.* **2007**, 4893–4902.
- [75] D. O’Hagan, *Chemical Society Reviews* **2008**, *37*, 308–319.
- [76] T. Ido, C.-N. Wan, V. Casella, J. S. Fowler, A. P. Wolf, M. Reivich, D. E. Kuhl, *J. Labelled Compd. Radiopharm.* **1978**, *14*, 175–183.
- [77] T. Toyokuni, J. S. D. Kumar, P. Gunawan, E. S. Basarah, J. Liu, J. R. Barrio, N. Satyamurthy, *Mol. Imaging Biol.* **2004**, *6*, 417.
- [78] P. Shah, A. D. Westwell, *J. Enzyme Inhib. Med. Chem.* **2007**, *22*, 527–540.
- [79] E. Differding, H. Ofner, *Synlett* **1991**, *1991*, 187–189.
- [80] F. Buckingham, A. K. Kirjavainen, S. Forsback, A. Krzyczmonik, T. Keller, I. M. Newington, M. Glaser, S. K. Luthra, O. Solin, V. Gouverneur, *Angew. Chem. Int. Ed.* **2015**, *54*, 13366–13369.
- [81] T. D. Beeson, D. W. C. MacMillan, *J. Am. Chem. Soc.* **2005**, *127*, 8826–8828.
- [82] I. S. R. Stenhagen, A. K. Kirjavainen, S. J. Forsback, C. G. Jørgensen, E. G. Robins, S. K. Luthra, O. Solin, V. Gouverneur, *Chem. Commun.* **2013**, *49*, 1386–1388.
- [83] M. Pretze, C. Wängler, B. Wängler, *Biomed Res Int* **2014**, *2014*, DOI 10.1155/2014/674063.

- [84] P. L. Jager, R. Chirakal, C. J. Marriott, A. H. Brouwers, K. P. Koopmans, K. Y. Gulenchyn, *J Nucl Med* **2008**, *49*, 573–586.
- [85] M. R. C. Gerstenberger, A. Haas, *Angew. Chem. Int. Ed. Eng.* **1981**, *20*, 647–667.
- [86] V. H. Jadhav, W. Choi, S.-S. Lee, S. Lee, D. W. Kim, *Chem. Eur. J.* **2016**, *22*, 4515–4520.
- [87] J. S. Kim, W. K. Lee, W. Sim, J. W. Ko, M. H. Cho, D. Y. Ra, J. W. Kim, *J. Inclusion Phenom.* **2000**, *37*, 359–370.
- [88] O. Jacobson, D. O. Kiesewetter, X. Chen, *Bioconjug. Chem.* **2015**, *26*, 1–18.
- [89] “Carbon-fluorine bond formation. - Abstract - Europe PMC,” can be found under <http://europepmc.org/article/med/18946845>, **2008**.
- [90] J. H. Clark, *Chem. Rev.* **1980**, *80*, 429–452.
- [91] D. W. Kim, D.-S. Ahn, Y.-H. Oh, S. Lee, H. S. Kil, S. J. Oh, S. J. Lee, J. S. Kim, J. S. Ryu, D. H. Moon, D. Y. Chi, *J. Am. Chem. Soc.* **2006**, *128*, 16394–16397.
- [92] J.-W. Lee, M. T. Oliveira, H. B. Jang, S. Lee, D. Y. Chi, D. W. Kim, C. E. Song, *Chem. Soc. Rev.* **2016**, *45*, 4638–4650.
- [93] J. A. K. Howard, V. J. Hoy, D. O’Hagan, G. T. Smith, *Tetrahedron* **1996**, *52*, 12613–12622.
- [94] M.-R. Zhang, K. Suzuki, *Curr Top Med Chem* **2007**, *7*, 1817–1828.
- [95] O. Jacobson, X. Chen, *Curr Top Med Chem* **2010**, *10*, 1048–1059.
- [96] T. Khotavivattana, S. Verhoog, M. Tredwell, L. Pfeifer, S. Calderwood, K. Wheelhouse, T. Lee Collier, V. Gouverneur, *Angew. Chem. Int. Ed.* **2015**, *54*, 9991–9995.
- [97] V. Jagannadham, T. L. Amyes, J. P. Richard, *J. Am. Chem. Soc.* **1993**, *115*, 8465–8466.
- [98] S. Verhoog, L. Pfeifer, T. Khotavivattana, S. Calderwood, T. L. Collier, K. Wheelhouse, M. Tredwell, V. Gouverneur, *Synlett* **2016**, *27*, 25–28.
- [99] J.-P. Meyer, K. C. Probst, A. D. Westwell, *J. Label Compd. Radiopharm* **2014**, *57*, 333–337.
- [100] T. J. Mangner, R. W. Klecker, L. Anderson, A. F. Shields, *Nucl. Med. Biol.* **2003**, *30*, 215–224.
- [101] B. Amaraesekera, P. D. Marchis, K. P. Bobinski, C. G. Radu, J. Czernin, J. R. Barrio, R. Michael van Dam, *Appl. Radiat. Isot.* **2013**, *78*, 88–101.
- [102] C. H. Tann, P. R. Brodfuehrer, S. P. Brundidge, C. Sapino, H. G. Howell, *J. Org. Chem.* **1985**, *50*, 3644–3647.
- [103] N. Turkman, V. Paolillo, J. G. Gelovani, M. M. Alauddin, *Tetrahedron* **2012**, *68*, 10326–10332.
- [104] N. Turkman, J. G. Gelovani, M. M. Alauddin, *J. Labelled Compd Radiopharm.* **2010**, *53*, 782–786.
- [105] C. Wodarski, J. Eisenbarth, K. Weber, M. Henze, U. Haberkorn, M. Eisenhut, *J Labelled Compd Radiopharm.* **2000**, *43*, 1211–1218.
- [106] A. Cavaliere, K. C. Probst, S. J. Paisey, C. Marshall, A. K. H. Dheere, F. Aigbirhio, C. McGuigan, A. D. Westwell, *Molecules* **2020**, *25*, 704.
- [107] M. T. Nguyen, A. V. Keer, T.-K. Ha, L. G. Vanquickenborne, *J Mol. Struct.* **1994**, *310*, 125–134.
- [108] D. H. Moon, D. Y. Chi, D. W. Kim, S. J. Oh, J.-S. Ryu, *Method for Preparation of Organofluoro Compounds in Alcohol Solvents*, **2006**, WO2006065038 (A1).
- [109] D. H. MOON, D. Y. CHI, D. W. KIM, S. J. OH, J. RYU, *United States Patent Application: 0100113763 - METHOD FOR PREPARATION OF ORGANOFUORO COMPOUNDS IN ALCOHOL SOLVENTS*, **2010**, 20100113763.
- [110] C. R. Schmid, J. D. Bryant, M. Dowlatzedah, J. L. Phillips, D. E. Prather, R. D. Schantz, N. L. Sear, C. S. Vianco, *J Org. Chem.* **1991**, *56*, 4056–4058.
- [111] D. I. MaGee, P. J. Silk, J. Wu, P. D. Mayo, K. Ryall, *Tetrahedron* **2011**, *67*, 5329–5338.
- [112] C. Chbib, *Bioorg. Med. Chem. Lett.* **2017**, *27*, 1681–1685.
- [113] D. Scarpì, L. Bartali, A. Casini, E. G. Occhiato, *Eur. J. Org. Chem.* **2013**, *2013*, 1306–1317.
- [114] C. P. Tripp, M. L. Hair, *Langmuir* **1995**, *11*, 149–155.

- [115] V. D. Romanenko, V. I. Tovstenko, L. N. Markovskii, *Chemischer Informationsdienst* **1981**, 12, DOI 10.1002/chin.198118108.
- [116] In *Comprehensive Organic Name Reactions and Reagents*, American Cancer Society, **2010**, pp. 3067–3072.
- [117] J. J. McAtee, R. F. Schinazi, D. C. Liotta, *J. Org. Chem.* **1998**, 63, 2161–2167.
- [118] M. Arisawa, T. Ichikawa, M. Yamaguchi, *Tetrahedron Lett.* **2013**, 54, 4327–4329.
- [119] H. Vorbrüggen, B. Bennua, *Chem. Ber.* **1981**, 114, 1279–1286.
- [120] H. Vorbrüggen, B. Bennua, *Tetrahedron Lett.* **1978**, 19, 1339–1342.
- [121] H. Vorbrüggen, K. Krolkiewicz, B. Bennua, *Chem. Ber.* **1981**, 114, 1234–1255.
- [122] H. Vorbrüggen, G. Höfle, *Chem. Ber.* **1981**, 114, 1256–1268.
- [123] V. Novohradsky, L. Zerzankova, J. Stepankova, O. Vrana, R. Raveendran, D. Gibson, J. Kasparkova, V. Brabec, *J Inorg Biochem.* **2014**, 140, 72–79.
- [124] A. Tai, D. Kawasaki, K. Sasaki, E. Gohda, I. Yamamoto, *Chem PharmBull.* **2003**, 51, 175–180.
- [125] *Org. Synth.* **2000**, 77, 162.
- [126] G. Tambutet, F. Becerril-Jiménez, S. Dostie, R. Simard, M. Prévost, P. Mochirian, Y. Guindon, *Org. Lett.* **2014**, 16, 5698–5701.
- [127] N.-S. Li, J. A. Piccirilli, *Chem. Commun.* **2012**, 48, 8754–8756.
- [128] A. Sniady, M. W. Bedore, T. F. Jamison, *Angew. Chem. Int. Ed.* **2011**, 50, 2155–2158.
- [129] J.-P. Meyer, K. C. Probst, I. M. L. Trist, C. McGuigan, A. D. Westwell, *J. Labelled Compd. Radiopharm* **2014**, 57, 637–644.
- [130] F. A. Davis, J. Lamendola, U. Nadir, E. W. Kluger, T. C. Sedergran, T. W. Panunto, R. Billmers, R. Jenkins, I. J. Turchi, *J. Am. Chem. Soc.* **1980**, 102, 2000–2005.
- [131] M. Leuenberger, A. Ritler, A. Simonin, M. A. Hediger, M. Lochner, *ACS Chem. Neurosci.* **2016**, 7, 534–539.
- [132] Y. Cen, A. A. Sauve, *J. Am. Chem. Soc.* **2010**, 132, 12286–12298.
- [133] P. Anne M. McDonnell, “Chemotherapeutic Agents and Their Uses, Dosages, and Toxicities,” can be found under <https://www.cancernetwork.com/cancer-management/chemotherapeutic-agents-and-their-uses-dosages-and-toxicities>, **2016**.
- [134] “Fieser and Fieser’s Reagents for Organic Synthesis Volumes 1 - 28, and Collective Index for Volumes 1 - 22 Set | Wiley,” can be found under <https://www.wiley.com/en-gb/Fieser+and+Fieser%27s+Reagents+for+Organic+Synthesis+Volumes+1+28%2C+and+Collective+Index+for+Volumes+1+22+Set-p-9781119231028>, **2016**.
- [135] G. Fang, X. Cong, G. Zaroni, Q. Liu, X. Bi, *Adv. Synth. Catal.* **2017**, 359, 1422–1502.
- [136] E. Lee, A. S. Kamlet, D. C. Powers, C. N. Neumann, G. B. Boursalian, T. Furuya, D. C. Choi, J. M. Hooker, T. Ritter, *Science* **2011**, 334, 639–642.
- [137] G. Li, A. K. Dilger, P. T. Cheng, W. R. Ewing, J. T. Groves, *Angew. Chem. Int. Ed.* **2018**, 57, 1251–1255.
- [138] W. Liu, X. Huang, M. S. Placzek, S. W. Krska, P. McQuade, J. M. Hooker, J. T. Groves, *Chem. Sci.* **2018**, 9, 1168–1172.
- [139] P. Xu, D. Zhao, F. Berger, A. Hamad, J. Rickmeier, R. Petzold, M. Kondratiuk, K. Bohdan, T. Ritter, *Angew. Chem. Int. Ed.* **2020**, 59, 1956–1960.
- [140] S. Y. Chen, M. M. Joullie, *J. Org. Chem.* **1984**, 49, 2168–2174.
- [141] C. B. Reese, Q. Wu, *Org. Biomol. Chem.* **2003**, 1, 3160–3172.
- [142] H.-J. J. Chen, D. A. DeGoey, J. Hartung, N. Ide, V. Kalthod, A. C. Krueger, Y.-Y. Ku, T. Li, J. T. Randolph, R. Wagner, J. Chau, G. T. Halvorsen, C. C. Marvin, E. Voight, *United States Patent Application: 0170057981 - Anti-Viral Compounds*, **2017**, 20170057981.